Wavelength dependency of phytoplankton photosynthesis : photoregulation and photoacclimation processes in coastal seas

Mónica Michel Rodriguez

École Doctorale de Sciences de la Matière, du Rayonnement et de l'Environnement

Spécialité Géosciences, Écologie, Paléontologie, Océanographie

Université de Lille

Laboratoire d'Océanologie et de Géosciences

UMR 8187 Univ. Lille, ULCO, CNRS

Wavelength dependency of phytoplankton photosynthesis: photoregulation and photoacclimation processes in coastal seas

Dépendance spectrale de la photosynthèse du phytoplancton : processus de photorégulation et de photoacclimatation en mer côtières

Thèse de doctorat présentée par **Mónica MICHEL RODRÍGUEZ**

Soutenue publiquement le 29 Janvier 2021 devant le jury composé de :

Pr. Christophe BRUNET, Stazione Zoologica Anton Dohrn (Italie)	Rapporteur
Dr. Vona MÉLÉDER, EA MMS, Université de Nantes	Rapporteur
Pr. Antoine SCIANDRA, LOV, CNRS	Examinateur (Président du Jury)
Dr. Valérie DAVID, EPOC, Université de Bordeaux	Examinateur
Pr. Sébastien LEFEBVRE, LOG, Université de Lille	Directeur de thèse
Dr. Fabrice LIZON, LOG, Université de Lille	Co-encadrant de thèse
Dr. Marianne JAUBERT, IBPC, Sorbonne Université	Invité

FOREWORD

I was founded by a PhD studentship of three years and three months from the University of Lille.

This work was partly funded by the state and the Region-Hauts de France though the CPER MARCO 2015-2020 and the University of Lille. The data presented in this thesis was partly collected during the ECOPEL LEG1 2018 campaign of the JERICO-NEXT.

Acknowledgements

First at all I would like to thank you Antoine Sciandra, Valérie David, Marianne Jaubert, Vona Méléder and Christophe Brunet for accepting being members of the jury and for evaluating this work.

Thank you, Sébastien Lefebvre and Fabrice Lizon, the supervisors of my thesis. Thank you for letting me be part of this project, thank you for everything you taught me, your time and help. Thank you, Fabrice, for all these meetings at the beginning of the thesis where times seemed to fly. Thank you Sébastien for keeping me (us) focused.

I would like also to thank the members of my two committees of advancement. Thank you, Emilie Poisson, Vincent Vantrepotte and Christophe Brunet, for your kind advice and productive discussions. Thank you, Emilie, for introducing me in the amazing tool of spectral clustering.

Thank you, François Schmitt, the director of the laboratory at the beginning of my thesis, and thank you Hubert Loisel, director at the end of my thesis. Thank you, Lionel Denis, director of the Marine Station. Thank you all for your welcoming.

Thank you, the members of Doctoral School, for your help in administrative issues.

At least half of the data in this thesis comes from the field work during the ECOPEL campaign in the English Channel. I would like you thank you Felipe Artigas for letting me participate and for his help on the use of phytoplankton net to concentrate my samples at the beginning of the campaign. Thank you, all the members of his team and the members of the ship.

The light quality data of this thesis have been treated with the python program developed by Xavier Mérieux who I thank you also for his kindness and time explaining to me how it works.

I would like to thank Sami Soussi and his collaborators Capucine Bialais and Paul Dayras for providing me with some algae cultures. These first tests with MULTI-COLOR-PAM helped me to set after the methodological approach of measuring with natural phytoplankton.

Thank you, Muriel Courvoisier, for nutrients analyses. I would also like to thank you also for your security advice in the laboratory and for bringing me home safe when the experiments took more time in late evenings.

Thank you very much to François Gevaert and Gwendoline Duong for your advice and analysis of the HPLC pigments samples.

Thank you Michèlle Pernak for your technical support using the FRRF Act2.

A special thank you goes for the ladies in the Marine Station secretary, thank you Helène, Nathalie, Lucdivine and Valérie for your help in all of these documents, tickets, reservations etc. I would warmly thank the personnel of the Marine Station, Dominique, Michel Thierry, Christine, Jossette, Christelle and Ghislaine, for helping always in many diverse stuff like the maintenance of the incubators, the property of my office and let me borrow some tools in some situations. But especially thank you for your warm welcoming.

Thank you, all of my mates, during these three years, the "young"(and not that young) team in Wimereux, PhD students, master students and so on. Thank you Jean Charles, Paul, Shagnika, Théo (I will always say Theito), Camille, Gwendoline, Lola, Marine, Noémie, Émilie, Florian, Clothilde, Dewi, Capucine, Nicolas, Guillaume (Plymouth conference time was very nice), all the people from MREN also!…all the internship students …Thank you all. Thank you Loïck for these tours coming back to Lille. Thank you, my dearest Angela, for bringing the sun every single day you were in the Marine Station. Thank you, Terete, for all of these conversations and all of these times you understood my "frañol" and the infinite messages of courage. Thank you, my great friend Shagnika, for your wisdom and warm heart. It was always easy to speak with you. Thank you, my big Lola, these two years working back-to-back have been more than a simple office mate stuff.

Thank you to my advisors and teachers before this thesis in this research journey.

Thank you, all of my friends, far, but always very close. Thank you, my dearest Lorena (you are the next one), Tamy, Ainhoa, Raul, Blanca, Tati, Aldo, Apolline, Gaisha, Ambar, and the all the others from my Marseille team and *las shurmis* de Cadiz! *Merci à tous, Gracias*. Thank you for always being there. Thanks to my friend Jeanne Marie for watching over me…Thanks to my family in Lille and Belgium. Of course, a very special thanks goes to you, my mum and dad. Thank you for your support, unconditional love and always believing in me. There are many things that I would never be able to express here in some simple sentences. And thank you Verschave, my life partner and beloved one…you who have been by my side and have seen all the process in live!

All these people have helped me closer or further in this thesis. However, if there is any mistake, it is of course only my fault.

INDEX

List of symbols and abbreviations

Abbreviation	Definition	Unit
α	Maximum light-use efficiency (initial slope of the light-response curve)	electrons/quanta
α(II)	α related to absolute absorption of PSII	electrons/quanta
AL	Actinic light	
Chl	Chlorophyll	
DIN	Dissolved Inorganic Nitrogen (NO_3+NO_2) (nitrites and nitrates)	μL^{-1}
E	Irradiance	$\mu molphotons.m^{-2}.s^{-1}$
E_k	Light saturation coefficient (the intersection of $ETR(II)_{max}$ and α)	quanta $m^{-2}s^{-1}$
E_k(II)	E_k related to absolute absorption of PSII	quanta(PS II s)$^{-1}$
E_{op}	PAR at ETR_{max}	µmol quanta m^{-2} s^{-1}
E_{op}(II)	PAR at $ETR(II)_{max}$	quanta(PS II s)$^{-1}$
ETR(II)	Electron transport rate related to PSII absorption	electrons(PS II s)$^{-1}$
ETR_{max}	Maximum electron transport rate	µmol electrons s^{-1}
F_0	Minimal fluorescence level obtained after the application of a saturation pulse	
F_m	Maximum fluorescence level obtained after the application of a saturation pulse on dark acclimated samples	
F_m'	Maximum fluorescence level obtained after the application of a saturation pulse on light acclimated samples	
FRR	Fast Repetition Rate	
F_v/F_m	Maximum quantum yield of PSII determined after 2.5 h of dark acclimation	unitless
G/B	Green/blue light quality ratio	
G/R	Green/red light quality ratio	
LHC	Light Harvesting complex	

λ	Wavelength	nm
ML	Measuring Light	
MT	Multi Turnover	
NPQ	Stern-Volmer type non-photochemical fluorescence quenching (Bilger and Björkman, 1990)	unitless
PAM	Pulse Amplitude Modulation	
PAR	Photosynthetically active radiation	µmol photons m^{-2} s^{-1}
PO_4	Phosphates	$µL^{-1}$
PS	Photosystem	
PSII	Photosystem II	unitless
PSU	Photosynthetic Unit	PSU
P-E	Light production curves	
PETλ	Photosynthetic electron transport	
r.ETR	Relative electron transport rate	µmol electrons m^{-2} s^{-1}
R/B	Red/blue light quality ratio	
RC	Reaction Center	
RLC	Rapid Light Curve	
RuBISCO	Ribulose-1,5-biphosphate carboxylase oxygenase	
$Si(OH)_4$	Silicate	$µL^{-1}$
$Sigma(II)_λ$	Wavelength-dependent cross section of PSII	nm^2
ST	Single Turnover	
XC	Xanthophyll's Cycle	
Y(II)	Effective quantum yield of PSII	unitless

General rationale and objectives

Light is one of the most dynamic controlling factors of primary production in aquatic environments (MacIntyre et al., 2000; Dubinsky & Schofield, 2010; Raven & Geider, 2003; Köhler et al., 2018) where phytoplankton must cope to multiple scales of light variations in time and space (Darecki et al., 2011; MacIntyre et al., 2000). At the surface, incident light varies seasonally on a year scale and depending on the cloud cover and surface wave frequency on short time scales. Once light penetrates the water column it decreases exponentially (Kirk, 2011). In offshore regions, light is able to penetrate to high depth while in coastal areas it is submitted to river outflows and resuspension of bottom sediments bringing organic and inorganic suspended matter which increase turbidity and ultimately impact primary production (Capuzzo et al., 2015; Philippart et al., 2013). Superimposed to light penetration issues, phytoplankton is dependent on hydrodynamics: under the effect of waves and turbulent mixing, which vary at different spa tio-temporal scales, cells are susceptible to be transported beyond the euphotic zone.

Coastal regions such as the English Channel, an epicontinental and megatidal ecosystem, are good working areas for the study of light variation in terms of light intensity, but also in terms of spectral composition of the available light also called “light quality”. Very briefly, long wavelengths in the red spectrum are more quickly absorbed by water than short ones in blue bands (Kirk, 2011). This is mainly the case of open coastal waters where phytoplankton is exposed to predominant blue and green bands at higher depths and a full spectrum only in surface, even if during the bloom the high concentration of phytoplankton biomass and the preferential absorption of blue wavelengths could induce an increase on the proportional available red wavelengths of light. In some ecosystems like estuaries, there are high concentrations of colored dissolved organic matter (CDOM). These substances absorb primarily UV and blue wavelengths and skew the light field to long wavelengths in the red spectrum (Lawrenz and Richardson, 2017). As a result, the different light quality ratios changes between blue, green and red wavelengths (red/blue, green/blue or green/red) can highly impact microalgae physiology with important effects on primary production (see some examples of variation in López-Figueroa, 1992; Brunet et al., 2014; Jaubert et al., 2017).

Phytoplankton has developed, in function of the plasticity of each phytoplankton group, sophisticated structures to cope with the dynamic variations of light intensity and quality at different time scales which goes for example from the lifetime of cells to the time that brings different phytoplankton community successions. For this, phytoplankton is able to photoregulate, photoacclimate and photoadapt (Falkowski & LaRoche, 1991; Kirk, 1994; Raven & Geider, 2003; Moore et al., 2006; Dubinsky & Stambler, 2009). The two first processes take place by phenotypic variations during the cell lifespan. These processes, also known as ontogenetic adaptations, can include the variations on electron rate, enzymatic activation, thylakoids structure variation or chloroplasts position change (Falkowski & Raven, 2007) at scales from seconds to minute (photoregulation), as well as pigment concentration and/or ratio variation, state of photoprotection, concentration of photosynthetic units (PSU), or ratio of PSII/PSI at medium and longer time scale from minutes to hours (photoacclimation). Concerning photoadaptation, also known as phylogenetic adaptation, it refers here to modifications of genotypes of microalgae and the development of specific strategies improving fitness across generations (Falkowski & LaRoche, 1991; Kirk, 2011; Moore et al., 2006).

In aquatic ecosystems, microalgae are subject to large differences in light intensity, which, unlike terrestrial plants, are amplified due to the attenuation effect of the different substances present in the aquatic environment and the fact that their position is determined by the movement of the water (Dubinsky & Stambler, 2009). That means that microalgae need to switch, with a different degree of plasticity, between high and low lights. On one hand, under high intensity lights, cells may photoregulate and acquire a photoprotective state to reduce a potential photoinhibition (even if photoreparation and its energetic cost can be a potential strategy assumed as already proved by Raven in 2011). That is to say, cells rely an energy-dissipation processes to avoid damage of photosynthetic apparatus (macro proteins of PSII) or the formation of free radicals and photoinhibition (Dubinsky & Schofield, 2010; Brunet & Lavaud, 2010; Demmig-Adams & Adams, 2006; Lavaud, 2007; Lavaud et al., 2007; Kaňa et al., 2012, 2019). On the other hand, at low lights photoacclimation may be focused on maximizing light absorption (Dubinsky & Schofield, 2010). Among these situations, it must be noted that photoacclimation takes places at the level of intracellular structures of photosynthetic systems and electron flow, being both in straight relation. In terms of structural changes, in response to light intensity and quality variations phytoplankton can vary their concentration and/or the proportion of pigments to adapt to the environment where they develop, but also the number and /or proportion of reaction centers, photosystems or ultrastructures such as the

number of thylakoids per grana for example (Dubinsky & Stambler, 2009). In terms of electron flow variations, phytoplankton also modulate the regulation of electron flow between photochemical reaction and non-photochemical quenching as thermal dissipation in case of excess of absorbed light.

In coastal regions, it has been proven that photosynthetic properties of phytoplankton vary at very different time and spatial scales (Lizon et al., 1995a; Brunet & Lizon, 2003; Houliez et al., 2013b, 2013a; Napoléon et al., 2012) but the dynamics of photoregulation/photoacclimation needs to be more developed in its complexity and take under consideration the combined variation of light quality and intensity (Combe et al., 2015). The question of spectral consideration in the water column in link with photosynthetic activity has evolved and been treated in different ways from field studies with different incubation systems, laboratory experiments first, and field and modelizations studies after (during the last 50 years) and the study of the different photosynthetic parameters derived from the light production curves (commonly known as P-E curves). Between the end of the 80' and the decade of the 90', the "action spectra" theory has shown important evolutions. Firstly, it was evidenced that the lack of consideration of a spectrally averaged initial slope α to predict photosynthesis under different optical waters would induce an underestimation of the integral photosynthesis in water column of 30% (Lewis et al., 1985a, 1985b). Lately, it has been also shown that the lack of consideration of the real spectral characteristic of submarine light and the real ability of phytoplankton to absorb light could lead to an underestimation of primary production rate by a factor of two (Laws et al., 1990). These facts support the need of using full spectra models (Kyewalyanga et al., 1992; Platt and Sathyendranath, 1988). Indeed, α could vary between different species and different light quality conditions in comparison to an α calculated in a simplified water column (Schofield et al., 1996) and P-E parameters could be corrected from the absorption spectra (Kyewalyanga et al., 1997). These questions have been discussed for many years but they were understudied in coastal areas to set the dynamics of photoregulation and photoacclimation processes as a general compromise between light quality and intensity and other controlling factors of available light for photosynthesis at the different scales of time and space of variation. This is possible now thanks to different technical tools.

While the question of variations of photosynthetic activity and primary production in relation to light quality has evolved, it has also been the case for the technical approaches used. Initially, studies have been performed with time consuming incubations in the so-called photosynthetrons which reproduced large numbers of narrow spectral bands of light for many

subsamples (Lewis et al., 1983). Nevertheless, since then the tools have evolved and the physiological variables measured have also evolved from ^{14}C (PP) to variable fluorescence and photophysiological variables, and the measure of the gross photosynthesis (GP) as a proxy of PP. Notably nowadays the techniques have evolved through the direction of variable fluorescence which allow the determination of precise physiological state variables at a higher frequency of sampling due to measuring times under the ^{14}C incubations. Nowadays, measures of photosynthetic activity are mostly performed with variable fluorescence tools that allow the determination of: ii) physiological state variables (PSII maximum quantum yield); ii)functional absorption cross section that can be measured with FRRFf (Kolber et al., 1998) and nowadays also with the new MULTI-COLOR-PAM (Schreiber et al., 2012); and iii) photosynthetic electron transport (PET) derived from other P-E parameters like rapid light curves (originally only with PAM methods (Schreiber et al., 1986) and nowadays also with new generation FRRf act2 (Chelsea UK). At the beginning of development of these techniques, only one light color of measuring light has been frequently considered. The blue light has been mainly employed based on the absorption properties of chlorophyll *a*, the dominant pigment within phytoplankton (Schreiber et al., 2012). In 2012, Schreiber et al. have published a new technical possibility called MULTI-COLOR-PAM (WALZ) with five different wavelengths of actinic light and measuring light as well as fast kinetics protocols to the measure of wavelength dependent absorption cross section of PSII ($Sigma(II)_{\lambda}$). This technical evolution was possible thanks to the resolution of the spectral light by the use of LED illumination (Schreiber et al., 2011). There are also other multi-spectral approach such as the development of a new mini-FIRe, (Gorbunov et al., 2020), a novel ultra-sensitive multispectral instrument, or other multispectral fluorometer with open hardware development platform controlled under Arduino (Hoadley and Warner, 2017). Thanks to these techniques, it is now more practical and efficient to measure the wavelength dependency of all photosynthetic parameters and light absorption capacities at different wavelength dependent photosynthetic processes.

Despite the evidence of both the influence of action spectra on photosynthetic parameter determination (Kyewalyanga et al., 1997; Lewis et al., 1985b), the knowledge of light quality sensing and wavelength dependent energy regulation on photosynthesis (López-Figueroa, 1992; Mouget et al., 2004; Depauw et al., 2012; Schellenberger Costa et al., 2013a; Brunet et al., 2014; Valle et al., 2014) and the development of new techniques of variable fluorescence with the capacity to discriminate the photosynthetic activity at different wavelengths of measurement (Gorbunov et al., 2020; Hoadley & Warner, 2017; Schreiber et al., 2012), the

study of wavelength dependency has been mainly studied in cultures with a limited range of experimental conditions (Schreiber et al., 2012; Schreiber & Klughammer, 2013; Szabó et al., 2014a, 2014b; Goessling et al., 2016; Hoadley & Warner, 2017; Goessling et al., 2018b). Multi-spectral data available with natural phytoplankton community are quite limited and apart from some studies with microphytobenthos in the laboratory (Goessling et al., 2018a), currently only Gorbunov et al (2020) work focused on physiological and taxonomic analysis of phytoplankton communities to our knowledge.

Therefore, this thesis has the goal to characterize the wavelength-dependency of photosynthesis in coastal phytoplankton communities. More precisely, this thesis aims:

(1) To test the wavelength-dependency of photosynthesis in natural phytoplankton communities

(2) To underline relationships between variations of wavelength dependency with biotic (phytoplankton community), and abiotic variables (light and physicochemical variables)

(3) To characterize the spatial and the temporal variability of wavelength dependency

(4) To define the potential dynamics of photoacclimation (including photoregulation at shorter time scale) at different scales

This thesis is structured into five main parts. The first part is a presentation of a state of the art in the subject with a development of the basis and the associated theories with i) photosynthetic structures and process involved on light sensing in microalgae (intensity/quality), ii) a presentation of spectral dependency theory with a glossary of terms used in the domain, iii) photoregulation and photoacclimation processes (as a response to variations of light intensity/quality), and iv) an overview of the methodological approach in terms of instrumentation and statistics used for the study of wavelength dependency. The goal of the first chapter is to introduce the next chapters of this thesis and to specify the theoretical basis of this work to help in the understanding of measurements made on natural communities. The second and third parts will focus on the results acquired in the field and the analysis of spatial (second chapter) and temporal (third chapter) variation of wavelength dependency. The second chapter will analyze wavelength-dependency of photosynthetic parameters in natural

phytoplankton communities in coastal open areas of the English Channel (an example of epicontinental and megatidal ecosystem) during a spring bloom period at different spatial scales and will present the analysis of the controlling factors of photosynthetic wavelength dependency. This second chapter presents in deep detail also the analytical and statistical approach developed during this thesis for multi spectral photosynthetic data. The third chapter will describe the time variability of wavelength-dependency between different seasons when the shifts of variation controlling factors are the most important. Finally, a synthesis of the main results and a general discussion followed by conclusions and future perspectives will be presented in the fourth chapter.

I. Theoretical background and methodologies

1.1. Variation of light in aquatic environments

Light variations are a central issue in this thesis because of their impact on primary production. Light is one of the most dynamic controlling factors of phytoplankton physiology and primary production (MacIntyre et al., 2000; Raven & Geider, 2003; Dubinsky & Schofield, 2010; Köhler et al., 2018). To understand the variations of wavelength dependency of photosynthesis, i.e., photoregulation and photoacclimation processes, it is important to first understand the variation of light (i.e., the light climate) in the aquatic ecosystem and more particularly in coastal regions. I will present a general background of the mechanisms leading to variations of the light climate in coastal areas.

The photosynthetic active radiation (PAR) is comprised between 400 and 700 nm and is known as the visible spectrum of light. There are different potential sources of variation of the underwater light climate: that the ones taking place in the atmosphere by the effect of clouds, the diurnal and seasonal cycles, and the light variations due physical processes occurring in the water column. This thesis will be focused on the last one. In water masses, there are two main sources of variations of light climate (i.e., intensity and quality). The first one is dependent on light absorption by water molecules themselves, and organic and inorganic constituents. Briefly, as light penetrates in the underwater field, the wavelengths that are absorbed by the different constituents become less available, while those that are not absorbed enrich the underwater body (Kirk, 2011). In function of the relative particles that compose the underwater field, the vertical profile of the total PAR light and each of the wavelengths (or narrow wavebands defined) would present a stronger or steeper exponential profile of attenuation. In standard conditions, the blue wavelengths are the ones with the highest capacity of penetration in the water column compared to the red wavelengths.

The variations on the presence of different constituents of the water body (organisms and organic and inorganic substances) lead to a variation of the light climate due to differential capacities of absorption of the different constituents. The light quality regime in underwater field is generally defined by the ratio among the different light colors which have paramount influence on physiological responses of microalgae (Figueroa et al., 1998; Ragni and Ribera d'Alcalà, 2004; Brunet et al., 2011; Jaubert et al., 2017). In this thesis, blue, green, and red light were studied by wavebands and defined by the integration of spectroradiometer measures between 410 and 490 nm, 480-580 and 600-700 nm, respectively, as described in chapter 2 in more details. Then, three different ratios are defined in the water surface: red/blue (R/B),

green/blue (G/B) or green/red (G/R). In coastal areas there are different water bodies with contrasted light quality profiles (Figure I.1). In areas like the English Channel it could be differentiated three different water masses as an example of the variations of light quality in the study area: an eastern and western coastal water body (Authie Bay and Brest Harbour respectively), and a clear offshore water body close to Jersey Islands. These profiles evidence the importance of variation of light quality in coastal regions.

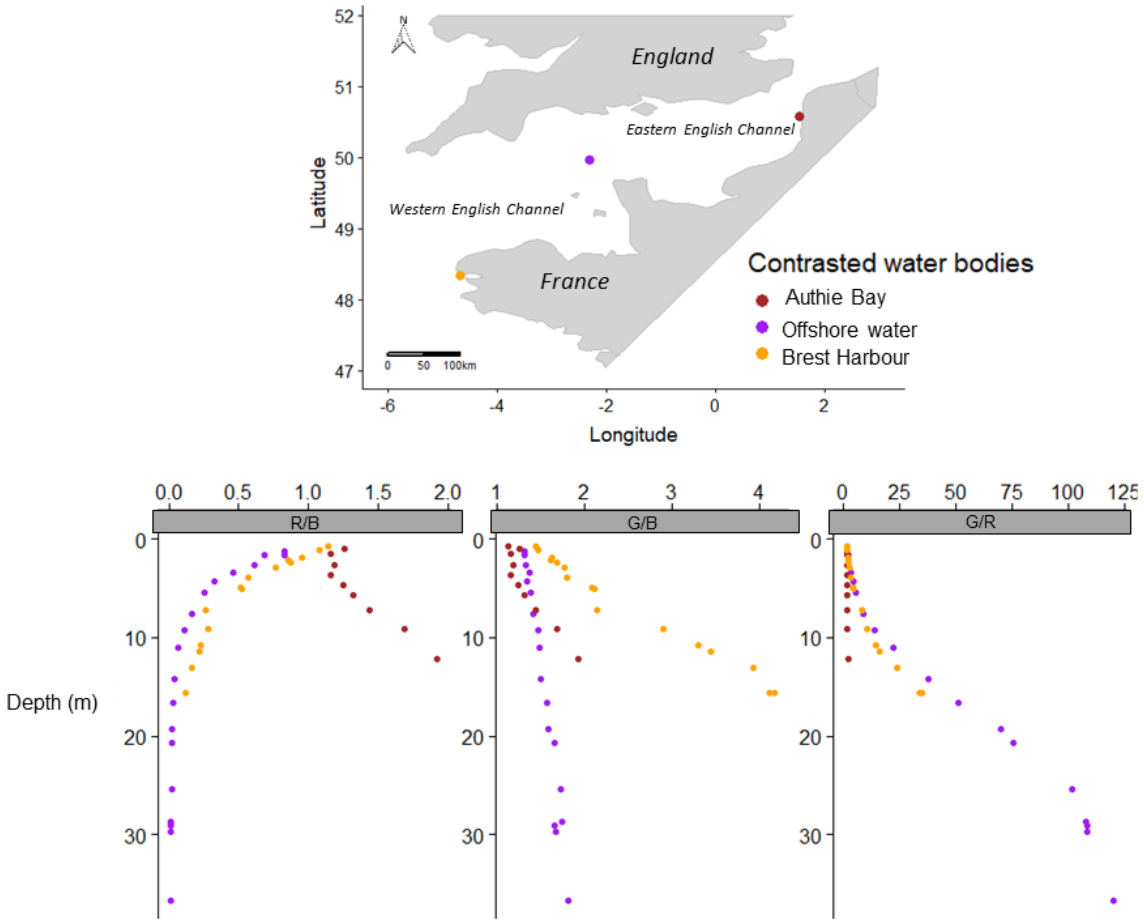

Figure I.1: Vertical profile of light quality ratios of three different water masses in the coastal area of the English Channel sampled during ECOPEL cruise (April 18th to Mai 3rd. The map in the top indicates the locations of the different water bodies: i) Authie Bay (brown circles) that was sampled on April 21st at 10:08 AM as an example of coastal water masses with influence of the Coastal flow (Brylinski et al., 1991) and the dominance of Phaeocystis globose; ii) the offshore sample close to Jersey Islands (purple circles) that was sampled on April 28th at 11:20 AM; and iii)the Brest Harbor (orange circles) and that was sampled on April 30th at 1:48 PM. In the bottom of the figure it is shown the vertical profil of red/blue (R/B), green/blue (G/B) and green/red (G/R) for each water mass.

In coastal areas, important river outputs are at the origin of the increase of the different organic and inorganic substances inducing a variation of the light climate because of the selective

absorption of these substances as previously cited. That is the case of the Colored Dissolved Organic Matter (CDOM). These substances are transported by the river outputs but they are also the result of the increase of phytoplankton biomass and degradation (Astoreca et al., 2009; Kirk, 2011; Vantrepotte et al., 2007). The characteristic of such substances is the absorption of blue wavelengths. This phenomena is responsible for the increase of red and green light that leads to development of dark waters in some estuaries with potential implications on the phytoplankton succession (Lawrenz & Richardson, 2017). These different considerations are illustrated in Figure I.2 which outlines the different parameters controlling the underwater light climate.

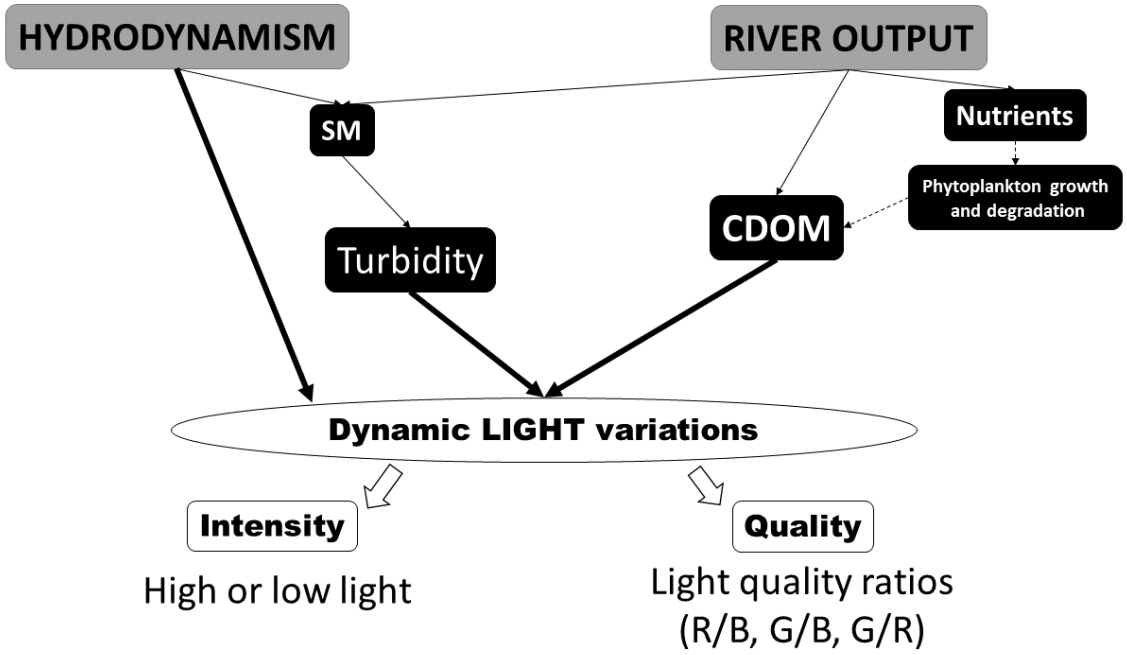

Figure I.2 : Schematic representation of light variations issues in coastal areas like English Channel. The intensity and quality dynamic variations are due the effect of hydrodynamism and river outputs. Hydrodynamism variate the concentration of Suspended matter (SM) that cause an increase of turbidity but also affect the ratio between euphotic and mixed upper layer where phytoplankton growths. The continental influence by river outputs generates an increase of Colored Dissolved organic matter (CDOM) and nutrients (that consequently the growth and development of natural phytoplankton communities and the concentration of CDOM after the degradation of phytoplankton biomass). Data in the following chapters showed that during this study nn the English Channel, light intensity varied between 10 to 1200 µmol photons.m^{-2}.s^{-1} and light ratios ranged between 0-2, 1-4 and 0-125 for R/B, G/B and G/R respectively.

Superimposed to these processes, the increase of turbidity due to resuspension of sediments (Capuzzo et al., 2015; Gohin et al., 2015) has important implications on the floristic composition and primary production (Philippart et al., 2013) (Figure I.2). This resuspension

takes place under the effect of hydrodynamism in coastal regions. Nevertheless, the effect of hydrodynamism does not only conduct effects on the light climate by suspended material. The hydrodynamics due to tide in megatidal seas are also responsible for vertical mixing. These factors change the depth of the mixed layer and export more or less cells through the vertical light gradient. The biological processes of photoregulation/photoacclimation relate to the intensity of hydrodynamism and the light climate described for example by the ratio between the euphotic and the mixed layer depths (Barlow et al., 2013; Dubinsky & Stambler, 2009; Kirk, 2011).

1.2. Light quality sensing and photosynthetic light reactions

Photosynthesis is at the interface of several disciplines. The study of light in the domain of photosynthesis occupies a primordial position in quite different domains such as biophysics, (eco)physiology, ecology, or genomics etc. due to the importance of light as a controlling factor of photosynthesis. Therefore, a survey in different disciplines in which light has a fundamental position is beyond the scope of this introduction. This section aims to help the reader to understand the process of light harvesting, energy transfer and photochemical reaction, photoregulation, photoacclimation and the action spectra or wavelength-dependency theory evolution in ecology research. At the end of this chapter the reader will also find a glossary of the terminology used in this thesis associated with the topic of the wavelength dependency.

1.2.1. Light absorption and energy transfer on photosynthetic organisms

The perception of light on microalgae at different wavelengths is produced due to a particular non-protein molecule called chromophore that serves as a primary site to photon absorption due to its chemical structure. The electron delocalization after photon absorption takes place on unsaturated carbon chains conjugated on a π system which confirms the general structure of chromophores. Moreover, the larger the chromophores are, the longuer is the wavelength they absorb (Möglich et al., 2010). These molecules are bound to proteins forming the photoreceptors. Photoreceptors are involved in light regulated biological responses and they are found in many different species. A special kind of photoreceptors in marine organisms is the light-harvesting complexes and the reaction centers where the photosynthetic pigments are

found with a critical role in photosynthesis. Its importance lies in the fact that they are not only capable of absorbing light, but also energy transfer before triggering a photochemical reaction.

Photosynthetic pigments are able to harvest light and transform it to a chemical potential gradient that is transferred across the thylakoid membrane among different compounds in the photosynthetic electron chain (Kirk, 2011; Möglich et al., 2010). During evolution, photosynthetic organisms have also developed other important photoreceptors which are worth citing. Indeed, these molecules take part on the perception of light as a source of information of the environment where microalgae develop and allow microalgae to adapt their physiology or behavior in function of environmental changes (Jaubert et al., 2017; Kianianmomeni and Hallmann, 2014). These photoreceptors are involved in multiple light mediated reactions such cell cycle progression (Huysman et al., 2013), movement (Cohn et al., 2015; Shikata et al., 2013), gene expression (Fortunato et al., 2016), sexual reproduction (Moulager et al., 2007) or specially on photoacclimation (Jungandreas et al., 2014; Schellenberger Costa et al., 2013b, 2013a). Indeed, photoreceptors can play an important role in some processes of feedback of regulation with the photosynthesis processes (Petroutsos et al., 2016; Schellenberger Costa et al., 2013a, 2013b).

In the following sections the optical properties of pigments and after some particularities of photoreceptors in relation to photosynthesis will be presented first and then, the pigment classification and the composition of light harvesting antenna, and how light energy is transferred through the reaction centers where the first photoreaction occurs.

a) Photosynthetic pigments and optical properties

Photosynthetic pigments are classified in three different groups as a function of the chemical structure of the pyrroles molecules that make up the chromophores. Four different chromophores have emerged in photosynthesis: open tetrapyrrole chain (in phycobilins), closed tetrapyrroles, which are divided on chlorins (in most of chlorophylls unless chlorophylls c) and porphyrins (for example, chlorophylls *c*), and finally the carotenoids (Falkowski & Raven, 2007; Kirk, 2011).

Chlorophylls a, b, d and f are pigments with a chlorins structure while chlorophyll c is a porphyrin-based molecule. The closed ring of chlorins and porphyrins lead to their characteristic absorption properties. Both chlorins and porphyrins have two major different

absorption bands: the blue-green absorption band named B band, or Soret band (the blue band called Soret in honor of the researcher who discovered it), and a red absorption band named Q band (Figure I.3). The former reflects three higher singlet states that after excitation are submitted to a quick decay to the lowest singlet state which is represented by the latter absorption band (Morot-Gaudry and Farineau, 2011). There are two differences between chlorins and porphyrins: the presence of a saturation C-C bond in the fourth ring and a lack of solubility in water of porphyrins in comparison to chlorins. Their structural differences lead to relevant consequences on Soret and red absorption bands due to the break of symmetry of the molecule. When the fourth bond of chlorins is saturated, it brings to a delocalization of electrons in the rings that leads to a large absorption band and lower energy states. In the case of porphyrins pigments, a comparable absorption band is either missing or largely attenuated (Falkowski & Raven, 2007).

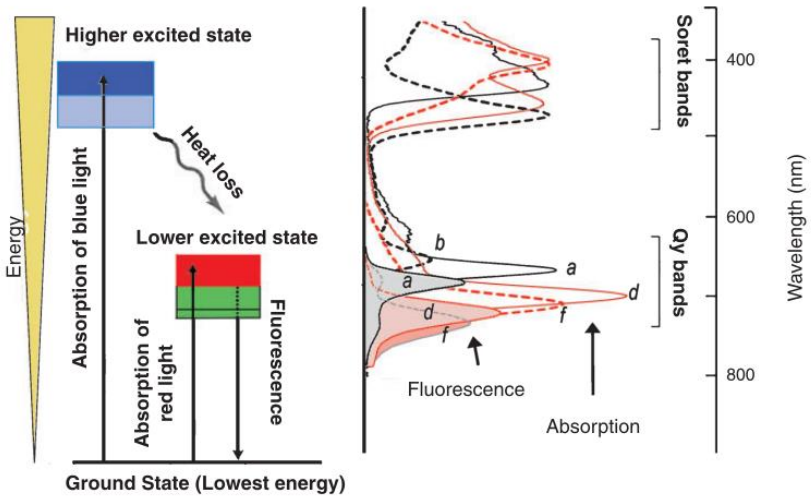

Figure I.3 : Schematic absorption and fluorescence spectra of chlorophylls (from Li and Chen, 2015). The blue and red boxes represent chl a absorption wavelength band. The grey-blue represents the absorption extension at blue light region (mainly by Chl b and Chl d), and green boxes represent the absorption extension at red light region (mainly by Chl d and Chl f). The upward vertical arrows represent the vibronic transitions between the ground state and excited states. The Soret bands with shorter wavelength correspond to a transition to a higher excited state. The Qy absorption band with longer wavelength of chlorophylls corresponds to light that has the energy required to produce the transition from the ground state to the first excited state. The downward vertical arrow indicates the fluorescence. Between absorption and fluorescence emission, relaxation processes as thermal equilibration occurs (heat loss). 'a, b, d and f' represent Chl a, Chl b, Chl d and Chl f respectively.

Chlorophyll *a* is the most widespread photosynthetic pigment. It is present in all known eukaryotic photosynthetic organisms and protists and has an essential role in photosynthesis. This pigment is found in reaction centers and the connection with the other peripheral pigments

is ensured due to the transfer of light energy between the peripheral pigments given their structure and spectroscopic properties. The role and association of other chlorophyll pigments in photosynthetic antenna are described in section 1.2.2.

Carotenoids are large molecules whose optical properties are derived from the length of the carbon molecule chain that constitutes the pigment, the conjugated bond, and the presence of oxygen groups. There are more carotenoids known than chlorophylls. The main carotenoids in phytoplankton are fucoxanthin, peridinin, lutein, violaxanthin, antheraxanthin, zeaxanthin and diadinoxanthin (Falkowski & Raven, 2007; Kuczynska et al., 2015). These molecules display a maximum absorption in the blue-green band. Carotenoids also present a larger spectral property of absorption in function of variations of the chemical structure. Fucoxanthin, a characteristic photosynthetic pigment in diatoms, is an example of the spectral range of carotenoids. This pigment is bound to other pigments in the photosynthetic antenna (see 1.2.2) and has different absorption properties in function of its position of light harvesting antenna. Indeed, fucoxanthin can be classified into high (blue) and low(red) energy absorption as well as two different energy intermediate states in green waveband (Premvardhan et al., 2009, 2008). This property has great relevance. In function of different light quality conditions, microalgae would be able to adapt their pigmentary composition and/or orientation (Section 1.3) and as a result, their capacity of absorption will be improved in this green waveband on light.

Phycobilins, presented in photosynthetic phycobilipigments, can be classified into three groups according to their structure: phycourobilin, phycoerythrobilin and phycocyanobilin and depending on the structure they can absorb blue-green, green, yellow or orange light.

b) Photoreceptors and their role in photosynthesis regulation

In marine microalgae, three different photoreceptors exist: i) photoreceptors absorbing blue such as the cryptochromes, phototrophins, aureochromes and proteins containing Light-Oxygen-Voltage (LOV) domaint; ii) the rhodopsins which absorbs green light; and iii) phytochromes in red band (Figure I.4).

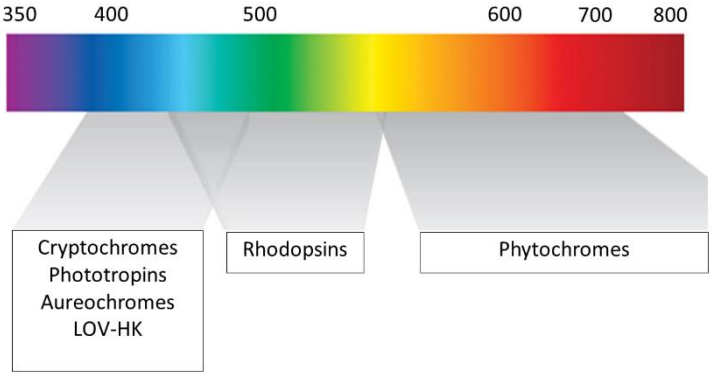

Figure I.4 : Photoreceptors in microalgae according to the range of visible light absorbed. Scheme based on Jaubert et al., (2017). LOV-HK are photoreceptors with a histidine kinase domain at the C-terminos of LOV domain containing proteins (Jaubert et al., 2017)

Considering the light quality variation in aquatic environments and the absorption of visible light in aquatic environments, the aquatic organism have been supposed to sense and adapt mainly in function of blue-green variations with little responses on the role of red light (Depauw et al., 2012; Fortunato et al., 2016). Using the new advances on molecular techniques, recent works have evidenced the role of some photoreceptors on processes of photoacclimation (Mann et al., 2017; Schellenberger Costa et al., 2013b) in diatoms and also in other green algae species like Chlamydomonas (Petroutsos et al., 2016). Schellenberger Costa et al., (2013b) showed that aureochrome, blue photoreceptors, were involved in photoacclimation and that blue light was essential for high light photoacclimation and the photoprotective state (Schellenberger Costa et al., 2013a). The red light plays nevertheless an important role too. Even if red light photon flux rapidly decreased in the photic zone (Kirk, 2011; Ragni & Ribera d'Alcalà, 2004), red light has an important role in metabolic changes like carbon allocation pattern (Jungandreas et al., 2014) and gene expression (Fortunato et al., 2016; Jaubert et al., 2017) but also phototaxis or pigment synthesis (López-Figueroa, 1992). In the particular case of gene expression, it must highlighted that phytochrome are sensors of red and far-red light. It has been shown that after a far-red exposition a phytochrome-dependent expression of a series of genewas produced. The presence of red light is an indicator or proximity to the surface where the intensity of light is normally higher and would need to photoacclimate (Depauw et al., 2012; López-Figueroa, 1992). It is hypothesized that phytochromes, as red/far-red light sensors, could perceive chlorophyll autofluorescence and therefore either monitor chloroplast activity of its own cell, or perceive the presence of other phototrophs in the neighbourhood (Ragni & Ribera d'Alcalà, 2004).

Previous studies showed that red light was required to develop a photoprotective state on *Pseudonitzschia multistriata* (Brunet et al., 2014).

1.2.2. Light harvesting Pigment Protein Complexes

Light harvesting pigment protein complexes are a group of proteins that bind pigments and transfer the absorbed light from the excitation to a photosynthetic reaction center. Such structures are used to keep pigments in the right position and to optimize light harvesting. These structures are frequently named as photosynthetic antenna. There are two types of pigment protein complexes: i) the chlorophyll-protein complexes (Jeffrey, 1980; Larkum & Barrett, 1983) and ii) the phycobiliproteins, which are water soluble molecules found in cyanobacteria, cryptomonads, Rhodophyceae or Glaucophyceae (fresh water microalgae) (Gantt, 1981). The composition of the light harvesting complex is especially important because in function of its composition, the phytoplankton present differentiated absorption capacities and differentiated spectral properties (Yentsch & Yentsch, 1979; Yentsch & Phinney, 1985; Beutler et al., 2002; MacIntyre et al., 2010). This classification differentiates five different groups: i) green algae, with a peripheral antenna composed of chlorophyll *a/b* bound to xanthophylls; ii) brown algae with chlorophyll *a/c* bound to xanthophylls; iii) blue algae, with phycobilisomes formed by phycocyanin; iv) red algae with phycobilisomes based on phycoerythrin; and v) a mixed group formed by a mixed of chlorophyll *a/c* and phycobiliproteins chlorophyll *a/c* and phycobiliproteins.

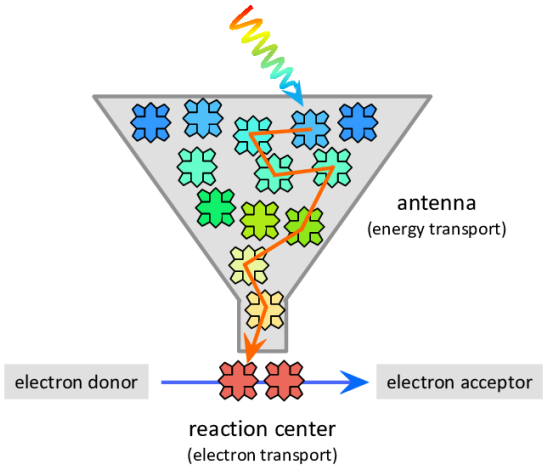

Figure I.5 : Light harvesting complex antenna. Schematic representation from Holtzegel, 2016. The different pigments are bound in the LHC forming a funnel where light energy (symbolized in a rainbow colored arrow) is transferred (see section 1.3.3).

It is important to note that within the photosynthetic antenna, many accessory pigments constituting the light harvesting complexes are found. These pigments are photosynthetically active by transferring absorbed energy to the reaction centers. In this group of pigments, it can be found some carotenoids like the previously cited fucoxanthin. In diatoms for example, the light harvesting complex is formed by the fucoxanthin-chlorophyll protein complex (Gelzinis et al., 2015; Kuczynska et al., 2015). However, in this pigment antenna, there are also photoprotective carotenoids which absorb light but do not transfer energy to reaction centers. That is the case for the β-carotene and the xanthophylls, diatoxanthin, diadinoxanthin, violaxanthin, antheraxanthin, and zeaxanthin, which are engaged in the xanthophyll cycle (later named as XC) (Brunet et al., 2011) that play an important role in the photoregulation processes of phytoplankton.

1.2.3. Photosynthetic energy transfer

The process of energy transfer takes place by a process of resonance. This process is based on the overlap of the Qy band of chlorophyll with fluorescence emission of other auxiliary pigments of the photosynthetic antenna. When an auxiliary pigment on the antenna relaxes from its excited singlet state, the ground state leads to the emission of energy that allows chlorophyll a to undergo a transition from the ground state to the lowest singlet state. This process of energy transfer is known as Föster mechanism (Falkowski & Raven, 2007).

The light absorption process itself does not constitute a photochemical reaction. The build up of reductants and oxidants in photosynthesis needs the absorbed light energy transferred through photosynthetic pigments to be involved in a chemical light reaction. This process occurs when light energy is used to excite and redistribute electrons from an electron donor. Electrons are then physically transferred from donors to receptors on a photochemically catalyzation of oxidation and reduction reactions and the creation of a potential gradient (Behrenfeld et al., 2008). These processes start when the excitation from light harvesting is conducted to the reaction center where the electron donors are found (water molecules for reaction center I for example) (Jeffrey & Vesk, 1977). The ultimate phase of electron transfer is the synthesis of an organic molecule on the Calvin cycle on the dark phase of photosynthesis.

The wavelength dependency of the photochemical reaction of photosynthesis is known as action spectra (Falkowski & Raven, 2007). The action spectrum theory and the application on primary production studies are described in section 1.5. In the next section (section 1.3), general

ecological strategies known to improve the light harvesting and light utilization in marine phytoplankton organisms are presented.

1.3. Ecological strategies to adapt to light climate

Different photophysiological processes are involved in phytoplankton to cope with the dynamics of variation of environmental controlling factors. Regulations and adaptations of photophysiological characteristics of phytoplankton are a central subject of study in ecology because of their effect on the primary production estimations. There are multiple and particularly good references that review the processes of photoregulation and photoacclimation to light intensity variations in phytoplankton. For an extended revision in this subject, the following papers can be consulted: Anning et al., 2000; Behrenfeld et al., 2008, 2004; Brunet et al., 2011; Dubinsky & Schofield, 2010; Dubinsky & Stambler, 2009; Falkowski & Raven, 2007; Kirk, 2011; MacIntyre et al., 2002; Subba Rao, 2006. Figure I.6 summarized the main processes of interest considered in the classical approaches with full light spectrum.

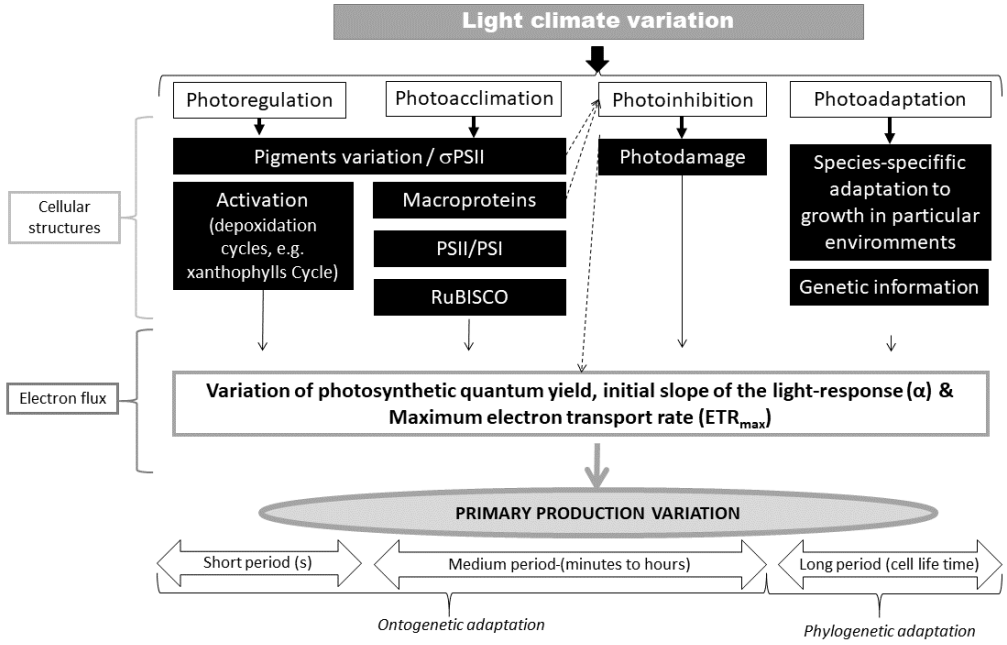

Figure I.6 : Diagram of physiological adaptations to light variations based on broad band (full light spectrum) classical approaches: Light climate variation induce to a response of phytoplankton and alteration of the photosynthetic structures and electron flux that influence the primary production. These responses take place at different time scales from long time scales (photoadaptation) to mid-scale (photoacclimation) and short time scales (activation of enzymes and epoxidation pigments). σ'_{PSII} *is the functional absorption cross section; PSII/PSI refers to the ratio of photosystem I and II; RuBISCO is the enzyme involved in carbon fixation in the Calvin Cycle. These terms are also found in the list of symbols and abbreviations (p.4) acronyms and the glossary (Table I.1).*

Photosynthetic responses of phytoplankton to light variations (Figure I.6) have been described in terms of time scales at which they take place and in function of structural and/or energy fluxes through photosynthetic machinery. Long time scale photoadaptations, also called phylogenetic ones, comprise the different strategies that different species follow to adapt to the environment (Kirk, 2011; Moore et al., 2006; Anning et al., 2000; Brunet et al., 2011).

Photoregulation and photoacclimation occur at short and mid time scales during the lifetime of a cell. Some reviews (Kirk, 2011) describe photoacclimation during cell life as ontogenetic adaptations. Since photoregulation takes place also during the lifetime of phytoplankton, this process can be also considered as ontogenetic adaptation. In the case of photoregulation, the different processes of energy regulation notably by the enzymatic de-epoxidation/epoxidation of acetylenic xanthophylls as a function of absorbed quanta in order to avoid and excess of energy and the formation of free radicals are considered (Brunet et al., 2011; Lohr & Wilhelm, 2001). In the case of photoacclimation, the different processes involve changes in cellular structures. First, cells can be submitted to a variation on concentration of pigment composition of light harvesting complexes (Green & Parson, 2003) and/or the size or the absorption cross section σ_{PSII}. The Photosynthetic Units (PSU) (with two photosystems PSII and PSI, and their pigment antenna) during photoacclimation can vary the size of their antennas and/or their concentration or number (described on the "Z schema" (Dubinsky & Stambler, 2009). The ratio of PSII and PSI can also be altered. Frequently an exposition to low light is associated to an increase of the size of the photosynthetic antenna while an exposition to high light intensity is associated to a decrease of size of photosynthetic antenna and an increase of the reaction centers (Moore et al., 2006)(Figure I.7). Pigment composition is adjusted in function of the variation of chla/Carbon ratio (Sakshaug et al., 1997; Brunet et al., 2011; Subba Rao, 2006). Otherwise, the variations on pigments can be studied by the analysis of the concentration and/or the ratio between pigments (MacIntyre et al., 2002). Note that cells can vary pigment concentration and consequently also vary their ratio among other pigments, but in some cases the ratio is not affected due to the parallel variation of both pigment's concentration used to calculate the pigment ratio studied. Photoacclimation refers also to changes on the ultrastructure of photosynthetic organisms with increases of thylakoids pre grana (Fisher et al., 1989) but also the variations on chloroplast on number, size and morphology (Kirk & Tilney-Bassett, 1978; Larkum & Vesk, 2003). An example of such photoacclimation is the case of *Phaeocystis antarctica* that modify the thylakoid stacking when exposed to low light (Moisan et al., 2006) (Figure I.6).

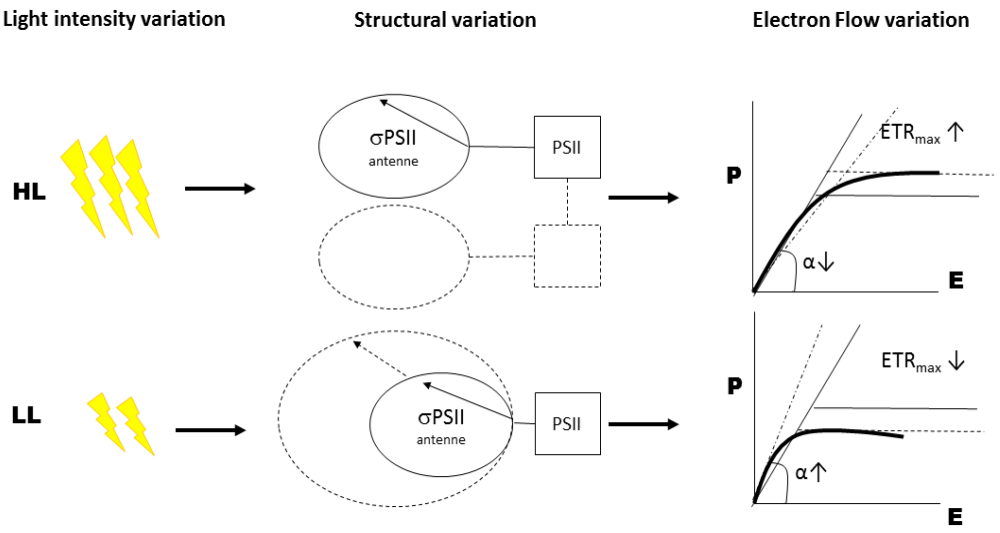

Figure I.7 : Schematic representation of full spectrum photoacclimation to high and low light (HL and LL respectively). Two main effects are shown: i) structural variations of photosynthetic antenna σPSII (represented here with circles) and photosynthetic system concentration (Photosynthetic system II named as PSII and represented with squares); ii) and the electron flow variation with the basic photosynthetic parameters variation in light curve analysis. Dotted lines symbolize cell responses after high or low light exposition. Under HL there are an increase of σPSII and PSII number, while under LL cells increase σPSII size and kept the same concentration of PSII. Arrows symbolize the direction of such variation (increase/decrease of σPSII size and increase /decrease of photosynthetic parameters fitted from P-E curves). The variation on photosynthetic antenna and the concentration of PSII is based on (Moore et al., 2006) and the variation of photosynthetic parameters in light curve is based on (Grobbelaar et al., 1996; MacIntyre et al., 2002).

The processes of photoacclimation can be analyzed by the study of the so-called light curves (Behrenfeld et al., 2004; Brunet et al., 2011; MacIntyre et al., 2002). The processes of photoregulation can be analyzed also by the study of the dynamics of non-photochemical quenching NPQ in fluorescence measurements which is considered the most important process of photoregulation. Briefly, NPQ is divided in three processes (Horton & Hague, 1988): i) qE or energy quenching first mediated by the regulation of transthylakoid proton gradient (ΔpH), ii) qT or quenching to due to state transitions (that does not exist in Diatoms) and iii) qI or quenching due to photoinhibition. The first analysis of qE associated with xanthophyll's Cycle (XC) was done by (Demmig-Adams, 1990). The energy quenching qE is also associated with XC in green (Demmig-Adams, 1990), brown (Brunet & Lavaud, 2010; Lavaud et al., 2007; Sakshaug et al., 1987) and red algae (Ritz et al., 1999) but in some species like cryptophytes, this energy regulation is associated to other system than the xanthophylls's cycle (for example: ions exchange in the membranes, or other pigment antenna according to Kaňa et al., 2019, 2013,

2012). Xanthophyll's Cycle of violaxanthin is based on the de-epoxidation of violaxanthin on antheraxanthin and zeaxanthin in the lumen of cells and the consecutive epoxidation in stroma. The Xanthophyll's Cycle of diadinoxanthin is based on the unique de-epoxidation of diadinoxanthin on diatoxanthin in the lumen or the diatoxanthin epoxidation in the stroma (Brunet et al., 2011).

In the field, the previous biological processes of photoacclimation are controlled by the light climate (quantity and quality) and the intensity of vertical mixing in the upper layer or through the water column (depending on the type of ecosystem, deep or not, with or without stratification, sustainable or temporary). The upper mixed layer (Z_{mix}) and euphotic layer (Z_{eu}) depths can be good proxies to study phytoplankton photoacclimation (Jensen et al., 1994; Wang et al., 2011; Bonamano et al., 2020). When the upper mixed layer is deeper than the euphotic mixed layer, phytoplankton is advected to depths with limiting light and the cells would develop photoacclimation to low light/dark conditions according to the vertical mixing intensity. For this, there must be a trade off between the rate of biological processes and the rate of turbulent movements. When phytoplankton develop in environments where the euphotic layer is deeper than mixed layer, cells will grow with potential high light intensities. (Barlow et al., 2013; Dubinsky & Schofield, 2010; Dubinsky & Stambler, 2009).

The most well-known examples of wavelength dependent photoacclimation are in cyanobacteria within the blue-green band. These processes are described in the bibliography as chromatic adaptation or ontogenetic adaptation of light spectral quality (Kirk, 2011; Kroon et al., 1993; Schofield et al., 1996). These previous works showed that phytoplankton can acclimate their quantum yield in function of different light quality. More recent works have evidenced the role of blue light to induce processes of photoprotection and induction of XC and NPQ, even if the red light sensing was required to develop these processes (Brunet et al., 2014). Other recent studies on diatoms and cryptophytes (Lawrenz & Richardson, 2017) compare the photoacclimation fitness of diatoms (*Skeletonema costatum*) and *Cryptophyceae* (*Rhodomonas salina*) under controlled conditions on light quality and quality in the laboratory. In this work it was found that cryptophytes followed an inverse chromatic adaptation while the diatom species showed a classical strategy of complementary chromatic adaptation (introduced by Engelman in 1883). While the classical chromatic adaptation theory assumes an increase of pigments able to absorb the light to which cells are exposed, the inverse chromatic strategy involves a variation of "pigment quotas en fonction of the absorption characteristics and the efficiency of energy transfer between PSI and PSI" (Bruce et al., 1986; Lawrenz & Richardson,

2017) and “the cryptophytes may regulate blue and green absorbing pigments when exposed to red light helping to balance the excitation energy received by the two photosynthstemss” (Lawrenz & Richardson, 2017).

1.4. Action spectra theory and evolution of multi-spectral photosynthetic data measurements in ecological studies

Previous sections described how phytoplankton absorbs light at different wavelengths that leads to wavelength dependency of absorption capacity, also called absorption spectra. Nevertheless, not all absorbed photons lead to a photochemical light reaction. Absorbed light can be dissipated as heat, fluorescence or other non-photochemical processes (see Havaux et al., 1991; Lavergne & Trissl, 1995). The term which defines the action or effect of different actinic wavelengths on photochemical reactions is named action spectra.

The first action spectra measurement comes from Engelman in 1882 (Drews, 2005; Engelmann, 1882). This first work highlighted the oxygen production and wavelength dependency of photosynthesis based on a qualitative approach. With the help of pieces of macroalgal tissues and a microspectral apparatus, he observed the movement of aerotaxis bacteria towards high oxygen production over the tissue through a gradient of different wavelengths of light. This experiment evidenced that bacteria were commutated in wavelengths of maximum production. In the middle of the 20th century, the techniques of measurements of action spectra were more developed. These advances were of prime importance because they first evidenced relevant discoveries on the physiology of photosynthetic organisms, and second, they allowed setting the basis for the study of light quality effect on primary production of phytoplankton under an ecological context.

Initial surveys focusing on the effect of light quality in the natural field and the implications on phytoplankton primary production started by experimental approaches using filters to simulate different light quality regimes (Jerlov, 1955). The same subject was addressed also with a theoretical model approach (Morel, 1978). In this work, after the comparison of the photosynthetic stored radiant energy (PSE) and the photosynthetic usable radiant energy (PUR) the authors estimated the quantum yield and its variation with the depth. I was deduced that for the calculation of the correct value of PUR, it was necessary to estimate the effective light absorption of phytoplankton that account for the absorption capacity of algae and the light

climate. These studies showed that the values of photosynthetic rate should not be estimated based on laboratory measurements of absorption capacity or surface based light values. *In situ* measurements were required to study the light quality variation effect on primary production estimations. As Lewis et al., (1985b) noticed, there may be a difference between the areal primary production estimated and measured due to the different algae absorption characteristics in relation to the ambient intensity and spectral distribution of light.

The evolution of action spectra measurements include advances in different techniques: carbon assimilation with ^{14}C (Nielsen, 1952) incubations in the so-called spectro-"photosynhetrons" (Lewis et al., 1985b); oxygen evolution by electrode as a proxy of photosynthetic efficiency (Haxo & Blinks, 1950) and fluorescence techniques (Emerson & Lewis, 1942; Neori et al., 1986; after first discover of changes in fluorescence in the 1930's by Kautsky) until the methods of *in vivo* fluorescence analysis (Lorenzen, 1966) and the development of a large number of fluorometers to measure chl a fluorescence rise induced by a specific non-actinic light. In fact, the development of a new type of oxygen electrode by Haxo et al (1950) led to the discovery of the existence of two reaction centers in the photosystem I and II. Oxygen evolution and lately fluorescence measurements allowed to establish the first action spectrum in the laboratory for different phytoplankton and macroalgae species (Haxo & Blinks, 1950; Neori et al., 1986). Nevertheless, initial action spectra measurements on the natural phytoplankton community were achieved lately with the development of the so-called "photosynthetrons" (Lewis and Smith, 1983) based on ^{14}C incubations (Nielsen, 1952) of short time and low volume. The spectro-"Photosynthetrons were 14C incubation chambers with different samples exposed to different light conditions. It is at this moment that natural phytoplankton samples started to be analyzed at different wavelengths simulating light quality variations with depth (Kyewalyanga et al., 2002, 1997; Lewis et al., 1985 a, b ; Schofield et al., 1991).

The spectro-photosynthetrons developed by Lewis in 1985 consisted in a modification from precedent prototypes (Lewis & Smith, 1983) by simulating the vertical gradient of light quality. These systems were composed of 96 bottles with *in situ* natural phytoplankton communities exposed to 12 different wavelengths at 8 different light intensities. Incubation data from such experiments allowed determining the photosynthesis vs. energy (P-E) curves for each spectral band. In these initial studies action spectra were defined by the initial slope of P-E (α or alpha). Measurements were done on the light limited region of P-E curves with assumed linear variation of photosynthesis in function of light. As Lewis et al., (1985b) noticed, estimations of areal primary production would present a higher relative error when the maximum photosynthetic

rate was used rather than the initial slope (Lewis & Smith, 1983; Platt & Jassby, 1976; Lewis et al., 1985b).

In this first measurement of natural phytoplankton community Lewis et al.(1985a) found that α was wavelength dependent. This work also evidenced a particular spectral shape with a variation of the amplitude in function of the chemical characteristics of the sampling area. Moreover, they found that the error in photosynthesis estimates could be 62% of the true *in situ* measurements with a simulated light source (Lewis et al., 1985b). This conclusion was confirmed in posterior C-incubations studies *in situ* with parallel measurements of radiation utilization, attenuation coefficients and phytoplankton specific absorption parameters (Laws et al., 1990; Schofield et al., 1991). The specific spectral print of quantum yield, absorption spectra and action spectra evidenced the capacity to reveal information on physiological characteristics of phytoplankton communities in link with the real *in situ* light climates. More accurate measurements of wavelength dependency of quantum yield were set in perspective to improve primary production estimations with bio-optical calculation models (Platt & Sathyendranath, 1988) in the water column.

Posterior works focused on the study of wavelength dependency of quantum yield by analysis at different narrow bands and combined light colors together (Schofield et al., 1996, 1991, 1990). One study summarized the importance of considering spectral irradiance vs white light estimations (Schofield et al. 1996). The authors compared a hypothetical vertical profile of chl-specific α, obtained from a white light incubation, and an *in situ* light quality incubation. These authors found that the difference of both values was higher in the depth than in the surface where cells are exposed to full spectrum. Moreover, the non-consideration of the spectral light variation with depth would induce a 12 to 49% error on α estimations and consequently also in the quantum yield used in bio-optical models. This error would be reduced by including the information of light absorption capacity of phytoplankton cells. Nowadays, the development of recent spectral fluorometers has allowed to measure photophysiological properties of phytoplankton with a relatively high sampling frequency. It is also possible to measure the absolute light absorption capacity to correct the values -or relative measures of photosynthetic parameters. Such measurements have important implications on the improvement of knowledge in ecological implications of wavelength dependent photoacclimation to light quality in the natural field.

1.5. Methodological overview of variable fluorescence and statistical approaches for multi-spectral photosynthetic data analysis

1.5.1. Variable fluorescence

Since the discovery of the so called Kautsky effect (Kautsky & Hirsch, 1931; revision on Govindje, 1995), variable fluorescence approach has become a largely used technique on the study of primary production thanks to the introduction in aquatic sciences of phytoplankton physiology studies through fluorescence rise in late 1980 (Cullen & Renger, 1979; Vincent, 1981). In this section, we present a general overview of the variable fluorescence principles with a particular focus on the multi-spectral fluorometers for multi spectral photosynthetic data acquisition. This section aims to help the reader to understand the basics of the techniques used in this thesis with a particular focus on multi wavelength fluorometers. Extended details and information can be found on reviews of the subject like for example: Oxborough, 2004; Papageorgiou & Govindjee, 2004; Govindjee, 2009; Suggett et al., 2010.

a) General considerations: definition of fluorescence and description of the principal differences between PAM and FRRf methods

The fluorescence variable techniques are based on the fact that light energy absorbed by a photosystems can be dissipated by three different competing pathways: photochemistry, thermal dissipation and fluorescence emission (Falkowski et al., 1986; Havaux et al., 1991; Kolber & Falkowski, 1993; Lavergne & Trissl, 1995). These techniques are not invasive and describe the photosynthetic activity. The fluorescence yield is correlated with the reaction centers as well as the redox state of the pool of plastoquinone (Schreiber, 1998). Only fluorescence of PSII is detectable at environmental temperatures. The characteristics of the fluorescence induction have been described first by Kautsky in the fluorescence curve induction developed in 1931 and that have been reviewed after that date by Govindje, (1995).

There are different variable fluorescence techniques and/or fluorometers. The Pulse Amplitude Modulation fluorometer (PAM) technique and Fast Repetition Rate Fluorometer (FFRf) (Kolber & Falkowski, 1992; Kolber et al., 1998) that have evolved in parallel; the Fluorescence Induction and Relaxation System (FIRe)(Gorbunov & Falkowski, 2004); or the Pump and probe Fluorometer (PandP)(Falkowski et al., 1986; Mauzerall, 1972) and the Induction Fluorometer/Continuous Excitation Fluorometer (Cosgrove & Borowitzka, 2010).

The PAM and FRRf methods, called active fluorometers, are based on the induction of fluorescence on the fast phase of the Kautsky by the saturation Pulse Method (Bradbury & Baker, 1984) for quantum yield measurements. These methods are based then on the fluorescence variable measurements. The minimal fluorescence (F_0) arrives when all the RCII are open after a dark acclimation (Figure I.8). When the samples have been dark acclimated, after the application of a saturation pulse the fluorescence level is maximal (F_m) and non-photochemical quenching is negligible. This Fm value decreases after illumination with the consequently increase of non-photochemical quenching. The determination of quantum yield and non-photochemical quenching is done from these measures of variable fluorescence which depend strongly on the recent light history and the photochemical efficiency of PSII themselves depending on the initial dark acclimation and the level of oxidation (capacity to accept electrons) of the primary electron acceptor called Quinones (Kromkamp & Forster, 2003). Consequently, differences between the measurements of the two techniques exist and have been described (Kromkamp & Forster, 2003).

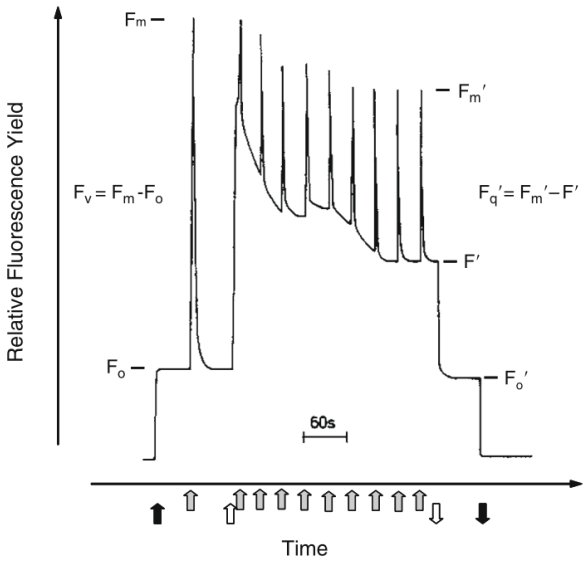

Figure I.8 : Fluorescence induction kinetics and application of the saturation pulse method. Dark arrows indicate measuring light on (up) and off (down). Gray arrows indicate application of short pulse of suturing light and open arrows the activation (Cosgrove & Borowitzka, 2010) modified from (Buchel & Wilhelm, 1993)

Initially, the difference between PAM and FRRf were based on the intensity and duration of the saturating pulse. PAM methods were based on Multi Turnover (MT) while FRRf on Single Turnover (ST). MT techniques were based on the application of a pulse that allowed the

multiple charge separation and reduction of the full all PSII electron acceptors (Q_A, Q_B and the pool of plastoquinone). ST techniques were based on the application of a light flash that only allowed the reduction of plastoquinone Q_A. These techniques have evolved in parallel but nowadays the new generations of fluorometers are equipped with the technical potential to produce MT and ST analysis. The classical light curves can be measured with the PAM and FRRf (for example FRRf ACT2, Chelsea) techniques as well as the functional absorption cross section (MULTI-COLOR-PAM or PhytoPAM (II)(Walz).

On the following section, we will focus on the multi spectral data acquisition. A comparison between the new multi spectral fluorometers will be done with a description of their differences. A focus will be done on the description of MULTI-COLOR-PAM, the instrumentation chosen for this thesis.

b) Multi spectral fluorometers

The development of LED lights has allowed the implementation of multiple techniques of spectral variable fluorescence (Schreiber et al., 2012).

The present work has been realized with the MULTI-COLOR-PAM, a particular device for multi spectral photosynthetic data acquisition. This instrument allows the acquisition of photosynthetic data at five different wavelengths. These five different light colors allow the construction of the so-called spectral print of a sample and carry to the definition of the wavelength dependence of photosynthetic parameters. The wavelengths analyzed are 440, 480, 540, 590 and 625 nm. These wavelengths have been chosen due to their interest for different photosynthetic. 440 nm is the absorption peak of chlorophyll *a*, 480 nm wavelengths are absorbed by carotenoids and chlorophyll *c/b*; 540 and 590 nm are the peak of absorption for phycoerythrin and also fucoxanthin in function of its location in the harvesting pigments complexe (Premvardhan et al., 2009, 2008), and 625 nm for phycocyanin but also the red band of chl c (Bricaud, 2004; Falkowski & Raven, 2007; Johnsen & Sakshaug, 2007)

The term “wavelength dependency” refers to a variation in function of specific wavelengths. In the case of ^{14}C incubations cited in previous sections (Lewis et al., 1985 a, b) these measurements spread over 12 wavelengths covering the visible light spectrum. In the case of MULTI-COLOR-PAM there are 5 analyzed wavelengths. It cannot be considered as a full spectrum and the terminology of wavelength dependency and its derivatives should be

privileged. Nevertheless, and even if the number of measurements is done on a reduced number of wavelengths, MC PAM wavelengths are chosen because of their importance in photosynthetic processes and are considered to give a suitable information whatever the microalgae group studied and its pigmentary composition.

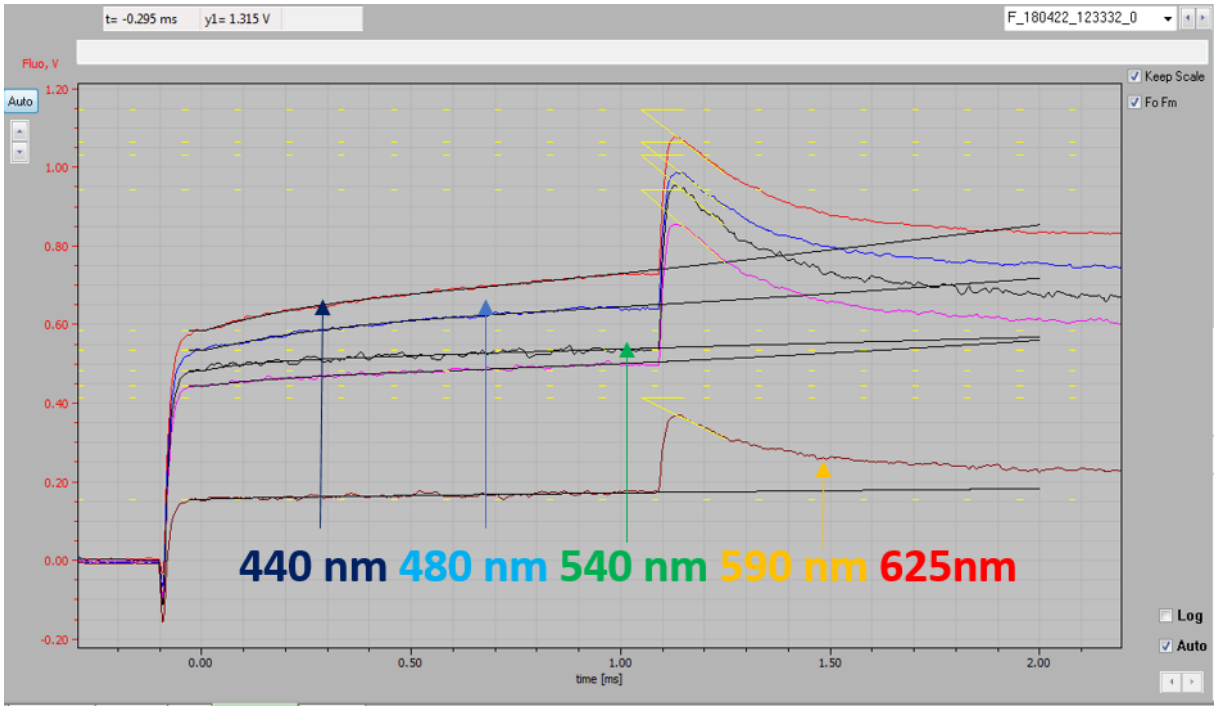

Figure I.9 : Fast kinetics analysis of fluorescence induction for Sigma(II)$_\lambda$ measurement with the triggering file "Sigma100.FMT" on the particular case of a natural phytoplankton community. Figure represent the variation of Fluorescence (in volts, V) in function of time (in ms). Each fluorescence induction curve at each of the the five wavelengths measured with MULTI-COLOR-PAM are indicated in the picture.

MULTI-COLOR-PAM has the potential to use the five different wavelengths for actinic and measuring light (AL and ML respectively) in Rapid Light Curves protocols (RLC with MT technique) as well as fast kinetics of fluorescence induction (with ST technique to measure Sigma(II)$_\lambda$). As described in Schreiber et al 2012, Sigma(II)$_\lambda$ is defined with a dedicated fitting routine controlled with a kinetic trigger file ("Sigma1000.FTM" example in Figure I.9) that allow the analyze of the O-I$_1$ fluorescence kinetics. This triggering includes a saturation single turnover of 50 µs and 1 ms of illumination period with strong actinic light of 5 colors. The functional absorption cross section measured with this technical approach refers to a quasi-dark acclimated sample and therefore, this measure is only valid for this reference state. This particularity sets the difference with the well-known functional absorption cross section from the FRRf methods (Ley & Mauzerall, 1982). Then, the term for functional absorption cross

section that would be used in the present Ph-D thesis is Sigma(II)$_\lambda$ and not σ_{PSII}. This parameter can be associated to the classical optical absorption cross section that describes the absorption capacity of cells unlike the σ_{PSII} which measures the probability to absorb a photon (Figure I.10) (Dubinsky, 1992; Falkowski & Raven, 2007).

A particular protocol of measurement has been developed in this thesis to analyze wavelength dependency in natural phytoplankton communities. Apart from the sample concentration required to get values in the good measurement range, it was necessary to increase to 6 the number of replicates for the Sigma(II)$_\lambda$ determination. The aim was to have a low variability of the measure for each of the 5 wavelengths analyzed. The methodological protocol of measure is described in detail in the results chapter II and III.

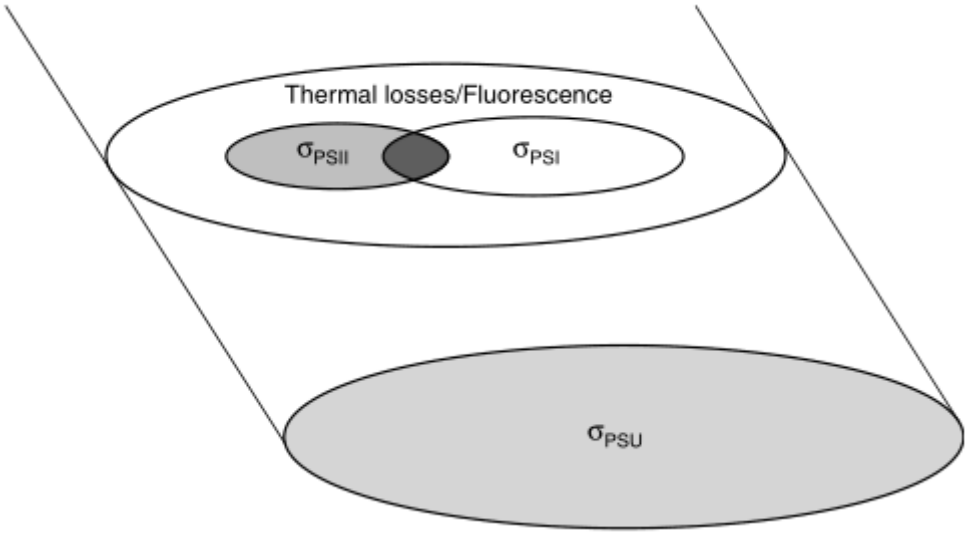

Figure I.10 : Schematic representation of functional absorption cross section (Falkowski & Raven, 2007; Fisher et al., 1989). The large elliptical area is the total energy harvested or PSU, the total light-harvesting area. The ellipses represent the fraction of the absorbed light that leads to photochemical reaction.

Nowadays the MULTI-COLOR-PAM is not the unique multi spectral instrument of variable fluorescence. In the same PAM methods, it can be found the new PhytoPAM(II) (Walz) which also allows the measure at 5 different wavelengths, the fast kinetics and RLC. Nevertheless, this instrument is focused on the measurements of the photosynthetic responses by phytoplankton groups (with a deconvolution algorithm). On the other hand, the new generation of FRRf (Act2 Chelsea) fluorometers present also different wavelengths and the capacity to measure functional absorption cross section and RLC but, apart from the basic differences

between FRRf and PAM methods of fluorescence induction, this instrument does not allow the deconvolution response by single wavelength (protocol are defined for 1, 2 or 3 wavelengths used as measuring light only and simultaneously; actinic light is white). The only study to the date with wavelength dependency analysis with other technical approaches is the work on the new mini-FIRe (Gorbunov et al., 2020). FIRe techniques allow measuring the functional absorption cross section σ_{PSII} but also maximum quantum yield measures. In these recent works developers have focused on a taxonomical approach as the PhytoPAM(II) of Walz and on monitoring programs. Apart from the classical variable fluorescence tools, a new multi wavelength instrument has been developed with open source software of exploitations by the control of Arduino (Hoadley & Warner, 2017). This last work realized on dinoflagellate *Symbiodinium spp*., have also shown the wavelength dependence of PSII absorption capacity and the necessity of measuring spectrally resolved photochemical measurements.

1.5.2. Statistical analysis of multi-spectral data

A specific approach integrating 3 different statistical methods was developed for both spatial and temporal scale studies (chapter II and III in this thesis respectively). This section presents an overview of each statistical method used to analyze multi spectral photosynthetic data. The aim of this methodological section is then to present in detail the steps carried out until the selection of the cascading statistical approach chosen as well as some basis and definitions of the statistical tools used.

a) Mixed effects models

Mixed effects models are characterized by the composition by two different components into the regression model. On one hand, there is a fixed effect (population) and on the other hand the so-called random (individual) effects. Fixed effects refers to the population tendency of the variable, i.e. the mean response for a set of measurements made on different samples. The random effects refers to the variance between the samples (Crawley, 2007). Random effects allow explaining how individuals differ into the population. Mixed models are an important tool in the present study because they allow us to analyze the individual response of each sample and do not consider the individual response as a part of the error but as an individual photoacclimation response. Mixed effects models were already used in precedent ecological

studies (Bolker et al., 2009; Chen, 2015; Duursma et al., 2014; Wang et al., 2018; Zolfaghari & Duguay, 2016).

There are different R packages that contain the functions using mixed effects models. "nlme"(Pinheiro and Bates, 2000), "lme4"(Bates et al., 2019, 2015) or "saemix"(Comets et al., 2019). The most well documented is “nlme” (for linear as well as for generalized and non-linear mixed models). The main difference between "nlme" and "lme4 "(the one used in this study) is that "lme4" uses recent and efficient linear algebra methods, and it includes generalized linear mixed models. Despite the fact that "lme4" is less flexible composing complex variance-covariance structures, it incorporates an implementation of crossed random effects in the way that they become easier and faster to calculate and it offers built-in facilities for likelihood profiling and parametric bootstrapping. Finally, "lme4" package also allows more flexibility for specifying different functions for optimizing over the random-effects variance-covariance parameters. In "lme4" there are any p-value calculations. "lmerTEST" package (Kuznetsova et al., 2019) allows the calculation of the likelihood ratio test by Satterwaite or Kenward-Roger approximations of degree of freedom and it reduces the convergence problems due to for example, the reduced number of data. Thanks to these packages it is also possible to estimate the p-values that are generally used in ecological studies to evaluate the statistical test performed.

b) Partial Triadic Analysis

Partial Triadic Analysis (PTA) (Thioulouse, 1987) is a special multivariate analysis of the so-called "cube-data" formed by different k-tables (Figure I.11) that belongs the family of the STATIS methods (Lavit, 1988). This kind of analysis is largely used in ecology studies to analyze the spatio-temporal variation of different environmental and biological parameters (Bertrand & Maumy-Bertrand, 2010; Mendes et al., 2010; Napoléon et al., 2012). In these studies, the different variables (columns of each k-tables) are measured at different stations (number of k-tables) at different dates (lines from each k-table) and a common spatial structure is analyzed for a stable temporal study. In this work the k-tables were defined by each of the wavelengths to analyze the variation of photosynthetic parameters among samples for each wavelength but also for a common spectral response.

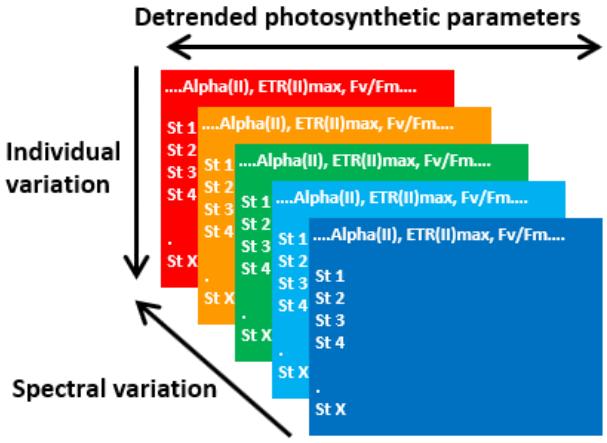

Figure I.11 : Representation of the cube data or k-table. Data for each wavelength analysed define de depthness of the cube data (bright blue, light blue, green, amber and light red table). Each k-table is composed by photosynthetic parameters in columns (detrended photosynthetic data (see chapter II for more details) and values at each sample in the lines (defined here with the labeling "st" followed by the number of the sample from 1 to X total samples).

In the following chapters of results, this specific analysis is used for both spatial and temporal studies. In this section the aim is to help the reader to briefly understand the data preparation and how the PTA is performed in this case. Data must be normed by color and organized in different k-tables. Once the PTA is performed, the results are presented in three different sections: the interstructure, the compromise and the intrastructure. The interstructure describes the relationship between the different k-tables. In this study the interstructure gives information of the relation or connection between wavelengths for all photosynthetic parameters and considering each sample unit. The compromise represents the common structure among wavelengths and allows us to summarize the general photosynthetic relation among the photosynthetic parameters. Finally, the intrastructure represents the differences to the compromise for each wavelength that define the k-tables. Therefore, intrastructure allows us to analyze the spectral responses for each sample.

1.6. General glossary

In this thesis it have been used several terms related to photosynthesis and photoacclimation concepts. In this glossary the reader will find a compililation of some terms related to light quality that are emploied in the following chapters. The terms presented here are used and described in the following sections and summarized here in (Table I.I). This glossary contains as well synonym terminology in relation to the action spectra theory or the MULTI-COLOR-PAM method used here that can be found in other works. The aim of this glossary is to allow the reader to have the standard nomenclature used in this research domain to better understand this work.

Table I.I : General glossary related to wavelength dependency of photosynthesis theory, photoacclimation and light quality terminology

Terminology	Synonyms	Definition
Spectrum and spectra		A band or a range of wavelengths for light. Here between 440 and 700 nm for PAR and visible light.
Wavelength	Light color Waveband Narrow band (in opposition to broad band) Spectral band	In this thesis wavelength color refers to each of the different wavelength analyzed with the MULTI-COLOR-PAM but these wavelengths (terminology used as well as technical report of Schreiber et al., 2011 and 2012) refers originally to a very narrow band
Wavelength-dependency	Spectral shape Spectral print Spectrally dependent	Significant variation of a biological parameter in function of wavelength
Action spectra		Wavelength dependency of photochemical reaction, through alpha measurements
Absorption spectra	a* ,absorption coefficient	Absorption capacity along the full spectrum of PAR

Optical absorption cross section	σPSU	Objective measurement of a molecule to absorb light at a given wavelength Absorption measurements with a spectrofluorometer.
Functional absorption cross section	Effective absorption cross section σPSII	Probability of a photon to be absorbed in PSII. i.e.,"size" of the photochemical target
Sigma(II)$_\lambda$ (Schreiber et al., 2012)		Wavelength dependent absorption cross section of PSII. Measurement at "referent" dark acclimated state independent of Chl a content
Chromatic adaptation or acclimation		Changes on quantum yield due to different spectral grown conditions, i.e different dominant wavelength color or narrow band pic (Kroon et al., 1993; Schofield et al., 1996). Implies Variation of pigment composition. It is also frequently associated with the vertical zonation of phytoplankton species (Hickman et al., 2009) and macroalgae (Kirk, 2011)
Enhanced light		Sum of colors of light in opposition to monochromatic or unenhanced light.
Photoregulation		Rapid tune of photosynthetic efficiency and increase of Non photochemical quenching. It is associated with a rapid cycle of xanthophylls (Brunet et al., 2011).

Photoacclimation	Ontogenetic adaptations (Kirk, 2011)	Phenotypic variations of macromolecular composition (pigments ratio and concentration, PSII/PSII, PSU units and RuBisCO as well as variations in α and ETR_{max} of Light responses curves
Photoadaptation	Phylogenetic adaptation (Kirk, 2011)	Changes in the genetic make-up of different species (Falkowski & LaRoche, 1991; Raven & Geider, 2003)
Photoprotection		Physiological state under high light conditions (with energy regulation and/or novo synthesis of photosynthetic pigments related to photoprotection: photoprotective carotenoids and/or xanthophylls.
PET_{λ}	Photosynthetic electron transport	Capacity of transport of electrons through the photosynthetic chain. This Capacity assessed by the photosynthetic parameters derived from light curves and together with non photochemical quenching and absorption capacity, it defines the photosynthetic status of cells

Light quality variations		Variation of the spectral properties of light. It is expressed by the variation of a color band (previously defined) or the ratio between different colors. Here the variations of light quality are defined for three spectrum bands of interest for photosynthesis (i.e. B for blue, G for green and R for red) which were obtained via quantum integration of spectral bands (410-490, 480-580 and 600-700 nm, respectively) and the variation of their ratio: R/B, G/R and G/B
Light climate	Light quantity and quality variations	Light quantity and quality variations in natural field

II. Wavelength dependence of microalgae photosynthetic parameters and functional absorption cross section of PSII in a temperate coastal sea

Wavelength dependence of microalgae photosynthetic parameters and underwater light climate in temperate sea

Michel-Rodriguez[1] M., Lefebvre[1] S., Courvoisier[2] M., Merieux[3] X. and Lizon[1] F.

Univ. Lille[1], CNRS[2], Univ. Littoral Côte d'Opale[3], UMR 8187 LOG, Laboratoire d'Océanologie et de Géosciences, Station Marine de Wimereux, 28 Avenue Foch, 62930 Wimereux, France

Submitted to PeerJ journal December 23th (accepted with minor revisions)

Abstract

Studying how natural phytoplankton adjust their photosynthetic properties to the quantity and quality of underwater light (i.e. light climate) is essential to understand primary production. A wavelength-dependent photoacclimation strategy was assessed using a multi-color pulse-amplitude-modulation chlorophyll fluorometer for phytoplankton samples collected in the spring at 19 locations across the English Channel. The functional absorption cross section of photosystem II, photosynthetic electron transport (PET_λ) parameters and non-photochemical quenching were analyzed using an original approach with a sequence of three statistical analyses. Linear mixed-effects models using wavelength as a longitudinal variable were first applied to distinguish the fixed effect of the population from the random effect of individuals. Population and individual trends of wavelength-dependent PET_λ parameters were consistent with photosynthesis and photoacclimation theories. The natural phytoplankton communities studied were in a photoprotective state for blue wavelengths, but not for other wavelengths (green, amber and light red). Population-detrended PET_λ values were then used in multivariate analyses (partial triadic analysis and redundancy analysis) to study ecological implications of PET_λ dynamics among water masses. Two wavelength ratios based on the microalgae saturation parameter E_k (in relative and absolute units), related to the hydrodynamic regime and underwater light climate, clearly confirmed the physiological state of microalgae. They also illustrate more accurately that natural phytoplankton communities can implement photoacclimation processes that are influenced by *in situ* light quality during the daylight cycle in temporarily and weakly stratified water. Ecological implications and consequences of PET_λ are discussed in the context of turbulent coastal ecosystems.

2.1. Introduction

In nature, phytoplankton must respond to multiple variations in the quantity and quality of light (i.e. light climate) at different temporal (from day to year) and spatial (from environmental coastal gradients to large hydrological structures) scales (MacIntyre et al., 2000; Dubinsky & Schofield, 2010). It is well known that microalgae have a strong ability to photoregulate, photoacclimate and photoadapt to these variations, as demonstrated by many articles and reviews (e.g. Anning et al., 2000; Dubinsky & Stambler, 2009). Kirk (2011) reviewed these photobiological processes and defined them as ecological strategies, highlighting the role of the light climate. Microalgae adapt to variability in the light climate through phylogenetic adaptations and ontogenetic acclimation. Evidence of phylogenetic adaptation has existed since Engelmann (1883) developed chromatic adaptation theory and has experienced some controversy (e.g. Bidigare et al., 1990; Falkowski & LaRoche, 1991). Pigment composition and thus cell absorption spectra, which determine light-use efficiency, have evolved to match the spectral characteristics of the prevailing light in a water mass. Ontogenetic acclimation in response to light conditions at the time of cell growth and development may modify a species' pigment composition and photosynthetic functioning, thus significantly influencing wavelength-dependent light absorption. Physiological state and photosynthetic properties of phytoplankton can be studied by using photosynthetic light-response (P-E) curves to estimate photosynthetic activity as light levels increase (Jassby & Platt, 1976). Light-use efficiency (initial slope, α) and maximum photosynthetic rate (ρmax) parameters of P-E curves are the two main parameters traditionally used to investigate biophysical, biochemical and metabolic processes that influence photosynthesis (MacIntyre et al., 2002; Falkowski & Raven, 2007) in response to variations in the light climate. Understanding better the response of cells to potential light stress in surface water also requires studying the distribution of light energy between the photochemical and non-photochemical pathways, which includes thermal dissipation of excess absorbed light energy (Lavaud, 2007). These processes are well documented for diatoms (Brunet & Lavaud, 2010) and can be studied easily by quantifying the light response (E) of non-photochemical quenching (NPQ, Serôdio & Lavaud, 2011).

Measuring the light absorption capacity of microalgae is essential to estimate the survival and production capacity of cells, and for ecologists to assess photosynthetic activity and primary production. To this end, a new generation of commercial fluorometers (e.g. multi-color pulse-amplitude-modulation (PAM) chlorophyll fluorometer (Heinz Walz GmbH, Germany), mini-

FIRe (Gorbunov et al., 2020) has been designed to study wavelength dependence of photosynthetic electron transport (PET_λ) in relation to the light absorption capacity and/or to focus on general photosynthetic activity of phytoplankton groups in a given ecosystem (e.g. a fast repetition rate fluorometer (Chelsea Technologies Group Ltd., United Kingdom), FFL-40 (Photon Systems Instruments, Czech Republic). In limnology and oceanography, nearly all studies that included in vivo chlorophyll *a* (Chla) variable fluorescence have measured direct light absorption capacity and photosynthesis for only one color of light. In most PAM techniques blue and red wavelengths (±470 and 650 nm) were typically used for measuring lights. In most recent FRR studies, blue wavelength (±450 nm) were typically used for measuring because it is one of the main spectral bands absorbed by Chla (400-500 nm), the most common and abundant photosynthetic pigment, and the dominant color in the marine environment (Schreiber et al., 2012). One exception is the recent study of Houliez et al., (2017), who performed the first *in situ* measurements of light absorption capacity and photosynthetic yield with blue (458 nm) and amber (593 nm) lights in the Baltic Sea. However, since it focused on the specific problem of measuring fluorescence rise in cyanobacteria, its results cannot be generalized to other phytoplankton groups.

Many studies have shown that pigment absorbance by microalgae is strongly correlated with the spectral transmittance of water and its components (Hickman et al., 2010; Lawrenz & Richardson, 2017). Colored dissolved organic matter (CDOM) and suspended particle concentrations can dramatically change the quantity and, especially, quality of light in coastal water (Kirk, 2011). To help Chla absorb light energy at different wavelengths, microalgae have a variety of accessory pigments. For example, the ecological success of diatoms is due to their pigment signature (Falkowski & Knoll, 2007), which includes Chla, Chlc and fucoxanthin (which expand the spectral absorption band to 580 nm), along with β-carotene and the xanthophylls involved in photoprotection (Brunet & Lavaud, 2010; Jeffrey et al., 2011). This diversity of pigments enables brown algae, such as diatoms, to be more effective than green or red algae (Lavaud, 2007) in many systemsin turbulent systems or in the mixed layer of the coastal ocean. However, the photosynthetic apparatus can acclimate to variations in light climate by changing cell pigment concentrations and/or ratios (MacIntyre et al., 2002). This can change the shape of the light-absorption spectrum and influence the efficiency of photosynthesis (Barlow et al., 2013, 2017). When light decreases, pigment concentrations usually increase in cells during growth, with or without wavelength-dependent changes in light absorption (Falkowski & LaRoche, 1991). In addition, pigment concentration can also increase

due to an increase in the size and/or number of photosynthetic units (i.e. antennas containing light-harvesting pigments) (Dubinsky & Stambler, 2009) depending on the phytoplankton group and ecosystem. Under high light conditions, cells increase the reaction center number with a smaller antenna size, inducing higher values of ρ_{max}. On the opposite, under low light conditions, cells increase their antenna size, inducing higher values of α. However, light harvesting by cells is not always correlated with pigment concentration due to mutual shading of the increasing density of pigment molecules, i.e. the "package effect" (Bidigare et al., 1990).

In response to changes in light color, an effective photoacclimation mechanism was observed in cyanobacteria that involves regulating "complementary chromatic adaptation" (CCA) (Kehoe & Gutu, 2006). CCA involves strong restructuring of photosynthetic antennas through pigment concentrations, including pigment-binding antenna proteins. Diatoms have fewer flexible binding proteins, such as fucoxanthin-chlorophyll *a/c*-binding antenna pigment-proteins complexe (FCPs), than cyanobacteria with which to perform classic CCA; however, diatom fucoxanthin may have different positions in the light-harvesting complex proteins of the antenna, which provide different levels of energy transfer as a function of light quality (Premvardhan et al., 2008). Through pigment analyses, Brunet et al., (2014) showed that spectral composition strongly influences the balance between light harvesting and photoprotective capacity of diatoms. Valle et al., (2014) and Schellenberger Costa et al., (2013a) observed that the energy transfer efficiency of light-harvesting pigments is wavelength-dependent and that diatoms' ability to activate photoprotection and repair a photodamaged photosystem II (PSII) effectively depends on light quality. Orefice et al., (2016) observed that variations in the light spectrum change the photophysiology and biochemistry of diatom cells. Many other wavelength-dependent responses of cyanobacteria and eukaryotic phytoplankton have been observed, especially in laboratory studies of cultures (Schreiber & Klughammer, 2013; Szabó et al., 2014a,b; Herbstová et al., 2015; Lawrenz & Richardson, 2017; Luimstra et al., 2018, 2020). Most field studies of wavelength-dependent acclimation focused on relationships between accessory pigments, the shape of phytoplankton absorption spectra and the underwater light climate (Hickman et al., 2009; Barlow et al., 2017), but few measured photosynthetic parameters at different wavelengths. Some early studies used the carbon absorption technique and determined α (in multispectral incubators), whose spectral correction through the water column and/or between different water masses has been studied intensively (Lewis et al., 1985 a,b; Kyewalyanga et al., 1992, 1997, 2002).

In the present study, we focused on wavelength-dependent parameters: α, ETR_{max}, E_k, non-photochemical quenching (NPQ) and light absorption capacity from 440-625 nm for different natural phytoplankton communities sampled across environmental gradients of a coastal sea. A specifically dedicated device − the multiple excitation wavelength chlorophyll fluorescence analyzer (MULTI-COLOR-PAM, Heinz Walz, Germany) − was used in its full capacity for the first time in a field study. α, ETR_{max}, E_k and E_{op} parameters were determined from PE measurements at five wavelengths as a function of the functional absorption cross section of PSII and NPQ for 19 locations sampled across the English Channel (EC). The EC is an epicontinental sea that is particularly suitable for studying photoacclimation strategies of microalgae, since its ecosystem has many environmental gradients between coastal and offshore water due to freshwater runoff and high tidal currents (Brunet et al., 1992; Brylinski et al., 1991). This area is dominated by diatoms and the *Haptophyceae Phaeocystis globosa* during the spring bloom (Breton et al., 2006; Houliez et al., 2013b, 2013a). The wavelength dependence of light absorption capacity is related to the composition of PSII antenna pigments, which changes in natural samples depending on phytoplankton community structure and specific photoacclimation processes in a given light climate. Therefore, we tested the hypothesis that phytoplankton PET_λ change in shape and level along environmental gradients of light quantity and/or quality and phytoplankton community structure (Figure II.1).

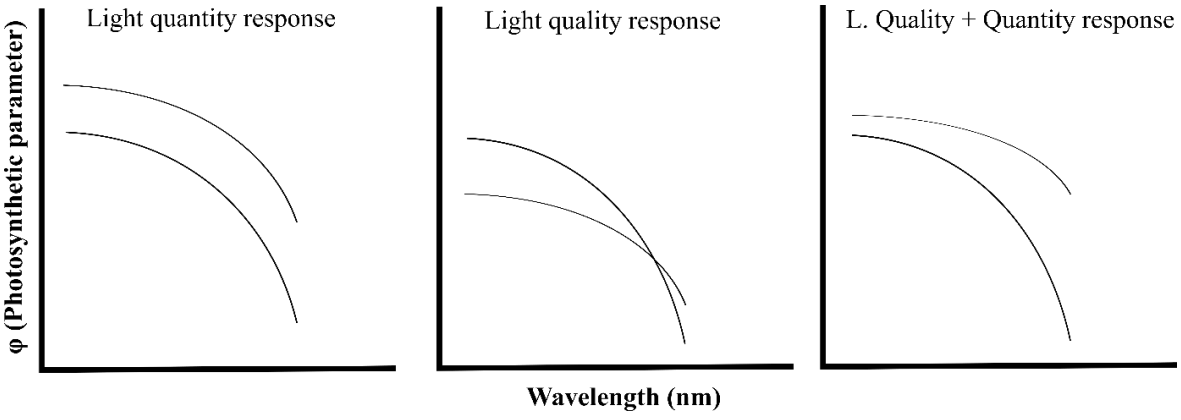

Figure II.1 : Conceptual diagram illustrating the hypothesis of photosynthetic parameter variation in function of wavelength under two contrasted and hypothetic light climate conditions (from the left to the right: light quantity variation, light quality variation and combined quality and quantity variation). The trend and shape of spectral variation aims to be an illustration and do not represent an expecific result of any photosynthetic parameters.

The specific questions investigated in this study lay in three categories:

- Are the photosynthesis responses by wavelength observed consistent with theories on photosynthesis and photoacclimation? Are there trends in the spectral signature of each PET_{λ} parameter?
- Are spectral photosynthesis responses consistent with environmental conditions? Which abiotic and abiotic variables best explain the physiological state of phytoplankton?
- What are the ecological implications of wavelength dependence and plasticity of PET_{λ} parameters?

To address these issues, an original analytical approach was developed that used three sequential statistical analyses: linear mixed-effects models, partial triadic analysis and redundancy analysis.

2.2. Materials and methods

2.2.1. Sampling area and strategy

Data were collected during a combined sampling campaign of the JERICO-NEXT program and the 2018 ECOPEL cruise in the EC, from the Strait of Dover (50°58.7' N, 1°36.64' E) to Brest (48°20.59' N, 5°25.03' W) from 18 April to 2 May 2018 (Figure II.2). Water was sampled at 19 locations at a depth of 2 m from inshore to offshore water (using a 20 L Niskin bottle) at different times of day. This zigzag sampling strategy was chosen to consider hydrobiological gradients between coastal/offshore and east/west waters (Vantrepotte et al., 2007b, 2012). To characterize the sampling hour, which can influence phytoplankton physiology, we calculated the number of hours that had elapsed since sunrise, which represents the recent light history of cells (i.e. time since sunrise named as TSS). The EC is an epicontinental macrotidal temperate system with strong hydrodynamics and substantial river inputs, which provide contrasting light climates that are useful for testing the wavelength-dependence hypothesis of photosynthesis in natural phytoplankton communities. The water bodies sampled were thus used to experiment with different light climates along environmental gradients and with changes in phytoplankton community structure.

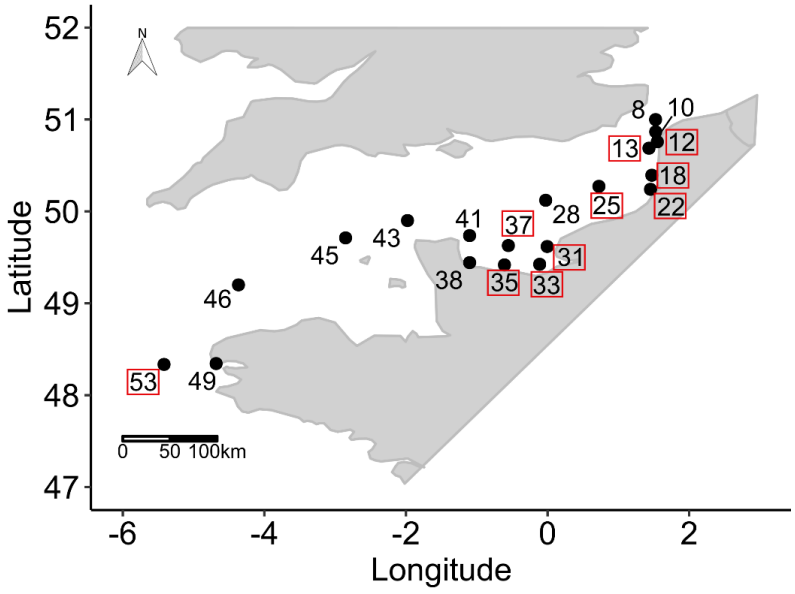

Figure II.2 : Sampling locations (n=19 among 55 locations sampled) for the study of phytoplankton wavelength dependence in the English Channel during the ECOPEL campaign in April 2018. The framed station numbers refer to thermal and haline stratified water columns.

2.2.2. Controlling variables of photosynthesis

Two types of variables that could control photosynthesis were analyzed as ex-situ experimental conditions under which the communities grew: i) abiotic variables and ii) biotic variables that describe the phytoplankton community structure.

a) Abiotic variables: Hydrological and light measurements

At each location, conductivity-temperature-depth (CTD) casts were conducted using a SBE25 CTD (Sea-Bird Scientific, USA). Water samples were filtered through a microfiber filter (Whatman GF/C or GF/F), and aliquots were then stored at -20°C until further processing for dissolved inorganic nutrient concentrations. Concentrations of dissolved inorganic nitrogen (DIN i.e. NO_3+NO_2), phosphate (PO_4), and silicate ($Si(OH)_4$) were measured with an Integral Futura Autoanalyzer II (Alliance Instruments) according to the method of Aminot et Kérouel (2004).

Underwater spectra were measured with a spectroradiometer RAMSES ACC-VIS hyperspectral radiometer (TriOS GmbH, Germany) throughout the euphotic layer, but the present study considered only spectroradiometer measurements at the surface to 2.5 m depth. Spectroradiometer measurements were made in triplicate (on all spectrum) in the water column, every 50 cm, from the depth where the sensor was not discovered by the waves.

Spectroradiometer measurements were made in triplicate (on all spectrum) in the water column, every 50 cm from the depth where the sensor was not discovered by the waves. The photon fluence rate was measured every 3 nm from 400-700 nm. Three spectrum bands of interest for photosynthesis (i.e. blue (B), green (G) and red (R)) were obtained via quantum integration of spectral bands (410-490, 480-580 and 600-700 nm, respectively). These spectral bands, expressed in µmol-photons.m^{-2}.s^{-1}, were chosen according to the study of Brunet et al., (2014). Intensity ratios for three pairs of spectral bands were then calculated (i.e. R/B, G/B and G/R) and used as light-quality ratios that depended on the overall chemical and biological characteristics of the waters sampled (Jaubert et al., 2017). Finally, averages of these ratios were calculated for replicates of the same depth and over a depth interval ranging between the first depth where it was possible to perform a measurement and the depth of 2.5 m. Depth profiles of photosynthetically active radiation (PAR; 400-700 nm) were obtained using a PAR quantameter (LI-193 4pi steradians from Biospherical Intruments Inc., USA) connected to the CTD. Vertical diffuse attenuation coefficients for PAR were calculated as follows:

$$K_{d(PAR)} = \frac{ln\,(I_0) - ln\,(I_z)}{z} \qquad (1)$$

where $K_{d(PAR)}$ is the downwelling diffuse attenuation coefficient of underwater light, and I_0 and I_z are photon fluence rates (µmol photons.m^{-2}.s^{-1}) at the surface and depth z (m), respectively (Kirk, 2011).

The depth of the euphotic layer (Z_{eu}), defined as the depth at which light intensity equals 1% of that at the surface, was then calculated (Eq. 2) for each location according to (Kirk, 2011):

$$Z_{eu} = \frac{4.6}{K_{d(PAR)}} \qquad (2)$$

Vertically averaged light intensity (E_{avg}) in the mixed layer was calculated (Eq. 3) according to Riley (1957):

$$E_{avg} = \frac{I_0\left(1 - e^{(-K_{d(PAR)} x Z_{uml})}\right)}{K_{d(PAR)} x Z_{uml}} \qquad (3)$$

The depth of the upper mixed layer (Z_{uml}) was defined from the CTD profiles using vertical density gradients, caused by vertical temperature and salinity gradients, according to (Van

Leeuwen et al., 2015). The water column was considered to be stratified if the difference in density between the surface layer (0-1.5 m below the surface) and the bottom layer exceeded 0.086 $kg.m^{-3}$, which corresponded to a difference of 0.5°C or 0.11 PSU for waters at 10°C and 34.5 PSU (Lowe et al., 2009). Thus, Z_{uml} is the depth of the water column without stratification. This approach allowed us to consider that water columns in the EC, which are usually considered to be mixed, may be occasionally stratified and thus influence phytoplankton physiology (Van Leeuwen et al., 2015). Finally, we calculated the ratio Z_{eu}/Z_{uml} for each sampling location as a measure of light availability in water, one of the key factors in phytoplankton photoacclimation (Jensen et al., 1994; Wang et al., 2011).

b) Biotic variables: phytoplankton groups, biomass and sample preparation

The FluoroProbe sensor (a multi-wavelength fluorometer, bbe Moldaenke GmbH, Germany) was used to estimate the composition of natural phytoplankton communities, as in several other studies (Houliez et al., 2013a, 2013b; Kring et al., 2014; Houliez et al., 2015). The FluoroProbe distinguished four groups of microalgae in vivo and instantaneously: i) diatoms plus dinoflagellates (i.e. "brown algae"); ii) *Haptophyceae*, concretely *Phaeocystis globosa* in the eastern EC (Houliez et al., 2012a); iii) *Cryptophyceae* and iv) *Cyanophyceae.* The biomass of each group was estimated as an equivalent concentration of Chla ($\mu g.L^{-1}$). See Beutler et al., 2002) for more details about the FluoroProbe. For all photosynthetic parameters parameters, phytoplankton samples were concentrated using a nylon phytoplankton net with a 20 µm mesh and 30 cm diameter (Aqatic Research Instrument, USA) and then kept in the dark under temperature-controlled conditions at temperature close to the water sampled and in air-conditioned laboratory before measuring photosynthesis. To measure photosynthesis accurately, the phytoplankton were concentrated to ensure that all samples had the same range of Chla concentration (ca. 100 $\mu g.L^{-1}$). Phytoplankton biomass in each group was estimated with the FluoroProbe before and after concentrating it. Since sampling with a net can change the structure of the original community, we considered the experimental conditions as ex situ. Regardless of the original structure of the natural communities sampled, concentrated samples responses were the focus of this study.

2.2.3. Wavelength-dependent photosynthesis parameters and functional absorption cross section of PSII

Wavelength-dependent PET_λ was studied using the MULTI-COLOR-PAM, which is particularly suitable for studying the PET_λ of phytoplankton (Schreiber et al., 2012; Szabó et al., 2014a). It provides pulse-modulated measuring light, continuous actinic light, single-turnover light pulses and multiple-turnover or saturation pulses with peak wavelengths at 440, 480, 540, 590 and 625 nm (i.e. bright blue, light blue, green, amber and light red, respectively). See Schreiber et al. (2012) for a full description.

Before measuring PET_λ, samples were first dark-acclimated for 2.5 h (a compromise between the analyses and sampling strategy), without far red exposure (that would blocked the device for too long for the many measurements required). The time of dark acclimation aims to optimize the maximum quantum yield of PSII measurements and neutralize the recent light history of cells (sampled in water columns of different depths and optical properties). It has been shown that there is not an universal protocol and the time required can exceed the classically considered time of 30 minutes and, in certain circumstances, periods of more than 2 hours are necessary (From et al., 2014). First, each dark acclimated sample was homogenized within an optical quarz cuvette with a magnetic stirrer then the light sensor US-SQS/WB Spherical Micro Quantum Sensor (Heinz Walz, Germany) was placed into the center of the cuvette to measure the photon flux density at each wavelength. This step provided the "PAR-list" file for each sample, which was used for all later measurements of that sample. Water samples filtered at 0.2 µm were used to determine the zero offset (i.e. the background signal to subtract from the total fluorescence signal at each wavelength). Next, a subsample of each dark acclimated sample was placed in a 2.5 mL cuvette with a 1 cm path length to adjust the measuring light and gain settings to it in order to obtain the same current fluorescence (F) level of 0.5 ± 0.05 (relative units) for all wavelengths and to get a good signal-noise ratio. This last step was used to compare fluorescence-rise kinetics (Szabó et al., 2014a).

Then, fast kinetic photosynthesis was measured to determine the wavelength-dependent functional absorption cross section of PSII (i.e. $Sigma(II)_\lambda$) by measuring $O\text{-}I_1$ fluorescence-rise kinetics repeatedly, as described by Schreiber et al. (2012). $Sigma(II)_\lambda$ was estimated using the pre-programmed fast kinetic trigger file "Sigma1000.FTM", in the same way as Szabó et al., (2014a, b) and Schreiber & Klighammer dit. In this phase of fast fluorescence, "O" was minimal fluorescence yield corresponding to all PSII reaction centers open. The full closure of

PSII reaction centers during a standard 1 ms long actinic illumination period was then induced and the corresponding fluorescence level was determined (I_1-level). Sigma(II)$_\lambda$ was calculated according to Schreiber et al. (2012) as:

$$Sigma(II)_\lambda = \frac{1}{\tau * L * PAR} \quad (4)$$

where τ is the time constant of light driven Q_A reduction (ms) determined from the fast fluorescence kinetics measurements, L the Avogadro's constant (6.022.1023 quanta.(mol photons)$^{-1}$), and PAR is the photon flux of the light driving the O–I_1 fluorescence rise.

Sigma(II)$_\lambda$ was calculated by the user software interface (PAM-Win-3, Heinz Walz) based on the fitted value of the time constant Tau (i.e. that of Q_A-reduction during the O-I_1 rise) obtained from three consecutive measurements separated by 10-s dark intervals, according to Klughammer & Schreiber (2015). Following this method, the estimate of Sigma(II)$_\lambda$ is independent of Chla concentration. Sigma(II)$_\lambda$ was determined from six subsamples to estimate the mean and variance of each natural community accurately (Figure II.3).

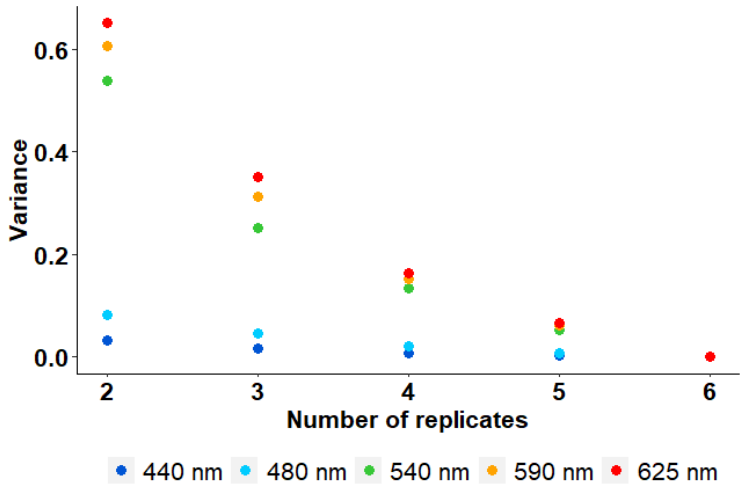

Figure II.3 : Variance of the functional absorption cross section of photosystem II (Sigma(II)$_\lambda$) by wavelength as a function of the number of replicates. See Schreiber et al. (2012) for more details about Sigma(II)$_\lambda$ and protocol measurements with the MULTI-COLOR-PAM (Heinz Walz GmbH, Germany)

Next, automated rapid light curves (RLC) of the PET$_\lambda$ were determined in triplicate (i.e. three independent samples) at each of the five wavelengths. For each RLC, samples were exposed to 14 actinic increasing light intensity levels, each 20 s long, as defined in the PAR-list file for each sample and wavelength. Hereafter, “PAR” refers to the photon flux measured at each

wavelength, and the same wavelength was always used for the measuring light and actinic light. Saturation pulse settings were defined at a width of 300 µs. The effective quantum yield of PSII (Y(II)) was calculated at each step (Eq. 5). An initial step at 0 µmol photons.m^{-2}.s^{-1} was used to determine the maximum Y(II) (F_v/F_m) for samples acclimated to the dark for a long period (2.5 h) (Eq. 6). The relative electron transport rate (r.ETR) was then determined using Y(II), the PAR intensity of the corresponding wavelength (from the PAR-list file) and an arbitrary factor of 0.5 to indicate that PSI and PSII absorb light equally (Eq. 7). The wavelength-dependent absolute electron transport rate of PSII (ETR(II)) was then calculated from $Sigma(II)_\lambda$ (nm^{-2}), Avogadro's number (L, $6.022.10^{23}$ quanta (mol $photons^{-1}$)) and the PAR intensity at each wavelength (Eq. 8 and 9).

$$Y(II) = \frac{F'_m - F}{F'_m} \quad (5)$$

$$\frac{F_v}{F_m} = \frac{(F'_m - F_0)}{F'_m} \quad (6)$$

$$rETR = Y(II)\ x\ PAR\ x\ 0.5 \quad (7)$$

$$PAR(II) = Sigma(II)_\lambda\ x\ L\ x\ PAR \quad (8)$$

$$ETR(II) = PAR(II)x\left(\frac{Y(II)}{\frac{F_v}{F_m}}\right) \quad (9)$$

NPQ was calculated as the normalized Stern-Volmer quenching coefficient (Eq. 10), according to Bilger & Björkman (1990):

$$NPQ = \frac{F_m}{F'_m} - 1 \quad (10)$$

All photosynthetic parameters were obtained in triplicate for the five wavelengths of MULTI-COLOR-PAM for each sample.

The Eilers and Peeters (1988) model was used to fit r.ETR vs. PAR and ETR(II) vs. PAR(II) curves to estimate three photosynthetic parameters for each wavelength: light-use efficiency (i.e. α, the initial slope of the ETR vs. PAR curve), the maximum electron transport rate (ETR_{max})) and the optimum light parameter (E_{op}) in relative (r) and absolute (II) units. The light

saturation parameter (E_k) was also calculated in the two units as $E_k = ETR_{max}/\alpha$ (Talling, 1957). To estimate the degree of photoacclimation of the phytoplankton communities, the $E_{k,440}/E_{avg}$ ratio in Z_{uml} at sampling was calculated for each location. The E_k ratios (in relative and absolute units) of three pairs of wavelengths (625/440, 540/440 and 540/625 nm) were calculated in the same way as the three pairs of *in situ* spectral bands (i.e. R/B, G/B and G/R measured at a depth of 2.5 m).

The Michaelis-Menten (1913) model was used to fit NPQ vs. PAR curves. A linear regression that forced the intercept to zero was used when the kinetics of these curves differed from the Michaelis-Menten model. Since two models were used, NPQ values were back-calculated using the calibrated models at two irradiances (of P-E curves) for each wavelength: low PAR (300 µmol photons.m^{-2}.s^{-1}) and, for saturating conditions, high PAR (1200 µmol photons.m^{-2}.s^{-1}), according to Szabó et al. (2014).

All P-E curves were fitted using the "fitEP" function of the "phytotools" package of R software specifically designed to fit phytoplankton photosynthesis curves using simulated annealing (Silsbe & Malkin, 2015). The curves for r.ETR vs. PAR, ETR(II) vs. PAR(II) and NPQ vs. PAR were fitted for the three aggregated replicates, and all photosynthetic parameters were obtained at each of the five wavelengths.

2.2.4. Statistical analyses

All statistical analyses were performed with R version 3.6.0 (R Core Team, 2020). For abiotic variables, the expectation-maximization with bootstrapping algorithm of Amelia II (Honaker et al., 2011) was used to determine missing values (n=2) of light quality data. Principal component analysis (PCA) (Legendre & Legendre, 2012) of abiotic and biotic variables was performed using the "PCA" function of the "FactoMineR" package (Husson et al., 2020) to determine the internal structure of locations that best explained the variance in teach datasets.

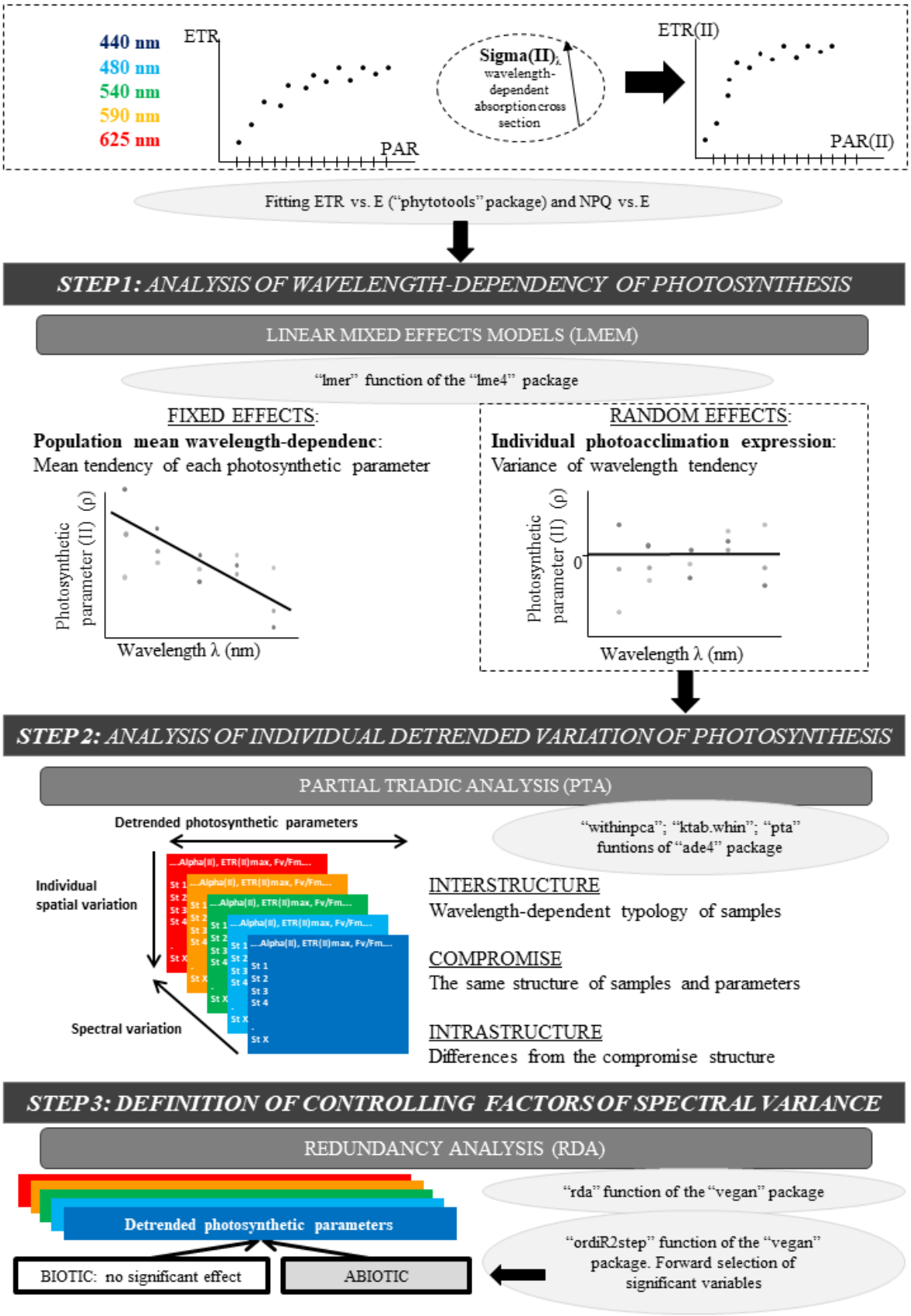

Figure II.4 : Diagram of the three-step numerical method used after fitting the electron transport rate (ETR) vs. photosynthetically active radiation (PAR) curve: linear mixed-effects models, Partial Triadic Analysis and Redundancy Analysis.

Statistical analysis of photosynthetic parameters followed a three-step approach (Figure II.4). First, wavelength dependence of each parameter was analyzed using a linear mixed-effects model (LMEM). Mixed-effects models are commonly used to fit regressions to repeated (i.e. longitudinal) measures (over time and/or space) by separating the variance explained by the main effects from that explained by random sampling, while considering the wavelength dependence of individuals. The most parsimonious model was linear, and higher-degree polynomials were not significant. LMEMs (Bates et al., 2015; Zuur, 2009) were thus used to analyze the population trend across wavelengths for each parameter. LMEMs were fitted using the "lmer" function of the "lmer4" package (Bates et al., 2019). Random effects, defined as differences of the locations from the population trend (intercepts and slopes), were used to study individual photoacclimation processes. Wavelengths from 440-625 nm were transposed to 0-185 nm to decrease uncertainty in the model intercept. Hypothesis tests were based on t-tests (for the intercept and slope of fixed effects) and likelihood-ratio tests based on the χ^2 null hypothesis (for random effects) (Pinheiro and Bates, 2000).

Second, each wavelength-dependent photosynthetic parameter was detrended by calculating individual differences from the population trend (from LMEMs) and then used in partial triadic analysis (PTA) (Thioulouse, 1987). PTA analyzes several two-way tables simultaneously (i.e. K-tables method). Five tables (one per wavelength) that contained 8 photosynthetic parameters (in columns) and 18 locations (in rows) were analyzed. Before analysis, all parameter values were centered and reduced based on their overall ranges from all tables. PTA identifies structures that are the same in all tables and assesses their stability among wavelengths. PTA was performed using the "pta" function of the "ade4" package (Dray et al., 2015), and related graphics were created with the “adegraphics” package (Siberchicot & Julien-Laferrière, 2018). PTA was applied in three steps − interstructure (an ordination), compromise and intrastructure analysis − which correspond to co-variance, mean and variance structure analysis, respectively (Lavit et al., 1994; Mendes et al., 2010).

Third, redundancy analysis (RDA) of the same five wavelength-detrended tables as for the PTA was performed to test for relationships between wavelength-dependent photosynthetic parameters and explanatory abiotic and biotic variables. Data were centered and reduced before analysis. Explanatory variables were selected for the model using an automatic stepwise model with the "ordiR2step" function of the "vegan" package (Oksanen et al., 2019) that performs forward selection based solely on the adjusted R^2 and p-value (199 permutations). At each step, the variable with the highest additional fit was added to the model.

2.3. Results

2.3.1. Abiotic and biotic variables

The ex situ experimental conditions determined by the abiotic PCA showed contrasting results. For abiotic variables the first two axes of the PCA explained 65.1% of total inertia (49.5% and 16.6%, respectively) (Figure II.5-A). The first axis distinguished samples based on their light-quality ratios (R/B, G/B and G/R), vertical light attenuation coefficient ($K_{d(PAR)}$), Z_{eu}, Z_{uml}, salinity and PO_4 concentration (Figure II.5 -A). The second axis distinguished samples based on their DIN concentration, temperature, $Si(OH)_4$ concentration and light intensity at a depth of 2 m (PAR_{2m}) (Figure II.5). Three groups of samples were distinguished. Group 1 (samples 22, 12, 18, 38, 33, 31 and 49) had intermediate-to-high DIN (>2 µmol.L^{-1}, up to 30 µmol.L^{-1} near Seine Bay) and temperatures (9.5-12.0°C), low-to-intermediate salinity (< 34 PSU) and PAR_{2m} (20-182 µmol photons.m^{-2}.s^{-1}), the highest R/B and G/B ratios (mean of 0.9 and 1.9, respectively), the highest $K_{d(PAR)}$ (0.2-0.5 m^{-1}), the shallowest Z_{eu} (9-23 m) and Z_{uml} (6.5-21.0 m), and the lowest G/R ratio (±2). On the opposite side of the factorial map, group 2 (samples 43, 45, 46, 28, 37 and 53) had the highest PO_4 and $Si(OH)_4$ concentrations (> 1 and 0.5-2.0 µmol.L^{-1}, respectively) and salinity (mean of 35 PSU), the lowest R/B and G/B ratios, the highest G/R ratios, the lowest $K_{d(PAR)}$ (0.07-0.17 m^{-1}), and the deepest Z_{eu} (26-63 m) and Z_{uml} (17-78 m). Group 3 (samples 8, 10, 13, 25, 35 and 41) had intermediate salinity (33.5-35.0 PSU), the lowest temperatures (<10°C) and DIN concentration, intermediate light-quality ratios, and the highest PAR_{2m}, but with high variability (116-930 µmol photons.m^{-2}.s^{-1}). Thus, PAR in the abiotic PCA did not distinguish sampling locations well, nor did TSS. Samples had TSS less than 2 h (samples 10, 18, 28, 33, 38, 46, 49 and 53), greater than 10 h (samples 22, 31, 37 and 45) or values between the two (samples 8, 10, 13, 25, 35, 41 and 43). Group 1 had locations near the coast, while group 2 had locations offshore. Detailed information on abiotic variables is shown in the Supplementary material, Figures SM II.1 and SM II.2.

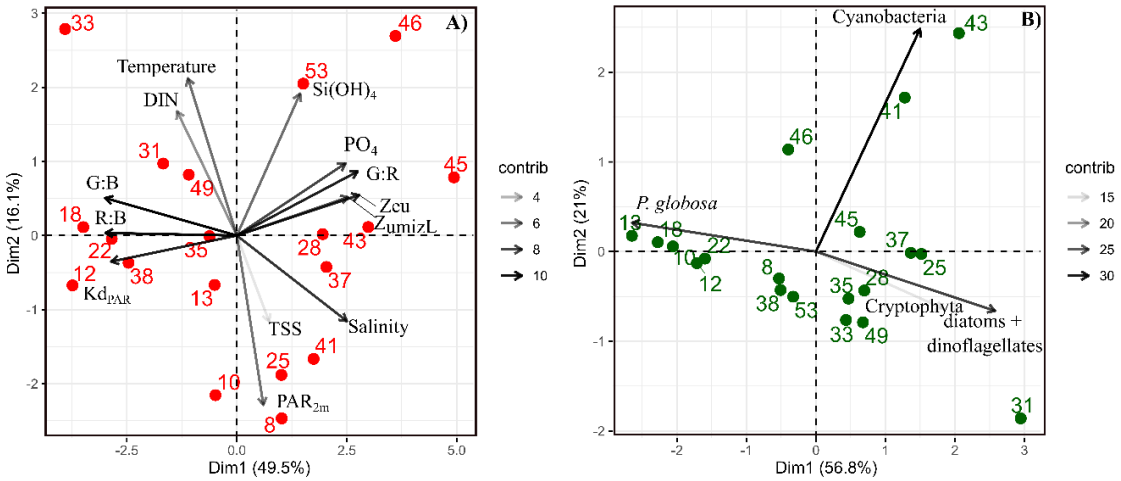

Figure II.5: The first two axes of the Principal Component Analyses (PCA) performed on: A) abiotic variables and B) biotic variables (biomass of the four phytoplankton groups determined by the bbe fluoroprobe), considering the 19 sampling stations. The % of explained variance for each axes is specified. The contribution (contrib) of each variable is indicated by a gray color scaling

The biotic PCA based on FluoroProbe measurements of the biomass of main phytoplankton groups (Figure II.5 B) distinguished samples mainly based on the biomass of *P. globosa*; however, the range of variation was low (±25%). The first axis distinguished *P. globosa* from other brown algae (diatoms and dinoflagellates) and cryptophytes, while the second axis distinguished Cyanobacteria (bluegreen). The results indicate that *P. globosa* co-dominated with diatoms at several locations, and *P. globosa* dominated only samples from locations 10, 12, 18 and 22. Samples from three locations (41, 43 and 46) contained the most cyanobacteria. Details of phytoplankton groups by location are shown in the Supplementary material, Figure SM II.3.

2.3.2. Wavelength-dependent photosynthetic parameters from linear mixed-effects models

Fixed effects of the LMEMs represented the population trend of each photosynthetic parameter once the spatial nature of the data sampling was considered (Figure II.6). All intercepts were significant, indicating that all parameters differed from zero in the bright blue wavelength (440 nm) (Table II.I). Wavelength dependence led to a significant slope of the fixed effect for all parameters except ETR_{max}(II) and E_{op}(II), but the sign of each slope varied among parameters.

While the slope of F_v/F_m was significant, its small decrease across wavelengths was considered null for simplicity.

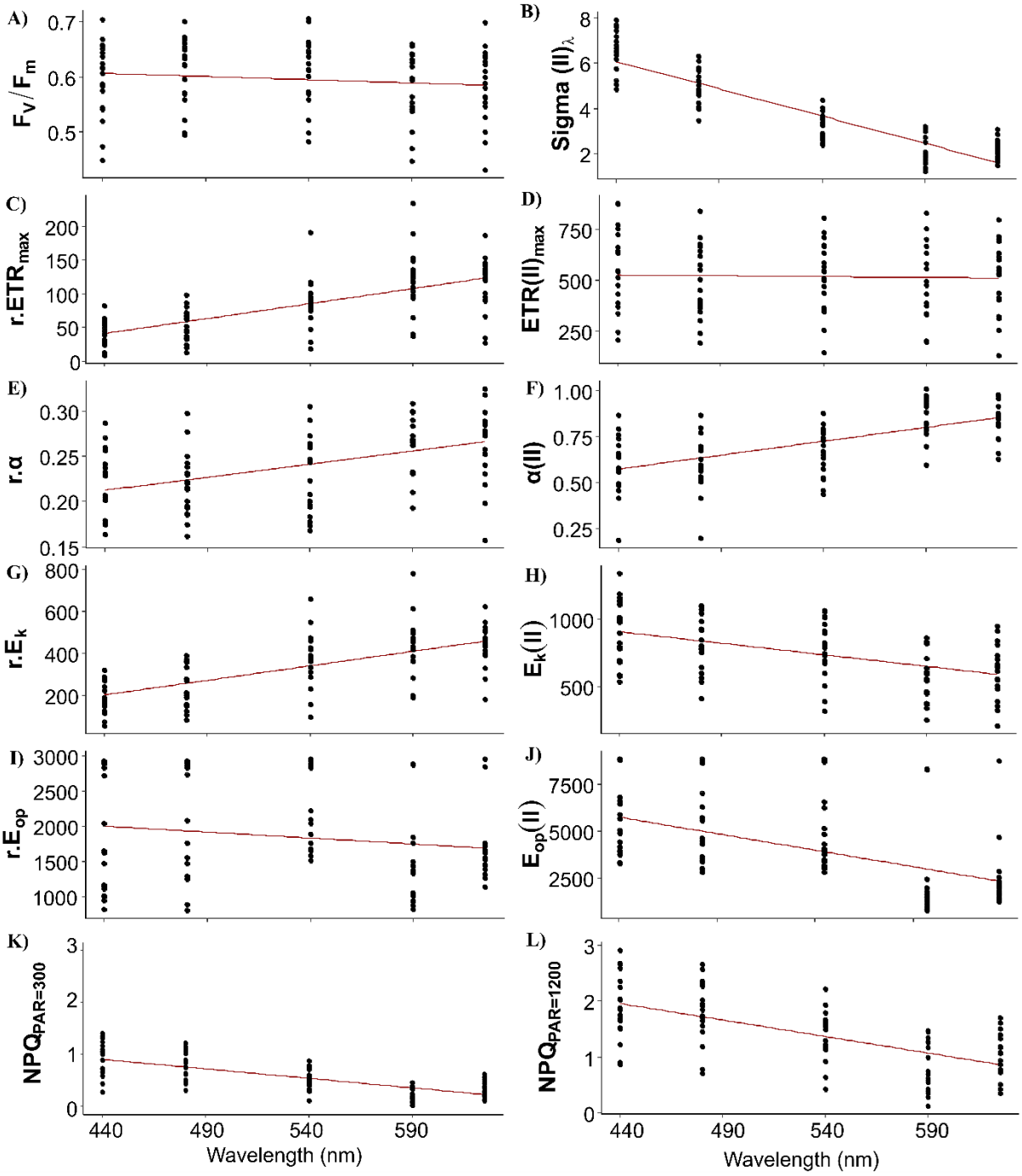

Figure II.6 : Raw data of each photosynthetic parameter (see glossary in section 1.6 and list of symbols and abbreviations for definitions) of the 19 samples by wavelength and the fixed effect (red line) of linear mixed-effect models (i.e., wavelength dependence at the population level).

*Table II.I : Results of the linear mixed-effects models for photosynthetic parameters (see glossary in section 1.6 and list of symbols and abbreviations for definitions): best estimates of standard error and significance (for fixed effects) and the significance of individual variation (for random effects). Hypothesis tests were based on t-tests (for the intercept and slope of fixed effects) and likelihood-ratio tests and the p-value based on χ2 statistics (for random effects). Significance codes: *** p <0.00, ** p <0.01, * p < 0.05, ns: non-significant.*

	Fixed effects				**Random effects**	
Parameters	**Intercept**	**Std. Errors**	**Slope**	**Std. Error**	**Intercept**	**Slope**
$\mathbf{F_V/F_m}$	0.61^{***}	0.01	-0.00012^{***}	0.00002	***	ns
$\mathbf{Sigma(II)_\lambda}$	6.08^{***}	0.03	-0.0241^{***}	0.0011	**	ns
$\mathbf{r.ETR_{max}}$	41.19^{***}	5.26	0.44^{***}	0.04	***	***
$\mathbf{ETR_{max}(II)}$	527.42^{***}	35.84	-0.09^{ns}	0.20	***	*
r.α	0.21^{***}	0.007	0.00029^{***}	0.00004	***	ns
α(II)	0.57^{***}	0.03	0.0015^{***}	0.0001	***	ns
$\mathbf{r.E_k}$	200.94^{***}	21.78	1.39^{***}	0.12	***	**
$\mathbf{E_k(II)}$	905.92^{***}	43.81	-1.72^{***}	0.32	***	**
$\mathbf{r.E_{op}}$	1998.90^{***}	141.01	-1.69^{ns}	0.90	***	ns
$\mathbf{E_{op}(II)}$	5737.18^{***}	405.36	-18.43^{***}	2.44	***	ns
$\mathbf{NPQ_{300}}$	0.90^{***}	0.06	-0.004^{***}	0.0003	***	ns
$\mathbf{NPQ_{1200}}$	1.94^{***}	0.111	-0.006^{***}	0.0004	***	ns

$Sigma(II)_\lambda$ is a key parameter since it connects relative and absolute parameters such as α, ETR_{max}, E_k and E_{op}. $Sigma(II)_\lambda$ decreased by a factor of 3 across wavelengths (from 6 to 2 nm^2). Conversely, $r.ETR_{max}$ increased by a factor of 3 (from 50 to 150), which may have counteracted the decrease in $Sigma(II)_\lambda$ and led to the null slope of $ETR_{max}(II)$. Parameters r.α and α(II) increased as wavelength increased, and sharply for the latter, which increased by a factor of 2. Since E_k is the ratio of ETR_{max} to α, $r.E_k$ increased and $E_k(II)$ decreased as wavelength increased. Since E_{op} values were highly scattered, they were not considered in later analyses. Since NPQ was estimated at low and high PAR from the P-E curves (300 and 1200 photons.m^{-2}.s^{-1},

respectively), trends in the NPQs were opposite to these in r.α and r.ETR_{max} and sometimes higher, which had more influence on the values of these parameters under the blue wavelengths (NPQ_{440} and NPQ_{480} ranged from 1-2) than under the red wavelength (NPQ_{625} reached 0.2 at PAR=300 µmol photons.m^{-2}.s^{-1}). The increasing trend in α(II) across spectrum could thus correspond to a strong decrease in α(II) under the blue wavelengths and not to an optimization under the light red wavelength.

For the random effects, intercepts of all parameters were highly significant, but their slopes were not, except for ETR_{max} and E_k in relative (r) and absolute (II) values (Table II.I). Thus, parameter values differed among samples but, except for ETR_{max} and E_k, had the same trend across wavelengths. This resulted in spatial differences in the spectral balance between bright blue and light red wavelengths for ETR_{max} and the photoacclimation parameters E_k (in relative and absolute units for the both).

When examining detrended values of absolute parameters among locations, those of ETR_{max}(II) and E_k(II) tended to differ among the five wavelengths by location, unlike those of the other parameters, which were generally more similar among the five wavelengths by location (Figure II.7). This was especially true for detrended values of α(II) and F_v/F_m, which differed little and almost not at all, respectively, among the five wavelengths by location. Because values of $Sigma(II)_\lambda$ under the light red wavelength were not always the lowest across wavelengths (i.e. a slightly non-linear distribution) (Figure II.6), its detrended values under the light red wavelength were higher than the population trend (Figure II.7). According to the statistical analyses, however, a linear model fit best to $Sigma(II)_\lambda$ values.

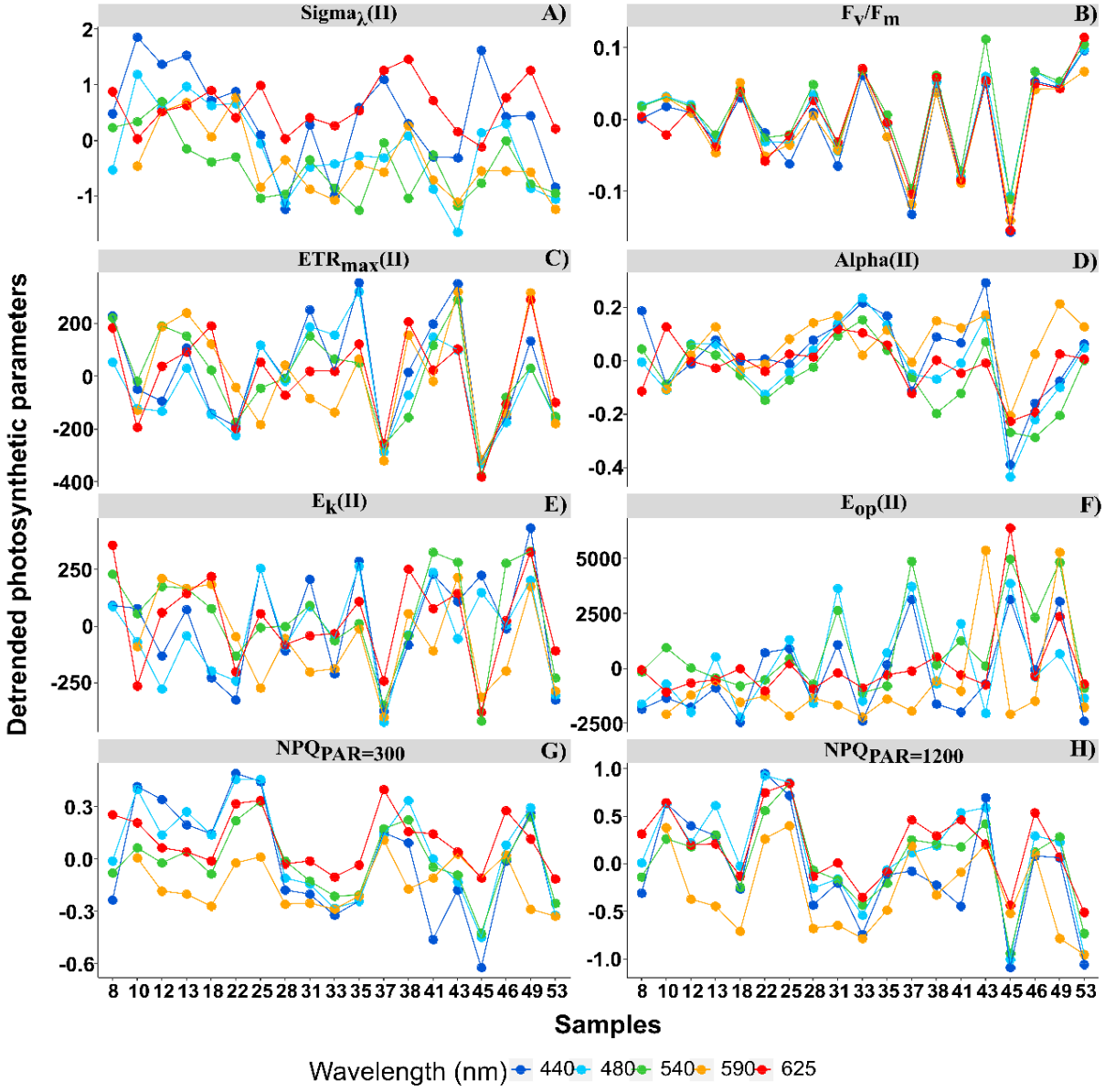

Figure II.7 : Detrended spectral photosynthetic parameters (see glossary in section 1.6 and list of symbols and abbreviations for definitions) resulted by calculating individual differences from the population trend (the linear mixed-effect models) among sampling locations. Point colors indicate each of the five wavelengths analyzed: 440, 480, 50, 590 and 625 nm.

2.3.3. Sample wavelength dependence of samples from the PTA

The first two axes of the PTA interstructure explained 85.38% of total inertia (Figure II.8), and the five wavelength tables had similar weights (0.38-0.47; Table II.III) and a significant representation (cos^2 close to 1; Table II.III). The PTA was thus adequate overall and highlighted similarities among the wavelengths. All five wavelengths were positively correlated and positively projected on the first axis (ca. 71.24% of the total inertia; Figure II.8) : Vector

correlation coefficients between the submatrix of photosynthetic parameters at each wavelength (nm), their weights in partial triadic analysis and cos^2., Figure II.8). The second axis separated the t blue and green wavelengths from the amber and light red wavelengths. The amber wavelength differed the most from the others and had the same correlation with the first and second axes.

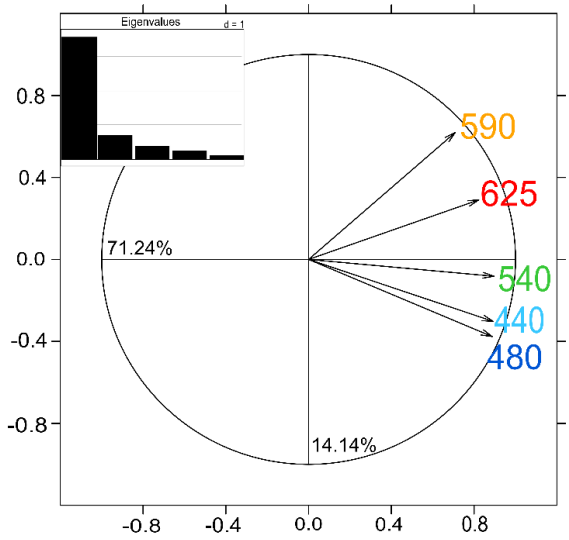

Figure II.8 : Correlation plot of partial triadic analysis interstructure analysis of detrended photosynthetic parameters measured at 440, 480, 540, 590 and 625 nm

Table II.II : Total inertia of partial triadic analysis (PTA) interstructure analyses, cumulative inertia of each PTA axis (Cum) and percentage of cumulative total inertia (Cum %).

Axe	Inertia	Cum	Cum (%)
1	10.56	10.56	37.76
2	8.54	19.10	66.49
3	4.51	23.61	82.18
4	2.42	26.03	90.61

Table II.III : Vector correlation coefficients between the submatrix of photosynthetic parameters at each wavelength (nm), their weights in partial triadic analysis and cos^2.

Wavelength	440	480	540	590	625	Weight	cos^2
440	1.00	0.88	0.74	0.50	0.59	0.47	0.91
480		1.00	0.77	0.43	0.60	0.47	0.90
540			1.00	0.54	0.69	0.47	0.89
590				1.00	0.61	0.38	0.69
624					1.00	0.44	0.80

When projecting the wavelength-dependent photosynthetic parameters on the compromise coordinates it explained 66.49 % of total inertia (Table II.III and Figure II.9-A), the relative positions of polygons indicated that PTA results generally met our expectations: opposition between the group of F_v/F_m, α(II) and ETR_{max}(II) vs. the group of Sigma(II)$_\lambda$ and $NPQ_{300\text{-}1200}$, with parameters related to photoacclimation (E_k and E_{op}) between these two groups. We observed the well-known relationships between variables related to energy flows (F_v/F_m and $NPQ_{300\text{-}1200}$), related to Sigma(II)$_\lambda$, and the major parameters that control PE relations in absolute units – α(II) and ETR_{max}(II) – which had a positive overall correlation.

The intrastructure of the PTA showed differences between photosynthetic parameter patterns among the five wavelengths (Figure II.9-B to F). Patterns for the main parameters, such as ETR_{max}(II), α(II), Sigma(II)$_\lambda$ and $NPQ_{300\text{-}1200}$, changed from the brith blue wavelength (440 nm) to light red wavelength (625 nm). The most evident change was the rotation of α(II) and NPQ300-1200 respected to the spectral pattern of Sigma(II)$_\lambda$. At blue wavelengths Sigma(II)$_\lambda$ and NPQ300-1200 were inversely correlated to α(II) (Figure II.9-A) but at amber and light red wavelengths there were any correlation (Figure II.9-D and E). (Figure II.9-D and E). Sigma(II)λ was incorrectly represented in the main plane at 625 nm (Figure II.9-E). The PTA intrastructure analysis also showed patterns for the locations among the five wavelengths (Figure II. 10). Wavelength dependence differed greatly among locations: polygons were largest for locations 33, 35, 43, 37 and 45, and smallest for locations 13, 18, 31, 46 and 53 (Figure II.10). In addition, the blue wavelengths (440 and 480 nm) displayed a general circular change among locations, moving from the right of the polygon for location 53 to the left for location 45 (Figure II.10).

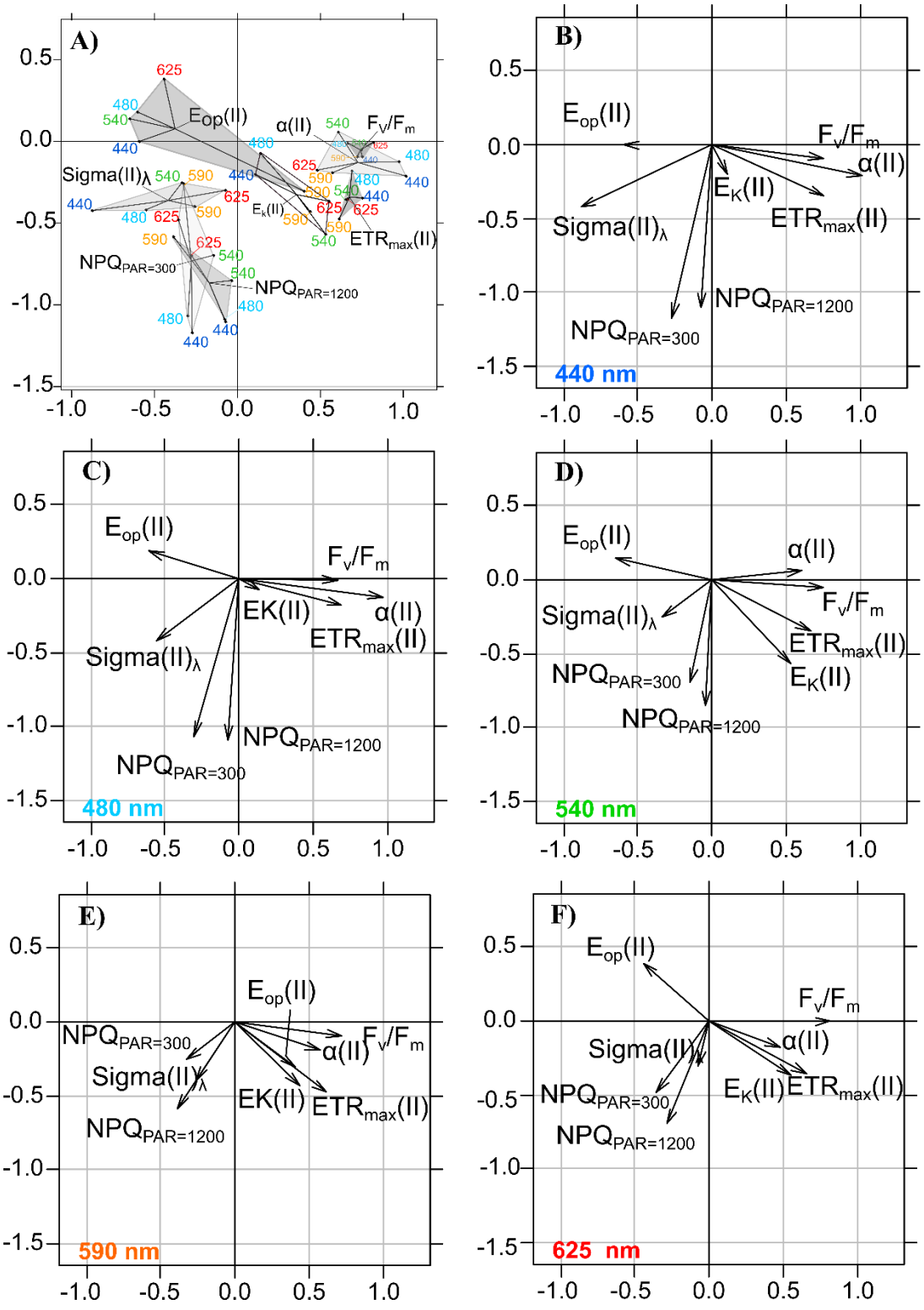

Figure II.9 : Results of intrastructure of the partial triadic analysis of detrended photosynthetic parameters $ETR_{max}(II)$, E_k, $\alpha(II)$, $E_{op}(II)$, $Sigma(II)_\lambda$, F_v/F_m and NPQ at 300 and 1200 µmol·photons·m-2s-1) projected on compromise coordinates (A). Each photosynthetic parameters coordinate is represented separately for each wavelength at 440 (B), 480 nm (C), 540 (D), 590 (E) and 625 (F) nm. See Table II.II for compromise contribution to total inertia and Table II.III for weight and cos2 of each of the wavelengths colors in PTA analysis.

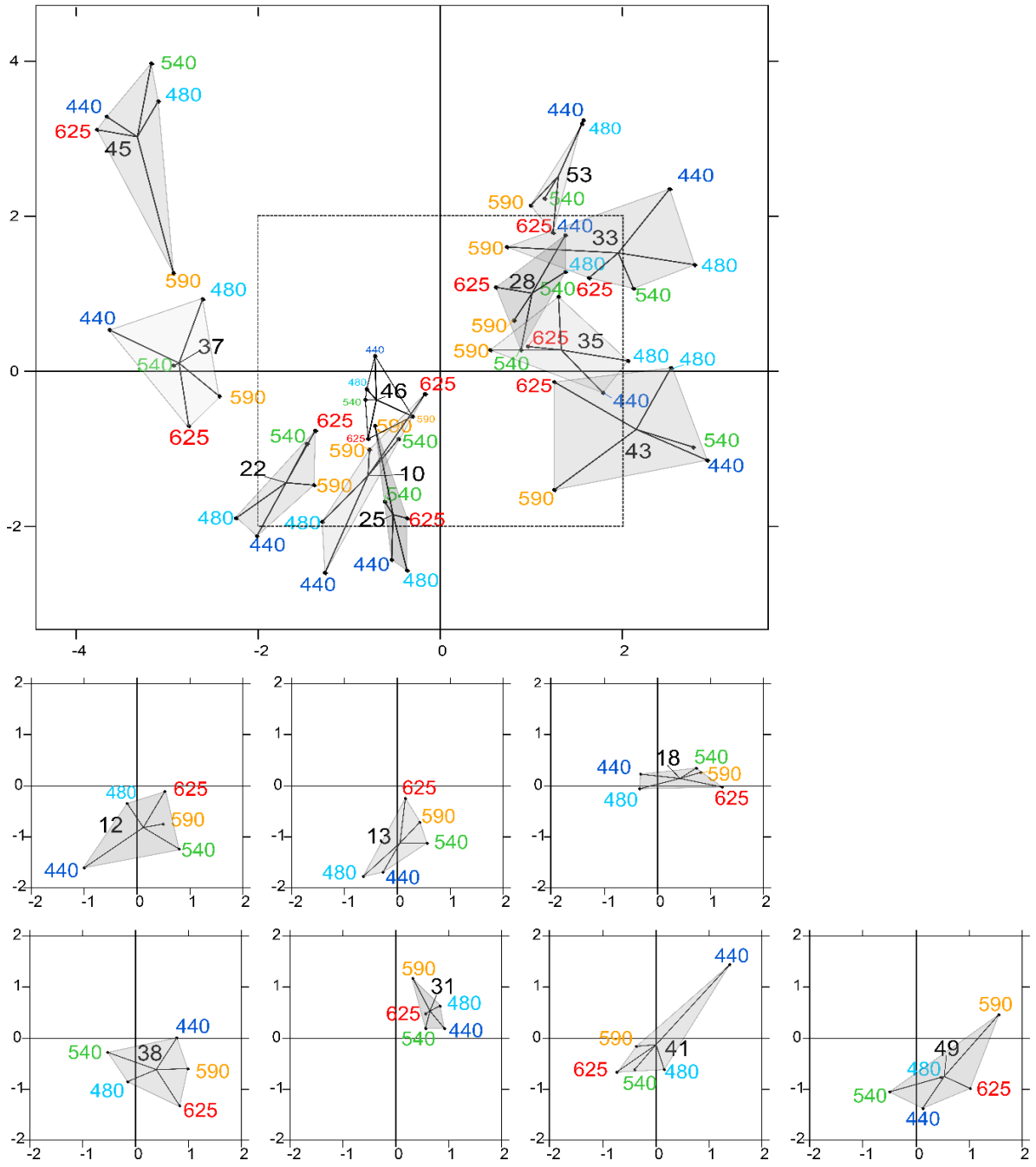

Figure II.10 : Partial triadic analysis intrastructure projected on compromise coordinates of photosynthetic parameters for each of the 18 locations: factorial map of spectral responses projected on compromise coordinates for each sample. The dotted line in the first figure represents the coordinates used to represent samples 12, 13, 18, 38, 41 and 49 separately to improve visualization of this part of the factorial map.

2.3.4. Explanatory variables of wavelength dependence from RDA and linear regression

The RDA results showed that abiotic variables related to light emerged first as explanatory variables (Table II.IV). Euphotic depth (Z_{eu}) was selected the most often, for three of the five wavelengths (Table II.IV), from 440-540 nm. TSS, which represents the recent light history of cells, was selected twice, for the light blue wavelength (480 nm) and the amber wavelength (590 nm). The G/R light ratios were selected for the amber wavelength. DIN concentration was the only non-light parameter selected, for the light blue wavelength. No variables were selected for the light red wavelength (625 nm), and PAR_{2m} did not seem to influence the parameters.

*Table II.IV : Results of redundancy analysis of detrended photosynthetic parameters at each wavelength: forward-selected explanatory variables, explained and residual variances, and the adjusted R^2 and associated p-value for abiotic and biotic variables. No biotic variable was selected, and the model for the red wavelength (625 nm) was not significant. Significance codes: *** p <0.00, ** p <0.01, ns: non-significant*

				Abiotic		Biotic	
Wavelength	**Model**	**Variance**	**Residual variance**	**adj R^2**	**p**	**adj R^2**	**p**
440	Z_{eu}	1.60	6.40	0.15	**	0.023	ns
480	Z_{eu}+TSS+K_d+DIN	4.16	3.82	0.38	***	-0.001	ns
540	Z_{eu}	2.35	5.65	0.20	**	0.010	ns
590	TSS+G/R	2.57	5.42	0.23	**	0.05	ns
625	None	6.00	1.99	0.10	ns	-0.111	ns

To further explore the influence of Z_{eu} and the difference in control of photosynthetic parameters under bright blue and light other significant red wavelengths, we sought specific connections between E_k and Z_{eu} (in ratios with E_{avg} and Z_{uml}, respectively), and between the ratio of E_k (in relative and absolute units) measured at 625 and 440 nm and the corresponding R/B light ratio ($E_{625/440}$) in water masses. Two significant linear trends were found between the $E_{k,440}/E_{avg}$ ratio (in relative and absolute units) and the Z_{eu}/Z_{uml} ratio for stratified water columns (Figure II.11-A). Correlations were non-significant for non-stratified water columns for $r.E_{k,440}$ and $E_k(II)_{440}$, as well as under the other wavelengths. Considering all sampling locations revealed other significant correlations between the absolute ratio $E_k(II)_{625/440}$ and (1) the red/blue light ratios in surface waters $E_{625/440}$ (see Figure II.11-B for correlation coefficients) and (2) the TSS factor (r=0.65, n=19, p<0.05, graph not shown).

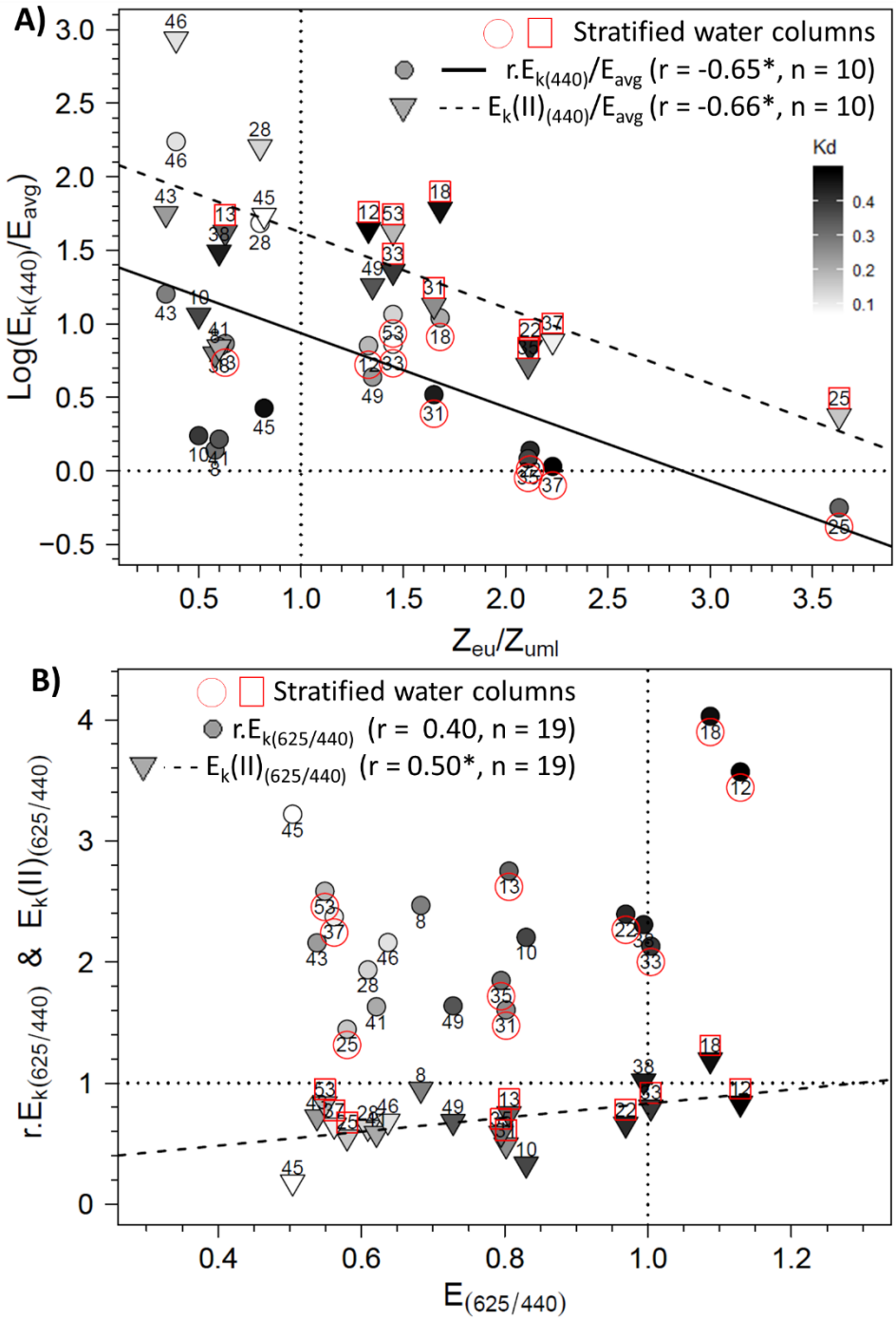

Figure II.11 : Relationships between (A) the E_k,440/E_{avg} ratio (the photoacclimation index measured at 440 nm to the vertically averaged PAR light intensity) (in relative (r) and absolute (II) units) and the Z_{eu}/Z_{uml} ratio (depth of the euphotic layer to that of the upper mixed layer) and (B) between E_k(II)(625/440) (ratio of photoacclimation index measured at red and blue wavelengths) and the corresponding red/blue wavelength ratios of light (E(625/440)) in water masses for the 19 locations. The regression equation in B is y = 0.5789 x + 0.2516 (F = 5.62; p = 0.0298). Pearson correlation coefficients, level of significance (p < 0.05) and the number of considered data are also reported on each graph.*

2.4. Discussion

Our results provide new insights into the wavelength dependence of photosynthetic parameters and PSII functional absorption cross section of coastal water phytoplankton communities. To date, the literature has focused on one or two species under a few growth conditions in the laboratory (Schreiber & Klughammer, 2013; Brunet et al., 2014; Szabó et al., 2014a; Luimstra et al., 2018) or older *in situ* studies that focused on the wavelength dependence of α in the water column (Lewis et al., 1985b, 1988; Kyewalyanga et al., 1992). Studying the present dataset including all photosynthetic parameters was complex due to environmental gradients and changes in community structure but made possible by the use of three powerful statistical methods. The wavelength dependence of photosynthetic parameters that was characterized at the population level and the sample level, will be discussed first in relation to the theories on photosynthesis and photoacclimation, and then from an ecological point of view.

2.4.1. Physiological meaning of wavelength dependence of photosynthetic parameters

a) Light absorption capacity

Since light absorption was measured according to the method of Schreiber, et al (2012), $Sigma(II)_{\lambda}$ can be considered an intrinsic property of the PSII units for each sample. Thus, the recent light history at sampling did not change the light absorption capacity of the 19 samples studied. Cell light absorption was thus a function of only pigment composition of photosynthetic units (Schreiber et al., 2012), even though the packaging effect may slightly skew the relation between $Sigma(II)_{\lambda}$ measurements and pigment concentration (Gorbunov et al., 2020). Since the slopes of the fixed (population level) and random (individual level) effects were significant and non-significant, respectively, all of the phytoplankton communities absorbed more light in the blue spectral range and with the same wavelength dependence, regardless of the sample.

Given the sampling area, we expected the decreasing trend in $Sigma(II)_{\lambda}$ across wavelengths. This is a typical result for cell communities dominated by brown algae with Chla as the main light-absorbing pigment (Kuczynska et al., 2015). The small increase (albeit not significant) under the light red wavelength (625 nm) is also consistent with this result (since Chla also absorbs red light), and with other $Sigma(II)_{\lambda}$ measurements for diatoms using the same method (Goessling et al., 2016, 2018a, 2018b). This is consistent with our group-based community-

structure measurements, which show that the diatom-dinoflagellate and haptophyte groups dominated all 19 samples. Consequently, the phytoplankton communities may not have been composed of species with completely opposite strategies for light absorption, as is common in experimental and theoretical modeling studies (Stomp et al., 2004, 2008; Luimstra et al., 2018, 2019; Gorbunov et al., 2020). Thus, the discussion focuses on the plasticity of typical brown algae communities to the wavelength dependence of light climates in coastal water depending on their physiological state.

Conversely, the absence of significant individual wavelength dependence for Sigma(II)$_\lambda$ among the 19 samples was unexpected; however, the light absorption capacity differed among samples regardless of the wavelength. Signature changes over the spectrum were expected because the spectral quality of light is crucial for microalgae to achieve optimal photoacclimation in the face of variable light quality and intensity during growth (Valle et al., 2014). Light quality can influence gene expression that adjusts pigment and protein compositions of specific antenna complexes (e.g. fucoxanthin-chlorophyll *a/c*-binding antenna pigment-protein complexes of diatoms called FCP), which changes spectral absorption by cells. Conversely, light quantity can influence pigment concentrations (Valle et al., 2014). In the present study, the changes in light quality may have been too small to induce significant changes in spectral absorption capacity among the 19 samples due to hydrodynamic conditions and the daylight cycle, which agrees with the results of Gorbunov et al., (2020). Cells could have managed variations in incident light quality via their photosynthetic apparatus without having to change their pigment composition. However, changes in light intensity were sufficient to produce significantly different spectral absorption capacities among samples.

The relatively high light absorption capacity of cells under the green wavelength (540 nm) agrees with results of Goessling et al., (2018b) for a planktonic diatom and for microphytobenthic diatoms (Goessling et al., 2018a), but does not agree with those of a brown-gold microalga (Szabó et al., 2014a) using the same method as in the present study. This could be because some or all cells in the communities of the present study were acclimated to green wavelengths in the water column. The green light ratios (G/B and G/R) measured always exceeded 1, indicating that green wavelengths dominated in all sampling conditions. It is well known that green light dominates coastal water during the algal blooms because the high chlorophyll concentration absorbs blue wavelengths (Kirk, 2011). This absorption capacity in the green spectral band could be due to an increase in the “green” absorption capacity of fucoxanthin, which absorbs more energy from 390-580 nm due to the basic structural and

functional properties of fucoxanthin in the light-harvesting complex proteins of the antenna (Premvardhan et al., 2008; Kuczynska et al., 2015). Burson et al., (2018) also showed continuous light absorption spectra, with better green light absorption capacity for a fucoxanthin diatom than for green and blue-green phytoplankton, in agreement with Valle et al., (2014).

b) General physiological state

The population trend across wavelengths and F_v/F_m values indicate that cells were in a good physiological state, considering the community composition based on diatoms and *Phaeocystis globosa* regardless of the wavelength and thus were not under high nutrient stress. The population trend of F_v/F_m was centered on 0.6 (the slope was almost null, albeit significant), and F_v/F_m values were never less than 0.4. Generally, the theoretical maximum of F_v/F_m is 0.7 (in a dark-adapted state, as in this study), and its critical value is 0.3 (Painter et al., 2010) for communities dominated by brown microalgae. We will not discuss here the complex links between nutrients and photosynthetic parameters, this is not our topic and this was done specifically in other works for the same ecosystem (Napoléon, et al., 2013b). In addition, the good nutrient status of water is confirmed by comparing nutrient concentration measurements in the present study to the seasonal nutrient cycle established for the EC (Gentilhomme & Lizon, 1998). Using a similar measurement method, Szabó et al., (2014b) observed similar values of F_v/F_m across wavelengths (which approached 0.7) for cultures in nutrient-replete conditions. Gorai et al., (2014) observed spectral independence of F_v/F_m when comparing physiological properties of a culture under blue and white lights.

c) Spectral trends and photoacclimation processes

In this context of samples with the same wavelength dependence of light absorption and good physiological state, wavelength photoacclimation can be investigated through trends in $ETR_{max}(II)$, $\alpha(II)$, NPQ and E_k. Although $r.ETR_{max}$ and $r.\alpha$ had a significant trend across wavelengths, they do not provide enough information to understand the spectral dependence of photosynthesis in detail, which is a function of light absorption, given here by $Sigma(II)_\lambda$ (Schreiber et al., 2012). These relative parameters are useful only to compare and better understand the influence of $Sigma(II)_\lambda$ on spectral photosynthetic processes in absolute units. Both parameters had a positive slope across wavelengths, indicating that $r.ETR_{max}$ and $r.\alpha$ spectra were the inverse of the $Sigma(II)_\lambda$ spectrum; conversely, in absolute units, the slope of

ETR_{max}(II) disappeared, while the positive slope of α(II) was maintained. These results were unexpected since water was sampled at different times of the day, and cells were kept in the dark for 2.5 h before being analyzed. An explanation could be that cells in the samples were in a wavelength-dependent photoprotective state due to the underwater light climate.

We expected the trend of ETR_{max}(II) to decrease over the spectrum because the cells grew in a natural environment in which blue and green light dominated, since red light is quickly absorbed in the water column (the R/B ratios were usually less than 1). Several studies involving phytoplankton and microphytobenthos observed increasing values of ETR_{max}(II) in the blue wavelength (Mercado et al., 2004; Szabó et al., 2014b; Goessling et al., 2016, 2018a) related to changing light conditions. Opposite results have also been found. Schreiber et al., (2012) indicated that photoinhibition could explain the decrease in ETR_{max}(II) under blue light, that the time needed to recover the starting values is much longer under bright blue than light red wavelengths, and that the recovery under blue light remains only partial after several hours. Correa-Reyes et al., (2001) observed that growth rates of eight microphytobenthic species decreased more under blue light than light of other colors. In the present study, given the higher light absorption in bright blue than light red wavelengths (625 nm), and since the high energy of blue wavelengths can cause photodamage (Dougher & Bugbee, 2001), the lack of slope for ETR_{max}(II) likely reflects a photoinhibition or photoprotective state of the communities towards blue wavelengths, which decreased $r.ETR_{max}$ values under blue light. For ETR_{max}(II), significant wavelength dependence among the 19 samples is superimposed on the non-significant population trend. Thus, some samples had different degrees of photoinhibition/photoprotection under blue light independent of other light colors. We can thus speculate about wavelength dependence of photoinhibition/photoprotection mechanisms.

We expected high r.α and especially α(II) under blue wavelengths and thus a decreasing trend from 440-590 nm, with a small increase at 625 nm. The variation in α as a function of light quality is the best known photosynthetic parameter because it was closely studied from the mid-1980s to the early 2000s by carbon-14 incorporation, for calculations of primary production rate (Lewis et al., 1985b, 1988; Kyewalyanga et al., 1992, 1997, 2002). At worst, a null slope of α(II) over the spectrum, like for ETR_{max}(II), was expected, but the consistently lower values in the blue wavelengths were unexpected given the $Sigma(II)_{\lambda}$ variations observed and previous studies of natural communities (Lewis et al., 1985a) or brown algae cultures (Haxo, 1960; Schofield et al., 1996). This result does not reflect an improvement in red light-use efficiency, since brown algae requires 24-48 h to photoacclimate to changes in red light (Valle et al., 2014),

which is consistent with properties of the underwater light climate. Unlike red light, high-intensity blue light can cause rapid changes in cells, such as energy allocation between photosynthetic and photoprotective pathways in coastal species (Lavaud, 2007; Brunet & Lavaud, 2010). As many experimental studies show, the cycle of xanthophyll (photoprotective pigment) and NPQ are fundamental photoprotective processes that are activated within seconds to minutes to dissipate excess absorbed light energy (Dimier et al., 2007a, 2007b, 2009a, 2009b). Energy dissipation by carotenoids can reduce photosynthetic rates under blue light, which increases NPQ (Brunet et al., 2014). Many other studies have used NPQ to measure the overall photoprotective capacity of the photosynthetic apparatus (e.g. Dimier et al., 2007b; Lavaud et al., 2007). The xanthophyll cycle (XC) photoprotective mechanism has been observed in the coastal sea of the EC for the same locations the phytoplankton communities in this study have been collected (Brunet et al., 1993; Brunet & Lizon, 2003) and in permanently well-mixed ecosystems (Alderkamp et al., 2011). Therefore, like for ETR_{max}(II), the decrease in the trend of α(II) observed over the spectrum could be due to photoinhibition and, more likely, photoprotection. Photoinhibition of α has been experimentally verified (Bjorkman 1987; Baker et al., 1994).

The hypothesis of a photoprotective influence on α (in relative and absolute units) requires that photoprotection occur early and at low light intensities. Consistent with this hypothesis, NPQ values were significant and always higher under blue than red light at low intensities. These results are confirmed by those of Goessling et al., (2018a) for suspensions of benthic diatoms and those of Tamburic et al.,(2014) for green algae. In the present study, NPQ was ca. 1 and 2 under low- and high-intensity blue light, respectively. According to Lefebvre et al., (2011), NPQ usually exceeds 1 for cells that face the sun and are not well adapted to high-intensity light.

Thus, since communities in the present study had adequate photoprotective capacity against blue light, maximum quantum efficiency F_v/F_m was always high regardless of the wavelength, while effective quantum efficiency, which influences α and ETR_{max}, decreased early under blue light (and probably green light). This created slightly different spectral signatures for α(II), which is determined under low light intensity, among the samples depending on the *in situ* light intensity, which thus likely decreased wavelength effects. Conversely, ETR_{max}(II) is determined under higher light intensity, in which individual spectral effects were efficient. To support this hypothesis, blue light is expected to be less prone to cause photoinhibition and photodamage than red light (Brunet et al., 2014) and cells have greater PSII repair capacity under blue light

than red light, since photoprotection and PSII repair are induced by protein-encoding genes under blue light, but are lacking under red light (Valle et al., 2014).

In this context, E_k varied across wavelengths due to relative variations in ETR_{max} and α, since $E_k=ETR_{max}/\alpha$. Values of $r.E_k$ were indeed lower in the blue wavelengths, while those of $E_k(II)$ were higher. These results are fairly consistent with our hypothesis for communities in the photoprotective state rather than the photoinhibition state, as are the high F_v/F_m values under blue wavelengths. This is supported by the two significant correlations observed between the $E_{k,400}$:E_{avg} ratio (in relative and absolute units) and the Z_{eu}/Z_{uml} ratio, indicating that the communities reflected well a high light availability in the mixed layer (Jensen et al., 1994; Wang et al., 2011). This is particularly true for the $rE_{k,400}/E_{avg}$ ratio, which tended towards the reference value of 1 at four locations that had stratified water columns. Values close to 1 indicate optimization of light absorption by photosynthetic metabolism (Anning et al., 2000). To our knowledge, these two correlations are new results for an ecosystem known for its high hydrodynamic regime. Most studies in dynamic coastal ecosystems observed cells in a photoacclimation state and $r.E_k$ values less than or greater than 1 (Tillmann et al., 2000; Claquin et al., 2010; Houliez et al., 2013a) One exception is Jouenne et al., (2005) in the Baie des Veys (French coast), who used carbon-14 measurements rather than active fluorescence measurements. The photoprotective state, based on NPQ under *in situ* irradiance, includes well-known processes that can operate continuously to protect microalgae from potential photoinhibition and, after photodamage, correspond well to photoacclimation processes (Alderkamp et al., 2011, 2013). The physiological plasticity of phytoplankton in limiting photodamage usually explains much of the diurnal variation in photosynthetic processes (Schuback et al., 2016). These include many processes of the photosynthetic apparatus that influence $r.E_k$ and $E_k(II)$ in response to *in situ* light intensity (Dubinsky & Schofield, 2010, 2010; Schofield et al., 2013).

The advantage of measuring photosynthesis at several wavelengths using the functional light absorption capacity of natural phytoplankton is revealed by the differing trends of the photosynthetic parameters observed over the spectrum. Comparing the spectral trends and estimating the absolute photosynthetic parameter were necessary to identify the photoacclimation state of the 19 samples.

2.4.2. Ecological meaning of sample spectral variability and controlling factors

To investigate the ecological meaning of our results for wavelength dependence, we addressed the variability in photosynthetic parameters outside of the population trends. This approach was based on the detrended measurements of the PTA and RDA by wavelength, and the relationships between the E_k(II) ratios and their controlling factors.

According to the PTA, the covariations observed among detrended values of photosynthetic parameters and their change over the spectrum are consistent with wavelength dependence at the population level of the parameters studied with the LMEMs. The PTA showed that the pattern of the parameters changed gradually and consistently between blue and red wavelengths, concretely for light absorption and photochemical quenching. Using the PTA to scan the intrastructure of the 19 samples revealed also that spectral variation patterns of the parameters of each sample differed from each other in size, shape and position on the factorial map. Sizes and shapes of these spectral polygons were not related to water column stratification (e.g. the polygon of the most stratified location (no. 33) was the same size as that of location 43, which was not stratified). According to the RDA, photosynthetic parameters measured by wavelength were influenced mainly by euphotic depth. The forward selection of the RDA first retained the most correlated variable in a group of abiotic variables that covaried with biotic variables. Consequently, since the euphotic depth (Z_{eu}), the light extinction coefficient (K_d(PAR)) and the three light-quality ratios were collinear or correlated variables (in the abiotic PCA), individual photosynthetic parameters could also be controlled by the underwater light quality and turbidity, since the RDA also selected K_d(PAR) and a wavelength ratio. Considering all photosynthetic parameters, the main RDA result is thus consistent with the significant relationship observed between the light saturation ratio ($E_k(II)_{625/440}$) and R/B light ratio ($E_{625/440}$). The RDA also selected the TSS variable discussed later. Mixing depth ($Zu_{mix}l$) was another interesting ecological parameter selected by the RDA. The RDA confirms the hydrodynamic regime's control of the photoacclimation index E_k previously displayed by the relationship between E_k (r and II) and Z_{eu}/Z_{umixl}. Since physical forcing in a given upper mixed layer controls certainly the level reached by E_k, wavelength dependency of photosynthetic parameters is generally a trade-off between the light quality of the different encountered water masses and changes in light quantity throughout the upper mixed layer due to the hydrodynamic regime. The RDA results and singular correlations with E_k (r and II) are consistent, but the correlations of $E_k(II)_{625/440}$ with critical environmental parameters provide better understanding

of the ecological mechanisms that influence phytoplankton photoacclimation. The results are interesting because they were obtained from the field, where light-quality ratios (between red and blue wavelengths for instance) are known to change with depth (data not shown, but see examples in Brunet et al., (2014) and Jaubert et al., (2017). It is likely that the influence of vertical changes in light-quality ratios on microalgae acclimation was small in the present study, especially because most upper mixed layers were shallow (6.5-14 m) and the residence times of the cells at a given depth were low. The spectral light saturation ratios $E_k(II)_{625/440}$ were therefore not correlated with the Z_{eu}/Z_{umixl} index.

The significant correlations between $E_k(II)_{625/440}$ and $E_{625/440}$ or TSS clearly highlight that natural phytoplankton communities can implement photoacclimation processes that are driven by the *in situ* light quality of the daylight cycle. Most samples had $E_{625/440}$ ratios less than 1, which indicates water in which blue wavelengths dominate red wavelengths, and phytoplankton have a higher $E_k(II)$ photoacclimation ratio in blue wavelengths than in red wavelengths. This original result is valid only for absolute $E_k(II)_\lambda$ parameters related to $Sigma(II)_\lambda$, not for relative parameters. Since $Sigma(II)_\lambda$ measured with the MULTI-COLOR-PAM is an intrinsic property of microalgae (Schreiber et al., 2012), and since microalgae can increase pigment concentration to absorb more light (Lawrenz & Richardson, 2017), differences in pigment concentrations may change the level of $Sigma(II)_\lambda$ measured during the day. Due to the differing variations in $r.E_k$ between blue and red wavelengths, $E_k(II)_{625/440}$ ratios are correlated with $E_{625/440}$ ratios in the water masses and with TSS. These relationships provide new information about the natural environment and are consistent with many experiments under controlled conditions. As several studies of monospecific cultures subjected to contrasting R/B ratios show (Schellenberger Costa et al., 2013a; Brunet et al., 2014), variations in the light spectrum and in blue vs. red wavelengths influence photoprotective capacity (e.g. activation of the diadinoxanthin-diatoxanthin xanthophyll cycle and the NPQ capacity) and the pigment composition of phytoplankton. (Schellenberger Costa et al., 2013a) conclude that photoprotection is regulated more by light quality (especially blue wavelengths) than by the overall light intensity. Kirk, (2011) stated that phytoplankton detect not so much the spectra of light, but rather differences between wavelength ratios received by PSI and PSII, using blue and red wavelength photoreceptors (Jaubert et al., 2017) that regulate photosynthesis and promote photoacclimation (Schellenberger Costa et al., 2013b; Petroutsos et al., 2016) This explains why the $E_k(II)$ for the green wavelength did not correlate significantly with the *in situ* light-quality ratios of the green

wavelengths. Photoacclimation mediation by *in situ* blue wavelengths, as discussed by Schellenberger Costa et al., (2013a), is thus consistent with our field study.

The $E_k(II)_{625/440}$ vs. $E_{625/440}$ correlation, like the abiotic PCA, indicates indirectly that variables such as temperature, PAR_{2m}, and DIN and $Si(OH)_4$ concentrations do not influence wavelength photoacclimation greatly. Previous studies in the EC showed that abiotic variables were the main variables that controlled spatial and/or temporal variations in relative photosynthetic parameters (Jouenne et al., 2005, 2007; Napoléon et al., 2012, 2013a; Houliez et al., 2013b, 2015). However, the variables that control these photosynthetic parameters may vary among geographic areas and/or seasons. In the present study, this correlation was determined over a large spatial scale.

2.4.3. Ecological implications and consequences

It is the general question of the absorption capacity of light in relation to the quality of light and its impact on primary production that is discussed here.

The precise examination of the $E_k(II)_{625/440}$ and $E_{625/440}$ relationship in link with the reference values of 1 indicates that the two ratios matched each other well. For example, at location 38, the $E_k(II)_{625/440}$ and $E_{625/440}$ ratios equaled 1, which could be because the water there was sampled before sunrise. However, other communities sampled before sunrise (e.g. at locations 28, 46 and 53) had $E_k(II)_{625/440}$ ratios > 1, related to the $E_{625/440}$ ratios of water masses. The regression model indicates that to observe an $E_k(II)_{625/440}$ ratio of 1, a theoretical $E_{625/440}$ ratio of 1.29 would be required, which is similar to our measurements. In this case, the blue wavelengths would decrease to 77 µmol photons.m^{-2}.s^{-1} given a red light of 100 µmol photons.m^{-2}.s^{-1}. Thus, the $E_{625/440}$ ratio indicates no strong imbalance in available energy and thus no stressful ecological situation for phytoplankton. In spring in temperate water, blue wavelengths are absorbed due to CDOM, terrestrial discharge near estuaries and phytoplankton blooms themselves (Vantrepotte et al., 2007; Astoreca et al., 2009). Lawrenz & Richardson, (2017) studied photoacclimation under extreme conditions, with a total absence of blue light (i.e. black water with high CDOM concentrations). They showed that, depending on the taxon, microalgae retain or lose their initial light absorption capacity on the spectrum, and their absorption capacity adapts to the light quality to which they were exposed, even with red wavelengths. Some species can survive under red light in the short term, but in the long term, cytoplasmic structures and chloroplast membranes degrade (Humphrey, 1983) and Chla

concentrations decline (Forster & Dring, 1992). Rivkin, (1989) showed the strong influence of blue light on carbon fixation and incorporation into amino acids and proteins. The $E_k(II)_{625/440}$ vs. $E_{625/440}$ correlation in the present study cannot be extrapolated beyond the measurement limits (i.e. to the completely unbalanced light ratios as Lawrenz & Richardson (2017) did), but includes representative conditions generally found in the EC or temperate systems.

In comparison, $E_k(II)_{625/440}$ ratios near 0 would indicate that blue wavelengths are ultra-dominant in the water mass and could activate strong photoprotection mechanisms or even cause photodamage, which would decrease $ETR_{max}(II)$ greatly under blue wavelengths. Under these conditions, given the intercept of the linear model, $E_k(II)$ values under blue wavelengths would be only 25% of those under the red wavelength, which suggests that primary production would decrease greatly. However, electron flows under green, amber and light red wavelengths remained high, and NPQ was not as strong as under blue wavelengths. This indicates that light absorption ($Sigma(II)_\lambda$) under these wavelengths was lower, as was the NPQ_λ developed. However, this raises the issue of using the spectral approach to calculate primary production based on the photosynthetic parameters of RLC relationships.

Previous studies of the wavelength dependence of photosynthesis specified the systematic error produced by measuring α under white-light incubators when comparing incubation light climates (Laws et al., 1990) or primary production models (Kyewalyanga et al., 1992). Most classic incubators do not reproduce light spectra at the low intensities that phytoplankton encounter in the water column because of the high variability in light quality with depth, but also with time, due to vertical mixing in the upper part of the water column. Schofield et al., (1996) examined the error caused by using the same or different α from cultures grown under different light qualities when calculating primary production in a theoretical and simplified water column. Depending on the species and growing conditions, differences between vertical primary production rates estimated by the two calculation methods ranged from 12-49%. Other studies showed that α values measured on board under artificial light, i.e. “broad-band” P-E experiments (Irwin et al., 1990), could be corrected from the shape of the phytoplankton absorption spectrum (Kyewalyanga et al., 1997; Sathyendranath et al., 1999). This approach involves the field of remote sensing in particular and includes “optical” and “full spectral” models (Platt & Sathyendranath, 1988; Sathyendranath & Platt, 1993; Behrenfeld & Falkowski, 1997a, 1997b). Recent studies (Kovač et al., 2017; Sathyendranath et al., 2020) combined a spectral model of underwater light with a model of the integrated spectral response of algal photosynthesis consistent with photoacclimation processes. These studies recommend using the

photosynthesis action spectrum or spectral correction of α in the water column, especially when differences in the shape of the action spectrum of α are larger than those in its magnitude at each wavelength (Sathyendranath & Platt, 1993). However, these studies did not consider that light-quality ratios in surface water can also greatly influence photoacclimation of microalgae. This was revealed in the present study by some individual wavelength-dependence phenomenon that differed significantly among the samples, and the $E_k(II)_{625/440}$ ratios, which involve $ETR_{max}(II)$ and α(II) (i.e. the photosynthetic apparatus), especially the functional absorption cross section of PSII and the maximum rate of PET_λ, according to the optical definition of E_k (Falkowski & Knoll, 2007). Parameters α(II) and $Sigma(II)_\lambda$ showed no significant individual wavelength dependence among water masses, unlike $ETR_{max}(II)$ and $E_k(II)$, which are involved in primary production at high light intensities. The central issue is thus how photosynthetic activity induced by wavelengths beyond 480 nm can compensate for the decrease in photosynthesis under strong blue light when estimating primary production in different water masses. Sensitivity analysis of physicochemical properties of water would pave the way for future research on wavelength dependence of phytoplankton photosynthesis, as well as spectral dependence at the seasonal scale, using current active fluorescence measurement technologies.

2.5. Conclusions

Our results indicate that natural phytoplankton communities can photoacclimate to light quality dynamically under contrasting environmental conditions in temperate coastal seas in response to the available energy balance between red and blue wavelengths. The high spatio-temporal variability in wavelength-dependent photosynthetic parameters of phytoplankton was consistent with theories of photosynthesis. With a general model of photoprotection against blue light based on NPQ of photosynthesis, the present study shows that natural phytoplankton communities were most adapted to high-intensity light when a large amount of light was absorbed (e.g. blue wavelengths) but appeared "shade" adapted when low-intensity light was absorbed (e.g. green, amber and light red wavelengths), to paraphrase Nielsen & Sakshaug (1993).

The results for dynamic photoacclimation processes showed a general trade-off between light quality and intensity, and also all related light factors (e.g. K_d(PAR), Zeu, Zumixl), which is difficult to find in experimental studies, through which photoacclimation has been discussed

for many years (Schofield et al.,1996; Brunet et al., 2014; Gorai et al., 2014). Experimental studies are generally performed with monocultures growing in the comfort of laboratories for generations and rarely with natural communities using conventional photosynthetic parameters. These cultures are subjected to photon flux of different wavelengths and/or intensities, with different frequencies of variation, different daylight cycles, etc. Experiments often consider the controlling variables separately but combining them simultaneously seems relevant for understanding processes of photoacclimation to light variations in the field, as discussed by Combe et al., (2015) in a modeling study.

2.6. Supplementary material

2.6.1. Supplementary material 1: Abiotic variables

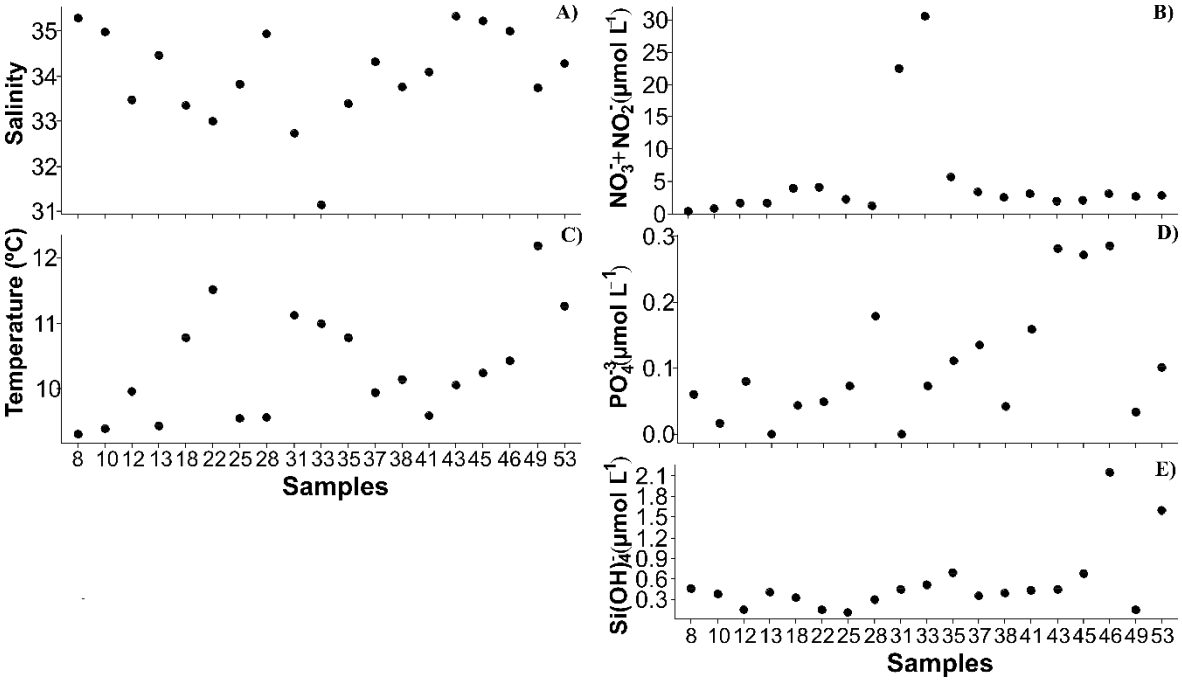

SM II-1 : Hydrological variables measured in surface water from conductivity-temperature-depth profiles at 19 locations across the English Channel: A) salinity; C) temperature; and B) NO_3+NO_2, D) phosphate (PO_4) and E) silicate ($Si(OH)_4$) concentrations

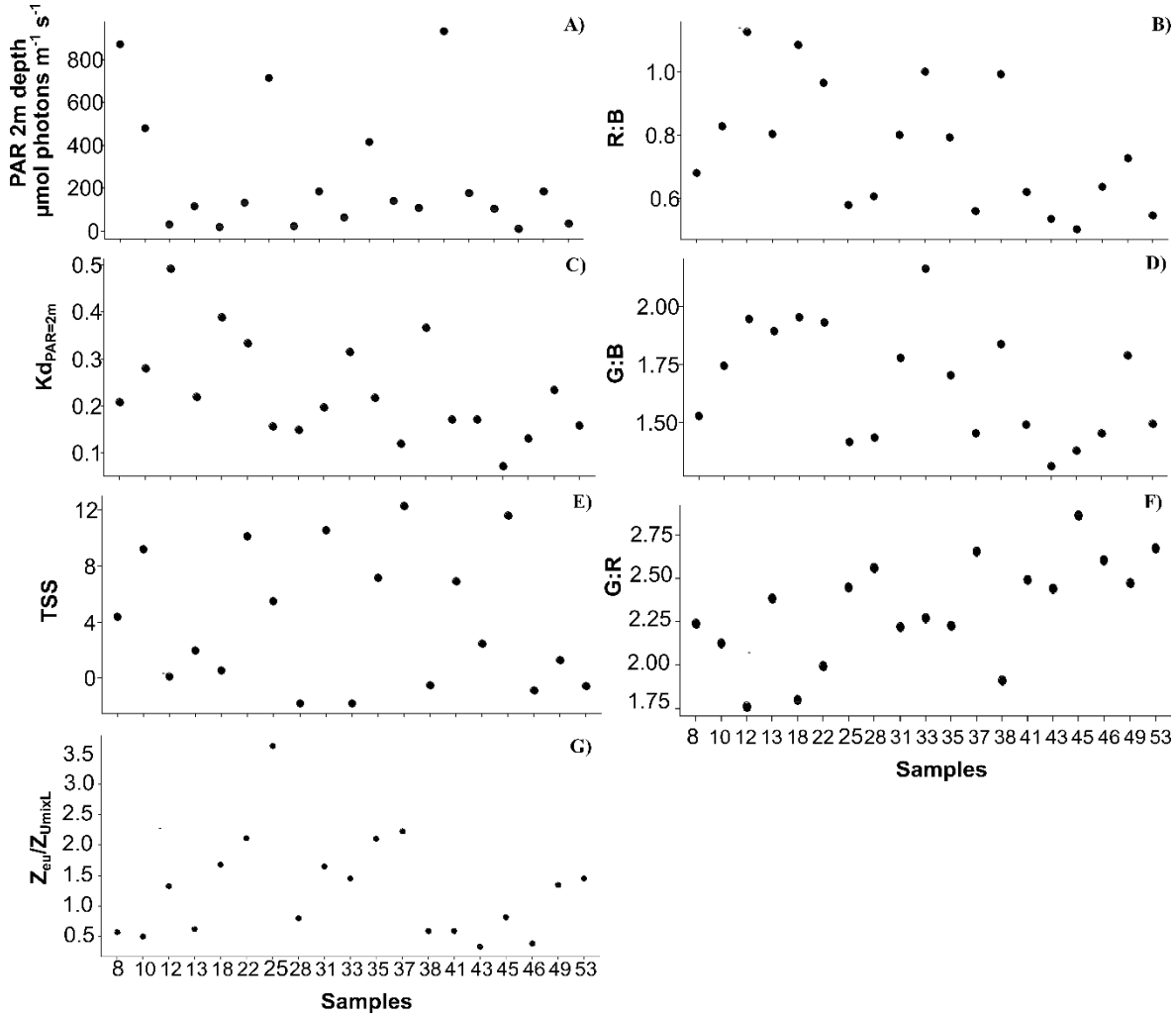

SM II-2 : Variables related to the light climate of the 19 locations: A) photosynthetically active radiation (PAR) at a depth of 2 m; (C) $K_{d(PAR)}$; (E) time since sunrise (h) (TSS); and light-quality ratios at the surface of (B) (R)ed:(B)lue, (D) (G)reen:(B)lue and (F) (G)reen:(R)ed wavelengths

2.6.2. Supplementary material 2: Biotic variables

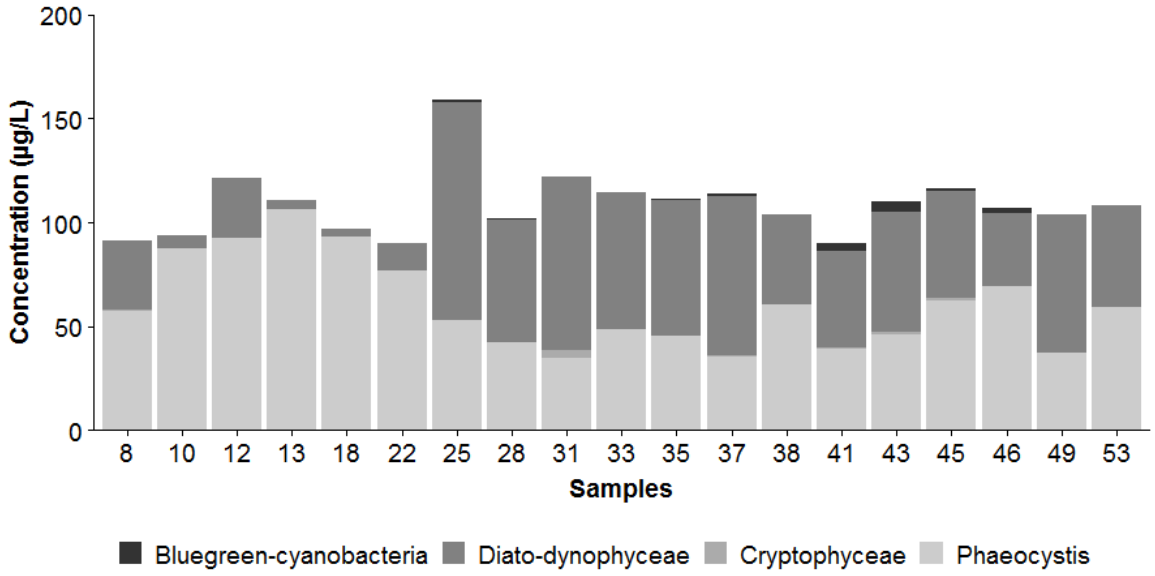

SM II-3 : Biomass of phytoplankton groups in concentrated samples using the FluoroProbe technique, in µg chlorophyll.L^{-1}. Shades of gray represent four phytoplankton groups: blue-green cyanobacteria, diatoms plus dinoflagellates, Cryptophyceae and Haptophyceae, which corresponds to Phaeocystis globosa in the English Channel

III. Time scales of wavelength-dependent photosynthesis from tides to seasons in coastal seas

Time scales of wavelength-dependent photosynthesis: from tides to seasons in a coastal sea

Michel-Rodriguez[1] M., Lefebvre[1] S., Duong[1] G., Courvoisier[2] M., Merieux[3] X., Gevaert[1] F., and Lizon[1] F.

Univ. Lille[1], CNRS[2], Univ. Littoral Côte d'Opale[3], UMR 8187 LOG, Laboratoire d'Océanologie et de Géosciences, Station Marine de Wimereux, 28 Avenue Foch, 62930 Wimereux, France

Abstract

The temporal patterns of wavelength dependency of photosynthesis were studied in a shallow coastal water body during 9-month (25 dates with 48 samples) near the Strait of Dovers. Photosynthetic electron transport $(PET)_\lambda$, absorption capacity absorption $(Sigma(II)_\lambda)$, physiological state (Fv/Fm_λ) and non-photochemical quenching (NPQ_λ) were assessed using a Multi-Color Pulse Amplitude Modulation (MULTI-COLOR-PAM Heinz, Walz) chlorophyll fluorometer on natural phytoplankton communities. Wavelength dependency of each photosynthetic parameter was analyzed using Linear Mixed Model Effects model and individual random effects were explained considering three different temporal scales: the three seasonal periods; the tidal effect (high and low tide) nested in the three seasons and, the individual level nested in the two previous ones. Population trends of wavelength dependent parameters were consistent with photosynthesis theory and with previous *in situ* studies in this coastal area. The analysis of detrended individual data with Principal triadic analysis (PTA) combined to Redundancy RDA analysis revealed that the seasonal phytoplankton succession controlled the spectral variations of photosynthesis parameters while at the tidal cycle scale within season, significant wavelength dependent variations of Sigma(II)λ emerged. In springtime, *Phaeocystis globosa* showed ability to photoacclimate to high light, combined to a particular rapid photoregulation, despite the low light due to high turbidity and hydrodynamical conditions of this shallow environment

Key words: Photosynthesis, Wavelength dependency, Photoregulation, Xanthophylls Cycle, *Phaeocystis globosa*, Tide cycle

3.1 Introduction

Phytoplankton is submitted to multitude of light variations in the natural field. To cope with such environmental variability, phytoplankton can photoacclimate, photoregulate and photoadaptate (Dubinsky & Stambler, 2009; Kirk, 2011). These processes have been mainly studied in relationship with the spatio-temporal variations of light intensity available for photosynthesis and classical environmental controlling factors in field studies (Houliez et al., 2015). Little work has focused on the light quality variations considering the characteristic temporal scales of these biological processes. Light quality control on natural microalgae communities was essentially studied in order to determine the action spectra and absorption spectra of cells with the purpose of estimating water column primary production rates using spectrally resolved photosynthesis light models (Kyewalyanga et al., 1992, 1997; Platt & Sathyendranath, 1988; Sathyendranath et al., 1989, 1995a). These earlier works, conducted using the technique of ^{14}C absorption, have evidenced that the action spectra or the so-called slope light utilization efficiency (α) of the photosynthesis light curve (PE) was spectrally dependent (Lewis et al., 1985b, 1985a), as the underwater light transmission and the phytoplankton absorption capacity related to intracellular pigment composition (Johnsen et al., 1994; Johnsen & Sakshaug, 1993; Schofield et al., 1996) and/or phytoplankton community structure (Hoepffner and Sathyendranath, 1992; Lutz et al., 2003; Schofield et al., 1996). Therefore, the shape of the wavelength dependency of α could vary according to i) the depth in the water column, ii) to the vertical mixing intensity and iii) to water masses properties (from an hydrological and biological point of view). The main issue that was addressed in this context was the systematic error in α when phytoplankton incubations were conducted under artificial white light, different from the real *in situ* light climate. This issue has been resolved by proposing α corrections using information based on the spectral dependence of this parameter with respect to measurements of the *in situ* light spectrum (Kyewalyanga et al., 1992; Laws et al., 1990; Schofield et al., 1991). At the same time, Laws et al., (1990) highlighted a good fit between the absorption spectra of microalgae and the underwater light quality, unlike Lewis et al., (1985a). In this last study, the sampled microalgae at different depths were probably not sufficiently conditioned to the *in situ* available light climate, subjected to intense vertical mixing (Laws et al., 1990).

Among the earlier works on wavelength dependency of α, the study of (Kyewalyanga et al., 2002) was one of the few interested in the temporal dynamic of α spectral dependency. Variations in absorption spectra have received more attention in time series measurements

(Sathyendranath et al., 1999; Lutz et al., 2003; Hickman et al., 2009; Lutz et al., 2016b; Barlow et al., 2017). The targeted time scale of Kyewalyanga et al., (2002) was the season since their sampling was conducted during 20 weeks between August and December, once a day at 9:00 a.m. for 4 depths. This previous study evidenced that it was the occurrence of a red tide bloom (*Mesodinium rubrum*) that caused the main change in the photosynthetic action spectra despite some significant changes of environmental factors at the same time. In other words, this result is consistent for a species with a unique pigmentary characteristic. It is clear that according to dominant microalgae groups, the spectral signatures of photosynthesis could be different without immediate link with the optical properties of water mass (Lewis et al., 1988). However, another factor is known to change the shape of photosynthetic action spectra: photoacclimation to light quality and intensity (Johnsen et al., 1994, p. 199; Johnsen & Sakshaug, 1993; Sakshaug, 1993; Schofield et al., 1996) a process more particularly studied on laboratory cultures (Glover et al., 1987; Holdsworth, 1985; Hauschild et al., 1991; Callieri et al., 1996; Mouget et al., 2005; Lawrenz and Richardson, 2017; Schofield et al., 1990, 1996; Schreiber & Klughammer, 2013; Szabó et al., 2014a, 2014b; Herbstová et al., 2015; Luimstra et al., 2018, 2020a). As a consequence, a fundamental question remains to be addressed: the question of the temporal variation of all photosynthetic parameters on P-E curves, measured spectrally on field samples, from the short (day) to the large temporal scale (seasons).

The study of temporal variation of wavelength dependency of photosynthesis on natural phytoplankton communities is relevant because nowadays techniques for reliably measuring photosynthetic parameters at 5 wavelengths in relative and absolute units have emerged (Gorbunov et al., 2020; Schreiber et al., 2012). In the past, measurements with the 14C tracer and multispectral phytoplankton incubations were a long and complex task to be carried out (Kyewalyanga et al., 1997). The current MULTI-COLOR-PAM and the work of Schreiber et al., (2012) measuring the functional absorption cross section of photosystem II ($Sigma(II)_{\lambda}$ at 5 wavelengths), i.e. showed the great potential of this tool to characterize the absolute absorbed light by the cells at the time of measurement, in association with the PSII pigments. In addition, α and $Sigma(II)_{\lambda}$ are directly related because α is proportional to the functional cross section and to the number (n) of photosynthetic units (PSU) (Falkowski, 1992; Falkowski & Raven, 2007). Therefore, this contemporary technical approach revives the interest of the question of the photosynthetic action spectra variations, related to biotic and abiotic disturbances of ecosystems at different time scales.

In coastal system like Eastern English Channel characterized by a strong bloom of *Phaeocystis globosa* in the spring, earlier works have already shown that microalgae photoacclimation can occur between two periods of vertical tidal mixing in neap tide (Lizon et al., 1995), but also potentially in spring tide condition (Lizon et al., 1998). They have also shown that a nested sampling design was required to characterize the short (tide and/or intraday) as well as long-term variability (within months, monthly and seasonal) of photosynthetic parameters to reliably estimate the temporal variability of photosynthetic activity of microalgae and avoid potential problems of aliasing (Houliez et al., 2015). During an specific period coastal temperate ecosystem,an spatial analysis carried out thanks to the current MULTI-COLOR-PAM (Chapter II cited below as Michel-Rodriguez in submission) have evidenced the wavelength dependency of photoacclimation processes thanks to the definition of the spectral balance of available energy between blue and red wavelengths. This work has proven that natural phytoplankton communities can photoacclimate to different light quality conditions by a general model of photoprotection against blue light despite the strong vertical mixing conditions. That work have been perfomerd during a bloom period with a stable phytoplankton community dominated with brown algae with a codomination of diatoms and *Phaeocystis globosa*. Considering the importance of photosynthetic activity variation in function of time, the question would be how may take place wavelength-dependent photoacclimation proceses, i.e.: how phytoplankton communities may response at that different time scales under the effects of environmental conditions and temporal phytoplankton succession with communities with different absorption capacity and photoprotection strategies.

In summary, the central issues of this study of wavelength dependency of photosynthesis are:

-Is the wavelength dependent photosynthetic activity and photoregulation/photoacclimation of *Phaeocystis sp*. Spring bloom singular? Do *Phaeocystis sp.* present a particular wavelength dependent absorption capacity, photoprotection strategy and energy allocation?

-How the wavelength dependency of the photosynthetic processes vary according to the tide and/or the season? That is to say: discreetly in response to environmental change regardless of the time scales involved, or continuously in relation with the phytoplankton successions? The environmental changes here may assume the physical and chemical parameters modulating the light available for photosynthesis at all time scales (of potential variations).

-How are the spectral balances of energy performed in function of the different photoprotection states and absorption capacity of the different phytoplankton groups?

To address these issues, a sequential framework of statistical analysis that has already shown reproducible results on spatial scale was carried out (Michel Rodriguez et al., in submission). This statistical analysis is based on Linear Mixed Effects Model (LMEM) with a specification of the temporal hierarchical structure of the data, Partial Triadic Analysis (PTA) and Redundancy Analysis (RDA) was carried in order to define the general wavelength dependency of photosynthesis and the posterior analysis of the individual variations quantification and the analysis of the controlling factors respectively.

3.2 Material and methods

3.2.1 Sampling area and strategy

Sampling was conducted in the foreshore surface waters near the Laboratory of Oceanology and Geosciences (LOG) at Wimereux (50º; 45'; 47''N 1º; 36', 18''E) located on the Eastern English Channel (France) (Figure III.1). The Strait of Dover is characterized by a macrotidal hydrodynamical regime with a tidal range between 3 and 9 meters during neap and spring tides respectively, and a parallel circulation to the coast known as "the coastal flow" (Brylinski et al., 1991). The sampling area is therefore likely to be impacted by river inputs from the south, as well as the coastal water mass up to the 20 or 30 m isobaths (Brylinski and Lagadeuc, 1990). Furthermore, this area is very productive (Brunet et al., 1992) and presents well defined seasonal phytoplankton succession characterized by a local *Pheaocystis globosa* bloom during spring and different diatom communities following that bloom in summer and autumn/winter (Houliez et al., 2013a; Schapira et al., 2008).

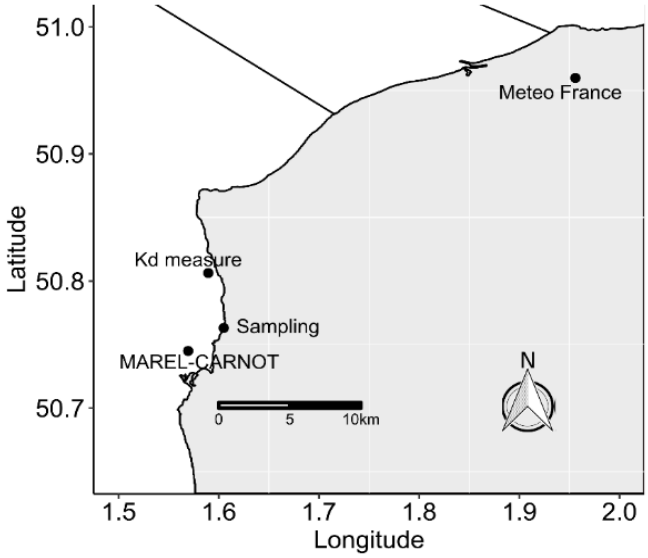

Figure III.1 : Locations of sampling and data acquisition. Latitude and longitude are given in decimal degrees.

A total of 48 samples were collected from 4th April to 2nd December 2019 at 25 dates with two sampling a day at high tide and low tide (except two dates with only one sample at low tide). Sampling was carried out weekly during the regional spring bloom period of *Phaeocystis globosa* (April and May) and fortnightly afterwards. Such a regular sampling frequency is only possible from the shore because of the strong wind conditions often encountered in the Eastern Channel. Cells from surface water were collected with a phytoplankton net with a mesh of 20 µm for further measurements. The phytoplankton community structure was determined in these concentrated samples. At the same time, surface water was sampled with a bucket for chemical measurements and natural (not concentrated) phytoplankton community structure determination. Sampling was carried out under the same tidal conditions but different diurnal conditions. To characterize the potential influence of light history in the physiology state of microalgae, the number of hours elapsed from sunrise to sampling time (TSS) was also calculated.

3.2.2 Controlling variables of wavelength-dependent photosynthesis

Natural phytoplankton communities were concentrated to obtain the sufficient density to perform quality measurements about sigma PSII with the technic used to study the wavelength dependency of photosynthesis, i.e. the MULTI-COLOR-PAM PAM (method described in

below sections). Environmental physicochemical variables of sea water together with light regime estimations were defined as the growth conditions of such phytoplankton community sampled. This approach of sample concentration have aready been used on photophysiological spectral signal analysis at a spatial scale proving a suitable method and providing quality results for the study of spectral photophysiological state of microalgae and its ecological implications (Michel-Rodriguez et al., in submission).

a) Abiotic variables: compilation of *in situ* environmental variable observations

Seawater aliquots were stored at -20°C until further processing for inorganic dissolved nutrient concentration. Concentrations of Nutrients (NO_3^-,NO_2^-, $Si(OH)_4^-$, PO_4^-) were measured with an Alliance Integral Futura Autoanalyser II according to the method of Aminot et Kérouel, (2007).

The Temperature (ºC), the salinity and the turbidity (ntu) were obtained from the Marel-Carnot automated measuring station (IFREMER) located 5 km south of the sampling site (50º44'42''N, 1º34'10''E) (Figure III.1). Data are available via the database Coriolis (Lefebvre et al., 2015) with a recorded resolution of 20 minutes and were hourly averaged. Only data corresponding to the sampling dates were selected. Tide height at sampling time was extracted from the French Hydrographic and Oceanographic Service of the Navy tables (for Boulogne-sur-Mer 50° 43' 38.8" N, 001° 34' 39.7"). The rainfall (mm) and Global Solar Radiation (GSR) (J cm^{-2} h^{-1}) were achieved from environmental data recorded at Calais (Figure III.1) (50°57'35"N, 1°57'21"N) (France) by Météo France (https://donneespubliques.meteofrance.fr/). From the daily rainfall data, the cumulative rainfall over two days was calculated to consider the potential rainfall effect on phytoplankton productivity. Hourly integrated measurements of GSR were used to estimate Photosynthetically Active Radiation (PAR µmol.photons.$m^{-2}s^{-1}$). First, GSR was converted to PAR (in the air surface of sea water) by assuming PAR being 50% of GSR and by considering 1 W m^{-2} = 0.36 µmol.photons.m^{-2} d^{-1} (Morel and Smith, 1974). Irradiance at sea surface (I_{W0}) was estimated assuming an additional average and theoretical loss of 50% due to the air-water interface (Kirk, 2011). In order to describe the light regime in the euphotic layer, the downwelling attenuation diffuse coefficient of underwater light (K_d) calculated from PAR vertical profiles (from TRIOS measurements) realized at the nearest coastal sampling point of an inshore-offshore transect in the Saint Jean Bay (just in front of the sampling site) during-regular campaigns to study seasonal

phytoplankton dynamics at sea, in coastal waters (DEPSEPC 2019 -CPER MARCO) was used. When dates did not match between the two sampling sites, a linear extrapolation was made between two consecutive dates in order to compute a $K_{d(PAR)}$ value. The subsurface light intensity (I_{wz}) was calculated following equation (1) at z=1m depth, considering the sample site:

$$I_{wo} = \frac{[I_{wz}\ (1 - \ e^{-K_d * z})]}{K_d * z} \qquad (1)$$

where K_d is the downwelling attenuation diffuse coefficient of underwater light, I_{w0} and I_{wz} are the photon fluency rates (µmol.photons.m^{-2}.s^{-1}) at the surface and at depth z (m) respectively (Kirk, 2011).

The averaged light intensity (E_{avg}) in mixing layer (Z_{uml}) in which sampling was caried out in order to evaluate the seasonal evolution of light, was calculated by the integration of K_d from open coastal water using equation 2 as (Riley, 1957). These values could be submitted to a certain overestimation due to the estimation of K_d

$$E_{avg} = \frac{I_0\left(1 - e^{\left(-K_{d(PAR)} x Z_{uml}\right)}\right)}{K_{d(PAR)} x Z_{uml}} \qquad (2)$$

Where Z_{uml} was fixed in this study at 1.5 m according to the depth of the water layer sampled by the net.

Yellow substances of sea water were measured by the FluoroProbe sensor (a multi spectral fluorometer, bbe, Moldaenke, described below) at 370 nm (see Beutler et al., (2002), for further informations). Yellow substances are known to influence the light quality regime in sea water and therefore the studied wavelength-dependent photosynthetic processes, more particularly at short wavelengths.

b) Biotic variables: phytoplankton groups and pigments analysis

Total biomass and the biomass of functional phytoplankton groups were estimated in a natural and in the concentrated sample (using a net) respectively by the multi-wavelength fluorescence technique of the FluorProbe sensor (bbe, Moldaenke). This fluorometer can discriminate four different spectral algal groups in mixed populations: i) diatomophyceae plus dinophyceae as

brown algae; ii) *Cryptophyceae*; iii) *Cyanophyceae* and iv)*Haptophyceae*, *Phaeocystis globosa* in the Eastern English Channel (see the work of Houliez et al., (2012b)). The same selection of spectral fingerprints (related to the previous cited groups) was kept during the full period of the present seasonal study as Houliez et al 2015. Previous works have shown that this method is effective and practical (Houliez et al., 2013a; Kring et al., 2014). Sample measurements were made using a dedicated cuvette of 25 mL and were always expressed in Chla equivalent ($\mu g.L^{-1}$) In order to accurately measure the photobiological variables, all samples were adjusted to a total Chla concentration of 150 $\mu g.L^{-1}$ by the Fluoroprobe immediately after sampling. The community of interest in this study is the actual one that resulted from the concentration process, independently of the community structure in the original sea water.

Pigment analysis was performed on concentrated samples on which photophysiological measurements were realized. First, samples were filtered through Whatman 25 mm GF/F glass-fiber filters. The filters were then stored at -80ºC until posterior High-Performance Liquid Chromatography (HPLC). Pigment content was extracted by grinding the filters with methanol and small drops of methylene chloride under dim light. Extracts were filtered on polytetrafluoroethylene membranes (0.45 μm) and dry-evaporated under nitrogen. Salt contents of the extract were removed in a distilled water: methylene chloride: mixture (50:50, v/v). The organic phase containing pigments was then evaporated with nitrogen and dissolved again in 40 μL methanol for injection. 20 μL were injected in a high performance liquid chromatography (HPLC) (Shimadzu, Nexera XR) equipped with a C18 reverse-phase column (Allure, Restek). Pigment contents were analyzed using a solvent delivery profile adapted from Arsalane et al., (1994).

In order to analyze the different energy transfer pathways within the phytoplankton communities and the photoacclimation state across the seasons, pigment concentration results were used to estimate :i) total photoprotective carotenoid pigments (PPC, following equation 3); ii) total photosynthetic carotenoids pigments (PSC, Eq. 4) as (Eisner et al., 2003; Barlow et al., 2013); iii) the de-epoxidation state (DES, Eq. 5) as Brunet et al 2014; i.e, the diadinoxanthin (Dd) de-epoxidation into Diatoxanthin (Dt); iv) total photosynthetic pigments (TP, following equation 6); For each calculation, the cis- and the trans- form of pigments were considered. Finally, total pigment concentrations were used to compute weighted values of PPC and PSC respectively, for each concentrated sample obtained at low and high tide.

$$\text{PPC} = \text{Violaxanthin} + \text{Zeaxanthin} + \beta\text{-carotenoid} + \text{Diadinoxanthin} + \text{Diatoxanthin} + \text{Alloxanthin} + \text{Lutein} \quad (3)$$

$$PSC = 19'Buta + 19'H + Peridinine + Fucoxanthin \quad (4)$$

Where 19'Buta is 19'-Butanoyloxyfucoxanthine and 19'H is 19'Hexanoyloxyfucoxanthine.

$$DES = Diatoxanthin/\ (Diadinoxanthin + Diatoxanthin) \quad (5)$$

$$TP = TChla+TChlb+TChlc+PSC+PPC \quad (6)$$

Where TChla, TChlb and TChlc are total chla, chlb and chlc respectively.

The objective of concentrate samples treatment was to keep the biomass concentration of samples constant. This is observed on fluoroprobe measurements results, but total pigment concentration presented a temporal increase trend from April to December. This trend was corrected with total pigment weighted values.

3.2.3 Wavelength-dependent photosynthesis measurements

Photosynthetic activity was studied following the same protocol as Michel-Rodriguez et al., (in in submission) to study the spectral dependency of phytoplankton at great spatial scale across the English Channel in spring 2018. For that, variable chlorophyll fluorescence measurements were conducted, using the Multiple Excitation Wavelength Chlorophyll Fluorescence Analyzer MULTI-COLOR-PAM (MC-PAM, Walz, Heinz Walz, GmbH, Germany). This device, fully described in Schreiber et al 2012, comprises 5 different peak-wavelengths (440, 480, 540, 590 and 625 nm) of pulse-modulated measuring light (ML) and continuous actinic light (AL) for single turnover and multi-turnover of saturation protocols (MT and SP, respectively).

In order to accurately measure physiological parameters without light history influence and completed oxidation of all reaction centers (RCII) (From et al., 2014), fast kinetics and automated rapid light curves measurements were realized on dark acclimated samples during a period of 1.5 h and kept in controlled conditions until analysis (temperature close to sea water and 100 rpp of agitation using a MINITRON Incubator). This dark acclimation time is the result of a compromise of sampling strategy. Samples were collected at high and low tide. The period of 1.5 dark acclimation before MULTI-COLOR-PAM aims to homogenize the time for both high and low tide while avoiding potential light perturbations on the transport of samples from

the field to the laboratory. Next, the PAR-list was measured for each sample with the help of a magnetic stirrer. The zero offset (background signal) was determined on 0.2µm filtered samples, and the current fluorescence Ft level was fixed to 0.5 ± 0.05 (relative units) by adjusting the measuring Light (ML) and the Gain settings (following Schreiber et al., 2012; Szabó et al., 2014a).

The wavelength-dependent functional absorption cross section of PS II, here called $Sigma(II)_{\lambda}$, was measured during fast kinetics measurements with the help of the pre-programmed fast kinetic trigger file "Sigma100.FTM" (Schreiber et al., 2012). Each $Sigma(II)_{\lambda}$ was obtained after three consecutive measurements separated by 10 seconds (Klugammer & Schreiber 2015) at each wavelength. The $Sigma(II)_{\lambda}$ values presented here are the result of measurements on six different sample pseudo-replicates. After that, the rapid light curves (RLC) were performed by triplicate at each of the five wavelengths cited above. RLC were measured using 14 increasing light intensity sequential pulses of 20 s and 300 µs width and intensity based on PAR-list with identical wavelength for ML and AL. The effective quantum yield was defined as Eq. 7 at each light step in function of the maximal fluorescence yield during illumination (F'_m) and the variable fluorescence ($F_v=F_m-F$ after dark acclimation and $F'_v=F'_m-F$ under actinic light). The maximum quantum yield of PSII (Y(II) or F_v/F_m) was defined with an initial step of 0 $\mu mol.m^{-2}.s^{-1}$ under dark acclimation conditions and was used together with an ETR factor of 0.5 (equal photon absorption between PSII and PSI) to define the relative electron turnover rate (rETR) (Eq 9). At each light step, the non-photochemical quenching (NPQ) was also calculated as the normalized Stern-Volmer quenching coefficient (Eq. 8). Finally, the photon absorption rate (PAR(II) as Schreiber et al 2012) was calculated following the Eq. 10. The electron turnover rate of PSII (ETR(II) in absolute absorption units was finally calculated following Eq. 11.

$$Y(II) = \frac{F'_m - F}{F'_m} \quad (7)$$

$$F_V/F_m = \frac{(F'_m - F_m)}{F_m} \quad (8)$$

$$rETR = Y(II)\ x\ PAR\ x\ 0.5 \quad (9)$$

$$PAR(II) = Sigma(II)_{\lambda}\ x\ L\ x\ PAR \quad (10)$$

$$ETR(II) = PAR(II)x \left(\frac{Y(II)}{F_V/F_m} \right) \quad (11)$$

Fitting was performed into three different light curves: i) rETR vs PAR; ii) ETR(II) vs PAR(II) and iii) NPQ vs PAR curves in order to estimate the photosynthetic parameters and the light dynamic of non-photochemical quenching. First, Eilers and Peeters, (1988) model was used to fit rETR vs PAR and ETR(II) vs PAR (II) curves and for estimation of the photosynthetic efficiency (hereafter α, the initial slope of RLC), the photosynthetic capacity or maximum electron turnover rate (ETR_{max}, the saturation level) and E_{op} (the optimum light parameter) in relative (r) and absolute (II) units. The light saturation parameter E_k (the curvature of the photosynthesis light curve) was also computed in the two units as $E_{k,\lambda} = ETR_{max,\lambda}/\alpha_\lambda$ (Talling, 1957). Light response curve fittings were achieved with "fit" function in R package "Phytotools". Secondly, The Michaelis-Menten model was used to fit NPQ vs. PAR curves. A linear regression forcing the intercept to pass through zero was used when kinetics of NPQ vs PAR curves differed from Michaelis Menten model. Fitting was achieved thanks to "nls2" for Michaelis-Menten model function and "lm" for linear regression. As two models were used, NPQ values were back-calculated using the calibrated models at two different irradiances (of photosynthesis light curves) for each of the five wavelengths: one at low PAR (100 µmolphotons.m^{-2}.s^{-1}) and a second at high PAR values (1000 µmolphotons.m^{-2}.s^{-1}) for very saturating conditions.

In order to estimate the phytoplankton photoacclimation state of each sample, the ratio between $E_{k,440}$ and E_{avg} in the sampling water column was calculated. In the same idea, the slope between different pairs of wavelengths of interest (625 and 440, 540 and 440 and 540 and 625 nm in this study) were also computed, i.e: $(param_{625}\text{-}param_{440})/(625\text{-}440)$; $(param_{540}\text{-}param_{440})/(540\text{-}440)$ and $(param_{625}\text{-}param_{540})/(625\text{-}540)$ for values of $Sigma(II)_\lambda$, $NPQ_{PAR=100}$, $NPQ_{PAR=1000}$ and E_k, in order to deepen the understanding of changes in spectral balance of light absorption capacity, energy utilization and photoacclimation state. These photosynthetic slopes were then compared to PCC/PSC ratios and DES from HPLC measurements (Eisner et al., 2003).

3.2.4 Statistical analysis

All statistical analyses were performed with R version 4.0.0.

Separated Principal Component Analysis (PCA, (Legendre & Legendre, 2012) were performed for abiotic and biotic variables in order to reveal the seasonal structure of our data with "PCA" function of "FactoMineR" package (Husson et al., 2020; Lê et al., 2008). Hierarchical Clustering on Principal Components was performed to analyze which was the temporal seasonal structure within abiotic and biotic variables. The agglomerative hierarchical cluster partition was defined as the one with the higher relative loss of inertia automatically proposed using "HCPC " function of "FactoExtra" R package. Results of both abiotic and biotic clusters were combined to set the seasonal periods which were considered for temporal structure on Linear Mixed Effects Model (LMEM, see below). Samples of the same day were always associated in the same period. In case of different aggregation among clusters for two samples of the same day, the more likely period considering the closer days to that date. For three dates, discrepancies appeared between samples for abiotic and biotic clustering. That was the case for May 15th, June 12th and October 16th (see results).

The statistical analysis of photosynthetic parameters followed here the same general approach used in our previous study about spatial variability (Michel-Rodriguez et al., in submission) with a series of cascading statistical analyses. For this temporal study, a particular attention has been paid to the hierarchical structure of the sampling time scales, since samples were collected at high and low tide within a day, for different days across different seasons.

First, linear mixed effects model (Bates et al., 2015; Zuur, 2009) was used to analyze the spectral dependency between dates of photosynthetic parameters by separating the explained variance from the main effects. LMMEs were fitted using the "lmer" function of "lme4" R package (Bates et al., 2019). Linear regression was used for all studied photobiological parameters. A nested temporal structure was defined in the random effects of the model considering that photosynthetic processes vary seasonally, fortnightly and/or at different tidal scales (Houliez et al., 2015). Henceforth, random effects were defined as the individual variation from the general tendency according to the tidal conditions and the seasonal periods (Figure III.2) that have been previously defined from the PCA clustering analysis results. The aim was here to clarify the temporal structure of environmental and phytoplankton community data sets as potential controlling factors of photosynthetic processes. The formulation of nested random effects significantly improved a single individual sample random effect compared to a case study without a hierarchical structure. As a result, random effects were studied between periods (3 grouping factors, see results), between different tidal conditions within each period (6 grouping factors) and between the 48 individual samples (the complete data set). Hypothesis

tested are based on F tests for fixed effects (using Satterthwaite's method for denominator degrees-of-freedom) and likelihood ratio tests for random nested models that asymptotically follow a χ^2 under the null hypothesis for random effects' (co-)variances (Pinheiro and Bates, 2000). The p-values for fixed and random effects were performed using "anova" and "ranova" functions "lmerTest" (Kuznetsova et al., 2019). Wavelength values were transposed from 440 to 625, to 0 to 185 nm in order to decrease the uncertainty of the model intercept.

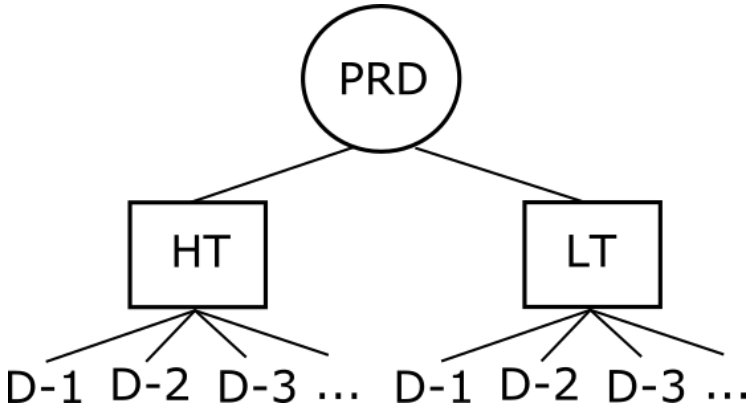

Figure III.2 : Diagram of nested temporal structure of random effects. PRD for period. HT and LT for high and low tide respectively and D for Day of sampling. This same nested temporal structure was implemented for each seasonal period PRD. Each PRD was defined in function of Hierarchical Clustering of abiotic and biotic variables (see results).

Secondly, the individual differences to the general mean spectral tendency (detrended spectral data) were calculated and used in a Partial Triadic Analysis (PTA) (Thioulouse, 1987). This analysis is a particular case of the so-called "multitable" analysis which aims to catch the overall typology among spectral photosynthetic responses, the commun responses and detailed description of differences to commum responses. PTA was performed with "pta" function of "ade4" package (Dray et al., 2018) and "adesgraphics" (Siberchicot and Julien-Laferrière, 2018) for graphical representation. The so-called cube data here was composed by five tables (one by measurement wavelength) with n=8 columns as number of photosynthetic parameters and N=48 rows as the number of total samples. Before PTA analysis, each wavelength k-table was centered, and the resulted tables together were normed and stocked as a ktab object for posterior PTA analysis ("withinpca" and "ktab" function of "ade4" R package). PTA analysis was performed following the well–known three steps analysis: interstructure, compromise and intrastructure for co-variance of wavelengths, mean and variance structure between samples respectively.

Third, a Redundancy Analysis (RDA) was performed on detrended spectral data of some photobiological parameters at each wavelength in order to characterize the relationships between individual spectral responses of photosynthetic activity and the potential controlling factors (abiotic and biotic variables). “forward.sel” function of “adespatial” (Dray et al., 2019) R Package was used in order to select the more parsimonious model. Forward selection was based on the R^2 adjusted value as well as the p-value for 199 permutations.

3.3 Results

3.3.1 Abiotic and biotic conditions

Abiotic and biotic variables displayed a clear common temporal structure with three distinct and contrasted periods (ou PRD) from Hiercharchical Clustering analysis: i) Spring period from April 4th to May 15th ; ii) Summer period from May 22nd to September 17th and iii) an Autumn period from October 24th to December (Figures III.3-B and III.4-B). May 15th and June 12th dates were assigned to spring and summer periods respectively, even if their characteristics differed between the two, abiotic and biotic, PCA. At these two dates, the phytoplankton community structures were similar to the other nearby samples in the first PCA plan of biotic variables, but their environmental conditions were different to the other nearby samples in the first PCA plan of the abiotic variables.

PCA 1st and 2nd axis of abiotic variables explained 46.3 % of total inertia (Figure III.3-A). First axis was related to nutrient concentrations, yellow substances, and rainfalls while the second axis is related to temperature, salinity, light intensity and light penetration capacity in water column (K_d) (Figure III.3-A). Spring period was characterized by high K_d values (ranging between 0.4 and 0.8), and low nutrient concentrations (under 2, 0.5 and 2 µmol.L^{-1} of dissolved nitrogen, phosphates and silicates respectively). Summer period presented the highest salinity and temperature values (34-35 salinity units and between 15 and 20 ºC), low K_d values (between 0.2 and 0.5) which progressively increased from summer to autumn when values reached 0.6. During spring and summer, irradiance varied between 100 and 600 µmol.photons.m^{-2}.s^{-1} while in autumn, values were the lowest (under 200 µmol.photons.m^{-2}.s^{-1}). Moreover, during autumn nutrient concentrations were the highest (reaching 5, over 0.5 and between 1 and 5 µmol L^{-1} of dissolved nitrogen, phosphates and silicates respectively) and rainfalls had the most important cumulated values (ranging 10 mm and reached values of 20 mm during the two dates discussed above, May 15th and June 12th). Autumn samplings were characterized by a clear increase of

yellow substances, (or Chromophoric Dissolved Organic Matter CDOM) with concentrations between 0.5 and 1 µg.L^{-1}. Turbidity had a low contribution to total explained variance, nevertheless this variable displayed some increases (over 50 ntu) at each of the three seasons evidenced on the time series plot of this parameter (beginning of May, July and December; Figure III.3-A). The sample light histories (described here by the TSS variable) and the tide height did not explain neither the seasonality from PCA analysis (Figure III.3-A) presenting both low contributions to PCA analyses. However, it should be noted (Figure SM III.1) that TSS values were highly variable during the spring period compared to the summer and autumn periods: TSS displayed variations ranging from 2 to 6h in spring, and less than 2h in autumn. All high tide samples were obtained with an averaged water height of 8 m while at low tide, averaged water height was only of 2m.

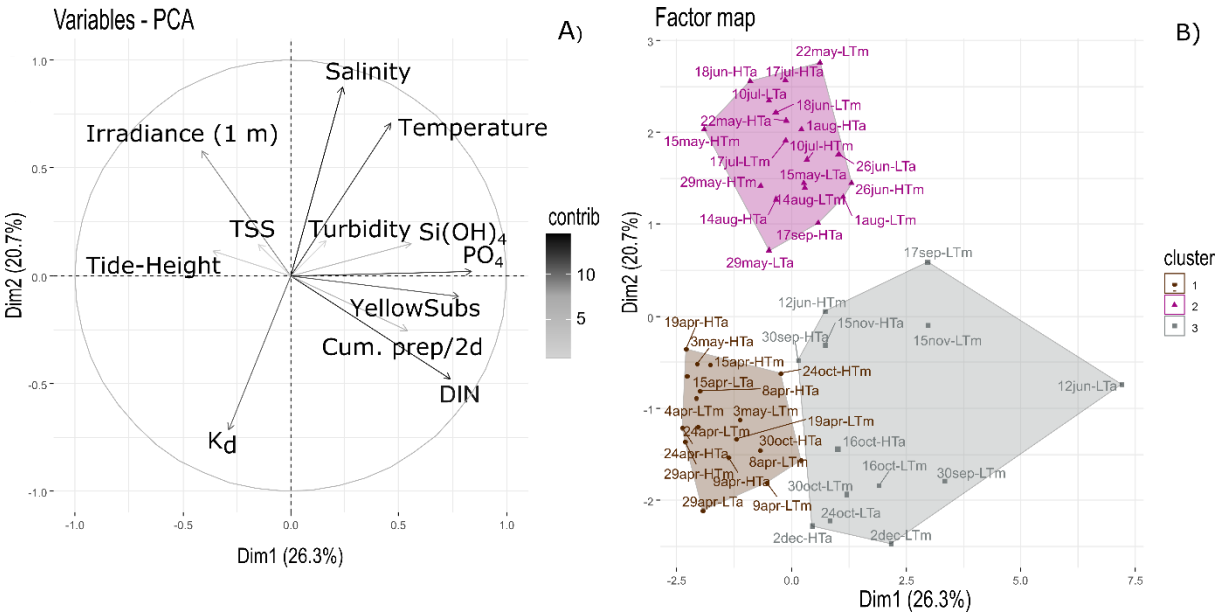

Figure III.3 : A) Principal components analysis (PCA) of environmental conditions (Temperature (◦C), Salinity, Turbidity (ntu), Silicates (Si(OH)2), NO_3+NO_2 (DIN) and phosphates (PO_4) in µmol.L^{-1} , PAR at 1 m depth (Irradiance in µmol photons m^{-2} s^{-1}), Tide Height (m), Time since sunshine (TSS in hours), 2 days cumulated rainfall("Cum.prep/2d", mm), yellows substances("Yellow Subs", µg.L^{-1}). Gray color scaling refers to the contribution (contrib) of each variable to PCA analyses. B) Hierarchical Clustering on PCA individuals. Labels of sampling dates are noted by the day and the month of sampling followed by the tide (LT for low tide and HT for High Tide) and "m" (if sampling was done in the morning) or "a" (if sampling was carried out in the afternoon). The significant clusters found (equivalent to seasonal periods named as PRD after) are: Spring (brown), Summer (purple) and Autumn (gray).

PCA on phytoplankton structure and pigment groups (PPC and PSC weighted to total pigments and de-epoxidation state or DES) showed similar temporal structure as abiotic variables (Figure

III.4-B). The main difference was the significant existence of a fourth cluster coñposed by sample on October 16th in low tide ("16oct_LT"). This sample presented a particular phytoplankton structure characterized by the total absence of *Phaeocystis globosa* in comparison to the rest of samples. This sample was collected during particular meteorological conditions of high hydrodynamism and turbidity (Figure SM III.2-D and 3). For simplicity, this fourth cluster was included with autumn period cluster and its particular characteristics considered in potential further discussions.

Spring period was characterized by the dominance of *Phaeocystis globosa* (95% of the total biomass) and an increase of de-epoxidation state (DES) corresponding to the fast photoprotective Cycle of Xanthophylls (diadinoxanthin (Dd) de-epoxidation into Diatoxanthin) (Figure III.4-A and Figure in SM III.4). By the end of April, DES decreased very sharply and showed some occasional and small increases in mid-June, late July and during the month of October (Figure SM III.4). Summer period had a co-dominance of *Phaeocystis globosa* with diatoms+dinoflagellates phytoplankton group and a correlation with high values of the photoprotective carotenoids (PPC) pool (Figure III.4-A and Figures SM III.3 and 4). The increase in PPC weighted to total pigments (TP) actually increased from the beginning of May until the end of July, then decreased and remained at median values until the end of the time series (Figure SM III.4). DES and PPC/TP were therefore generally alternating during the spring and summer periods. Finally, the Autumn period was defined mainly by the increase of *Cryptophyta* to more than 50 % of total biomass. *Cyanobacteria* covaried with diatoms+dinoflagellates and their presence varied between 10 and 20 % of total biomass during summer and autumn. Note that PSC/TP (Photosynthetic carotenoids weighted to total pigments TP) kept a constant value among sampling dates without any covariation with a specific phytoplankton group estimated from Fluoroprobe measurements (Figure III.4-A and Figures SM III.3 and 4).

Detailed description of abiotic variables can be found on supplementary materials on Figures SM III.1 and SM III.2 and in figures SM III.3 and SM III.4 for phytoplankton groups, PPC, PSC and DES from pigments HPLC analysis.

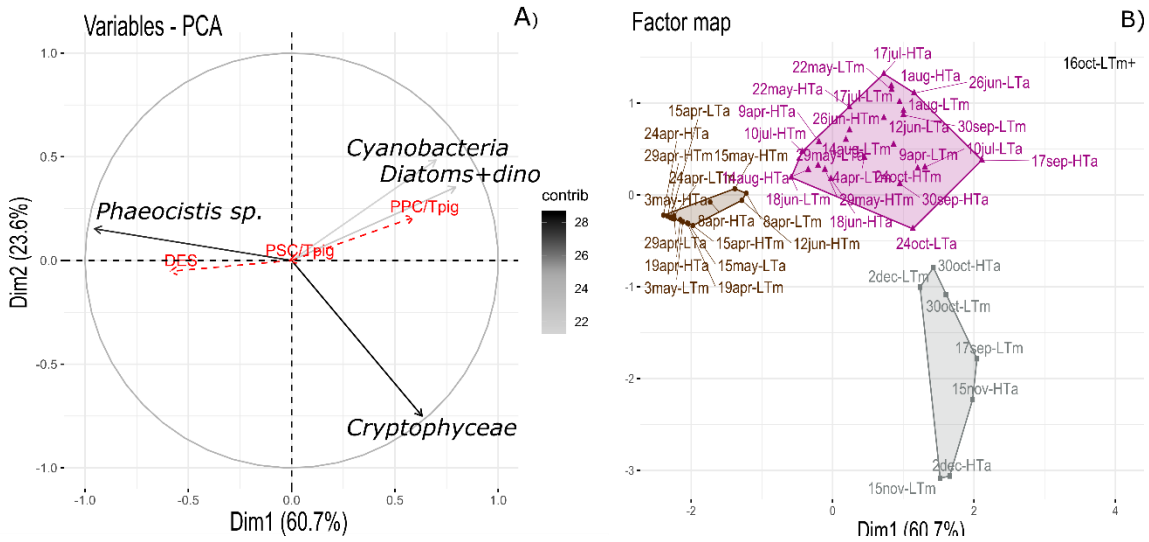

Figure III.4 : A) Principal components analysis (PCA) of phytoplankton biomass estimated with a FluoroProbe (Cryptophyceae, Diatoms+dinoflagellates named as "diatoms+dino", Cyanobacteria and Phaeocystis sp.). Gray scale color refers to the contribution of each variable to PCA analyses. Supplementary variables of energy regulation from HPLC pigment analysis (PSC: Total pigments and PPC: total pigments and DES) are shown in red. B) Agglomerating Hierarchical Clustering on PCA. Labels of sampling dates are noted by the day and the month of sampling followed by the tide (LT for low tide and HT for High Tide) and m (if sampling was done on the morning) or a (if sampling was carried in the afternoon) .The significant clusters found (equivalent to seasonal periods named as PRD after) are: Spring (brown), Summer (purple) and Autumn (gray)

3.3.2 Wavelength-dependent photosynthesis parameters

Raw data are displayed on figure III.5 and all statistical results of LMEM are reported in Table III.I. Population wavelength-dependencies were here first characterized by significant spectral trends of fixed effects of LMEM for half of the measured physiological parameters ($Sigma(II)_{\lambda}$, Fv/Fm, $r.ETR_{max}$, $ETR_{max}(II)$, $r.E_K$ and NPQ_{100}). In addition, four of the twelve physiological parameters ($Sigma(II)_{\lambda}$, $r.ETR_{max}$, $ETR_{max}(II)$ and NPQ_{100}) evidenced significant individual spectral trends considering the overall significance of the model (last column of Table III.I).

*Table III.I : Fixed estimates of linear mixed effects regression for photosynthetic parameters with standard error(SE) and significant codes for random variation at intercept (a) and slope (b) between periods (PRD), tides within periods (Tide/PRD) and between all samples (Sp/tide/PRD). Significant codes next to parameters refers to the significant analysis of the model (significant spectral variation). Hypothesis tests are based on t tests for fixed effects coefficients intercept and slope and likelihood ratio tests and p-value based on χ2 statistics. Significant code: 0 p-value <0.001'***' <0.01 '**' <0.05 '*' p-value>0.05 '.' Marginal significicativity (p-value >0.05 < 0.08), ns for non-significant values*

Fixed effects					**Random effects**						**Sig. of the model**
Estimates					Intercept (a) effects			Slope (b) effects			
	A (Intercept)	S.E	**B (slope)**	S.E	Sp/tide/PRD	Tide/PRD	PRD	Sp/tide/PRD	Tide/PRD	PRD	
Sigma(II)$_\lambda$	6.60 *	0.84	-0.03 *	0.003	***	ns	***	ns	***	**	*
Fv/Fm	$5.63\cdot10^{-1}$ ***	$2.89\cdot10^{-2}$	$-1.27\cdot10^{-4}$*	$2.80\cdot10^{-5}$	***	ns	ns	ns	ns	ns	*
ETR$_{max}$(II)	767.77 ns	94.43	-1.09 *	0.32	***	ns	***	ns	.	*	*
r.ETR$_{max}$	57.01ns	10.10	0.42 *	0.05	***	ns	ns	**	ns	ns	*
alpha(II)	0.70 ns	0.07	$8.33\cdot10^{-4}$ ns	$3.29\cdot10^{-4}$	***	ns	ns	ns	***	ns	ns
r.alpha	0.23 ***	$1.37\cdot10^{-2}$	$9.36\cdot10^{-5}$ns	$6.35\cdot10^{-3}$	***	ns	ns	ns	ns	ns	ns
E$_k$(II)	1141.66 *	154.94	-2.65 ns	1.09	***	ns	**	ns	ns	**	ns
E$_k$	250.26 ns	51.69	1.52 **	0.14	***	ns	ns	ns	ns	ns	**
E$_{op}$(II)	4068.45 **	516.84	-13.16 ns	4.30	***	ns	*	ns	ns	.	ns
E$_{op}$	1431.55 *	251.93	0.36 ns	1.12	***	ns	*	ns	**	.	ns
NPQ$_{100}$	0.29 ns	0.04	$-1.02\cdot10^{-3}$ *	$2.22\cdot10^{-4}$	***	ns	ns	ns	.	*	*
NPQ$_{1000}$	2.01 ns	0.34	$-6.14\cdot10^{-3}$.	$1.55\cdot10^{-3}$	***	ns	*	ns	ns	**	.

The analysis of fixed effects of LMEM revealed relevant information on light absorption capacity and energy flux variations as a function of wavelength. Firstly, Sigma(II)$_\lambda$ (the parameter that connects relative and absolute photosynthetic parameters) displayed a 4-fold decreasing trend along the spectrum from 6 to 1.5 nm^2. On the opposite, r.ETR$_{max}$ showed a 2.5 fold increasing trend (values ranged from 57 to 135 µmol electrons m^{-2} s^{-1}) in relative units. This trend was largely counterbalanced by Sigma(II)$_\lambda$ and the absolute parameter ETR$_{max}$(II) decreased significantly across the spectrum from bright blue (440nm) to light red (625nm) wavelengths (Figure III.5). Although α (in relative and absolute units) did not show a general significant trend on the spectrum, the r.E$_k$ parameter (resulting from the ratio between r.ETR$_{max}$

and r.α) displayed 2 fold increasing trend (values varied from 250 to 530 quanta $m^{-2}s^{-1}$) across the spectrum. On the other hand, E_k(II) did not present a significant trend despite the fact that mean values decreased from 1142 to 625 quanta(PSII.s^{-1}) at 440 and 625 nm respectively (a net 2 fold decrease). Finally, the maximum photochemical quantum yield F_v/F_m, which relates also the cell physiological state, and the two non-photochemical quenching estimates showed the same kind of decreasing trend as Sigma(II)$_\lambda$ but with different slopes (Table III.I). Fv/Fm (generally varying between 0.3 and 0.7 regardless of wavelength) evidenced a slight spectral trend, with 1.7 times higher values at 440 nm than at 625 nm but slope values close to zero. The population spectral trend for the two NPQ estimates would be related to the light intensity. Indeed, NPQ_{100} (i.e at low PAR values of 100 µmol electrons m^{-2} s^{-1}) showed the same trend (values ranging from 0.3 to 0.1) as Sigma(II)$_\lambda$, while for NPQ_{1000} (i.e. at saturated PAR of 1000 µmol.photons.m^{-2}·s^{-1}) there was no significant spectral trend (only a marginal significance was observed).

Random effects of LMME accounts for differences of samples to the population fixed tendency across wavelengths were analysed according to the hierarchical structure of the temporal sampling strategy. The results (Table III.I) evidenced significant individual spectral trends for Sigma(II)$_\lambda$, r.ETR_{max}, ETR_{max}(II) and NPQ_{100} but in different ways for each of these parameters according to time scales. At individual sample level, all parameters evidenced significant different intercepts indicating that the levels achieved by parameters were all different, but only $rETR_{max}$ showed significant different spectral slopes (Table III.I). Considering the sampling level in relation to the high and low tides, all parameters displayed non-significant different intercepts, but different slopes were achieved for Sigma(II)$_\lambda$ whatever the seasonal periods (considering the significant models, Table III.I). With regard to the three seasons, Sigma(II)$_\lambda$ and ETR_{max}(II) evidenced significant different intercepts, while Sigma(II) $_\lambda$, ETR_{max}(II) and NPQ_{100} revealed significant different spectral trends (slope) between seasons (Table III.I).

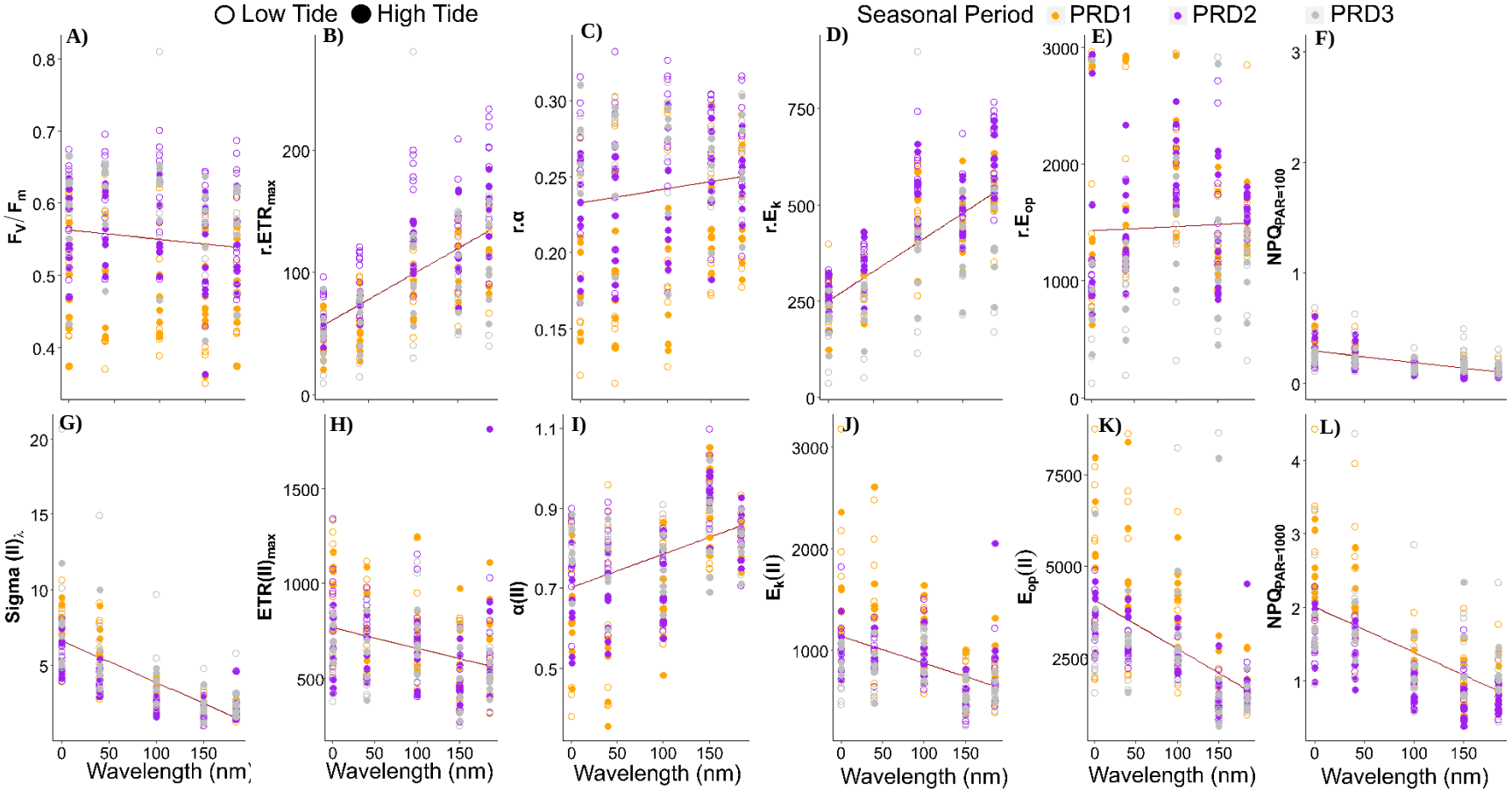

Figure III.5 : Spectral variation patterns of F_v/F_m (A), Sigma(II) (nm^2) (B), NPQ at 100 (K) and 1000 (L) µmol·photons·$m^{-2}s^{-1}$ and relative (C, E, G, I) and absolute (D, F, H, J) of relative and absolute ETR_{max} (µmol electrons s^{-1} and electrons(PS II s)$^{-1}$ respectively), relative and absolute α (electrons/quanta for both respectivelly), relative and absolute E_k (quanta $m^{-2}s^{-1}$ and quanta(PS.II.s)$^{-1}$ respectively), and relative and absolute E_{op} (µmol.quanta.m^{-2}·s^{-1} and quanta(PS.II.s)$^{-1}$respectivelly) measurements at high (closed circles) and low tide (open circles) at each seasonal period characterized on PCA and Hierchical Clustering of abiotic and biotic variables (PRD1 in brown for late spring PRD2 in purple for summer ; and PRD3 in gray for autumn). Fitted linear mixed effects model is shown with a solid dark red line. 440, 480, 540, 590 and 625 nm of measure have been transposed to 0, 40, 100, 150 and 185 nm in X axes for Linear Mixed Effets Model ditting(see M&M for details)

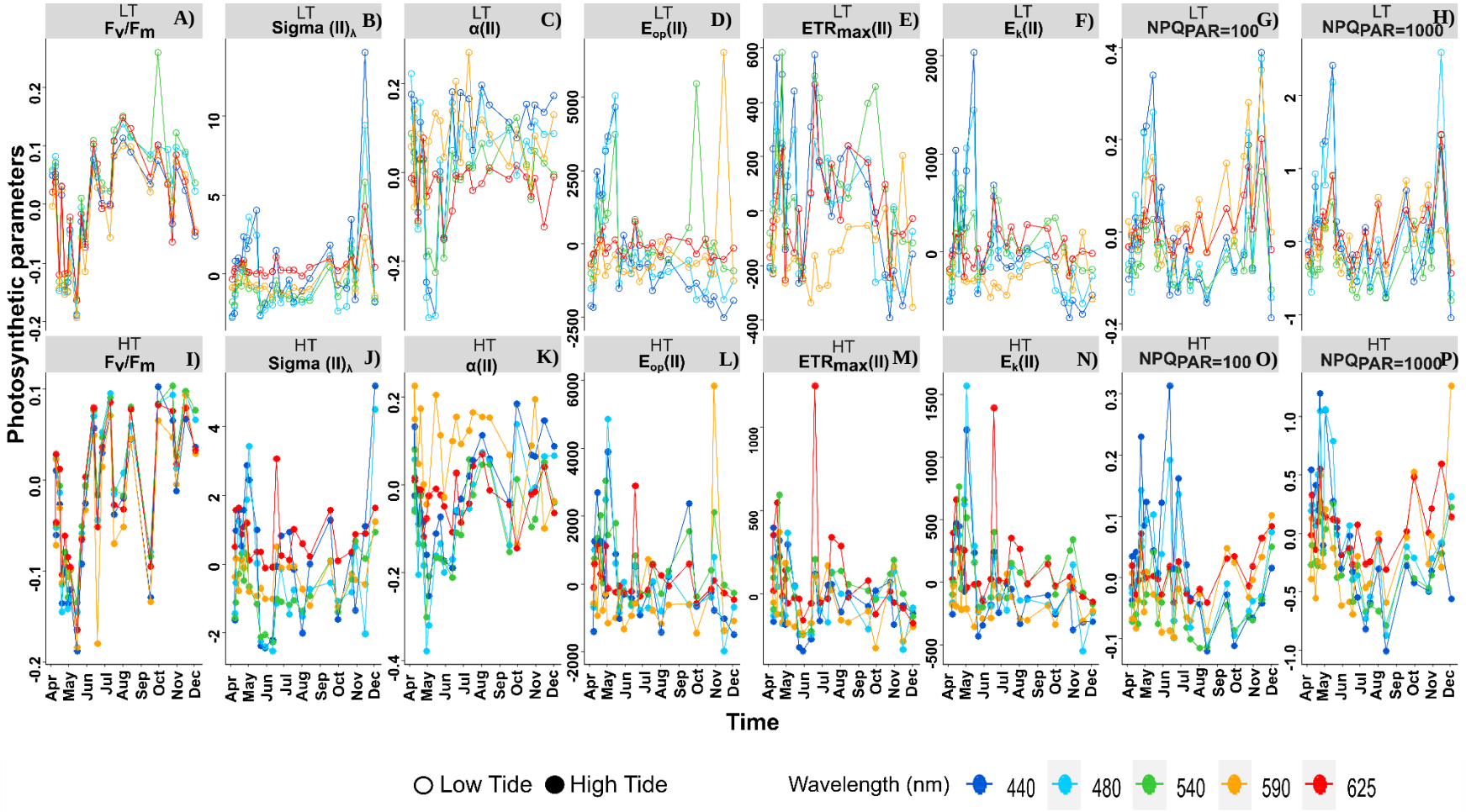

Figure III.6 : Variation of detrended photosynthetic spectral measurements of: F_v/F_m,(A and I) Sigma(II)$_\lambda$(B and J), α(II) (C and K), E_{op}(II)(D and L), ETR_{max}(II)(E and M), E_k(II)(F and N), and NPQ at 100 (G and O)and 1000 (H and P) µmol·photons·$m^{-2}s^{-1}$ for each photosynthetic parameter and samples for low tide (LT, open symbols) (A, B, C, D, F, G, H) and high tide (HT, closed symbols))(I, J, K, L, M, N, O, P). Point colors refer to each of the 5 wavelengths analyzed: bright blue, light blue, green, amber and light red for 440, 480, 50, 590 and 625 nm respectively

Figure III.6 displays the detrended photosynthetic parameters at each measured wavelength obtained from LMEM analyses. Random effects can be observed from the scattering as well as the time course of the five wavelength curves which differ according to the seasons for the three parameters cited above ($Sigma(II)_{\lambda}$, $ETR_{max}(II)$ and NPQ_{100}). This is particularly clear for the $Sigma(II)_{\lambda}$ at low tide and NPQ_{100} at high tide, but less for $ETR_{max}(II)$ (Figure III.6). Note that NPQ_{100} as well as NPQ_{1000} were particularly high at 440 nm in spring at high tide. Moreover, generally all parameters showed in blue higher variability from the zero level (which refers to the population mean value in LMEM) than amber and light red responses.

3.3.3 Sample wavelength-dependency as shown by Partial Triadic Analysis

A multivariate analysis through a PTA (K-tables method) analysis was conducted on detrended photosynthetic parameters obtained from LMEM analyses in order to capture the similarities within the five wavelength tables concerning all photosynthetic parameters. This analysis also highlights the changes in the relationships between the five measuring wavelengths. The analysis and its interpretation follow a three-step process: interstructure, compromise and intrastructure.

As a reminder, **interstructure** of PTA evidences the common features between variables of the five wavelength measures. The first two axes of PTA interstructure explained 65% of total inertia (Figure III.7-A) and the five wavelength tables presented similar weight (values ranging from 0.33 to 0.49; Table III.II) and a significant representation with cos^2 close to 1, excepted for the amber wavelengths (590nm table, Table III.II). There is a clear positive correlation (Figure III.7-A) between the five wavelengths which are all positively projected on the first axis (ca 65.26% of the total inertia Figure III.7-A) which account to relatively similar evolution of temporal detrended values. Axis 2 (18.36% of the total inertia, Figure III.7-A) discriminates between light red and amber wavelengths on the positive side and green and blue wavelengths on the negative side of this axis (Figure III.7-A). Amber wavelengths were also distinguished by being a little away from the other wavelengths.

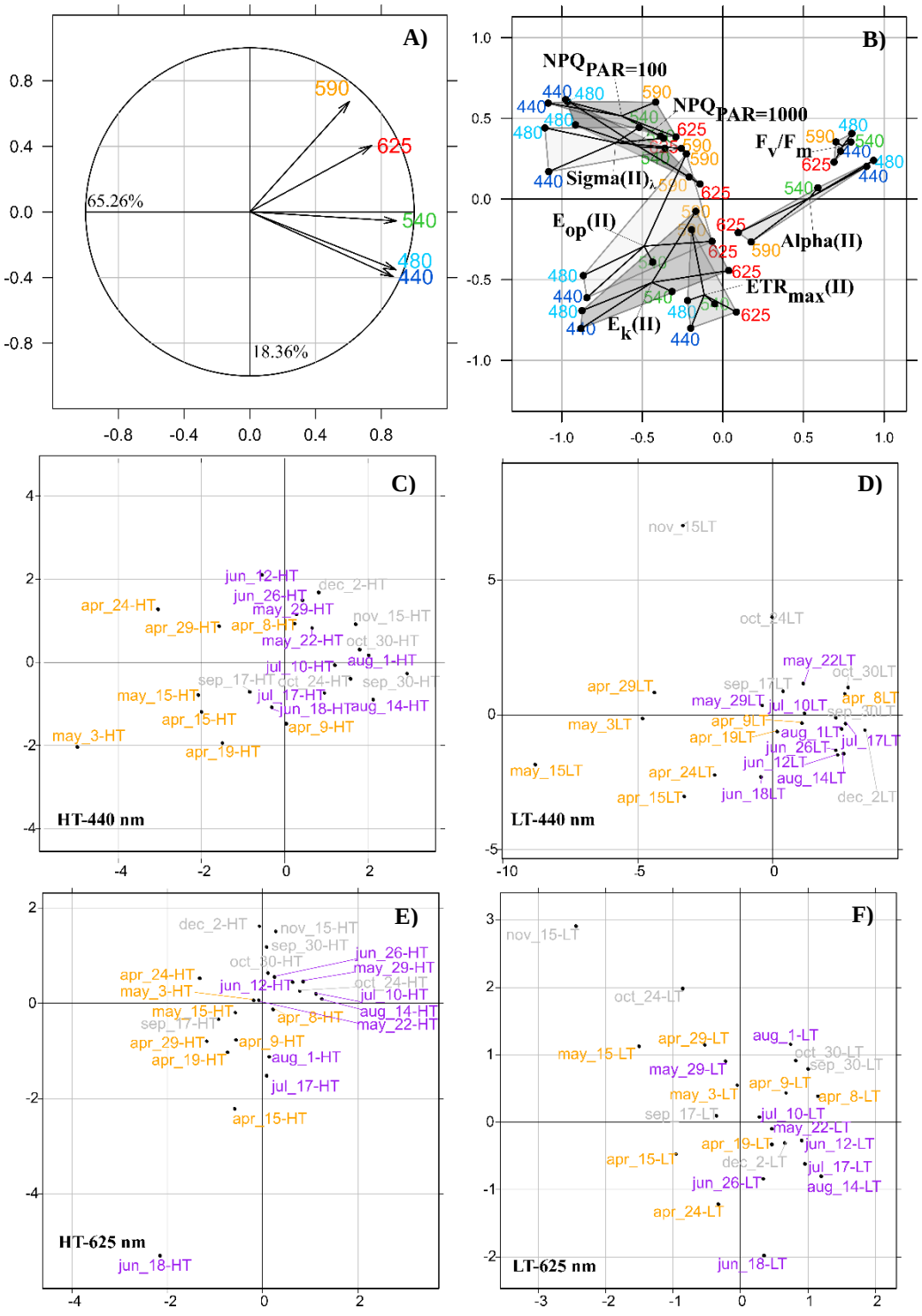

Figure III.7 : Partial Triadic Analysis (PTA) results for: A) interstructure; B)intrastructure (axes of the polygons) and compromise (center of polygons) of photosynthetic parameter; and intrastructure projections of individual samples at 440 nm (C and D) and at 625 nm (E and F) for High (C and D) and Low tide (D and F). In figure A, intrastructure responses at each wavelength are labeled with the wavelength value in bright blue, light blue, green, amber and light red (440, 480, 540, 590 and 625 nm respectively). Individual labels are composed by the day of the sampling date followed by the month, LT or HT for low and high tide respectively, and "m" or "a" for morning or afternoon samplings. Colors of individuals refer to the seasonal period (brown for sprint, purple for summer and gray for winter/autumn) resulting from PCA analysis and Hierchical Clustering.

Table III.II : Matrix of vector correlation coefficients between sub-matrix of photosynthetic parameters at each wavelength color, their weights in PTA analysis and cos^2

Wavelength (nm)	440	480	540	590	625	Weight	cos^2
440	1	0.90	0.72	0.29	0.47	0.48	0.91
480		1	0.75	0.35	0.47	0.49	0.93
540			1	0.46	0.61	0.49	0.88
590				1	0.52	0.33	0.54
624					1	0.41	0.69

The two axes of the **compromise** PTA analysis contributed to 73.84% (Table III.III) of total inertia and gave an accurate overview of the common structure among photosynthetic parameters for each measured wavelength (center of polygons in Figure III.7-B) and sample dates (median distance between wavelength values at 440 and 625 nm in Figure III.7 C,D,E and F). The relative position of each polygons highlighted proximities and oppositions that are well consistent with the theoretical expectations for photosynthetic processes. Fv/Fm and α are close and on the positive side of the first axis, while E_k(II) and E_{op}(II) are opposite, with ETR_{max}(II) in the intermediate position (Figure III.7-B). On a perpendicular axis defined by previous parameters, the two intrastructure polygons of the NPQ and Sigma(II)$_\lambda$ are arranged very close to each other on the positive side of the second axis (Figure III.7-B). Concerning the size of the polygons, Fv/Fm shows here the smallest polygon, that is to say the smallest spectral variability of all the studied photosynthetic parameters, as on Figure III.6. The rest of the parameters displaed similar polygon sizes, i.e. similar spectral variabilities outside the population trends, since data have been detrended here (Figure III.7-B).

Table III.III : PTA compromise analyses of the first 2 axes with Total Inercia, cumulated inertia (Cum) of each PTA axes (Cum) and % of cumulated total inertia (Cum %).

	Inertia	Cum	Cum (%)
Axe 1	13.08	13.08	48.54
Axe 2	6.82	19.90	73.84
Axe 3	3.98	23.89	88.62
Axe 4	1.40	25.28	93.80

Each of the edges of the polygons represents the **intrastructure** of photosynthetic parameters. Values at short wavelengths blue (440 and 480 nm) are for all photosynthetic parameters opposed to long amber and light red wavelengths at (590 and 625 nm). Moreover, blue values

are found generally further from the center of the factorial plan which was directly linked to the higher variability from the mean response compared to the more stable red values. The intrastructure polygon of ETR_{max}(II) evidenced a particular spectral pattern at 625 nm with a particular.

Results of PTA **intrastructure** of samples are here focused on two characteristic wavelengths (440 and 625nm) for clarity and in order to compare high and low tide individual sample measurements (Figure III.7-C, D, E and F). The analysis of individual samples evidenced a general temporal structure corresponding to the three seasonal periods of abiotic and biotic conditions that have been previously defined, more particularly at high tide. At high tide and 440nm, individual samples were clearly structured in periods from the left to the right of the first axis, that is from spring to autumn (except for the September 17th sample corresponding to a non-typical spectrum) being spring period the most different from the others. At high tide and 625nm, individual samples from spring and summer were discriminated (except for the June 18th and September 17th samples corresponding to a non-typical spectrum), while samples from autumn were in an intermediate position with less clear discrimination. At low tide these variations in patterns tended to disappear, especially at 625nm (Figure III.7-C, D, E and F).

3.3.4 Controlling factors of photophysiology

In an effort to identify the controlling factors of individual variations of the photosynthetic parameters individual variations, a redundancy analysis (RDA) was carried out on detrended photosynthetic data. The forward-selected explanatory variables allow explaining significantly each measured wavelengths (p-value < 0.05, Table III.IV) with a percentage of total variance between 20 and 40 depending on the wavelengths (around 40% in bright blue, 25% for light red and green and 19% for amber wavelengths, Table III.IV). Biotic and the combination of biotic and abiotic factors explained systematically a higher percentage of variance than abiotic parameters (Table III.IV). At 440, 480 and 540 nm, the yellow substances were the only abiotic parameters selected. This is an interesting result because yellow substances, or CDOM concentration, absorb light at short wavelengths, from ultraviolet to blue. At 590 and 625 nm, the abiotic forward selected variables were sub-surface light intensity (at 1m depth), in addition to light extinction coefficient at 590nm and water turbidity at 625nm.

Table III.IV : Results of RDA analysis of detrended photosynthetic parameters at each wavelength and the forward-selected explanatory variables. At each wavelength analyzed, the forward selected variables in the model are listed for environmental variables, the variance explained, the residuals and the R^2 adjusted (R^2adj) are shown.

Wavelength	Model	% abiotic Variables (a)	% explanation biotic variables (c)	% explanation Combined biotic +abiotic (b)	Residuel	p-value
440	Y.subs+ *Phaeocystis*+dinoflagellates+ diatoms	1.12	17.93	18.51	62	**
480	Y.subs+ *Phaeocystis*+dinoflagellates+ diatoms	1.35	21.44	16.87	60.34	***
540	Y.subs Diatoms+dinoflagellates+ Cryptophycee	0.6	17.10	8.09	74.13	***
590	I(1m)+kD+PO4 Cryptophycee	6.88	3.88	7.25	81.99	***
625	I(1m)+Turbidity+ Diatoms+dinoflagellates+ Cryptophycee	9.65	12.86	4.01	74.47	***

In parallel, the biotic forward selected variables corresponding to phytoplankton community structure displayed some differences according to the measured wavelengths (Table III.V and Figure. III.8). concerning brown microalgae, the diatom plus dinoflagellate group was always forward selected at each wavelength unless at 590nm, while *Phaeocystis globosa* biomass was only selected at 440 and 480nm. C*ryptophyceae* biomass was forward selected at 540, 590 and 625nm (Table III.IV). Therefore, there seems to be an ecological tuning between the forward selected microalgae groups and the measuring wavelengths of detrended photosynthetic parameters. It is a very interesting result given that it was obtained from natural phytoplankton communities.

In this context, temporal structure of samples were clearly reported on RDA biplots for 440 and 625 nm (Figure III.8-A B). These figures illustrate several results identified in Table III.IV and stated on PTA analysis. Sigma(II)$_\lambda$ and NPQ covaried at these two wavelengths and were linked to total phytoplankton biomass, but to different phytoplankton groups in function of the measuring wavelengths (Figure III.8). On the opposite, on the first axis, Fv/Fm and α are correlated at 440nm, in link with the diatom plus brown algae, diatoms and dinoflagellates group, while they were uncorrelated at 625nm (with F_v/F_m always correlate to brown algae). Note that *Cryptophyceae* biomass were well correlated with NPQ at 625nm while at 440 nm NPQ is correlated to *Phaeocystis sp*. and inversely correlated with diatoms+dinoflagellates

biomass. This variation of NPQ correlation would indicate a particular photoprotection mechanism between these species with different absorption capacity. $ETR_{max}(II)$ and $E_k(II)$ were negatively correlated to yellow substance at 440nm, while they are positively correlated to turbidity and sub-surface light intensity at 625nm (Figure III.8).

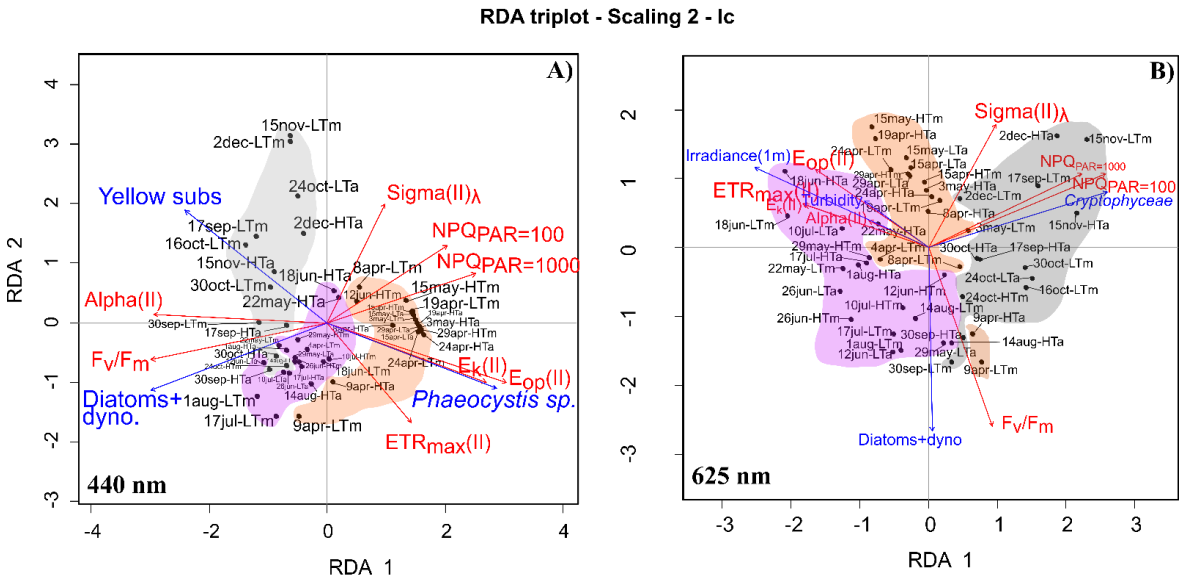

Figure III.8 : Redundancy Analysis (RDA) using scaling 2 triplot (correlation biplot: distances between objects are not approximate of Euclidean distances and angles between all vectors reflect linear correlation). Controlling factors and (blue arrows) of photosynthetic variables (red arrows). Individuals (black) are labeled with the day, month tide (high HT or Low LT tide) and the moment of sampling in the day (m for morning and for afternoon). The colored areas of samples represent the aggregation of these samples considering the seasonal periods resulting from PCA on abiotic and biotic variables and clustering analyses. Brown group samples for Spring period; Purple group samples for Summer period and gray color groups samples for Autumn period.

In order to go deeper in the study of the controlling factors of spectral variations of photosynthetic data, a focus was first made on the photoacclimation index E_K, divided by the averaged light intensity E_{avg} in the shallow sampling water column (Figure III.9).

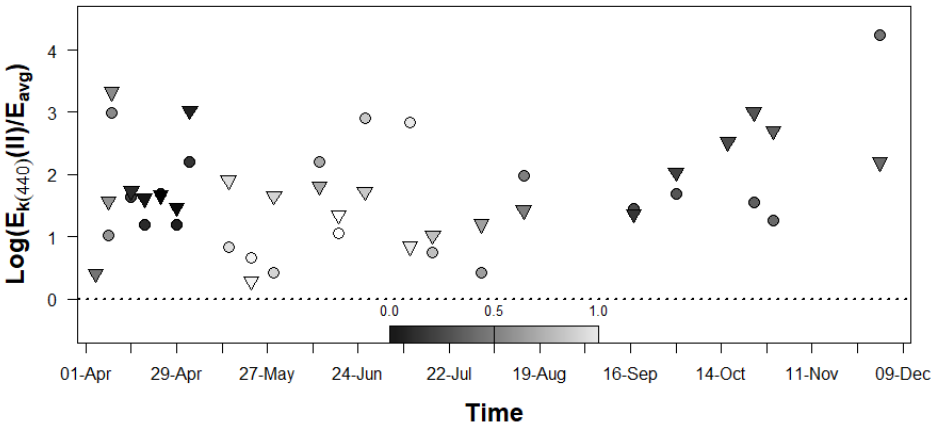

Figure III.9 : Temporal variations of the photoacclimation index E_k (in absolute units, measured at 440nm) divided by the vertically averaged light (Eavg) in Log scale at low tide (. Circles) are for pointsand at high tide (while triangles) low light.The gray scale bar indicates de KdPAR values at each sample

Temporal variations of such a classical ratio (Tillmann et al., 2000) showed that the phytoplankton communities presented a good photoacclimation state since values generally close to 1, but in some cases also above 1 (reaching a value of 4) (Figure III.9). This photoacclimate state could be due to the right strategy of photoprotection developed by microalgae. This was observed comparing the temporal evolution of the individual slope of $Sigma(II)_{\lambda}$ and NPQ_{100} between 440 and 625 nm (Figure III.10) with the temporal evolution of de-epoxidation state (DES) and the ratio between the photoprotective carotenoids and photosynthetic carotenoids (SM III-4). Recall that these last variables describe respectively the rapid cycle of activation of xanthophylls (XC) and energy transfer pathways within phytoplankton cells. Indeed, the spectral slope of the absorption capacity and the non-photochemical quenching at low lights decrease at the end of April and increase at the beginning of the declared summer period (middle of May) (Figure III.9). This temporal evolution is parallel to the decrease of the maximum values of DES and the increase of PPC/PSC ratio. Moreover, these variables showed a significant correlation with the light extinction coefficient K_d (Spearman r = 0.51 and -0.55 respectively) (Figure III.11).

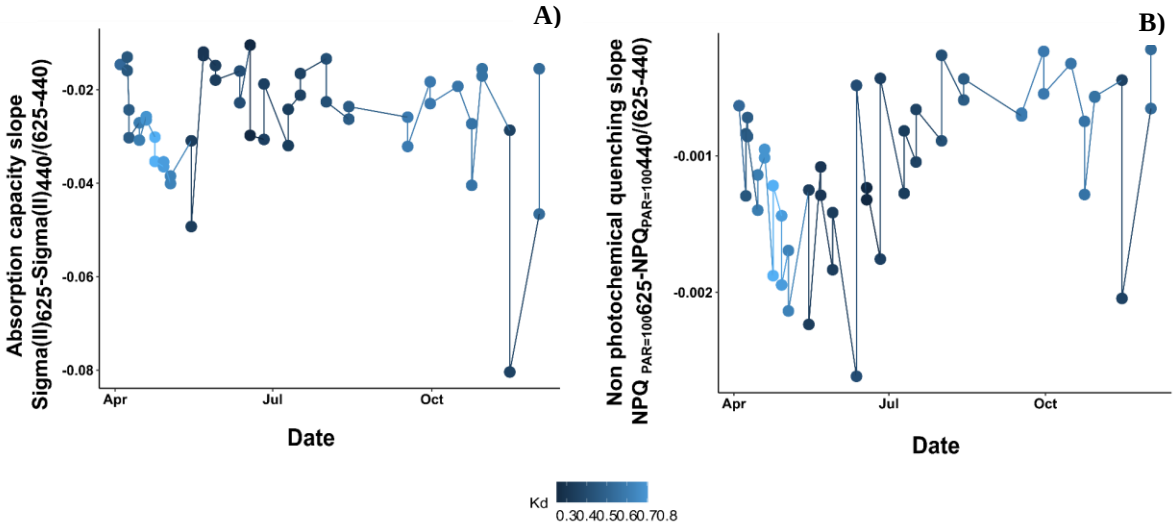

Figure III.10 : Plots of the temporal evolution of the absorption capacity Sigma(II)$_\lambda$ (A) and non photochemical quenching NPQ (at 100 µmol.photons.m^{-2}s^{-1})(B) slope between 440 and 625 nm in function of time (Date). The blue color graduation refers to K_d estimates from open coastal waters in the study area.

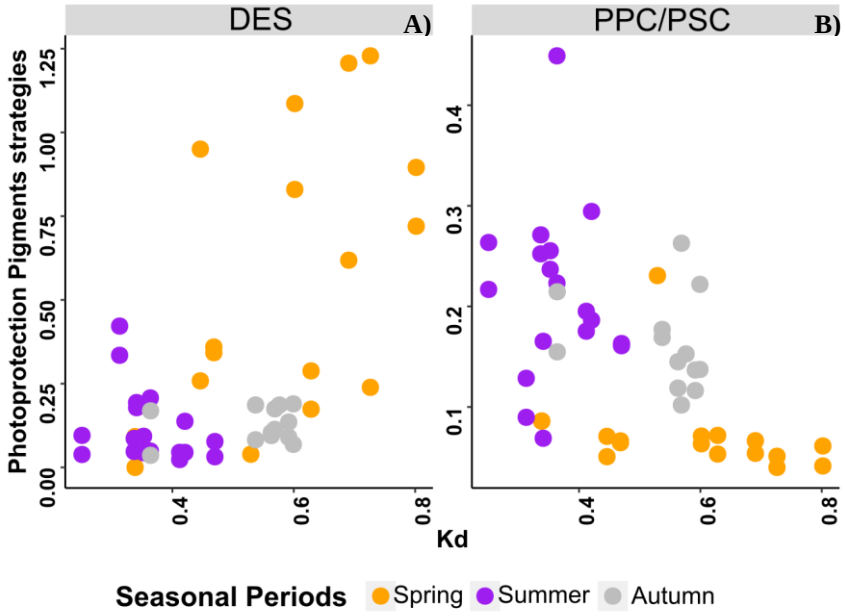

Figure III.11 : XY pigment XY plots of coefficients DES (A) and PPC/PSC (B) in function of K_d estimates (coefficient of light extinction) from open coastal waters in the study area for each seasonal period: spring (brown), summer (purple) and Autumn (gray).

3.4 Discussion

In this study we examined the wavelength dependency of multiple parameters referring to Photosynthetic Electron Transport (PET)$_\lambda$, absorption capacity of PSII and non-photochemical

quenching in a coastal temperate sea during 9 months with a total of 48 samples. In particular, this work provides new insights about the temporal variation of wavelength dependency of photosynthesis in relation with phytoplankton community structure shifts, their respective photoacclimation strategies and plasticity to cope with seasons and the tide scale changes. To date, only few works dealt with action spectra measured *in situ* and were only focused on the variations of α (the initial slope of P-E) during bloom of species with specific pigmentation structure (e.g *Mesodinium rubrum*; Kyewalyanga et al., 2002). Nevertheless, these studies did not consider the potential of phytoplankton cells to photoacclimate at shorter temporal scales within seasons. Indeed, other works on photosynthesis (but not spectral ones) have shown that photosynthetic activity could vary at very different temporal scales (Houliez et al., 2015) and that photoacclimation could happen in mixed coastal waters in relative stable conditions, between high and low tide and in neap tide conditions (Lizon et al., 1995; Lizon, 2002). In this study, we go further in the domain of wavelength dependency research in comparison to these previous works due to the complexity of the data acquired while considering the temporal scale effects. For that, an innovative statistical framework was used consisting in a sequential use of Linear Mixed Effects Model (LMEM), Partial Triadic Analysis (PTA) and Redundancy analyses (RDA). Here, the particularity was to nest temporal scales in the LMEM approach.

In this section, we first discuss the wavelength-dependency of each photosynthetic parameter in link to the theories of photosynthesis and photoacclimation, and the physiological implications. Secondly, we will discuss the wavelength dependency time variability and its controlling factors. This discussion will be carried out considering three different temporal scales: the three seasonal periods; the tide effect (high and low tide) nested in the three periods and, the individual level nested in the two previous ones.

3.4.1 Population wavelength dependency of photosynthesis

Wavelength-dependency has been characterized with Linear Mixed Effects Model on population level (fixed effects) and at individual level (random effects). In this section we will discuss the meaning of the wavelength dependency of these parameters in relation to the general photosynthetic and photoacclimation theories in fixed effects. Recall that our results showed that except α (in relative and absolute units), E_k(II) and NPQ at 1000 µmol.photons.$m^{-2}s^{-1}$, all photosynthetic parameters displayed a significant population trend over wavelength.

Absorption capacity of PSII

Absorption capacity was estimated by Sigma(II)$_\lambda$ following the method of Schreiber et al (2012) as an estimation of the absolute absorption capacity of PSII in a reference dark acclimate state, an intrinsic feature of the PSII. This parameter presented a decreasing population trend in function of wavelengths with still high values of absorption at 540 nm (green) that reached in this study 2.1 nm^2. Previous works using MULTI-COLOR PAM showed the same magnitude of absorption capacity during the bloom in English Channel (Michel-Rodriguez et al., in submission) at this same wavelength. These results were expected because they are characteristic of brown microalgae. Diatoms-dinoflagellate and haptophyte groups were most of the time dominant in the samples as in Michel-Rodriguez et al., (in submission). Brown microalgae displayed a dominance of chlorophyll a but also fucoxanthin pigments which can absorb green light depending on their position in light harvesting antenna (Premvardhan et al., 2008). Similar results were obtained also using the same MULTI-COLOR-PAM in diatoms (Goessling et al., 2018).

Physiological state

As for Sigma(II)$_\lambda$, the PSII maximum quantum efficiency or F_v/F_m needs to be discussed before focusing on photosynthetic parameters trend and photoacclimation strategies since it is related to the physiological state of the samples. This parameter presented a very marginal wavelength dependency and can be considered wavelength independent (even if the slope was significant). Spectral trends have already been characterized for this parameter (Lewis et al., 1988; Schofield et al., 1996; Falkowski & Raven, 2007). This result was expected because it was already observed in the spring at the Channel scale for phytoplankton communities dominated by brown microalgae (Michel-Rodriguez et al in submission). Here the values of F_v/F_m ranged between 0.4 and 0.6, with an average around 0.55. This range is not critical and does not imply a severe potential physiological stress. These values are only the general population trend. Individual variations were observed and will be discussed later in this study.

Photosynthetic parameters

The population trend of photosynthetic parameters allowed understanding the general management of light energy and electron flow from a physiological point of view related to

photosynthesis theory. The population trend in LMEM of photosynthetic parameters was guided by the spring-time values. A general strategy of photoacclimation will not be considered here at the population level but after a particular focus at each temporal scale defined from LMEM analysis (see section 4.2). This is supported by the fact that variations of wavelength dependency were significant for some photosynthetic parameters at population level and/or individual level depending on the nested temporal scale.

First, the expected result for ETR_{max} would be an increasing trend in relative units and a wavelength independency in absolute units according to previous studies on natural phytoplankton communities in the same coastal region at spatial scale (Michel-Rodriguez et al., in submission). Nevertheless what is observed here is that ETR_{max}(II) presented a wavelength decreasing trend. This result was remarkably interesting considering the shallow sampling area and the potential turbidity. In some previous studies, higher ETR_{max}(II) in blue wavebands were associated to photoacclimation due to increasing light intensities in blue wavelengths (Szabó et al., 2014a) and a change in PSII/PSI ratio generating a redistribution of the electron transport of blue photons through PSI (Schreiber et al., 2012). Such high values in blue wavelengths were also observed on microphytobenthos species in laboratory (Goessling et al., 2018), for benthic diatoms growing under blue light. In our case, higher ETR_{max}(II) in blue wavebands could be explained by a photoacclimation of advected cells of *Phaeocystis globosa* from initially clearer waters. Indeed, during the bloom, our results showed that phytoplankton biomass was high, as well as the turbidity and therefore K_d values. Brunet et al., (1993) reported inverse significant correlation between DES indexes and the light extinction coefficients K_d across the inshore-offshore environmental gradient of this ecosystem. On the shore, we were in different conditions: not on the environmental gradient but in a shallow water generating sand resuspension and thus probably masking the potential relationship between DES and K_d that could take place at sea. These seasonal values of ETR_{max}(II), as we will discuss in section 3.4.2 in detail, could control the population trend in LMEM.

Secondly, we observed a wavelength independency of α, the initial slope of P-E curves, in absolute and relative units. This result is consistent with what was measured initially by Schreiber et al. in their initial publication of MULTI-COLOR-PAM (2012), but differs to what was observed for cultures of brown algae (Goessling et al., 2018; Schofield et al., 1996) for which values showed a decreasing spectral trend. This was also the case for *in situ* measurements of previous and initial works of (Lewis et al., 1985b, 1985a) in which α showed a decreasing spectral trend close to the light absorption spectra (a*). The lack of higher values

for α(II) at 440 nm on the contrary to ETR_{max}(II) could be explained by the fact that advected cells were acclimated to high light at the beginning of the springtime, as previously described with high values of DES and $ETR(II)_{max}$. For this photosynthetic parameter the population trend could be guided by spring time trend.

Finally, we observed that E_k presented an increasing wavelength dependency in relative units and a wavelength independence in absolute units. Given that E_k is calculated as ETRmax/α, E_k(II) was here the result of the mutual compensation between α(II) and ETR_{max}(II). It resulted at population level a lack of significant trend that could be explained by the high variability of individual measurements. This parameter showed an amplitude of variation over 1500 quanta(PS II s)$^{-1}$ that can reach 2000 quanta(PS II s)$^{-1}$ at 440 nm. This was not the case in the study of Michel-Rodriguez et al (in submission) in which a significant decreasing wavelength dependency was observed. It is possible that E_k(II) variability at 440 nm specially prevented here the observed trend to be significant. This hypothesis could be also true for α(II).

These population wavelength dependent responses of photosynthesis showed some significant variations at some specific temporal scale that will now be discussed in connection with the environmental controlling factors.

3.4.2 Individual wavelength dependency and controlling factors according to time scales

Wavelength dependency of individual variations will be presented from detrended data (after subtraction of the spectral population signal) from LMEM in relation to controlling factors (in RDA analysis) according to the time scales considered in the LMEM analysis: i) seasonal scale; i) the daily tidal cycle scale with High (HT) and Low Tide (LT); and iii) the sample or individual scale. Results evidence that at least one of the temporal scales was significant for all photosynthetic parameters. The most significant temporal structure was the season. A secondary temporal structure was evidenced at the daily tidal cycle scale nested in the seasonal scale (that means that for each season we find differences between high tide and low tide values). The controlling factors were different at each of the temporal scales defined.

a) Seasonal scale

Spectral variability at seasonal level was driven by phytoplankton community succession and their respective photoacclimation strategies. A significant variation of wavelength dependency was observed for the light absorption capacity $Sigma(II)_{\lambda}$, $ETR_{max}(II)$, NPQ at 100 µmol.photons$m^{-2}s^{-1}$. Note that the significant values of LMEM random analyses indicate that at least one season was significantly different from the general population trend. A similar observation can be done in PTA and RDA analyses in which detrended data were grouped also under the criterion of seasonal periods. Recall that the seasonal periods were defined as spring, summer and autumn and were coherent and resulted from with the temporal variation analysis (Hierarchical Clustering and PCA analysis) of controlling factors observed in the Eastern English Channel (Breton et al., 2000; Gentilhomme & Lizon, 1997; Houliez et al., 2015, 2013; Lizon et al., 1995; Schapira et al., 2008; Seuront et al., 2006). The spring period was characterized by the growth of a high biomass dominated after mid-April by *Phaeocystis globosa* which led to a decrease in the nutrient stock that had been regenerated after winter. The summer period corresponded to high temperature and low nutrient concentrations and a mixed community of diatoms and surprisingly of *Phaeocystis*. Finally, the autumn period was characterized by low light intensity and a regeneration of nutrients stock with an increase of *Cryptophyceae* in the diatom with P*haeocystis* mix. In similar temperate macrotidal systems, the gradual variations of environmental parameters induce such a shift of phytoplankton structure at seasonal scales (Houliez et al., 2015; Jouenne et al., 2007).

The phytoplankton succession resulted in different patterns of pigment compositions and therefore could explain the different $Sigma(II)_{\lambda}$ signatures observed between seasons. In Spring, the community was highly dominated by *Phaeocystis globosa* which is characterized by the presence of auxiliary pigments like chlorophyll C3 or 19'Hexanoyloxyfucoxanthine (19H')(Breton et al., 2000; Brunet & Lizon, 2003). Indeed, these pigments are found in our samples in all the time series and are considered on total pigment (TP), and in 19H' in photosynthetic carotenoid pigments (PSC). The total pigment weighted values of these pigment concentrations showed higher values of Chl C3 in spring season (data not shown). Springtime was also characterized by a maximum value of de-epoxidation of diadinoxanthin (de-epoxidation state or DES) Figure SM.III-4). These pigments belong to the group of xanthophyll pigments that could explain, as said in the previous paragraph, the state of photoacclimation of cells to strong lights when the waters are still clear before the strong biomass. This is consistent with RDA results in which it was observed that in spring the absorption capacity and total

biomass were correlated in springtime at blue wavelengths only. In summer, the phytoplankton structure showed a co-dominance of *Phaeocystis* with Diatoms+dinoflagellates in combination with a presence of 10 % of cyanobacteria. This last group is characterized by an absorption spectrum developed in red wavelengths thanks to phycobilisomes as it is shown in the particular HPLC works of pigments absorption spectrum and properties (Roy, 2011). Note nevertheless that phycobilisomes areis not considered in the total pigment biomass in HPLC analysis. In the particular case of the red band in MULTI-COLOR-PAM, the 625 nm light was initially designed for this phytoplankton group, concretely *Synechocystis* (Schreiber et al., 2011 and methodological manual MULTI-COLOR-PAM). In our data the increase of $Sigma(II)_{\lambda}$ was in the light red band at 625 nm while the amber band at 590 nm values are lower in comparison to red band ones. Finally, during autumn, which is characterized by the presence of *cryptophytes* in more than 30 % of the samples, the spectral band enhanced was a green and amber band with values that reached 5 nm^2 and even 10 nm^2 for some dates (Figure III.5). Higher $Sigma(II)_{\lambda}$ values during autumn can be here due to an increase of alloxanthin concentration. This pigment is included in the pool of total photoprotective carotenoids (PPC). The ratio PPC/TP (Figure SM III.4) showed here an increase in autumn season that can be explained by the increasing concentration of alloxanthin in time (data not shown). In autumn, total pigment shows a general increasing trend (Figure SM III.4) while the absorption capacity $Sigma(II)_{\lambda}$ showed a general enhancement at all wavelengths, as in springtime. The explanation is nevertheless related to different factors. During autumn, the increase of $Sigma(II)_{\lambda}$ would be explained by a decrease of available blue light in the water column due to higher concentrations of CDOM but in spring it is due to the higher absorption of blue lights after a liberation of excess of energy by the action of xanthophylls cycle with high DES values. This pattern among seasons of absorption capacity is evidenced. Redundancy Analysis in which the yellow substances (proxy of CDOM concentrations or biomass degradation (Astoreca et al., 2009) were forward selected for the blue wavelengths. This assumption is also consistent with RDA results which showed that at red wavelengths, the absorption capacity and total biomass were associated with *cryptophyte* biomass.

The phytoplankton community succession controlled the absorption capacity among seasons but also highlighted different strategies of photoregulation through NPQ. This relation between absorption capacity and NPQ was observed with a systematic correlation of $Sigma(II)_{\lambda}$ and NPQ in RDA and in PTA intrastructure. On one hand, there is a dominance of *Phaeocystis globosa* in spring and a rapid cycle of Xanthophylls with a high de-epoxidation state (DES) and

high NPQ values. On the other hand, in summer the main strategy of photoregulation was the increase of the pool of photoprotective carotenoids but not the rapid cycle of Xanthophylls that acts at longer time scales and after longer expositions to high light intensities (Alderkamp et al., 2012; Meyer et al., 2000). During the spring, the phytoplankton community was exposed to a seasonal increase of light even in a turbid shallow environment. Spring cells set up then a fast photoregulation by de-epoxidation of diadinoxanthin which was observed in the peak of DES while increasing the non-photochemical quenching (NPQ_{λ}). In summer, cells develop in a more stable water column and higher light intensities allowing them to develop a long term photoacclimation characterized by the synthesis of the pool of photoprotective pigments and lower NPQ values. Recall that in summer there is a codominance of *Phaeocystis globosa* and diatoms+dinoflagellates. This increase of diatoms would explain the opposite energy regulation strategy of summer period. This opposite strategy has already been observed in previous works (Meyer et al., 2000). These authors evidenced that *Phaeocystis globosa* developed a fast rapid xanthophyl's cycle (linked to a reduce cost of synthesis other pigments (Brunet et al., 1993)) when growing at different lights intensities, while a diatom specie (*Thalassiossira sp*) developed that strategy of photoregulation only when growing in low lights (under 10 $\mu mol.photons.m^{-2}s^{-1}$) which is not the case in summer season. This is consistent with our results. Indeed the temporal evolution of the individual slope of $Sigma(II)_{\lambda}$ and NPQ at 100 $\mu mol.photons.m^{-2}s^{-1}$ showed a shift between the end of spring and the beginning of summer, what evidence then a change in absorption capacity and energy regulation (Figure III.10). In autumn, $NPQ_{PAR=100}$ at 440nm were similar to summer. PPC/PT evolution (Figure SM III.3) showed some peaks but in general any singular photoprotection strategy on carotenoids was found in this season. This result should be explained by a particular contribution to NPQ by cryptophyte not related to photoprotective pigments of xanthophylls (Kaňa et al., 2019, 2013, 2012).

The photoregulate and photoacclimation states cited previously would be related to the variations from general population wavelength dependency of $ETR_{max}(II)$ (Table III.I, marginal significant variations of $ETR_{max}(II)$ at seasonal scale). Recall that in LMEM analysis the significant variations appear even if only one season has a different variation from general population wavelength dependency. If we focus on the spring and in summer data only (Table SM 1), the variation of this parameter in function of wavelength shows a decreasing trend and an almost null trend for spring and summer respectively (SM). In spring the $ETR_{max}(II)$ decreasing trend and higher blue values would result from the rapid photoregulation. In summer

the spectral trend was steeper because of a photoacclimation in blue wavelengths that result in a reduction of ETR_{max}(II) and α(II) but NPQ was not high enough to induce a strong decrease of α(II) at blue wavelengths and α(II) LME trend result as not significant. This result would evidence a photoprotection state that has already been observed in coastal waters with a co-dominance of *Phaeocystis globosa* and diatoms+dinoflagellates during the bloom in spring period in well mixed areas (Michel-Rodriguez et al., in submission).

The seasonal pattern of photosynthetic parameters was carried out mainly by responses at blue light, whether it is at the level of energy regulation or photoprotection. This has been observed on the amplitude of variation of photosynthetic parameters values at bright blue light band, which were always higher. Moreover, photosynthetic parameter ETR_{max}(II) showed as cited above photoacclimative state at this wavelength. Detrended data at amber and red light were closed to the general population trend with a less evidenced seasonal trend. This result is evidenced on PTA results where blue detrended data was systematically better represented with a clear seasonal structurr of intrastructure responses. The higher variability at blue wavelengths is explained by the fact that our phytoplankton community is dominated by species with a high efficiency of blue absorption but also because photoacclimation and photoregulation responses at that wavelength are described in literature to occur at shorter time scale than under red lights (Valle et al., 2014). This is particularly the case for example of the processes of energy regulation by NPQ which are faster at blue lights (Brunet et al., 2014). This result is also consistent with previous analysis at spatial scale with this same method of analysis (Michel-Rodriguez et al., in submission).

b) Tidal cycle scales

At this scale we observed that the capacity of absorption (Sigma(I)λ) showed significant variations from the general population trend and in a marginal degree of significantly, also for ETR_{max}(II) and NPQ at low lights. As α(II) model appear as non-significant due to the miss of general population trend, the variation of this photosynthetic parameter at tidal temporal scale will not be discussed here.

Phytoplankton community exchanges between offshore and shallow coastal waters due to the tide could explain observed variations of cited parameters at this short time scale. This physical process could be responsible for the transport and mixing of phytoplankton communities of the same structure but with different light history. Growing under different light quality regimes

provoked the different absorption strategy observed in link with a particular plasticity of communities for photosynthetic pigment conversions. This conversion of pigment would be a switch to photoprotective pigments strategy because of a photoregulation. It is well known that in estuaries environments, species are able to induce the activation of protective pigments (Lavaud et al., 2007). Recent studies highlight the importance of a photoacclimation to high lights even in environments with high turbidity and low light under the effect of tide variation in estuaries (McLaughlin et al., 2020). A study on microphytobenthos and phytoplankton community in an estuary at different time scales carried out hourly, along four spring-neap tidal cycles distributed along 1 year (Frankenbach et al., 2020) showed that Sigma(II)$_\lambda$ (only at blue wavelengths) can vary at fortnight time scales for phytoplankton as our high and low tide periods here. This was also the case for Fv/Fm. We suggest here then that the significant variation of Sigma(II)$_\lambda$ wavelength dependency can be explained then by an activation or switch of auxiliary pigments as these of photoprotection. The observation of the different values at different tide periods showed that low tide presented the higher spectral trend of Sigma(II)$_\lambda$(Table SM III.1). This result is consistent with this scenario of variation of absorption strategy by the activation of photoprotective pigment in the blue band of the absorption capacity. This phytoplankton community trapped in shallow waters could then photoregulate/photoacclimate in a shallower water column with potential strong turbidity.

Tidal temporal pattern is observed on the intrastructure of samples in PTA analysis. These results showed that the seasonal structure of samples was more clearly defined at blue wavelengths in high tide. However, that was not observed at low tide because of the photoregulation/photoacclimation state that cells reached during the tide period when they are exposed to the light climate of the shallow waters. One important point to highlight is the fact that this effect is not enhanced at neap or spring tide for Sigma(II)$_\lambda$. In the analysis of the intrastructure, which resume the full photosynthetic state of the sample, samples at neap tides with tide coefficient under 45 (April 29th, May 29th, June 26th) and samples at spring with a tide coefficient over 100 (September 30th, October 30th or April 19th) appear with the same spectral distance between 440 and 625 nm than the rest of the samples (with a coefficient of tide between 45 and 100). Note that this threshold is arbitrary and aimed to highlight only the more extreme tide periods. An important explanation to the lack of this effect is the fact that each sample, which presents a significant random effect at the intercept and then at the intensity level, presents different light histories. A specific variability at the monthly scale of the tide could be masked by the random variability of the available light at this time scale (Lizon et al., 1998). In

this scenario we would suppose that these different light intensities hide the effect of the hydrodynamics of neap and spring tides (Blauw et al., 2012).

3.5 Conclusions

In this work, wavelength dependence of phytoplankton has been studied at different time scales in a very coastal and shallow sampling area. This area is nevertheless connected to open coastal water by tidal circulation of water masses in the north-south and east-west directions. Therefore some exchanges between water bodies along the inshore-offshore gradient occurred during tidal cycles (Brylinski et al, 1991). Mixtures of cells of different origin and or light histories could be encountered in shallow waters. It is under these specific conditions that this study showed that spectral photoacclimation of natural phytoplankton communities was possible with an optimization of the maximum electron transfer rate ($ETR_{max}(II)$) in the blue wavelength. This is fully evidenced by the spectral approach of photosynthetic parameters measurement, more particularly by a comparison between the blue and light red wavelengths. There is no reason to believe that these observed processes cannot be transposed to the rest of the coastal waters if a tuning is possible between photoacclimation time scales and the duration of the water column stability given its turbidity.

To respond concisely our initial questions in link with the discussion, we can thus say:

i) Is the wavelength signature of Phaeocystis sp. bloom singular? With a rapid xanthophylls cycle and high values of epoxidation of diatoxathin (DES) values, a pronounced spectral trend of NPQ in this season and also an increase of $ETR_{max}(II)$ and a decrease of $\alpha(II)$ in blue wavelengths (even if $\alpha(II)$ not significant), we can deduce that during that season there is a clear and singular photoregulation strategy. A wavelength dependency due to a presence of a particular phytoplankton group was also evidenced in previous works of action spectra at seasonal scale with the difference that the absorption strategy of this species in that particular work were very different from the global population (absorption and action spectra with peaks in green band) (Kyewalyanga et al., 2002). Here the particularity was that even if there was a phytoplankton succession, the spectral absorption capacity was not very contrasted.

ii) *How the wavelength signatures of the photosynthetic processes vary: according to the tide and/or the season?* The variations of wavelength dependency take place at both seasonal and tidal temporal scale, but the controlling factors of such variations differs between

both temporal scales. At seasonal scale, the control factor was the phytoplankton succession while at tidal scale, it was the variation of absorption capacity that emerged because of a different plasticity of photoacclimation.

iii) *How are the spectral balances of energy performed in function of the different photoprotection and absorption capacity of the different phytoplankton groups?* In the case of the seasonal scale, the different groups presented a very different photoprotective state between spring and summer. In summer this process was mediated by a longer time scale process with the synthesis of new pool of photoprotective carotenoids while in spring it is due to the xanthophyll cycle and a rapid photoregulation process with very high NPQ capacity in blue wavelengths which are worked out in higher turbidity conditions than in summer.

3.6 Supplementary material

2.6.1. Supplementary material 1: Abiotic variables

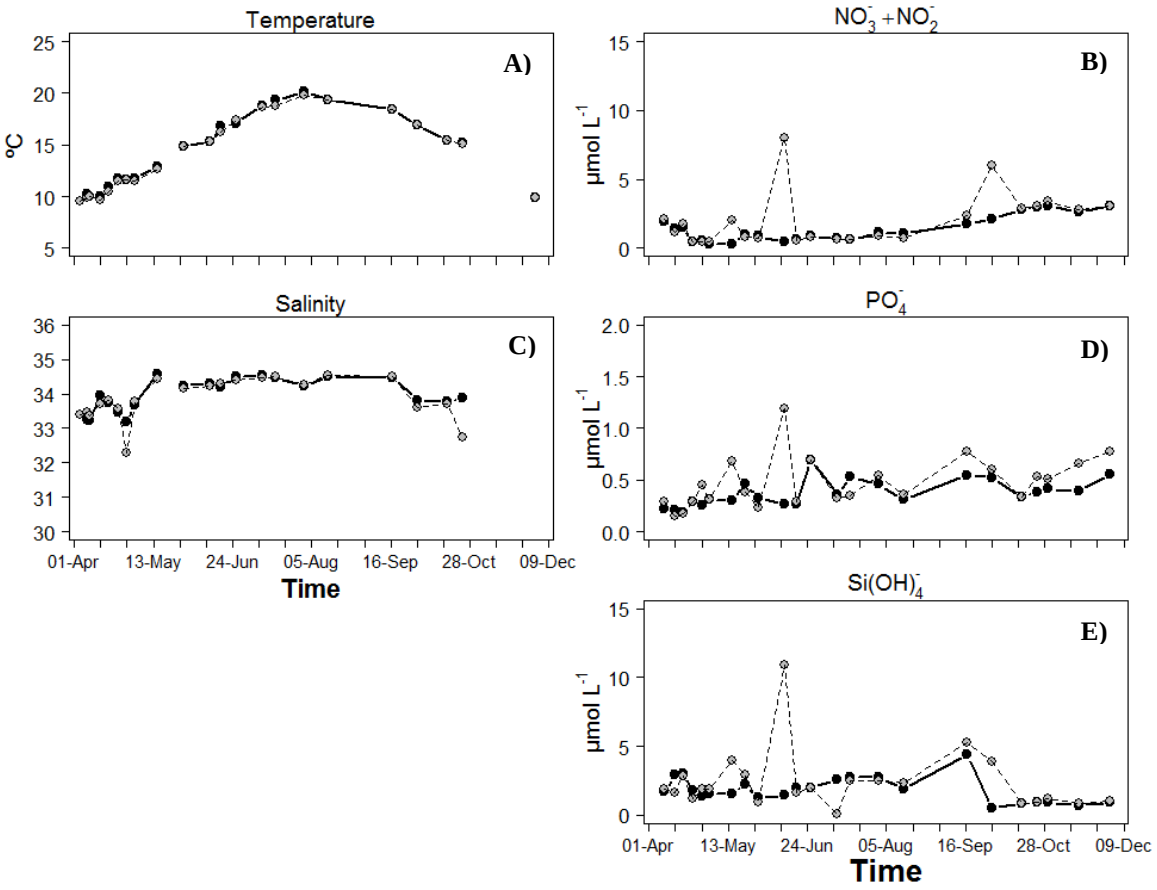

SM III-1 Abiotic parameters A) Temperature; B)NO_3+NO_2, C) Salinity; D)PO_4 and E) $Si(OH)_4$ G)concentration in µmolL^{-1} . Gray and black symbols represent low and high tide values respectively.

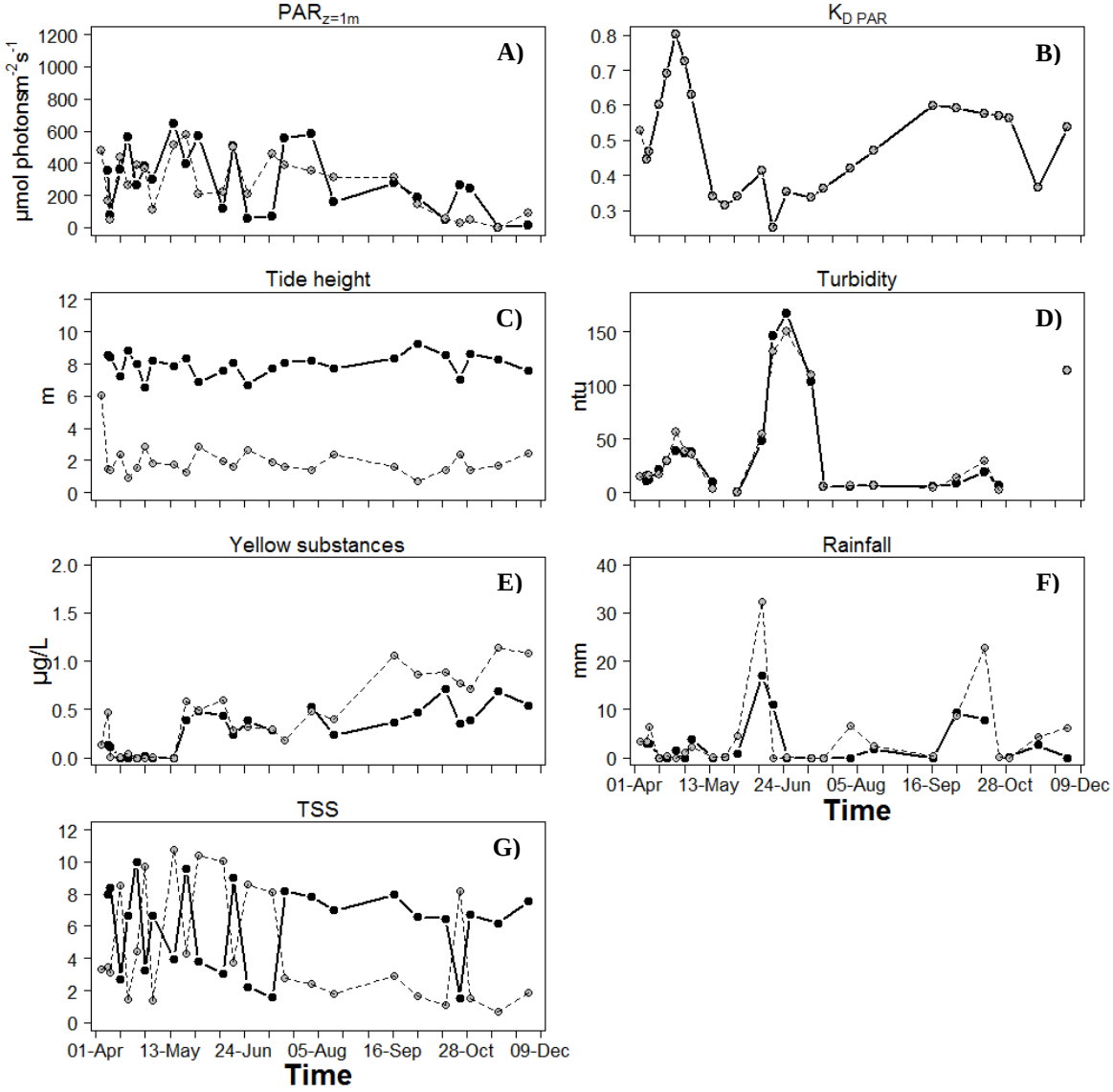

SM III-2 : Abiotic parameters A)PAR in µmol·photons·m^{-2}s^{-1} at 1m depth (estimated from GSR in open coastal waters extinction coefficients(see M&M for details); B) coefficient of light extinction K_d in offshore waters from of the sampling area (see M&M for details); C) Tide height (m); D) Turbidity(ntu); E) Yellow substances µg L^{-1}; F) rainfalls (mm) per day (black closed symbols and solid line) and two days cumulated rainfall (gray closed circles and dashed line) G) Time since sunshine in hours (TSS), Except for F, gray and black symbols refers to low and high tide values respectively.

3.6.2. Supplementary material 2: Biotic variables

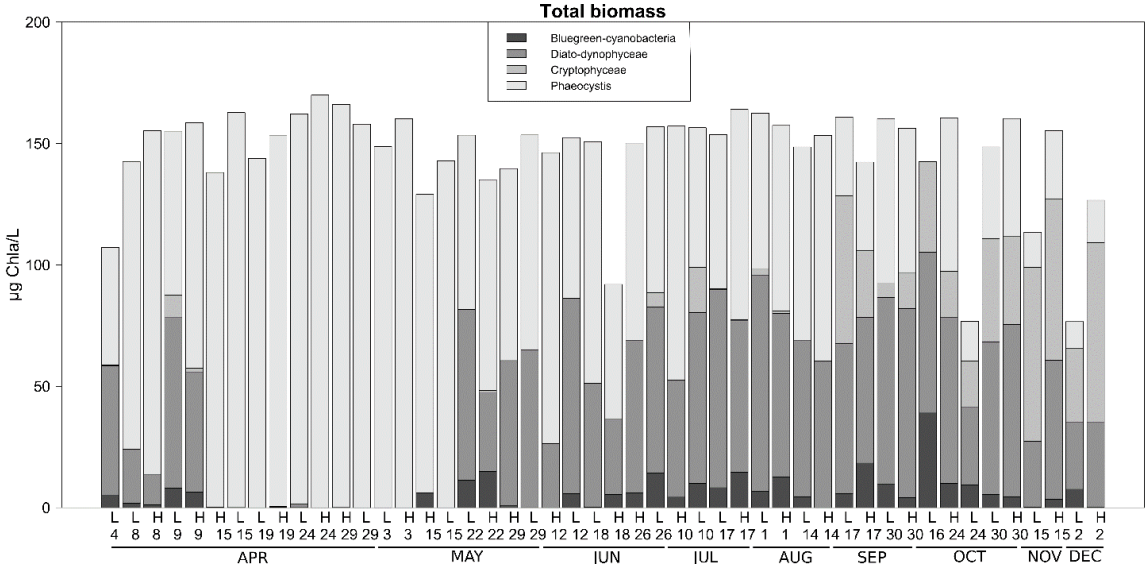

SM III-3 : Stack bar charts of biomass estimations by phytoplankton groups on concentrated samples using the FluoroProbe technique, in unit of µgChlL^{-1}. Color scale of bars charts represent the 4 phytoplankton groups: black for "blue-green cyanobacteria; dark gray for diatom plus dinoflagellate group; gray for Cryptophyceae; and light gray for the Haptophyceae group corresponding to Phaeocystis globosa in the English Channel.

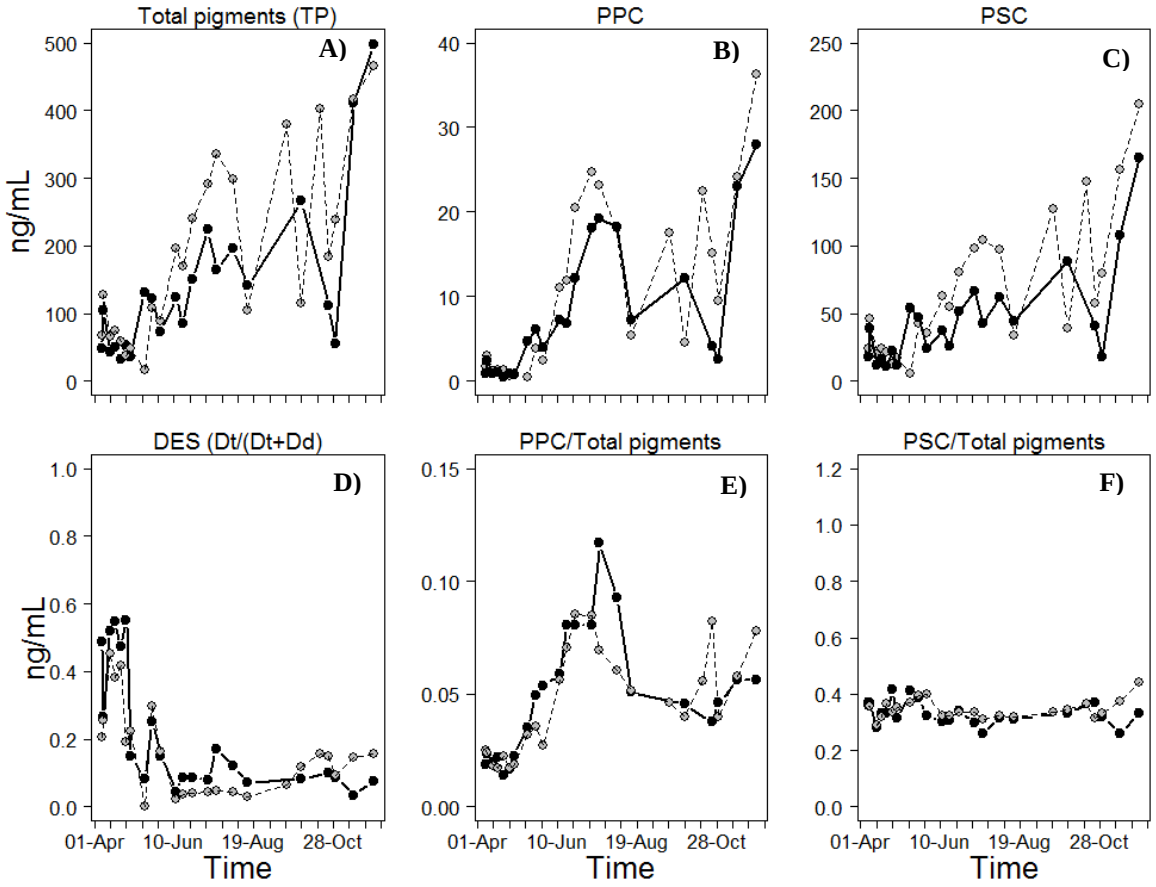

SM III-4 : Temporal variations of A)Total Photosynthetic pigments (TP) , B) photoprotective carotenoids (PPC), C) Photosynthetic carotenoids (PSC), D)De-epoxidation state (DES=Dt/(Dt+Dd)); and the total pigments concentration weighted values of PPC(E) and PSC (F)for high tide samples (black circles and solid line) and low tide samples (gray circles and dashed line).

3.6.3. Supplementary material 3: population trend focus by seasons and tide periods

Table SM 1 : Table of intercept and slope of linear regression model performed at each season. Only photosynthetic parameters with a significant random variation from LMEM are shown in this table.

ESTIMATES by season

	Intercept (values at 440 nm)			Slope		
Photosynthetic param	**Sprint**	**Summer**	**Autumn**	**Sprint**	**Summer**	**Autumn**
$ETR_{max}(II)$	881.6 ***	749.35**	664.01***	-1.69 ***	-0.84*	-0.71*
$Sigma(II)_{\lambda}$	7.12 ***	5.09***	7.59 ***	-0.031***	-0.021***	-0.031***
$NPQ_{PAR=100}$	0.39 ***	0.26***	0.27***	-0.00013 ***	-0.0011***	-0.0005**

Table SM 2 : Table of intercept and slope of linear regression model performed at each tide of the season. Only photosynthetic parameters with a significant random variation from LMEM are shown in this table.

ESTIMATES for HT

	Intercept (values at 440 nm)			Slope		
Photosynthetic param	**Sprint**	**Summer**	**Autumn**	**Sprint**	**Summer**	**Autumn**
$Sigma(II)_{\lambda}$	6.38***	6.39***	6.38***	-0.026***	-0.026***	-0.026***

ESTIMATES for LT

	Intercept (values at 440 nm)			Slope		
Photosynthetic param	**Sprint**	**Summer**	**Autunm**	**Sprint**	**Summer**	**Autunm**
$Sigma(II)_{\lambda}$	6.61***	6.61***	6.61***	-0.03***	-0.029***	-0.028***

IV. General discussion and perspectives

General discussion and perspectives

The aims of this thesis were (i) to study the wavelength dependency of microalgae photosynthesis in coastal systems; (ii) to analyze its variability and its controlling factors at various temporal and spatial scales in order to characterize the spectral dynamics of photoregulation and photoacclimation and finally, (iii) to suggest some perspectives on complementary laboratory experiments.

4.1. How the *in situ* approach and the analytical method allowed to evidence the wavelength dependency of photosynthesis related to the light climate?

The results of this thesis have been characterized following an innovative approach. Indeed, this is the first time these multi-wavelength measurements of photosynthesis were performed on natural phytoplankton communities: photosynthetic electron transport (PET_λ), non-photochemical quenching (NPQ_λ), maximum quantum yield ($F_v/F_{m\lambda}$) and light absorption capacity (functional absorption cross section of PSII, $Sigma(II)_\lambda$) were estimated at five different wavelengths of interest. Studies on this topic so far have been done only on monospecific cultures under a reduced number of conditions (Goessling et al., 2018b, 2016; Hoadley and Warner, 2017; Schreiber et al., 2012; Schreiber & Klughammer, 2013; Szabó et al., 2014a, 2014b) or by analyzing ex situ natural microphytobenthic community samples kept under controlled conditions in laboratory (Goessling et al., 2018a). In this thesis, for the first time, natural phytoplankton was used for wavelength dependent studies of photoregulation and photoacclimation related to the underwater light climate variations (light quantity and quality) with new multi-spectral variable fluorescence techniques and associated statistics.

The MULTI-COLOR-PAM (Walz) fluorometer was recently employed in field works (Frankenbach et al., 2020; Morelle et al., 2018; Morelle & Claquin, 2018) but by reducing the spectral measuring potential of this device. This device allows the measurement of the $I\text{-}O_1$ fast kinetics to estimate the functional absorption cross section of PSII, $Sigma(II)_\lambda$, of a dark-acclimated sample. This allows the determination of absolute rate of PSII electron turn-over. In

previous studies, Sigma(II)$_\lambda$ was only measured at 440 nm because it is the main absorbed wavelength by chlorophyll of photosynthetic organisms. One of the aims of Morelle et al (2018) and Franckenbach et al (2020) works was to study the electron requirements for carbon fixation in order to estimate primary production rates from ETR_{max}(II) measurements. Nevertheless, the significant role of the blue-red spectral balance determination has been highlighted in understanding the physiological and photoacclimation state in which a natural phytoplankton community was at a given season or in a given water column.

The acquisition and analysis of the unique and complex multi-spectral data set obtained in this work have required the development of a unique protocol of sample measurement and data analysis. Other multi-spectral fluorometers exist: the FRRf Act2 (Chelsea UK) does not deconvolute the wavelength measurement signal; the mini-FIRe (Gorbunov et al., 2020) has only physiological and taxonomic absorption capacity analysis without RLC derived photosynthetic parameters consideration; The Phyto-PAM(II) (Walz, Germany) used the different wavelengths for determining the photosynthetic parameters by phytoplankton groups.

The use of MULTI-COLOR-PAM required sample concentration for natural communities to get a stable measuring signal, especially for Sigma(II)$_\lambda$. The first analysis made with MULTI-COLOR-PAM (Schreiber et al., 2012) was performed on cultures with a concentration ranging between 200 and 300 µg Chla L^{-1}. Such microalgae densities can be considered as optically thin suspensions (Klughammer & Schreiber, 2015; Szabó et al., 2014b) but they have notably higher concentration than field samples. Phytoplankton biomass in the English Channel ranges between 2 and 30 µg. L^{-1} with specific events of biomass concentration reaching 90 µgL^{-1} (e.g.(Houliez et al., 2015, 2013a). That is why, it was necessary to concentrate the samples for reproducible measurements. However, the concentration process did not avoid the extrapolation of ecological implications results since concentrated communities remained consistent with the structure of natural phytoplankton communities encountered all over the year.

Measurements were performed in triplicate for RLC measurements and in 6 replicates for Sigma(II)$_\lambda$. A specific statistical approach has been implemented to analyze the population spectral trend (or spectral balance) and the individual wavelength variations around the population trend. For each photosynthetic parameter, five different values were obtained, one for each of the analyzed wavelengths. The goal was then to study the photosynthetic activity variability considering not only the interconnection between wavelengths. It is thanks to the use of a unique cascading statistical tools —Linear Mixed model Effects for spectral trend,

Principal Triadic Analysis (PTA, never used to the date with this kind of data) and RDA on detrended data— that it was possible to understand the general wavelength dependency of photosynthesis and to analyze the individual processes of wavelength dependent photoregulation and photoacclimation.

All of these considerations on MULTI-COLOR-PAM data acquisition and the unique statistical approach developed in this thesis were crucial and allowed evidencing new insights in the study of wavelength dependent photoacclimation and photoregulation processes. Thanks to the spectral approach, it was possible to study how phytoplankton integrate the light climate changes and how the photoregulation and photoacclimation are shaped in function of light wavelengths. The potential of phytoplankton to integrate the light quality for growing conditions is a prime of importance. Previous studies (Brunet et al., 2014) evidenced that NPQ and photoprotection were determined by blue light but sensing red light was required to allow photoregulation. In this thesis, it was also evidenced that the spectral balance among wavelengths was controlled by the underwater light climate. As it will be detailed in the next paragraph, this fact was evidenced at spatial scale in the upper mixed layer of stratified water columns and at temporal scale, by different strategies related to phytoplankton successions and cell plasticity over time. If only one wavelength response would have been measured, e.g. blue wavelength, the quantification of spectral balance of photosynthetic proceses of absorption and energy regulation would not have been possible and as a consequence, it would not have been possible to interpret the whole photosynthetic processes in reation to abiotic and biotic factors.

The wavelength dependency of photosynthesis related to underwater light climate is well-known in ecophysiology and primary production computation from satellite data. The spectral consideration in primary production models have been treated in the past by some field and computational studies (Kyewalyanga et al., 1992; Platt & Sathyendranath, 1988; Sathyendranath et al., 1995b, 1989). The measurements of photosynthetic action spectra in the field was relatively complicated. These measurements could be done on broad band models and posterior correction with absorption coefficient (Kyewalyanga et al., 1997). Nevertheless, these measurements miss information about energy regulation processes like non photochemical quenching and a complete light curve parameters acquisition. The results of this thesis produce absolute absorption measurements of photosynthesis and sensitive measurements of energy spectral balance for natural phytoplankton communities. Moreover, new modelling studies highlighted the importance of including photoacclimation processes in primary production computation (Kovač et al., 2017; Sathyendranath et al., 2020). This kind of model could be

useful in order to assess the impact of the photosynthesis wavelength dependency, characterized here by an innovate approach for natural communities, on the daily and seasonal rates of PP. Spectral consideration of photosynthesis could also have implications on water quality monitoring programs, as already highlighted by Gorbunov et al., (2020) with their new multi-wavelength tool for analysis of phytoplankton taxonomic groups and physiological characteristics. Specifically $E_k(II)_{625/440}$ measured at spatial scale could be a good proxy for water quality in coastal areas since it describes the photoacclimation state of phytoplankton communities and integrates light regime even in well mixed conditions.

4.2. How are controlled wavelength dependent photoacclimation and photoregulation processes in coastal areas?

Results of this thesis have also evidenced that variations of wavelength dependency of photosynthesis take place differently at spatial and temporal scales involving different controlling factors. At spatial scale, for a given phytoplankton community, it was evidenced that, cells were able to photoregulate/photoacclimate to the light quality variations in function of the water column stability and light penetration. At temporal scale, the wavelength dependency was mainly evidenced at seasonal scale due to environmental conditions that drives phytoplankton succession, in a consistent way with the classical and local seasonal pattern (Breton et al., 2000; Jouenne et al., 2007, 2005; Schapira et al., 2008). Abiotic factors mainly controlled wavelength dependent photoacclimation at spatial scales. At temporal scale, it was the community structure mediated by environmental factors, such as turbidity or CDOM concentration at temporal scale.

More precisely, at spatial scale and during a spring bloom with a similar phytoplankton community adopting the same light absorption strategy, the recent light history of cells, explained by the light quality in the euphotic layer, appeared as the determinant factor controlling individual photoacclimation responses. In this case, characterization of a tuning between photoregulation/photoacclimation and the light climate was done using the photosynthetic saturation parameter E_k. Spectral ratio of E_k between 440 and 625 nm was in correlation with the same pair of light quality ratio and the time since sunrise (light history). These results highlight the combination of quality and quantity variation of light in the photoacclimation state. This light and physiological E_k ratio should be included in future monitoring of water quality in regional observation programs as previously cited.

At temporal scale, it was shown that despite hydrodynamism occurring in shallow coastal waters under the effects of tide, the different phytoplankton communities that succeed over time displayed different photoacclimation state consistent with their absorption capacity strategy and their photoprotective pigment composition. The spectral balance between blue and red wavelengths for parameters such as absorption capacity and non-photochemical quenching ($Sigma(II)_{\lambda}$ and NPQ respectively) showed a shift in the transition between two different phytoplankton communities in correlation with a shift between the two main indicators of photoprotective strategy (epoxidate state DES,photoprotective carotenoids and photosynthetic carotenoids ratio (PPC/PSC)). During the succession from spring to summer, encountered communities were not on rapid xanthophyll cycle based for photoprotection but rather on photoprotective carotenoid pool. Moreover, at the diurnal tidal cycle scale, comparison of high and low tide measurements evidenced that phytoplankton was able to adapt their absorption capacity. α and $ETR_{max}(II)$ at 590 nm presented also a strong temporal dynamic in link with the seasonal phytoplankton succession when high and low tide values were observed.

Another important result from the time serie measurements highlights a particular spectral response of photosynthesis optimization under blue light, by the increase of $ETR_{max}(II)$ at 440 nm and the rapid non-photochemical quenching associated.. This particular spectral behavior was observed in the early spring bloom of *Phaeocystis globosa*, but not observed during the full developed bloom period of this species (at spatial scale, cf Chapter II p.). This may be because this campaign was a spatial one shot at a "t" time. The same phenomenon could have been observed before or after the campaign. This emphasizes the necessity of monitoring to fully understand the photoacclimation dynamics of the natural phytoplankton communities.

4.3. Analytical and methodological consideration of multi spectral data analysis for future improvements

In this study, all the 5 wavelengths of measuring and actinic light of MULTI-COLOR-PAM have been analyzed. This was necessary in a first approach but -time consuming, due to the dark acclimation period and measurements in replicate for light absorption capacity and the RLC (6 and 3 respectively). A potential improvement of this protocol would be to focus on specific wavelengths of interest to determine the spectral tuning between photosynthesis and the light climate. The time of analysis would be reduced by 2/5 if only blue, green, and red wavelengths were measured. Despite the reduction of measurements to build the spectral print,

the main spectral balance of photoacclimation state would be still studied. Reduction of time in data acquisition would allow field measuring at higher frequency for both space studies at sea and time series in fixed location to avoid potential aliasing phenomena. This reduction of wavelengths must respond to the general characteristics of the encountered phytoplankton. If for example an area or a period of study is known to present a community with phycoerythrin of phycocyanin pigments (as communities dominated by cyanobacteria or Cryptophyta, Kyewalyanga et al., 2002) the choice of measuring wavelengths could be modulated. In these cases, the reduction should not be done for amber, green wavelength. This reduction of measured wavelengths suggested here is based on the case of the English Channel dominated by brown algae.

The statistical approach has been here focusing on the linear variation of photosynthetic measurements among wavelengths and their linear correlations with controlling factors. Now, the spectral print of all photosynthetic parameters is not always. In this study the aim was to get a general overview of spectral balances of individual photosynthetic responses, considering the initial hypothesis and scientific questions. If the aim of the study is to analyze the spectral print, it is possible to adapt a mixed model effects formula and on focus on the polynomial spectrum.

4.4. Perspectives

4.4.1. Study of the neap and spring tidal cycles and their potential impact on wavelength dependency

Given the results of photoacclimation at the tidal and seasonal cycles described in chap3, a potential axis of research would be the study of wavelength dependent variations of photoacclimation during a full tide period of high and low lights. The results at temporal scale showed that phytoplankton among seasons could have different plasticity and strategy to photoacclimate to the tidal cycle conditions. Even if the seasonal temporal scale was the most highlighted, significant variations of wavelength dependency could also be observed at the monthly tidal cycle scale.

Given that cells integrated the intensity and the light quality variations at high and low tides, the control by the monthly tidal cycles could also be studied by seasons in order to consider the light intensity, nutrient conditions, temperature and community structure influences. Analysis by seasons implies a reduction of the power of analysis with LMEM due to the reduction of the

number of observations, except if the frequency measurement is increased. An increasing number of observations can be done per day and/or per week or per month within the same season in order to better characterize the hydrodynamic control of wavelength dependency processes. It can be hypothesized that in spring tide, population trend across wavelengths could be the lowest, without $ETR_{max}(II)$ optimization for exemple, due to high vertical mixing intensity and acclimation to averaged light of the mixed layer. On the opposite, in neap tide, population trend across wavelengths could be the highest, with an $ETR_{max}(II)$ optimization, due to low vertical mixing intensity. The processes of photoprotection under blue wavelengths could also occur in neap tide in summer or on very sunny days.

4.4.2. Comparison between photosynthetic parameters measured under full spectrum of light and individual wavelength.

The analysis of the wavelength dependency of photoacclimation was performed by the analysis of Rapid Light Curves at five different wavelengths of actinic light. The next question arising from results of this study is: how energy is managed in the case of a full spectrum (white light) of actinic light? What is the multi-wavelength light measurement added value compared to independent wavelengths of actinic light? Can the measurements under independent wavelengths be added, integrated and compared to the full spectrum according to the spectral light absorption capacity?

A first approach of this question has been done with this same device (the MULTI-COLOR-PAM) on benthic centric diatoms (Goessling et al., 2016). In their study they measured $Sigma(II)_{\lambda}$ and P-E curves parameters and compared results at red, blue and white light, which is also proposed on MULTI-COLOR-PAM. These results were achieved by providing the same number of photons at each light climate. Results of this study showed significant lower alpha, $ETR_{max}(II)$ and $Sigma(II)_{\lambda}$ under white light compared to red and blue wavelengths. Previous authors found that for all photosynthetic parameters, the white light results were lower than responses at red, and red ones lower than blue responses. A mean value between red and blue responses was not observed but more detailed measures must be performed to evaluate and quantify the differences on the full spectrum vs independent wavelength illumination, first on monospecific cultures and then on natural communities.

4.4.3. Light climate transfer experiments under controlled conditions in laboratory

In previous chapters, it was discussed the role of energy regulations in photosynthetic apparatus that account for different quantity and quality light growing conditions of phytoplankton. It has been shown that the intensity of light as well as the rate of variation of light quality in natural field play an important role in the spectral balance of energy allocation of cells. Light climate transfer experiments on natural phytoplankton communities could be realized in stable and controlled conditions in the laboratory in order to specify the temporal dynamics of spectral photoacclimation. In previous chapters, the photoacclimation state has been characterized as a compromise of the combination of the light intensity and quality. The measurement under controlled conditions in the laboratory, would allow to control the different parameters affecting the dynamics of photoacclimation. To quantify exactly the light quality variations, the light intensity could be fixed, as well as other physico-chemical conditions (for example, without random variations due to cloud cover and/or turbulence for light). *In sit*u cells perform a compromise between intensity and quantity variations because light climate changes arrive at the same time. If the intensity of light is fixed and the light quality ratios modulated, new insights on the dynamics of light quality integration could be obtained at high and low light. These experimentations could allow to quantify the range of variation between the photoacclimation state at one initial light condition and the photoacclimative state after the light transition, but also the kinetic of this spectral change.

Light transfer experiments could be performed on natural phytoplankton communities but also with monospecific species. The perspective of light transfer could allow analyzing a specific light absorption strategy for a given community with a specific light history but also photoacclimation plasticity (two different species of the same genre can have different photobiological properties (Suggett et al., 2015). The wavelength dependent plasticity of photoacclimation of a dominant species could also be an additional definition element of functional traits in microalgae.

References

Alderkamp, A. C., Garcon, V., de Baar, H. J., & Arrigo, K. R. (2011). Short-term photoacclimation effects on photoinhibition of phytoplankton in the Drake Passage (Southern Ocean). *Deep Sea Research Part I: Oceanographic Research Papers*, *58*(9), 943-955.https://doi.org/10.1016/j.dsr.2011.07.001

Alderkamp, A.C., Mills, M.M., van Dijken, G.L., Arrigo, K.R. (2013). Photoacclimation and non-photochemical quenching under *in situ* irradiance in natural phytoplankton assemblages from the Amundsen Sea, Antarctica. *Marine Ecology Progress. Series. 475*, 15–34. https://doi.org/10.3354/meps10097

Aminot, A., Kérouel, R., (2007). *Dosage automatique des nutriments dans les eaux marines: méthodes en flux continu*. Editions Quae.

Aminot, A., Kérouel, R., (2004). Dissolved organic carbon, nitrogen and phosphorus in the N-E Atlantic and the N-W Mediterranean with particular reference to non-refractory fractions and degradation. *Deep Sea Res. Part I: Oceanographic Research Papers, 51*(12), 1975–1999. https://doi.org/10.1016/j.dsr.2004.07.016

Anning, T., MacIntyre, H.L., Pratt, S.M., Sammes, P.J., Gibb, S., Geider, R.J., (2000). Photoacclimation in the marine diatom *Skeletonema costatum*. *Limnology and Oceanography. 45(8),* 1807–1817. https://doi.org/10.4319/lo.2000.45.8.1807

Arsalane, W., Rousseau, B., Duval, J.-C., (1994). Influence of the pool size of the xanthophyll cycle on the effects of light stress in a diatom: competition between photoproteci'ion and photoinhibition. *Photochemistry and photobiology*, *60*(3), 237–243. https://doi.org/10.1111/j.1751-1097.1994.tb05097.x

Astoreca, R., Rousseau, V., Lancelot, C., (2009). Coloured dissolved organic matter (CDOM) in Southern North Sea waters: Optical characterization and possible origin. *Estuarine, Coastal and Shelf Science*, *85*(4), 633–640. https://doi.org/10.1016/j.ecss.2009.10.010

Barlow, R., Lamont, T., Britz, K., Sessions, H., (2013). Mechanisms of phytoplankton adaptation to environmental variability in a shelf ecosystem. *Estuarine, Coastal and Shelf Science*, *133*, 45–57. https://doi.org/10.1016/j.ecss.2013.08.006

Barlow, R., Lamont, T., Gibberd, M.-J., Airs, R., Jacobs, L., Britz, K., (2017). Phytoplankton communities and acclimation in a cyclonic eddy in the southwest Indian Ocean. *Deep Sea Research Part I: Oceanographic Research Papers*, *124*, 18–30. https://doi.org/10.1016/j.dsr.2017.03.013

Bates, D., Mächler, M., Bolker, B., Walker, S.,(2015). Fitting linear mixed-effects models using lme4. *Journal of Statistical Software*, *67*. https://doi.org/10.18637/jss.v067.i01

Bates, D., Maechler, M., Bolker, B., Walker, S., Christensen, R.H.B., Singmann, H., Dai, B., Scheipl, F., Grothendieck, G., Green, P., Fox, J., (2019). lme4: Linear Mixed-Effects Models using "Eigen" and S4.

Behrenfeld, M.J., Falkowski, P.G., (1997a). A consumer's guide to phytoplankton primary productivity models. *Limnology and oceanography*, *42*(7), 1479–1491. https://doi.org/10.4319/lo.1997.42.7.1479

Behrenfeld, M.J., Falkowski, P.G., (1997b). Photosynthetic rates derived from satellite-based chlorophyll concentration. *Limnology and oceanography*, *42*(1), 1–20. https://doi.org/10.4319/lo.1997.42.1.0001

Behrenfeld, M.J., Halsey, K.H., Milligan, A.J., (2008). Evolved physiological responses of phytoplankton to their integrated growth environment. *Philosophical Transactions of the Royal Society B: Biological Sciences*, *363*(1504), 2687–2703. https://doi.org/10.1098/rstb.2008.0019

Behrenfeld, M.J., Prasil, O., Babin, M., Bruyant, F., (2004). In search of a physiological basis for covariations in light-limited ad light-saturated photosynthesis: photosynthetic variability in algae. *Journal of Phycology*. *40*(1), 4–25. https://doi.org/10.1046/j.1529-8817.2004.03083.x

Bertrand, F., Maumy-Bertrand, M., 2010. Using partial triadic analysis for depicting the temporal evolution of spatial structures: assessing phytoplankton structure and succession in a water reservoir. *Case Studies In Business, Industry And Government Statistics*, *4*(1),23-43, http://www.bentley.edu/csbigs/documents/bertrand2.pdf.

Beutler, M., Wiltshire, K.H., Meyer, B., Moldaenke, C., Lüring, C., Meyerhöfer, M., Hansen, U.-P., Dau, H., (2002). A fluorometric method for the differentiation of algal populations *in vivo* and *in situ*. *Photosynthesis research*, *72*(1), 39–53. https://doi.org/10.1023/A:1016026607048

Bidigare, R.R., Ondrusek, M.E., Morrow, J.H., Kiefer, D.A., (1990). *In-vivo* absorption properties of algal pigments, in: Spinrad, R.W. (Ed.), Presented at the Orlando '90 *Ocean Optics X*, 16-20 April, Orlando, FL, United States, p. 290 https://doi.org/10.1117/12.21451

Bilger, W., & Björkman, O. (1990). Role of the xanthophyll cycle in photoprotection elucidated by measurements of light-induced absorbance changes, fluorescence and photosynthesis in leaves of Hedera canariensis. *Photosynthesis research*, *25*(3), 173-185.

Bolker, B.M., Brooks, M.E., Clark, C.J., Geange, S.W., Poulsen, J.R., Stevens, M.H.H., White, J.-S.S., (2009). Generalized linear mixed models: a practical guide for ecology and evolution. *Trends in ecology & evolution*, *24*(3), 127–135. https://doi.org/10.1016/j.tree.2008.10.008

Bonamano, S., Madonia, A., Piermattei, V., Stefanì, C., Lazzara, L., Nardello, I., Decembrini, F., Marcelli, M., (2020). Phyto-VFP: a new bio-optical model of pelagic primary production based on variable fluorescence measures. *Journal of Marine Systems*, *204*, 103304. https://doi.org/10.1016/j.jmarsys.2019.103304

Bradbury, M., Baker, N.R., (1984). A quantitative determination of photochemical and non-photochemical quenching during the slow phase of the chlorophyll fluorescence induction curve of bean leaves. *Biochimica et Biophysica Acta (BBA)-Bioenergetics*, *765*(3), 275–281. https://doi.org/10.1016/0005-2728(84)90166-X

Breton, E., Brunet, C., Sautour, B., Brylinski, J.-M., (2000). Annual variations of phytoplankton biomass in the Eastern English Channel: comparison by pigment signatures and microscopic counts. *Journal of Plankton Research*, *22*(8), 1423–1440. https://doi.org/10.1093/plankt/22.8.1423

Breton, E., Rousseau, V., Parent, J.Y., Ozer, J., Lancelot, C., (2006). Hydroclimatic modulation of diatom/*Phaeocystis* blooms in nutrient-enriched Belgian coastal waters (North Sea). *Limnology and Oceanography*, *51*(3), 1401–1409. https://doi.org/10.4319/lo.2006.51.3.1401

Bricaud, A., Claustre, H., Ras, J., Oubelkheir, K., (2004). Natural variability of phytoplanktonic absorption in oceanic waters: Influence of the size structure of algal populations. *Journal of Geophysical Research: Oceans*, *109*(C11). https://doi.org/10.1029/2004JC002419

Bruce, D., Biggins, J., Steiner, T., Thewalt, M., (1986). Excitation energy transfer in the cryptophytes. Fluorescence excitation spectra and picosecond time-resolved emission spectra of intact algae at 77 K. *Photochemistry and photobiology*, *44*(4), 519–525. https://doi.org/10.1111/j.1751-1097.1986.tb04702.x

Brunet, C., Brylinski, J., Lemoine, Y., (1993). *In situ* variations of the xanthophylls diatoxanthin and diadinoxanthin: photoadaptation and relationships with a

hydrodynamical system in the eastern English Channel. *Marine Ecology Progress Series, (102)*, 69–77. https://doi.org/10.3354/meps102069

Brunet, C., Brylinski, J.M., Frontier, S., (1992). Productivity, photosynthetic pigments and hydrology in the coastal front of the Eastern English Channel. *Journal of Plankton Research*, *14*(11), 1541–1552. https://doi.org/10.1093/plankt/14.11.1541

Brunet, C., Chandrasekaran, R., Barra, L., Giovagnetti, V., Corato, F., Ruban, A.V., (2014). Spectral Radiation Dependent Photoprotective Mechanism in the Diatom *Pseudo-nitzschia multistriata*. *PLoS One* 9(1), e87015. https://doi.org/10.1371/journal.pone.0087015

Brunet, C., Johnsen, G., Lavaud, J., Roy, S., (2011). Pigments and photoacclimation processes In Roy S., Llewellyn CA, Egeland ES and Johnsen G.[eds.], Phytoplankton Pigments: Characterization, Chemotaxonomy and Applications in Oceanography, pp. 445–471. https://doi.org/10.1017/CBO9780511732263.017

Brunet, C., Lavaud, J., (2010). Can the xanthophyll cycle help extract the essence of the microalgal functional response to a variable light environment?. *Journal of Plankton Research*, *32*(12), 1609–1617. https://doi.org/10.1093/plankt/fbq104

Brunet, C., Lizon, F., (2003). Tidal and diel periodicities of size-fractionated phytoplankton pigment signatures at an offshore station in the southeastern English Channel. *Estuarine, Coastal and Shelf Science*, *56*(3-4), 833–843. https://doi.org/10.1016/S0272-7714(02)00323-2

Brylinski, J.-M., Lagadeuc, Y., (1990). L'interface eaux côtières/eaux du large dans le Pas-de-Calais (côte française): une zone frontale. *Comptes rendus de l'Académie des sciences. Série 2, Mécanique, Physique, Chimie, Sciences de l'univers, Sciences de la Terre*, *311*(5), 535-540

Brylinski, J.-M., Lagadeuc, Y., Gentilhomme, V., Dupont, J.P., Lafite, R., Dupeuple, P.A., Huault, M.F., Auger, Y., Puskaric, E., Wartel, M., Cabioch, L., (1991). Le fleuve côtier: un phénomène hydrologique important en Manche Orientale. Exemple du Pas-de-Calais. *Oceanologica Acta, Special issue*, 197–203.

Buchel, C., Wilhelm, C., (1993). In vivo analysis of slow chlorophyll fluorescence induction kinetics in algae: progress, problems and perspectives. *Photochemistry and Photobiology*, *58*(1), 137-148.

Burson, A., Stomp, M., Greenwell, E., Grosse, J., Huisman, J., (2018). Competition for nutrients and light: testing advances in resource competition with a natural phytoplankton community. *Ecology*, *99*(5), 1108–1118. https://doi.org/10.1002/ecy.2187

Callieri, C., Amicucci, E., Bertoni, R., Vörös, L., (1996). Fluorometric characterization of two picocyanobacteria strains from lakes of different underwater light quality. *Internationale Revue der gesamten Hydrobiologie und Hydrographie*, *81*(1), 13–23. https://doi.org/10.1002/iroh.19960810103

Capuzzo, E., Stephens, D., Silva, T., Barry, J., Forster, R.M., (2015). Decrease in water clarity of the southern and central North Sea during the 20th century. *Global change biology*, *21*(6), 2206–2214. https://doi.org/10.1111/gcb.12854

Chen, B., (2015). Patterns of thermal limits of phytoplankton. *Journal of Plankton Research*, *37*(2), 285–292. https://doi.org/10.1093/plankt/fbv009

Claquin, P., Longphuirt, S.N., Fouillaron, P., Huonnic, P., Ragueneau, O., Klein, C., Leynaert, A., (2010). Effects of simulated benthic fluxes on phytoplankton dynamic and photosynthetic parameters in a mesocosm experiment (Bay of Brest, France). *Estuarine, Coastal and Shelf Science*, *86*(1), 93–101. https://doi.org/10.1016/j.ecss.2009.10.017

Cohn, S.A., Halpin, D., Hawley, N., Ismail, A., Kaplan, Z., Kordes, T., Kuhn, J., Macke, W., Marhaver, K., Ness, B., Olszewski, S., Pike, A., Rice, E., Sbarboro, J., Wolske, A.,

Zapata, Y., (2015). Comparative analysis of light-stimulated motility responses in three diatom species. *Diatom Research*, *30*(3), 213–225. https://doi.org/10.1080/0269249X.2015.1058295

Combe, C., Hartmann, P., Rabouille, S., Talec, A., Bernard, O., Sciandra, A., (2015). Long-term adaptive response to high-frequency light signals in the unicellular photosynthetic eukaryote *Dunaliella salina*. *Biotechnology and bioengineering*, *112*(6), 1111–1121. https://doi.org/10.1002/bit.25526

Comets, E., Lavenu, A., & Lavielle, M. (2011). SAEMIX: Stochastic Approximation Expectation Maximization (SAEM) Algorithm. *R package version*, *1*.

Correa-Reyes, J.G., Sánchez-Saavedra, M. del P., Siqueiros-Beltrones, D.A., Flores-Acevedo, N., 2001. Isolation and growth of eight strains of benthic diatoms, cultured under two light conditions. *Journal of Shellfish Research*, *20*(2), 603-610.

Cosgrove, J., Borowitzka, M.A., (2010). Chlorophyll fluorescence terminology: an introduction. In *Chlorophyll a fluorescence in aquatic sciences: methods and applications* (pp. 1-17). Springer, Dordrecht, pp. 1–17. https://doi.org/10.1007/978-90-481-9268-7_1

Crawley, M.J., (2007). *The R book*. John Wiley & Sons

Cullen, J.J., Renger, E.H., (1979). Continuous measurement of the DCMU-induced fluorescence response of natural phytoplankton populations. *Marine biology*, *53*(1), 13–20. https://doi.org/10.1007/BF00386524

Darecki, M., Stramski, D., Sokólski, M., (2011). Measurements of high-frequency light fluctuations induced by sea surface waves with an Underwater Porcupine Radiometer System. *Journal of Geophysical Research: Oceans*, *116*(C7). https://doi.org/10.1029/2011JC007338

Demmig-Adams, B., (1990). Carotenoids and photoprotection in plants: a role for the xanthophyll zeaxanthin. *Biochimica et Biophysica Acta (BBA)-Bioenergetics*, *1020*(1), 1–24. https://doi.org/10.1016/0005-2728(90)90088-L

Demmig-Adams, B., Adams, W.W., (2006). Photoprotection in an ecological context: the remarkable complexity of thermal energy dissipation. *New Phytologist*, *172*(1), 11–21. https://doi.org/10.1111/j.1469-8137.2006.01835.x

Depauw, F.A., Rogato, A., Ribera d'Alcala, M., Falciatore, A., (2012). Exploring the molecular basis of responses to light in marine diatoms. *Journal of experimental botany*, *63*(4), 1575–1591. https://doi.org/10.1093/jxb/ers005

Dimier, C., Brunet, C., Geider, R., Raven, J.,(2009a). Growth and photoregulation dynamics of the picoeukaryote Pelagomonas calceolata in fluctuating light. *Limnology and Oceanography*, *54*(3), 823–836. https://doi.org/10.4319/lo.2009.54.3.0823

Dimier, C., Corato, F., Saviello, G., Brunet, C., (2007). Photophysiological Properties of the Marine Picoeukaryote Picochlorum Rcc 237 (*trebouxiophyceae*, Chlorophyta). *Journal of phycology*, *43*(2), 275–283. https://doi.org/10.1111/j.1529-8817.2007.00327.x

Dimier, C., Corato, F., Tramontano, F., Brunet, C., (2007b). Photoprotection and xanthophyll-cycle activity in three marine diatoms 1. *Journal of Phycology*, *43*(5), 937–947. https://doi.org/10.1111/j.1529-8817.2007.00381.x

Dimier, C., Giovanni, S., Ferdinando, T., Brunet, C., (2009b). Comparative ecophysiology of the xanthophyll cycle in six marine phytoplanktonic species. *Protist*, *160*(3), 397–411. https://doi.org/10.1016/j.protis.2009.03.001

Dougher, T.A.O., Bugbee, B., (2001). Differences in the Response of Wheat, Soybean and Lettuce to Reduced Blue Radiation¶. *Photochemistry and Photobiology*, *73*(2), 199–207. https://doi.org/10.1562/0031-8655(2001)0730199DITROW2.0.CO2

Drews, G., (2005). Contributions of Theodor Wilhelm Engelmann on phototaxis, chemotaxis, and photosynthesis. *Photosynthesis research*, *83*(1), 25–34. https://doi.org/10.1007/s11120-004-6313-8

Dubinsky, Z., (1992). The functional and optical absorption cross-sections of phytoplankton photosynthesis. In *Primary productivity and biogeochemical cycles in the sea* (pp. 31-45). Springer, Boston, MA.. https://doi.org/10.1007/978-1-4899-0762-2_3

Dubinsky, Z., Schofield, O., (2010). From the light to the darkness: thriving at the light extremes in the oceans. *Hydrobiologia*, *639*(1), 153–171. https://doi.org/10.1007/s10750-009-0026-0

Dubinsky, Z., Stambler, N., (2009). Photoacclimation processes in phytoplankton: mechanisms, consequences, and applications. *Aquatic Microbial Ecology*, *56*(2-3), 163–176. https://doi.org/10.3354/ame01345

Duursma, R.A., Barton, C.V.M., Lin, Y.-S., Medlyn, B.E., Eamus, D., Tissue, D.T., Ellsworth, D.S., McMurtrie, R.E., (2014). The peaked response of transpiration rate to vapour pressure deficit in field conditions can be explained by the temperature optimum of photosynthesis. *Agricultural and Forest Meteorology*, *189*, 2-10. https://doi.org/10.1016/j.agrformet.2013.12.007

Eilers, P.H.C., Peeters, J.C.H., (1988). A model for the relationship between light intensity and the rate of photosynthesis in phytoplankton. *Ecological modelling*, *42*(3-4), 199–215. https://doi.org/10.1016/0304-3800(88)90057-9

Eisner, L.B., Twardowski, M.S., Cowles, T.J., Perry, M.Jane., (2003). Resolving phytoplankton photoprotective: photosynthetic carotenoid ratios on fine scales using *in situ* spectral absorption measurements. *Limnology and Oceanography*, *48*(2), 632–646. https://doi.org/10.4319/lo.2003.48.2.0632

Emerson, R., Lewis, C.M., (1942). The photosynthetic efficiency of phycocyanin in Chroococcus, and the problem of carotenoid participation in photosynthesis. *The Journal of general physiology*, *25*(4), 579–595. https://doi.org/10.1085/jgp.25.4.579

Engelmann, Th.W., (1882). Ueber Sauerstoffausscheidung von Pflanzenzellen im Mikrospektrum. Pflüg. Arch. Für Gesammte Physiol. Menschen Thiere 27, 485–489. https://doi.org/10.1007/BF01802976

Engelmann, T.W., (1883). Farbe und Assimilation. Bot Zeit 41, 1-13,17-29.

Falkowski, P.G., (1992). Molecular ecology of phytoplankton photosynthesis. In *Primary productivity and biogeochemical cycles in the sea* (pp. 47-67). Springer, Boston, MA. https://doi.org/10.1007/978-1-4899-0762-2_4

Falkowski, P.G., Knoll, A.H. (Eds.), (2007). *Evolution of primary producers in the sea*. Academic Press.

Falkowski, P.G., LaRoche, J., (1991). Acclimation to spectral irradiance in algae. *Journal of Phycology*, *27*(1), 8-14. https://doi.org/10.1111/j.0022-3646.1991.00008.x

Falkowski, P.G., Raven, J.A., (2007). *Aquatic photosynthesis*. Princeton University Press.

Falkowski, P.G., Wyman, K., Ley, A.C., Mauzerall, D.C., (1986). Relationship of steady-state photosynthesis to fluorescence in eucaryotic algae. *Biochimica et Biophysica Acta (BBA)-Bioenergetics*, *849*(2), 183-192. https://doi.org/10.1016/0005-2728(86)90024-1

Figueroa, F.L., Niell, F.X., Figueiras, F.G., Villarino, M.L., 1998. Diel migration of phytoplankton and spectral light field in the Ria de Vigo (NW Spain). *Marine Biology*, *130*(3), 491-499. https://doi.org/10.1007/s002270050269

Fisher, T., Shurtz-Swirski, R., Gepstein, S., Dubinsky, Z., (1989). Changes in the levels of ribulose-l, 5-bisphosphate carboxylase/oxygenase (rubisco) in tetraedron minimum (chlorophyta) during light and shade adaptation. *Plant and cell physiology*, *30*(2), 221-228.

Forster, R.M., Dring, M.J., (1992). Interactions of blue light and inorganic carbon supply in the control of light-saturated photosynthesis in brown algae. *Plant, Cell & Environment, 15*(2), 241-247. https://doi.org/10.1111/j.1365-3040.1992.tb01478.x

Fortunato, A.E., Jaubert, M., Enomoto, G., Bouly, J.-P., Raniello, R., Thaler, M., Malviya, S., Bernardes, J.S., Rappaport, F., Gentili, B., Huysman, M.J.J., Carbone, A., Bowler, C., d'Alcalà, M.R., Ikeuchi, M., Falciatore, A., (2016). Diatom phytochromes reveal the existence of far-red-light-based sensing in the ocean. *The Plant Cell, 28*(3), 616-628. https://doi.org/10.1105/tpc.15.00928

Frankenbach, S., Ezequiel, J., Plecha, S., Goessling, J.W., Vaz, L., Kühl, M., Dias, J.M., Vaz, N., Serôdio, J., (2020). Synoptic spatio-temporal variability of the photosynthetic productivity of microphytobenthos and phytoplankton in a tidal estuary. *Frontiers in Marine Science, 7*. https://doi.org/10.3389/fmars.2020.00170

From, N., Richardson, K., Mousing, E.A., Jensen, P.E., 2014. Removing the light history signal from normalized variable fluorescence (Fv/Fm) measurements on marine phytoplankton. *Limnology and Oceanography: Methods*, *12*(11), 776-783. https://doi.org/10.4319/lom.2014.12.776

Gaidukov, N., (1902). Über den Einfluß farbigen Lichts auf die Färbung lebender Oscillatorien.

Gantt, E., (1981). Phycobilisomes. *Annual Review of Plant Physiology*, *32*(1), 327-347. https://doi.org/10.1146/annurev.pp.32.060181.001551

Gelzinis, A., Butkus, V., Songaila, E., Augulis, R., Gall, A., Büchel, C., Robert, B., Abramavicius, D., Zigmantas, D., Valkunas, L., (2015). Mapping energy transfer channels in fucoxanthin–chlorophyll protein complex. *Biochimica et Biophysica Acta (BBA)-Bioenergetics*, *1847*(2), 241-247. https://doi.org/10.1016/j.bbabio.2014.11.004

Gentilhomme, V., Lizon, F., (1998). Seasonal cycle of nitrogen and phytoplankton biomass in a well-mixed coastal system (Eastern English Channel). *Hydrobiologia* 361, 191–199. https://doi.org/10.1023/A:1003134617808

Glover, H.E., Keller, M.D., Spinrad, R.W., (1987). The effects of light quality and intensity on photosynthesis and growth of marine eukaryotic and prokaryotic phytoplankton clones. *Journal of Experimental Marine Biology and Ecology*, *105*(2-3), 137-159.. https://doi.org/10.1016/0022-0981(87)90168-7

Goessling, J.W., Cartaxana, P., Kühl, M., (2016). Photo-protection in the centric diatom *Coscinodiscus granii* is not controlled by chloroplast high-light avoidance movement. *Frontiers in Marine Science, 2*, 115. https://doi.org/10.3389/fmars.2015.00115

Goessling, J.W., Frankenbach, S., Ribeiro, L., Serôdio, J., Kühl, M., (2018a). Modulation of the light field related to valve optical properties of raphid diatoms: implications for niche differentiation in the microphytobenthos. *Marine Ecology Progress Series*, *588*, 29-42. https://doi.org/10.3354/meps12456

Goessling, J.W., Su, Y., Cartaxana, P., Maibohm, C., Rickelt, L.F., Trampe, E.C.L., Walby, S.L., Wangpraseurt, D., Wu, X., Ellegaard, M., Kühl, M., (2018b). Structure-based optics of centric diatom frustules: modulation of the in vivo light field for efficient diatom photosynthesis. *New Phytologist*, *219*(1), 122-134. https://doi.org/10.1111/nph.15149

Gohin, F., Bryère, P., Griffiths, J.W., (2015). The exceptional surface turbidity of the North-West European shelf seas during the stormy 2013–2014 winter: Consequences for the initiation of the phytoplankton blooms?. *Journal of marine systems*, *148*, 70-85. https://doi.org/10.1016/j.jmarsys.2015.02.001

Gorai, T., Katayama, T., Obata, M., Murata, A., Taguchi, S., (2014). Low blue light enhances growth rate, light absorption, and photosynthetic characteristics of four marine phytoplankton species. *Journal of experimental marine biology and ecology*, *459*, 87-95. https://doi.org/10.1016/j.jembe.2014.05.013

Gorbunov, M., Shirsin, E., Nikonova, E., Fadeev, V., Falkowski, P., (2020). A multi-spectral fluorescence induction and relaxation (FIRe) technique for physiological and taxonomic analysis of phytoplankton communities. *Marine Ecology Progress Series*, *644*, 1-13. https://doi.org/10.3354/meps13358

Gorbunov, M.Y., Falkowski, P.G., (2004). Fluorescence induction and relaxation (FIRe) technique and instrumentation for monitoring photosynthetic processes and primary production in aquatic ecosystems. Presented at the 13th International Congress of Photosynthesis, Montreal, pp. 1029–1031.

Gorbunov, M.Y., Kolber, Z.S., Falkowski, P.G., (1999). Measuring photosynthetic parameters in individual algal cells by Fast Repetition Rate fluorometry. *Photosynthesis Research, 62*(2), 141-153. https://doi.org/10.1023/A:1006360005033

Govindje, E., (1995). Sixty-Three Years Since Kautsky: Chlorophyll a Fluorescence. *Functional Plant Biology,22,* 131–160. https://doi.org/10.1071/pp9950131

Govindjee, (2009). List of biography and history published mostly in Photosynthesis Research, 1988–2008. *Photosynthetic research, 99,* 139. https://doi.org/10.1007/s11120-008-9392-0

Green, B.R., Parson, W.W. (Eds.), 2003. Light-Harvesting Antennas in Photosynthesis, Advances in Photosynthesis and Respiration. Springer Netherlands, Dordrecht. https://doi.org/10.1007/978-94-017-2087-8

Grobbelaar, J.U., Nedbal, L., Tichý, V., (1996). Influence of high frequency light/dark fluctuations on photosynthetic characteristics of microalgae photoacclimated to different light intensities and implications for mass algal cultivation. *Journal of Applied Phycology*, *8*(4), 335-343. https://doi.org/10.1007/BF02178576

Hauschild, C.A., McMurter, H.J.G., Pick, F.R., (1991). Effect of Spectral Quality on Growth and Pigmentation of Picocyanobacteria1. *Journal of phycology*, *27*(6), 698–702. https://doi.org/10.1111/j.0022-3646.1991.00698.x

Havaux, M., Strasser, R.J., Greppin, H., (1991). A theoretical and experimental analysis of the qP and qN coefficients of chlorophyll fluorescence quenching and their relation to photochemical and nonphotochemical events. *Photosynthetic Research, 27*(1), 41–55. https://doi.org/10.1007/BF00029975

Haxo, F.T., (1960). The wavelength dependence of photosynthesis and the role of accesory pigments. Comp. Biochem. Photoreact. Syst. Academic Press, New York, 339–360.

Haxo, F.T., Blinks, L.R., (1950). Photosynthetic action spectra of marine algae. *The Journal of general physiology*, *33*(4), 389-422. https://doi.org/10.1085/jgp.33.4.389

Herbstová, M., Bína, D., Koník, P., Gardian, Z., Vácha, F., Litvín, R., (2015). Molecular basis of chromatic adaptation in pennate diatom *Phaeodactylum tricornutum*. *Biochimica et Biophysica Acta (BBA)-Bioenergetics*, *1847*(6-7), 534-543. https://doi.org/10.1016/j.bbabio.2015.02.016

Hickman, A., Dutkiewicz, S., Williams, R., Follows, M., (2010). Modelling the effects of chromatic adaptation on phytoplankton community structure in the oligotrophic ocean. *Marine Ecology Progress Series*, *406*, 1-17. https://doi.org/10.3354/meps08588

Hickman, A.E., Holligan, P.M., Moore, C.M., Sharples, J., Krivtsov, V., Palmer, M.R., (2009). Distribution and chromatic adaptation of phytoplankton within a shelf sea thermocline. *Limnology and Oceanography*, *54*(2), 525-536. https://doi.org/10.4319/lo.2009.54.2.0525

Hoadley, K.D., Warner, M.E., (2017). Use of Open Source Hardware and Software Platforms to Quantify Spectrally Dependent Differences in Photochemical Efficiency and Functional Absorption Cross Section within the Dinoflagellate Symbiodinium spp. *Frontiers in Marine Science, 4*, 365. https://doi.org/10.3389/fmars.2017.00365

Hoepffner, N., Sathyendranath, S., 1992. Bio-optical characteristics of coastal waters: Absorption spectra of phytoplankton and pigment distribution in the western North Atlantic. *Limnology and oceanography*, *37*(8), 1660-1679. https://doi.org/10.4319/lo.1992.37.8.1660

Holdsworth, E.S., (1985). Effect of growth factors and light quality on the growth, pigmentation and photosynthesis of two diatoms, *Thalassiosira gravida* and *Phaeodactylum tricornutum*. *Marine Biology*, *86*(3), 253-262. https://doi.org/10.1007/BF00397512

Holtzegel, U., (2016). The Lhc family of Arabidopsis thaliana. *Endocytobiosis and Cell Research*, *27*(2), 71-89.

Honaker, J., King, G., Blackwell, M., Honaker, J., King, G., & Blackwell, M. (2011). Amelia II: A program for missing data. *Journal of statistical software*, *45*(7), 1-47.

Horton, P., Hague, A., (1988). Studies on the induction of chlorophyll fluorescence in isolated barley protoplasts. IV. Resolution of non-photochemical quenching. *Biochimica et Biophysica Acta (BBA)-Bioenergetics*, *932*, 107-115. https://doi.org/10.1016/0005-2728(88)90144-2

Houliez, E., Lefebvre, S., Lizon, F., Schmitt, F.G., (2017). Rapid light curves (RLC) or non-sequential steady-state light curves (N-SSLC): which fluorescence-based light response curve methodology robustly characterizes phytoplankton photosynthetic activity and acclimation status?. *Marine Biology*, *164*(8), 1-17. https://doi.org/10.1007/s00227-017-3208-8

Houliez, E., Lizon, F., Artigas, L.F., Lefebvre, S., Schmitt, F.G., (2013a). Spatio-temporal variability of phytoplankton photosynthetic activity in a macrotidal ecosystem (the Strait of Dover, eastern English Channel). *Estuarine, Coastal and Shelf Science*, *129*, 37-48. https://doi.org/10.1016/j.ecss.2013.06.009

Houliez, E., Lizon, F., Lefebvre, S., Artigas, L.F., Schmitt, F.G., (2015). Phytoplankton photosynthetic activity dynamics in a temperate macrotidal ecosystem (the Strait of Dover, eastern English Channel): Time scales of variability and environmental control. *Journal of Marine Systems*, *147*, 61-75. https://doi.org/10.1016/j.jmarsys.2014.05.001

Houliez, E., Lizon, F., Lefebvre, S., Artigas, L.F., Schmitt, F.G., (2013b). Short-term variability and control of phytoplankton photosynthetic activity in a macrotidal ecosystem (the Strait of Dover, eastern English Channel). *Marine biology*, *160*(7), 1661-1679. https://doi.org/10.1007/s00227-013-2218-4

Houliez, E., Lizon, F., Thyssen, M., Artigas, L.F., Schmitt, F.G., (2012a) Spectral fluorometric characterization of Haptophyte dynamics using the FluoroProbe: an application in the eastern English Channel for monitoring *Phaeocystis globosa*. *Journal of plankton research*, *34*(2), 136-151. https://doi.org/10.1093/plankt/fbr091

Humphrey, G.F., (1983). The effect of the spectral composition of light on the growth, pigments, and photosynthetic rate of unicellular marine algae. *Journal of Experimental Marine Biology and Ecology*, *66*(1), 49-67. https://doi.org/10.1016/0022-0981(83)90027-8

Husson, F., Josse, J., Le, S., Mazet, J., 2020. FactoMineR: Multivariate Exploratory Data Analysis and Data Mining.

Huysman, M.J.J., Fortunato, A.E., Matthijs, M., Costa, B.S., Vanderhaeghen, R., Daele, H.V. den, Sachse, M., Inzé, D., Bowler, C., Kroth, P.G., Wilhelm, C., Falciatore, A., Vyverman, W., Veylder, L.D., (2013). AUREOCHROME1a-mediated induction of the diatom-specific cyclin dsCYC2 controls the onset of cell division in diatoms (*Phaeodactylum tricornutum*). *The Plant Cell*, *25*(1), 215-228. https://doi.org/10.1105/tpc.112.106377

Irwin, B., Anning, J., Caverhill, C., Platt, T., (1990). *Primary production on the Labrador Shelf and in the Strait of Belle Isle in May 1988*. Department of Fisheries and Oceans, Marine Fish Division, Biological Sciences Branch, Biological Station.

Jaubert, M., Bouly, J.-P., Ribera d'Alcalà, M., Falciatore, A., 2017. (2017). Light sensing and responses in marine microalgae. *Current opinion in plant biology*, *37*, 70-77. https://doi.org/10.1016/j.pbi.2017.03.005

Jeffrey, S.W., 1980. Algal Pigment Systems, in: Falkowski, P.G. (Ed.), Primary Productivity in the Sea, Environmental Science Research. Springer US, Boston, MA, pp. 33–58. https://doi.org/10.1007/978-1-4684-3890-1_3

Jeffrey, S.W., Vesk, M., (1977). Effect of Blue-Green Light on Photosynthetic Pigments and Chloroplast Structure in the Marine Diatom Stephanopyxis Turris1. *Journal of Phycology*, *13*(3), 271-279. https://doi.org/10.1111/j.1529-8817.1977.tb02927.x

Jeffrey, S.W., Wright, S.W., Zapata, M.,(2011). Microalgal classes and their signature pigments, in: Roy, S., Llewellyn, C., Egeland, E.S., Johnsen, G. (Eds.), Phytoplankton Pigments. Cambridge University Press, Cambridge, pp. 3–77. https://doi.org/10.1017/CBO9780511732263.004

Jensen, J.P., Jeppesen, E., Olrik, K., Kristensen, P., (1994). Impact of nutrients and physical factors on the shift from cyanobacterial to chlorophyte dominance in shallow Danish lakes. *Canadian Journal of fisheries and aquatic sciences*, *51*(8), 1692-1699. https://doi.org/10.1139/f94-170

Jerlov, N.G., (1955). The Particulate Matter in the Sea as Determined by Means of the Tyndall Meter. Tellus 7, 218–225. https://doi.org/10.1111/j.2153-3490.1955.tb01155.x

Johnsen, G., Nelson, N.B., Jovine, R.V.M., Prézelin, B.B., (1994). Chromoprotein-and pigment-dependent modeling of spectral light absorption in two dinoflagellates, Prorocentrum minimum and Heterocapsa pygmaea. *Marine Ecology Progress Series*, 245-258.

Johnsen, G., Sakshaug, E., (2007). Biooptical characteristics of PSII and PSI in 33 species (13 pigment groups) of marine phytoplankton, and the relevance for pulse-amplitude-modulated and fast-repetition-rate fluorometry 1. *Journal of Phycology*, *43*(6), 1236-1251. https://doi.org/10.1111/j.1529-8817.2007.00422.x

Johnsen, G., Sakshaug, E., 1993. Bio-Optical Characteristics and Photoadaptive Responses in the Toxic and Bloom-Forming Dinoflagellates Gyrodinium Aureolum, Gymnodinium Galatheanum, and Two Strains of Prorocentrum Minimum1. *Journal of Phycology*, *29*(5), 627-642. https://doi.org/10.1111/j.0022-3646.1993.00627.x

Jouenne, F., Lefebvre, S., Véron, B., Lagadeuc, Y., (2007). Phytoplankton community structure and primary production in small intertidal estuarine-bay ecosystem (eastern English Channel, France). *Marine Biology*, *151*(3), 805-825. https://doi.org/10.1007/s00227-006-0440-z

Jouenne, F., Lefebvre, S., Véron, B., Lagadeuc, Y., (2005). Biological and physicochemical factors controlling short-term variability in phytoplankton primary production and photosynthetic parameters in a macrotidal ecosystem (eastern English Channel). *Estuarine, Coastal and Shelf Science*, *65*(3), 421-439. https://doi.org/10.1016/j.ecss.2005.05.023

Jungandreas, A., Schellenberger Costa, B., Jakob, T., von Bergen, M., Baumann, S., Wilhelm, C., (2014). The Acclimation of *Phaeodactylum tricornutum* to Blue and Red Light Does Not Influence the Photosynthetic Light Reaction but Strongly Disturbs the Carbon Allocation Pattern. *PLoS One 9*, e99727. https://doi.org/10.1371/journal.pone.0099727

Kaňa, R., Kotabová, E., Prášil, O., (2013). Presence of Flexible Non-Photochemical Quenching in Cryptophytes (Rhodomonas Salina), in: Photosynthesis Research for Food, Fuel and

the Future. Springer Berlin Heidelberg, Berlin, Heidelberg, pp. 489–492. https://doi.org/10.1007/978-3-642-32034-7_103
Kaňa, R., Kotabová, E., Šedivá, B., Kuthanová Trsková, E., (2019). Photoprotective strategies in the motile cryptophyte alga Rhodomonas salina—role of non-photochemical quenching, ions, photoinhibition, and cell motility. *Folia microbiologica*, *64*(5), 691-703. https://doi.org/10.1007/s12223-019-00742-y
Kaňa, R., Kotabová, E., Sobotka, R., Prášil, O., (2012). Non-Photochemical Quenching in Cryptophyte Alga Rhodomonas salina Is Located in Chlorophyll a/c Antennae. *PLoS ONE 7*, e29700. https://doi.org/10.1371/journal.pone.0029700
Kautsky, H., Hirsch, A., (1931). Neue Versuche zur Kohlensãureassimilation. Naturwissenschaften 19, 964–964. https://doi.org/10.1007/BF01516164
Kehoe, D.M., Gutu, A., (2006). Responding to color: the regulation of complementary chromatic adaptation. *Annu. Rev. Plant Biol.*, *57*, 127-150. https://doi.org/10.1146/annurev.arplant.57.032905.105215
Kiang, N.Y., Siefert, J., Govindjee, Blankenship, R.E., (2007). Spectral signatures of photosynthesis. I. Review of Earth organisms. *Astrobiology*, *7*(1), 222-251. https://doi.org/10.1089/ast.2006.0105
Kianianmomeni, A., Hallmann, A., (2014). Algal photoreceptors: in vivo functions and potential applications. *Planta 239*(1), 1-26. https://doi.org/10.1007/s00425-013-1962-5
Kirk, J.T.O., (2011). Light and Photosynthesis in Aquatic Ecosystems, 3rd ed. Cambridge University Press, Cambridge. https://doi.org/10.1017/CBO9781139168212
Kirk, J.T.O., Tilney-Bassett, R.A.E., (1978). The plastids, their chemistry, structure, growth, and inheritance, Rev. 2d ed. ed. Elsevier/North Holland Biomedical Press ; sole distributors for the U.S.A. and Canada, Elsevier/North-Holland, Amsterdam ; New York : New York.
Klughammer, C., Schreiber, U., (2015). Apparent PS II absorption cross-section and estimation of mean PAR in optically thin and dense suspensions of Chlorella. *Photosynthetic Research*, *123*, 77–92. https://doi.org/10.1007/s11120-014-0040-6
Köhler, J., Wang, L., Guislain, A., Shatwell, T., (2018). Influence of vertical mixing on light-dependency of phytoplankton growth. *Limnology and Oceanography*, *63*(3), 1156-1167. https://doi.org/10.1002/lno.10761
Kolber, Z., Falkowski, P.G., (1993). Use of active fluorescence to estimate phytoplankton photosynthesis *in situ*. *Limnology and Oceanography, 38*, 1646–1665. https://doi.org/10.4319/lo.1993.38.8.1646
Kolber, Z.S., Falkowski, P.G., (1992). Fast Repetition Rate fluorometer for making *in situ* measurements of primary productivity. Presented at the Proceedings of IEEE Ocean 92th Conference, Newport, Rhode island, pp. 637–641.
Kolber, Z.S., Prášil, O., Falkowski, P.G., (1998). Measurements of variable chlorophyll fluorescence using fast repetition rate techniques: defining methodology and experimental protocols. *Biochimica et Biophysica Acta (BBA)-Bioenergetics*, *1367*(1-3), 88-106. https://doi.org/10.1016/S0005-2728(98)00135-2
Kovač, Ž., Platt, T., Sathyendranath, S., Antunović, S., (2017). Models for estimating photosynthesis parameters from *in situ* production profiles. *Progress in Oceanography, 159*, 255-266. https://doi.org/10.1016/j.pocean.2017.10.013
Kring, S.A., Figary, S.E., Boyer, G.L., Watson, S.B., Twiss, M.R., (2014). Rapid *in situ* measures of phytoplankton communities using the bbe FluoroProbe: evaluation of spectral calibration, instrument intercompatibility, and performance range. *Canadian journal of fisheries and aquatic sciences*, *71*(7), 1087-1095. https://doi.org/10.1139/cjfas-2013-0599

Kromkamp, J.C., Forster, R.M., (2003). The use of variable fluorescence measurements in aquatic ecosystems: differences between multiple and single turnover measuring protocols and suggested terminology. *European Journal of Phycology*, *38*(2), 103-112. https://doi.org/10.1080/0967026031000094094

Kroon, B., Prézelin, B.B., Schofield, O., (1993). Chromatic Regulation of Quantum Yields for Photosystem Ii Charge Separation, Oxygen Evolution, and Carbon Fixation in Heterocapsa Pygmaea (pyrrophyta). *Journal of phycology*, *29*(4), 453-462. https://doi.org/10.1111/j.1529-8817.1993.tb00146.x

Kuczynska, P., Jemiola-Rzeminska, M., Strzalka, K., 2015. (2015). Photosynthetic pigments in diatoms. *Marine drugs*, *13*(9), 5847-5881. https://doi.org/10.3390/md13095847

Kuznetsova, A., Brockhoff, P.B., Christensen, R.H.B., (2019). lmerTest: Tests in Linear Mixed Effects Models.

Kyewalyanga, M., Piatt, T., Sathyendrath, S., (1992). Ocean primary production calculated by spectral and broad-band models. *Marine Ecology Progress Series*, 171-185. https://doi.org/10.3354/meps085171

Kyewalyanga, M., Platt, T., Sathyendranath, S., (1997). Estimation of the photosynthetic action spectrum:implication for primary production models. *Marine Ecology Progress Series*, 146, 207–223. https://doi.org/10.3354/meps146207

Kyewalyanga, M., Sathyendranath, S., Platt, T., (2002). Effect of Mesodinium rubrum (= Myrionecta rubra) on the action and absorption spectra of phytoplankton in a coastal marine inlet. *Journal of plankton research*, *24*(7), 687-702. https://doi.org/10.1093/plankt/24.7.687

Larkum, A.W.D., Barrett, J., (1983). Light-harvesting processes in algae [Includes taxonomic basis]. Adv. Bot. Res.

Larkum, A.W.D., Vesk, M.,(2003). Algal Plastids: Their Fine Structure and Properties, in: Larkum, A.W.D., Douglas, S.E., Raven, J.A. (Eds.), Photosynthesis in Algae, Advances in Photosynthesis and Respiration. Springer Netherlands, Dordrecht, pp. 11–28. https://doi.org/10.1007/978-94-007-1038-2_2

Lavaud, J., Fast regulation of photosynthesis in diatoms: mechanisms, evolution and ecophysiology. *Functional Plant Science and Biotechonology*, *1*, 267-287.

Lavaud, J., Strzepek, R.F., Kroth, P.G., (2007). Photoprotection capacity differs among diatoms: possible consequences on the spatial distribution of diatoms related to fluctuations in the underwater light climate. *Limnology and Oceanography*, *52*(3), 1188-1194. https://doi.org/10.4319/lo.2007.52.3.1188

Lavergne, J., Trissl, H.W., (1995). Theory of fluorescence induction in photosystem II: derivation of analytical expressions in a model including exciton-radical-pair equilibrium and restricted energy transfer between photosynthetic units. *Biophysical journal*, *68*(6), 2474-2492.

Lavit, C., (1988). Presentation de la méthode STATIS permettant l'analyse conjointe de plusieurs tableaux de données quantitatives. *Cachiers de la Recherche Développement*, *18*, 49-60.

Lavit, C., Escoufier, Y., Sabatier, R., Traissac, P., (1994). The ACT (STATIS method). *Computational Statatitistical Data Analysis. 18*, 97–119. https://doi.org/10.1016/0167-9473(94)90134-1

Lawrenz, E., Richardson, T.L., Differential effects of changes in spectral irradiance on photoacclimation, primary productivity and growth in *Rhodomonas salina* (*Cryptophyceae*) and *Skeletonema costatum* (*Bacillariophyceae*) in simulated blackwater environments. *Journal of phycology*, *53*(6), 1241-1254. https://doi.org/10.1111/jpy.12578

Lawrenz, E., Smith, E.M., Richardson, T.L., (2013). Spectral Irradiance, Phytoplankton Community Composition and Primary Productivity in a Salt Marsh Estuary, North Inlet, South Carolina, USA. *Estuaries Coasts 36*, 347–364. https://doi.org/10.1007/s12237-012-9567-y

Laws, E.A., DiTullio, G.R., Carder, K.L., Betzer, P.R., Hawes, S., (1990). Primary production in the deep blue sea. Deep Sea Res. Part Oceanogr. *Res. Pap. 37*, 715–730. https://doi.org/10.1016/0198-0149(90)90001-C

Lefebvre, A., (2015). MAREL Carnot data and metadata from Coriolis Data Centre. https://doi.org/10.17882/39754

Lefebvre, S., Mouget, J.-L., Lavaud, J., (2011). Duration of rapid light curves for determining the photosynthetic activity of microphytobenthos biofilm *in situ*. *Aquatic botany*, *95*(1), 1-8. https://doi.org/10.1016/j.aquabot.2011.02.010

Legendre, P., Legendre, L., (2012). Numerical ecology, Third English edition. ed, Developments in environmental modelling. Elsevier, Amsterdam.

Lewis, M.R., Smith, J.C., (1983). A small volume, short-incubation-time method for measurement of photosynthesis as a function of incident irradiance. *Marine ecology progress series. Oldendorf*, *13*(1), 99-102.

Lewis, M.R., Ulloa, O., Platt, T., 1988. (1988). Photosynthetic action, absorption, and quantum yield spectra for a natural population of Oscillatoria in the North Atlantic 1. *Limnology and Oceanography*, *33*(1), 92-98. https://doi.org/10.4319/lo.1988.33.1.0092

Lewis, M.R., Warnock, R.E., Irwin, B., Platt, T., (1985a). Measuring Photosynthetic Action Spectra of Natural Phytoplankton Populations. *Journal of Phycology, 21*, 310–315. https://doi.org/10.1111/j.0022-3646.1985.00310.x

Lewis, M.R., Warnock, R.E., Platt, T., (1985b). Absorption and photosynthetic action spectra for natural phytoplankton populations: Implications for production in the open ocean 1. *Limnology and Oceanography*, *30*(4), 794-806. https://doi.org/10.4319/lo.1985.30.4.0794

Ley, A.C., Mauzerall, D.C., (1982). Absolute absorption cross-sections for photosystem II and the minimum quantum requirement for photosynthesis in *Chlorella vulgaris*. *Biochimica et Biophysica Acta (BBA)-Bioenergetics*, *680*(1), 95-106. https://doi.org/10.1016/0005-2728(82)90320-6

Li, Y., Chen, M., (2015). Novel chlorophylls and new directions in photosynthesis research. *Functional Plant Biology*, *42*(6), 493-501. https://doi.org/10.1071/FP14350

Lizon, F., Lagadeuc, Y., Brunet, C., Aelbrecht, D., Bentley, D., (1995). Primary production and photoadaptation of phytoplankton in relation with tidal mixing in coastal waters. *Journal of plankton research*, *17*(5), 1039-1055. https://doi.org/10.1093/plankt/17.5.1039

Lizon, F., Seuront, L., Lagadeuc, Y., (1998). Photoadaptation and primary production study in tidally mixed coastal waters using a Lagrangian model. *Marine Ecology Progress Series*, *169*, 43-54. https://doi.org/10.3354/meps169043

Lohr, M., Wilhelm, C., (2001). Xanthophyll synthesis in diatoms: quantification of putative intermediates and comparison of pigment conversion kinetics with rate constants derived from a model. *Planta*, *212*(3), 382-391. https://doi.org/10.1007/s004250000403

López-Figueroa, F., (1992). Diurnal Variation in Pigment Content in Porphyra laciniata and Chondrus crispus and its Relation to the Diurnal Changes of Underwater Light Quality and Quantity. *Marine Ecology, 13*, 285–305. https://doi.org/10.1111/j.1439-0485.1992.tb00356.x

Lorenzen, C.J., (1966). A method for the continuous measurement of in vivo chlorophyll concentration. In *Deep Sea Research and Oceanographic Abstracts* (Vol. 13, No. 2, pp. 223-227). https://doi.org/10.1016/0011-7471(66)91102-8

Lowe, J., Howard, T., Pardaens, A., Tinker, J., Holt, J., Wakelin, S., Milne, G., Leake, J., Wolf, J., Horsburgh, K., Reeder, T., Jenkins, G., Ridley, J., Dye, S., Bradley, S., (2009). UK Climate Projections science report: Marine and coastal projections.

Luimstra, V.M., Schuurmans, J.M., de Carvalho, C.F.M., Matthijs, H.C.P., Hellingwerf, K.J., Huisman, J., (2019). Exploring the low photosynthetic efficiency of cyanobacteria in blue light using a mutant lacking phycobilisomes. *Photosynthetic Research, 141,* 291–301. https://doi.org/10.1007/s11120-019-00630-z

Luimstra, V.M., Schuurmans, J.M., Hellingwerf, K.J., Matthijs, H.C.P., Huisman, J., 2020a. Blue light induces major changes in the gene expression profile of the cyanobacterium Synechocystis sp. PCC 6803. *Physiologia plantarum*, *170*(1), 10-26. https://doi.org/10.1111/ppl.13086

Luimstra, V.M., Schuurmans, J.M., Verschoor, A.M., Hellingwerf, K.J., Huisman, J., Matthijs, H.C.P., (2018). Blue light reduces photosynthetic efficiency of cyanobacteria through an imbalance between photosystems I and II. *Photosynthetic Research. 138,* 177–189. https://doi.org/10.1007/s11120-018-0561-5

Luimstra, V.M., Verspagen, J.M.H., Xu, T., Schuurmans, J.M., Huisman, J., (2020b). Changes in water color shift competition between phytoplankton species with contrasting light-harvesting strategies. *Ecology, 101*(3), e02951. https://doi.org/10.1002/ecy.2951

Lutz, V., Frouin, R., Negri, R., Silva, R., Pompeu, M., Rudorff, N., Cabral, A., Dogliotti, A., Martinez, G., (2016). Bio-optical characteristics along the Straits of Magallanes. *Continental Shelf Research, 119,* 56-67. https://doi.org/10.1016/j.csr.2016.03.008

Lutz, V., Sathyendranath, S., Head, E., Li, W., (2003). Variability in pigment composition and optical characteristics of phytoplankton in the Labrador Sea and the Central North Atlantic. *Marine Ecology Progress Series*, *260*, 1-18. https://doi.org/10.3354/meps260001

MacIntyre, H.L., Kana, T.M., Anning, T., Geider, R.J., 2002. (2002). Photoacclimation of photosynthesis irradiance response curves and photosynthetic pigments in microalgae and cyanobacteria 1. *Journal of phycology*, *38*(1), 17-38. https://doi.org/10.1046/j.1529-8817.2002.00094.x

MacIntyre, H.L., Kana, T.M., Geider, R.J., (2000). The effect of water motion on short-term rates of photosynthesis by marine phytoplankton. *Trends in plant science*, *5*(1), 12-17. https://doi.org/10.1016/S1360-1385(99)01504-6

MacIntyre, H.L., Lawrenz, E., Richardson, T.L., 2010. Taxonomic Discrimination of Phytoplankton by Spectral Fluorescence, in: Suggett, D.J., Prášil, O., Borowitzka, M.A. (Eds.), Chlorophyll *a* Fluorescence in Aquatic Sciences: Methods and Applications. Springer Netherlands, Dordrecht, pp. 129–169. https://doi.org/10.1007/978-90-481-9268-7_7

Mann, M., Serif, M., Jakob, T., Kroth, P. G., Wilhelm, C., 2017. PtAUREO1a and PtAUREO1b knockout mutants of the diatom *Phaeodactylum tricornutum* are blocked in photoacclimation to blue light. *Journal of plant physiology*, *217*, 44-48. https://doi.org/10.1016/j.jplph.2017.05.020

Mauzerall, D., (1972). Light-induced fluorescence changes in *Chlorella*, and the primary photoreactions for the production of oxygen. *Proceedings of the National Academy of Sciences*, *69*(6), 1358-1362. https://doi.org/10.1073/pnas.69.6.1358

Mendes, S., Fernández-Gómez, M.J., Jorge Pereira, M., Azeiteiro, U., Galindo Villardón, M.P., (2010). The efficiency of the Partial Triadic Analysis method: an ecological application. *Biometr Lett*, *47*, 83-106.

Mercado, J.M., del Pilar Sánchez-Saavedra, M., Correa-Reyes, G., Lubián, L., Montero, O., Figueroa, F.L., (2004). Blue light effect on growth, light absorption characteristics and

photosynthesis of five benthic diatom strains. *Aquatic Botany*, *78*(3), 265-277. https://doi.org/10.1016/j.aquabot.2003.11.004

Michaelis, L., & Menten, M. L. (1913). Die kinetik der invertinwirkung. *Biochem. z*, *49*(333-369), 352.

Möglich, A., Yang, X., Ayers, R.A., Moffat, K., (2010). Structure and function of plant photoreceptors. *Annual review of plant biology*, *61*, 21-47. https://doi.org/10.1146/annurev-arplant-042809-112259

Moisan, T.A., Ellisman, M.H., Buitenhuys, C.W., Sosinsky, G.E., (2006). Differences in chloroplast ultrastructure of *Phaeocystis antarctica* in low and high light. *Marine Biology*, *149*(6), 1281-1290. https://doi.org/10.1007/s00227-006-0321-5

Moore, C.M., Suggett, D.J., Hickman, A.E., Kim, Y.-N., Tweddle, J.F., Sharples, J., Geider, R.J., Holligan, P.M., (2006). Phytoplankton photoacclimation and photoadaptation in response to environmental gradients in a shelf sea. *Limnology and Oceanography*, *51*(2), 936-949. https://doi.org/10.4319/lo.2006.51.2.0936

Morel, A., (1978). Available, usable, and stored radiant energy in relation to marine photosynthesis. *Deep Sea Research*, *25*(8), 673-688. https://doi.org/10.1016/0146-6291(78)90623-9

Morel, A., Smith, R.C., (1974). Relation between total quanta and total energy for aquatic photosynthesis 1. *Limnology and Oceanography*, *19*(4), 591-600. https://doi.org/10.4319/lo.1974.19.4.0591

Morelle, J., Claquin, P., (2018). Electron requirements for carbon incorporation along a diel light cycle in three marine diatom species. *Photosynthetic Research*, *137*, 201–214. https://doi.org/10.1007/s11120-018-0491-2

Morelle, J., Schapira, M., Orvain, F., Riou, P., Lopez, P.J., Pierre-Duplessix, O., Rabiller, E., Maheux, F., Simon, B., Claquin, P., (2018). Annual phytoplankton primary production estimation in a temperate estuary by coupling PAM and carbon incorporation methods. *Estuaries and Coasts*, *41*(5), 1337-1355..https://doi.org/10.1007/s12237-018-0369-8

Morot-Gaudry, J.-F., Farineau, J., (2011). La photosynthèse Processus physiques, moléculaires et physiologiques. Editions Quae, Paris.

Mouget, J.-L., Rosa, P., Tremblin, G., (2004). Acclimation of Haslea ostrearia to light of different spectral qualities–confirmation ofchromatic adaptation'in diatoms. *Journal of Photochemistry and Photobiology B: Biology*, *75*(1-2), 1-11. https://doi.org/10.1016/j.jphotobiol.2004.04.002

Mouget, J.-L., Rosa, P., Vachoux, C., Tremblin, G., (2005). Enhancement of marennine production by blue light in the diatom Haslea ostrearia. *Journal of applied phycology*, *17*(5), 437-445. https://doi.org/10.1007/s10811-005-0561-7

Moulager, M., Monnier, A., Jesson, B., Bouvet, R., Mosser, J., Schwartz, C., Garnier, L., Corellou, F., Bouget, F.-Y., (2007). Light-dependent regulation of cell division in Ostreococcus: evidence for a major transcriptional input. *Plant physiology*, *144*(3), 1360-1369. https://doi.org/10.1104/pp.107.096149

Napoléon C, Fiant L, Raimbault V, Claquin P. 2013a. Study of dynamics of phytoplankton and photosynthetic parameters using opportunity ships in the western English Channel. *Journal of Marine Systems* 128:146–158. DOI: 10.1016/j.jmarsys.2013.04.019.

Napoléon C, Raimbault V, Claquin P. 2013b. Influence of Nutrient Stress on the Relationships between PAM Measurements and Carbon Incorporation in Four Phytoplankton Species. *PLoS ONE* 8:e66423. DOI: 10.1371/journal.pone.0066423.

Napoléon, C., Raimbault, V., Fiant, L., Riou, P., Lefebvre, S., Lampert, L., Claquin, P., (2012). Spatiotemporal dynamics of physicochemical and photosynthetic parameters in the central English Channel. *Journal of Sea Research*, *69*, 43-52. https://doi.org/10.1016/j.seares.2012.01.005

Neori, A., Vernet, M., Holm-Hansen, O., Haxo, F.T., (1986). Relationship between action spectra for chlorophyll *a* fluorescence and photosynthetic O2 evolution in algae. *Journal of Plankton Research*, *8*(3), 537-548.

Nicklisch, A., (1998). Growth and light absorption of some planktonic cyanobacteria, diatoms and *Chlorophyceae* under simulated natural light fluctuations. *Journal of Plankton Research*, *20*(1), 105-119.

Nielsen, E.S., (1952). The use of radio-active carbon (C14) for measuring organic production in the sea. *ICES Journal of Marine Science*, *18*(2), 117-140. https://doi.org/10.1093/icesjms/18.2.117

Nielsen, M.V., Sakshaug, E., (1993). Photobiological studies of *Skeletonema costatum* adapted to spectrally different light regimes. *Limnology and oceanography*, *38*(7), 1576-1581. https://doi.org/10.4319/lo.1993.38.7.1576

Oksanen, J., Blanchet, F.G., Friendly, M., Kindt, R., Legendre, P., McGlinn, D., Minchin, P.R., O'Hara, R.B., Simpson, G.L., Solymos, P., Stevens, M.H.H., Szoecs, E., Wagner, H., (2015). Vegan: community ecology package. Ordination methods, diversity analysis and other functions for community and vegetation ecologists. *R package ver*, 2-3.

Orefice, I., Chandrasekaran, R., Smerilli, A., Corato, F., Caruso, T., Casillo, A., Corsaro, M.M., Piaz, F.D., Ruban, A.V., Brunet, C., (2016). Light-induced changes in the photosynthetic physiology and biochemistry in the diatom *Skeletonema marinoi*. *Algal research*, *17*, 1-13. https://doi.org/10.1016/j.algal.2016.04.013

Oxborough, K., (2004). Imaging of chlorophyll a fluorescence: theoretical and practical aspects of an emerging technique for the monitoring of photosynthetic performance. *Journal of Experimental Botany*, *55*(400), 1195-1205. https://doi.org/10.1093/jxb/erh145

Painter, S.C., Lucas, M.I., Stinchcombe, M.C., Bibby, T.S., Poulton, A.J., (2010). Summertime trends in pelagic biogeochemistry at the Porcupine Abyssal Plain study site in the northeast Atlantic. *Deep Sea Research Part II: Topical Studies in Oceanography*, *57*(15), 1313-1323. https://doi.org/10.1016/j.dsr2.2010.01.008

Palenik, B., (2001). Chromatic Adaptation in Marine Synechococcus Strains. *Applications of Environmental Microbiology*, *67*, 991–994. https://doi.org/10.1128/AEM.67.2.991-994.2001

Papageorgiou, G.C., Govindjee (Eds.), 2004. Chlorophyll a fluorescence: a signature of photosynthesis, Advances in photosynthesis and respiration. Kluwer Academic, Dordrecht.

Petroutsos, D., Tokutsu, R., Maruyama, S., Flori, S., Greiner, A., Magneschi, L., Cusant, L., Kottke, T., Mittag, M., Hegemann, P., Finazzi, G., Minagawa, J., (2016). A blue-light photoreceptor mediates the feedback regulation of photosynthesis. *Nature 537*, 563–566. https://doi.org/10.1038/nature19358

Philippart, C.J.M., Salama, Mhd.S., Kromkamp, J.C., van der Woerd, H.J., Zuur, A.F., Cadée, G.C., (2013). Four decades of variability in turbidity in the western Wadden Sea as derived from corrected Secchi disk readings. *Journal of sea research*, *82*, 67-79. https://doi.org/10.1016/j.seares.2012.07.005

Pinheiro, J.C., Bates, D.M., (2000). Mixed-effects models in S and S-PLUS, Statistics and computing. Springer, New York.

Platt, T., Jassby, A.D., 1976. The Relationship Between Photosynthesis and Light for Natural Assemblages of Coastal Marine Phytoplankton1. *Journal of Phycology*, *12*(4), 421-430. https://doi.org/10.1111/j.1529-8817.1976.tb02866.x

Platt, T., Sathyendranath, S., (1988). Oceanic primary production: estimation by remote sensing at local and regional scales. *Science*, *241*(4873), 1613-1620. https://doi.org/10.1126/science.241.4873.1613

Premvardhan, L., Bordes, L., Beer, A., Büchel, C., Robert, B., (2009). Carotenoid structures and environments in trimeric and oligomeric fucoxanthin chlorophyll *a/c2* proteins from resonance Raman spectroscopy. *The Journal of Physical Chemistry B*, *113*(37), 12565-12574. https://doi.org/10.1021/jp903029g

Premvardhan, L., Sandberg, D.J., Fey, H., Birge, R.R., Büchel, C., van Grondelle, R., (2008). The charge-transfer properties of the S2 state of fucoxanthin in solution and in fucoxanthin chlorophyll-*a/c2* protein (FCP) based on stark spectroscopy and molecular-orbital theory. *The Journal of Physical Chemistry B*, *112*(37), 11838-11853. https://doi.org/10.1021/jp802689p

R Core Team, (2020). R: A language and environment for statistical computing. R Foundation for statistica Computing [WWW Document]. URL https://www.r-project.org/ (accessed 12.1.20).

Ragni, M., Ribera d'Alcalà, M., (2004). Light as an information carrier underwater. Journal of *Plankton Research. 26,* 433–443. https://doi.org/10.1093/plankt/fbh044

Raven, J.A., (2011). The cost of photoinhibition. *Physiologia plantarum*, *142*(1), 87-104. https://doi.org/10.1111/j.1399-3054.2011.01465.x

Raven, J.A., Geider, R.J., 2003. Adaptation, Acclimation and Regulation in Algal Photosynthesis, in: Larkum, A.W.D., Douglas, S.E., Raven, J.A. (Eds.), Photosynthesis in Algae, Advances in Photosynthesis and Respiration. Springer Netherlands, Dordrecht, pp. 385–412. https://doi.org/10.1007/978-94-007-1038-2_17

Richardson, K., Beardall, J., Raven, J.A., (1983). Adaptation of unicellular algae to irradiance: an analysis of strategies. *New Phytologist. 93*, 157–191. https://doi.org/10.1111/j.1469-8137.1983.tb03422.x

Riley, G.A., 1957. (1957). Phytoplankton of the north central sargasso sea, 1950–52 1. *Limnology and Oceanography*, *2*(3), 252-270. https://doi.org/10.1002/lno.1957.2.3.0252

Ritz, M., Neverov, K.V., Etienne, A.-L., (1999). ΔpH-dependent fluorescence quenching and its photoprotective role in the unicellular red alga Rhodella violacea. *Photosynthetica*, *37*(2), 267-280. https://doi.org/10.1023/A:1007164207022

Rivkin, R., (1989). Influence of irradiance and spectral quality on the carbon metabolism of phytoplankton. I. Photosynthesis, chemical composition and growth. *Marine ecology progress series. Oldendorf*, *55*(2), 291-304. https://doi.org/10.3354/meps055291

Sakshaug, E., (1993). The relationship between phytoplankton growth rate and production with emphasis on respiration and excretion. In *ICES Marine Science Symposia* (Vol. 197, pp. 63-68).

Sakshaug, E., Bricaud, A., Dandonneau, Y., Falkowski, P.G., Kiefer, D.A., Legendre, L., Morel, A., Parslow, J., Takahashi, M., (1997). Parameters of photosynthesis: definitions, theory and interpretation of results. *Journal of Plankton Research*, *19*(11), 1637-1670. https://doi.org/10.1093/plankt/19.11.1637

Sakshaug, E., Demers, S., Yentsch, C., (1987). Thalassiosira oceanica and T. pseudonana: two different photoadaptational responses. *Marine Ecology Progress Series*, 275-282. https://doi.org/10.3354/meps041275

Sathyendranath, S., Longhurst, A., Caverhill, C.M., Platt, T., (1995). Regionally and seasonally differentiated primary production in the North Atlantic. *Deep Sea Research Part I: Oceanographic Research Papers*, *42*(10), 1773-1802. https://doi.org/10.1016/0967-0637(95)00059-F

Sathyendranath, S., Platt, T., (1993). Remote senting of water-colum primary production. Presented at the ICES Marine Sciences Symposia, pp. 237–243.

Sathyendranath, S., Platt, T., Kovač, Ž., Dingle, J., Jackson, T., Brewin, R.J.W., Franks, P., Marañón, E., Kulk, G., Bouman, H.A., (2020). Reconciling models of primary

production and photoacclimation. *Applied optics*, *59*(10), C100-C114. https://doi.org/10.1364/AO.386252

Sathyendranath, S., Prieur, L., Morel, A., (1989). A three-component model of ocean colour and its application to remote sensing of phytoplankton pigments in coastal waters. *International Journal of Remote Sensing*, *10*(8), 1373-1394. https://doi.org/10.1080/01431168908903974

Sathyendranath, S., Stuart, V., Irwin, B.D., Maass, H., Savidge, G., Gilpin, L., Platt, T., (1999). Seasonal variations in bio-optical properties of phytoplankton in the Arabian Sea. *Deep Sea Research Part II: Topical Studies in Oceanography*, *46*(3-4), 633-653. https://doi.org/10.1016/S0967-0645(98)00121-0

Schapira, M., Vincent, D., Gentilhomme, V., Seuront, L., (2008). Temporal patterns of phytoplankton assemblages, size spectra and diversity during the wane of a *Phaeocystis globosa* spring bloom in hydrologically contrasted coastal waters. *Marine Biological Association of the United Kingdom. Journal of the Marine Biological Association of the United Kingdom*, *88*(4), 649. https://doi.org/10.1017/S0025315408001306

Schellenberger Costa, B., Jungandreas, A., Jakob, T., Weisheit, W., Mittag, M., Wilhelm, C., (2013a). Blue light is essential for high light acclimation and photoprotection in the diatom *Phaeodactylum tricornutum*. *Journal of experimental botany*, *64*(2), 483-493. https://doi.org/10.1093/jxb/ers340

Schellenberger Costa, B., Sachse, M., Jungandreas, A., Bartulos, C.R., Gruber, A., Jakob, T., Kroth, P.G., Wilhelm, C., (2013b). Aureochrome 1a Is Involved in the Photoacclimation of the Diatom *Phaeodactylum tricornutum*. *PLoS ONE 8*, e74451. https://doi.org/10.1371/journal.pone.0074451

Schofield, O., Bidigare, R., Prézelin, B., 1990. Spectral photosynthesis, quantum yield and blue-green light enhancement of productivity rates in the diatom Chaetoceros gracile and the prymnesiophyte Emiliania huxleyi. *Marine Ecology Progress Series*, 175-186. https://doi.org/10.3354/meps064175

Schofield, O., Moline, M., Cahill, B., Frazer, T., Kahl, A., Oliver, M., Reinfelder, J., Glenn, S., Chant, R., (2013. Phytoplankton productivity in a turbid buoyant coastal plume. *Continental Shelf Research*, *63*, S138-S148. https://doi.org/10.1016/j.csr.2013.02.005

Schofield, O., Prézelin, B., Johnsen, G., (1996). Wavelength Dependency of the Maximum Quantum Yield of Carbon Fixation for Two Red Tide Dinoflagellates, Heterocapsa Pygmaea and Prorocentrum Minimum (pyrrophyta): Implications for Measuring Photosynthetic Rates1. *Journal of phycology*, *32*(4), 574-583. https://doi.org/10.1111/j.0022-3646.1996.00574.x

Schofield, O., Prezelin, B., Smith, R., Stegmann, P., Nelson, N., Lewis, M., Baker, K., (1991). Variability in spectral and nonspectral measurements of photosynthetic light utilization efficiencies. *Mar. Ecol. Prog. Ser*, *78*, 253-271. https://doi.org/10.3354/meps078253

Schreiber, U., (2004). Pulse-Amplitude-Modulation (PAM) Fluorometry and Saturation Pulse Method: An Overview, in: Papageorgiou, G.C., Govindjee (Eds.), Chlorophyll *a* Fluorescence. Springer Netherlands, Dordrecht, pp. 279–319. https://doi.org/10.1007/978-1-4020-3218-9_11

Schreiber, U., (1998). Chlorophyll fluorescence: New Instruments for Special Applications, in: Garab, G. (Ed.), Photosynthesis: Mechanisms and Effects: Volume I–V: Proceedings of the XIth International Congress on Photosynthesis, Budapest, Hungary, August 17–22, 1998. Springer Netherlands, Dordrecht, pp. 4253–4258. https://doi.org/10.1007/978-94-011-3953-3_984

Schreiber, U., Klughammer, C., (2013). Wavelength-dependent photodamage to *Chlorella* investigated with a new type of multi-color PAM chlorophyll fluorometer. *Photosynthetic Research. 114*, 165–177. https://doi.org/10.1007/s11120-013-9801-x

Schreiber, U., Klughammer, C., Kolbowski, J., (2012). Assessment of wavelength-dependent parameters of photosynthetic electron transport with a new type of multi-color PAM chlorophyll fluorometer. *Photosynthetic Research, 113*, 127–144. https://doi.org/10.1007/s11120-012-9758-1

Schreiber, U., Klughammer, C., Kolbowski, J., (2011). High-end chlorophyll fluorescence analysis with the MULTI-COLOR-PAM. I. Various light qualities and their applications. 21.

Schreiber, U., Schliwa, U., Bilger, W., (1986). Continuous recording of photochemical and non-photochemical chlorophyll fluorescence quenching with a new type of modulation fluorometer. *Photosynthetic Research, 10*, 51–62. https://doi.org/10.1007/BF00024185

Schuback, N., Flecken, M., Maldonado, M.T., Tortell, P.D., (2016). Diurnal variation in the coupling of photosynthetic electron transport and carbon fixation in iron-limited phytoplankton in the NE subarctic Pacific. *Biogeosciences 13*, 1019–1035. https://doi.org/10.5194/bg-13-1019-2016

Serôdio, J., Lavaud, J., (2011). A model for describing the light response of the nonphotochemical quenching of chlorophyll fluorescence. *Photosynthetic Research, 108*, 61–76. https://doi.org/10.1007/s11120-011-9654-0

Shikata, T., Matsunaga, S., Iseki, M., Nishide, H., Higashi, S.-I., Kamei, Y., Yamaguchi, M., Jenkinson, I.R., Watanabe, M., (2013). Blue light regulates the rhythm of diurnal vertical migration in the raphidophyte red-tide alga Chattonella antiqua. *Journal of Plankton Research. 35*, 542–552. https://doi.org/10.1093/plankt/fbt006

Shimada, A., Maruyama, T., Miyachi, S., (1996). Vertical distributions and photosynthetic action spectre of two oceanic picophytopianlcters, *Prochlorococcus marinus* and *Synechococcus sp*. *Marine Biology, 127*(1), 15-23.. https://doi.org/10.1007/BF00993639

Siberchicot, S.D. and A., Julien-Laferrière, with contributions from J.T.B. on earlier work by A., (2018). adegraphics: an S4 lattice-based package for the representation of multivariate data. *R Journal, 9*(2).

Silsbe, G.M., Malkin, S.Y., (2015). phytotools: Phytoplankton Production Tools.

Stomp, M., Huisman, J., de Jongh, F., Veraart, A.J., Gerla, D., Rijkeboer, M., Ibelings, B.W., Wollenzien, U.I.A., Stal, L.J., 2004. Adaptive divergence in pigment composition promotes phytoplankton biodiversity. *Nature 432*, 104–107. https://doi.org/10.1038/nature03044

Stomp, M., van Dijk, M.A., van Overzee, H.M.J., Wortel, M.T., Sigon, C.A.M., Egas, M., Hoogveld, H., Gons, H.J., Huisman, J., (2008) The timescale of phenotypic plasticity and its impact on competition in fluctuating environments. *The American Naturalist, 172*(5), E169–E185. https://doi.org/10.1086/591680

Subba Rao, D.V. (Ed.), (2006). Algal cultures, analogues of blooms and applications. Science Publishers, Enfield, NH.

Suggett, D.J., Goyen, S., Evenhuis, C., Szabó, M., Pettay, D.T., Warner, M.E., Ralph, P.J., 2015. Functional diversity of photobiological traits within the genus *Symbiodinium* appears to be governed by the interaction of cell size with cladal designation. *New Phytolgist. 208*, 370–381. https://doi.org/10.1111/nph.13483

Suggett, D.J., Prášil, O., Borowitzka, M.A. (Eds.), (2010). Chlorophyll *a* Fluorescence in Aquatic Sciences: Methods and Applications. Springer Netherlands, Dordrecht. https://doi.org/10.1007/978-90-481-9268-7

Szabó, M., Parker, K., Guruprasad, S., Kuzhiumparambil, U., Lilley, R.Mc.C., Tamburic, B., Schliep, M., Larkum, A.W.D., Schreiber, U., Raven, J.A., Ralph, P.J., (2014a). Photosynthetic acclimation of *Nannochloropsis oculata* investigated by multi-

wavelength chlorophyll fluorescence analysis. *Bioresource Technology, 167*, 521–529. https://doi.org/10.1016/j.biortech.2014.06.046

Szabó, M., Wangpraseurt, D., Tamburic, B., Larkum, A.W.D., Schreiber, U., Suggett, D.J., Kühl, M., Ralph, P.J., (2014b). Effective light absorption and absolute electron transport rates in the coral *Pocillopora damicornis*. *Plant physiology and biochemistry, 83*, 159-167. https://doi.org/10.1016/j.plaphy.2014.07.015

Talling, J.F., 1957. The phytoplankton population as a compound photosynthetic system. *New phytologist*, *56*(2), 133-149. https://doi.org/10.1111/j.1469-8137.1957.tb06962.x

Tamburic, B., Szabó, M., Tran, N.A.T., Larkum, A.W.D., Suggett, D.J., Ralph, P.J., (2014). Action spectra of oxygen production and chlorophyll *a* fluorescence in the green microalga *Nannochloropsis oculata*. *Bioresource technology*, *169*, 320-327. https://doi.org/10.1016/j.biortech.2014.07.008

Thioulouse, J., (1987). Les analyses multitableaux en écologie factorielle 20.

Tillmann, U., Hesse, K.-J., Colijn, F., 2000. Planktonic primary production in the German Wadden Sea. *Journal of Plankton Research*, *22*(7), 1253-1276. https://doi.org/10.1093/plankt/22.7.1253

Valle, K.C., Nymark, M., Aamot, I., Hancke, K., Winge, P., Andresen, K., Johnsen, G., Brembu, T., Bones, A.M., (2014). System Responses to Equal Doses of Photosynthetically Usable Radiation of Blue, Green, and Red Light in the Marine Diatom *Phaeodactylum tricornutum*. *PLoS ONE 9*, e114211. https://doi.org/10.1371/journal.pone.0114211

Van Leeuwen, S., Tett, P., Mills, D., Molen, J. van der, (2015). Stratified and nonstratified areas in the N orth S ea: Long-term variability and biological and policy implications. *Journal of Geophysical Research: Oceans*, *120*(7), 4670-4686. https://doi.org/10.1002/2014JC010485

Vantrepotte, V., Brunet, C., Mériaux, X., Lécuyer, E., Vellucci, V., Santer, R., 2007. Bio-optical properties of coastal waters in the Eastern English Channel. *Estuarine Coastal Shelf Science. 72*, 201–212. https://doi.org/10.1016/j.ecss.2006.10.016

Vantrepotte, V., Loisel, H., Dessailly, D., Mériaux, X., 2012. Optical classification of contrasted coastal waters. *Remote Sensing of Environment*, *123*, 306-323. https://doi.org/10.1016/j.rse.2012.03.004

Vincent, W.F., (1981). Photosynthetic capacity measured by DCMU-induced chlorophyll fluorescence in an oligotrophic lake. *Freshwater biology*, *11*(1), 61–78. https://doi.org/10.1111/j.1365-2427.1981.tb01242.x

Wang, H., Zhu, R., Zhang, J., Ni, L., Shen, H., Xie, P., (2018). A novel and convenient method for early warning of algal cell density by chlorophyll fluorescence parameters and its application in a highland lake. *Frontiers in plant science*, *9*, 869. https://doi.org/10.3389/fpls.2018.00869

Wang, L., Cai, Q., Xu, Y., Kong, L., Tan, L., Zhang, M., (2011). Weekly dynamics of phytoplankton functional groups under high water level fluctuations in a subtropical reservoir-bay. *Aquatic. Ecology*, *45*(2), 197–212. https://doi.org/10.1007/s10452-010-9346-4

Yentsch, C.S., Phinney, D.A., (1985). Spectral fluorescence: an ataxonomic tool for studying the structure of phytoplankton populations. *Journal of Plankton Research. 7*, 617–632. https://doi.org/10.1093/plankt/7.5.617

Yentsch, C.S., Yentsch, C.M., (1979.) Fluorescence spectral signatures: the characterization of phytoplankton populations by the use of excitation and emission spectra. *J. mar. Res*, *37*(3), 471-483.

Zolfaghari, K., Duguay, C., (2016). Estimation of water quality parameters in lake Erie from meris using linear mixed effect models. *Remote Sensing*, *8*(6), 473. https://doi.org/10.3390/rs8060473

Zuur, A.F. (Ed.), (2009). Mixed effects models and extensions in ecology with R, Statistics for biology and health. Springer, New York, NY.

Abstract

Phytoplankton photoregulation and photoacclimation are controlled by variations in the light climate (i.e. quantity and quality of light) at different temporal and spatial scales. In coastal and megatidal seas such as the English Channel, the underwater light climate is also affected by the hydrodynamics and river outputs. In one hand, the strong hydrodynamism leads to resuspension processes and to intense vertical mixing, transporting cells through the euphotic layer and beyond, in the disphotic layer. In another hand, large river outputs generate an increase of turbidity with particulate matter and with carbon dissolved organic matter (CDOM). All these processes induce a decrease of light penetration in the water column and a general modification of the light climate. For instance, the CDOM absorbs better blue wavelengths.

The wavelength dependent processes of phytoplankton such as photoregulation and photoacclimation have been studied for the first time on natural communities thanks to a new generation of multi-spectral fluorometer called MULTI-COLOR-PAM PAM (Walz). Photosynthesis light curves (P-E) were measured after long dark acclimation at 5 wavelengths, as well as the functional light absorption coefficient of photosystem II ($Sigma(II)_{\lambda}$). Furthermore, the development of an original protocol of data analysis including Linear Mixed Effects Models (LME), Principal Triadic Analyses (PTA) and Redundancy Analyses (RDA) have helped the interpretation of this unique dataset and have highlighted the wavelength dependency of photosynthetic processes at different spatial and temporal scales.

First, a spatial study across the English Channel (From Dunkerque to Brest, France) in springtime have evidenced the capacity of phytoplankton to photoacclimate and to photoregulate despite the high vertical mixing in this megatidal sea. The real photoacclimation state of cells was characterized through the spectral comparison of photosynthetic parameters of the PE (more particularly the light use efficiency $\alpha(II)$) and thanks to the calculations of specific indexes involving the light saturation parameter $E_k(II)$ and the average light of the mixed layer. The phytoplankton photoacclimation state was characterized by a general photoprotective state to blue wavelengths whatever the water masses of the coastal seas. Secondly, a study at seasonal scale evidenced that wavelength dependent photoacclimation and photoregulation were controlled by phytoplankton community structure and succession. This time series revealed that photoacclimation to high lights with an optimization of the maximum photosynthetic capacity ($ETR(II)_{max}$) of cells was possible in springtime. This was observed in parallel to the activation of rapid cycle of xanthophylls. In summer period, characterized by the

increase of the pool of photoprotective carotenoids, ETR(II)max optimization was no longer observed. Simultaneously with the change in the photoprotection model, a sudden transition in the spectral slope of the functional light absorption capacity (Sigma $(II)_{625-440}$) was observed in relation to an increase in the non-photochemical quenching ($NPQ_{625-440}$). Indeed, each of the phytoplanktonic community at each season would have a differentiated strategy to also ensure a photoregulation/photoacclimation to variations in the light climate as a function of the tidal cycle, between high and low tide.

This study therefore presents new results on the spectral dependency of photosynthesis and photoacclimation strategies of natural phytoplankton communities in coastal seas subjected to high hydrodynamics. It highlights potential indicators that could be included in future ecosystem quality monitoring programs.

Key words:

Photosynthesis, Wavelength-dependency, Photoregulation, Photoacclimation, Variable fluorescence, Oceanology

Résumé

La photorégulation et la photoacclimatation du phytoplancton sont contrôlées par les variations du climat lumineux (c'est-à-dire la quantité et la qualité de la lumière) à différentes échelles temporelles et spatiales. Dans les zones côtières telles que la Manche, le climat lumineux est affecté par l'hydrodynamisme et les apports fluviaux. D'une part, le fort hydrodynamisme conduit à des processus de resuspension et à un intense mélange vertical, transportant les cellules à travers la couche euphotique et au-delà, dans la couche disphotique. D'autre part, les débits importants des rivières génèrent une augmentation de la turbidité avec les matières en suspension et avec la matière organique dissoute dans le carbone (CDOM). Tous ces processus induisent une diminution de la pénétration de la lumière dans la colonne d'eau et une modification générale du climat lumineux. Par exemple, le CDOM absorbe mieux les longueurs d'onde du bleu.

Les processus de dépendance spectrale du phytoplancton tels que la photoregulation et la photoacclimation ont été étudiés pour la première fois sur des communautés naturelles grâce à un fluorimètre multispectral de nouvelle génération appelé MULTI-COLOR-PAM (Walz). Les relations photosynthèses-énergie (PE) ont été mesurées après une longue période d'acclimatation au noir à 5 longueurs d'onde, ainsi que le coefficient d'absorption fonctionnel de la lumière des photosystèmes II ($Sigma(II)_{\lambda}$). Le développement d'un protocole original d'analyse de données combinant les techniques de Modèles linéaires à effets mixtes (LME), l'analyse triadique principale (PTA) et les analyses de redondance (RDA) a permis d'analyser un ensemble de données unique et complexe ainsi que de mettre en évidence la dépendance aux longueurs d'onde des processus photosynthétiques à différentes échelles spatiales et temporelles.

Dans un premier temps, une étude à l'échelle spatiale à travers la Manche (de Dunkerque à Brest, France) au printemps a mis en évidence la capacité du phytoplancton à photoréguler et à se photoacclimater malgré les mélanges verticaux élevés de cette mer mégatidale. L'état réel de photoacclimatation des cellules au climat de lumière a été caractérisé à travers la comparaison spectrale des paramètres photosynthétiques des relations PE (plus particulièrement l'efficacité d'utilisation de la lumière $\alpha(II)$ en unité absolue) et grâce aux calculs d'indices impliquant le paramètre de saturation de la lumière $E_k(II)$ et la lumière moyenne de la couche de mélange. L'état de photoacclimatation du phytoplancton a était caractérisé comme un état général de photoprotection aux longueurs d'onde bleu quel que soit la masse d'eau de cette mer côtière.

Deuxièmement, une étude à l'échelle saisonnière a montré que les variations de la dépendance spectrale de la photoacclimatation et de la photorégulation étaient contrôlées par la structure et la succession des communautés phytoplanctoniques. Cette série temporelle a révélé qu'une photoacclimatation aux fortes lumières avec une optimisation de la capacité photosynthétique maximale ($ETR(II)_{max}$) des cellules était possible au printemps, pendant le bloom de *Phaeocystis globosa*. Ceci a été observé parallèlement à l'activation du cycle rapide des xanthophylles. Pendant l'été, caractérisée par l'augmentation du pool de caroténoïdes photoprotecteurs, l'optimisation de ETR(II)max n'était plus observée. De façon simultanée au changement du mode de photoprotection, une transition brutale de la pente spectrale de la capacité d'absorption fonctionnelle de la lumière ($Sigma\ (II)_{625-440}$) a été observé en lien avec une augmentation du quenching non-photochimique ($NPQ_{625-440}$). De plus, à chaque saison, chaque communauté phytoplanctonique aurait une stratégie différenciée pour assurer également une photorégulation/photoacclimatation aux variations du climat de lumière en fonction du cycle de marée, entre haute et basse mer.

Cette étude présente donc de nouveaux résultats sur la dépendance spectrale de la photosynthèse et des stratégies de photoacclimatation des communautés naturelles de microalgues en milieux côtiers soumis à un fort hydrodynamisme. Elle met en évidence de potentiels indicateurs qui pourraient être inclus dans les futurs programmes de surveillance de la qualité des écosystèmes.

Mots Clés :

Photosynthèse, Dépendance spectrale, Photorégulation, Photoacclimatation, Fluorescence variable, Océanologie